Enhancing Resilience and Self-Centering of Reinforced Concrete Single and Coupled Shear Walls with Externally Bonded Fibre Reinforced Polymer Composites

by

Ali ABBASZADEH

MANUSCRIPT-BASED THESIS PRESENTED TO ÉCOLE DE TECHNOLOGIE SUPERIEURE IN PARTIAL FULFILLMENT FOR THE DEGREE OF DOCTOR OF PHILOSOPHY
Ph.D.

MONTREAL, SEPTEMBER 08, 2024

ÉCOLE DE TECHNOLOGIE SUPÉRIEURE
UNIVERSITÉ DU QUÉBEC

BOARD OF EXAMINERS

THIS THESIS HAS BEEN EVALUATED

BY THE FOLLOWING BOARD OF EXAMINERS

Mr. Omar Chaallal, Thesis Supervisor
Department of Construction Engineering, École de technologie supérieure

Mr. Hakim Bouzid, President of the board of examiners
Department of Mechanical Engineering, École de technologie supérieure

Mr. Georges El-Saikaly, Member of the jury
Department of Construction Engineering, École de technologie supérieure

Mr. Amar Khaled, Member of the jury
Department of Construction Engineering, École de technologie supérieure

Mr. Hassan Aoude, External examiner
Department of Civil Engineering, University of Ottawa

THIS THESIS WAS PRENSENTED AND DEFENDED

IN THE PRESENCE OF A BOARD OF EXAMINERS AND THE PUBLIC

ON AUGUST 28, 2024

AT ÉCOLE DE TECHNOLOGIE SUPÉRIEURE

ACKNOWLEDGEMENTS

I express my deepest gratitude to my Ph.D. supervisor, Professor Omar Chaallal, whose guidance, expertise, and unwavering support have been invaluable throughout my academic journey. Professor Chaallal's mentorship has shaped my research and instilled in me a deeper understanding of the subject matter. His insightful feedback, encouragement, and dedication have been instrumental in shaping the direction of this thesis. I am profoundly grateful for his patience, wisdom, and encouragement, which are pivotal in every step of this academic pursuit.

I also express my heartfelt gratitude to every member of the esteemed jury for their invaluable time and expertise in assessing my thesis.

I owe my deepest gratitude to my parents, whose persistent love, support, and sacrifices have been the foundation of my academic journey. Their encouragement, belief in my abilities, and sacrifices have been my constant source of strength and inspiration. I am profoundly grateful for their tireless support, which has enabled me to pursue my academic aspirations with confidence and determination.

I am immensely thankful to my beautiful wife for her persistent love, understanding, and encouragement throughout this challenging yet rewarding journey. Her patience, support, and unwavering belief in me have been my driving force during uncertainty and self-doubt. Her presence and unwavering support have been a constant source of comfort and motivation, for which I am deeply grateful.

Lastly, I want to express my heartfelt appreciation to my friends for their encouragement, camaraderie, and unwavering support throughout this journey.

Amélioration de la résilience et du recentrage des murs de cisaillement isolés et couplés en béton armé avec des composites en polymère renforcés de fibres collés en surface externement

Ali ABBASZADEH

RÉSUMÉ

Les murs de cisaillement isolés (MCI) et les murs de cisaillement couplés (MCC) sont des éléments cruciaux en génie sismique pour améliorer la capacité d'une structure à résister aux forces sismiques. Ces structures sont soigneusement conçues pour résister aux forces latérales des tremblements de terre tout en conservant la ductilité et en fournissant une rigidité suffisante pour transmettre ces forces à la fondation. De plus, ils peuvent dissiper l'énergie sismique en formant des rotules plastiques sous charges cycliques de mouvement du sol. La conception de murs de cisaillement efficaces nécessite une attention méticuleuse aux détails. Un principe de conception crucial pour les murs de cisaillement plus grands est de garantir que la rupture par flexion ait lieu avant la rupture par cisaillement. Dans la conception des MCC, une attention particulière est accordée aux poutres de couplage (PC), qui sont des éléments essentiels pour transférer les forces de cisaillement entre les murs. Ces poutres sont conçues pour éviter de subir une rupture en cisaillement afin de maintenir leur intégrité et leur fonctionnalité. En même temps, elles sont conçues de manière stratégique pour permettre la formation de rotules plastiques à leurs extrémités, incarnant le concept de poutre faible - colonne forte.

Bien que la création de rotules plastiques dans les murs de cisaillement puisse dissiper une quantité significative d'énergie sismique, elle peut également entraîner un déplacement résiduel dans ces composants essentiels. Les effets persistants de ces déplacements peuvent poser des défis quant à l'intégrité structurelle des bâtiments après un tremblement de terre. Par conséquent, pour améliorer la fonctionnalité des bâtiments et minimiser les coûts liés aux dommages dus aux tremblements de terre, il est essentiel de développer une stratégie efficace qui réduise le déplacement résiduel dans les murs de cisaillement existants. La présente étude propose une configuration de renforcement efficace pour les murs de cisaillement situés à Vancouver et à Montréal, qui représentent respectivement les zones sismiques de l'ouest et de l'est du Canada. L'approche suggérée implique l'utilisation de polymères renforcés de fibres collés en surface (PRFCS) pour améliorer la capacité de recentrage, minimisant ainsi le déplacement résiduel dans les murs après les mouvements sismiques du sol.

Le déplacement permanent dans les murs de cisaillement a été mesuré en utilisant le rapport de déformation résiduelle inter-étages (RDRI). Une analyse non linéaire temporelle (ANLT) utilisant le logiciel RUAUMOKO 2D a été utilisée pour évaluer le RDRI dans ces murs. Pour répondre aux exigences en matière de risque sismique spécifiées par le CNRC 2020, 15 mouvements du sol ont été sélectionnés pour Vancouver et 11 pour Montréal, ensuite mis à l'échelle au niveau de risque sismique requis (2% par 50 ans). Dans chaque mur de cisaillement, le point de référence pour le déplacement résiduel a été établi en sélectionnant la valeur

maximale moyenne de RDRI. Dans la phase suivante, trois stratégies de renforcement différentes utilisant des composites en PRFCS ont été mises en œuvre dans les murs de cisaillement, et leurs valeurs RDRI résultantes ont été comparées aux valeurs de contrôle.

Pour créer des prototypes conformes aux spécifications du CNRC 2020 et du CSA A23.3-19, dans un premier temps, quatre modèles de MCC ont été conçus à Montréal et à Vancouver, variant de 15 à 20 étages, ont été renforcées à l'aide de bandes PRFCS verticales et horizontales pour augmenter leur résistance en flexion et en cisaillement. Les poutres de couplage ont été renforcées avec des enveloppes et des bandes PRF supplémentaires pour augmenter leur confinement et leur résistance en flexion, respectivement. Dans la prochaine étape, quatre MCI ont été conçus et évalués avec la même hauteur et la même zone. Les murs ont été renforcés avec trois configurations différentes de feuilles PRFCS verticales associées à des enveloppes en PRF augmentant leur résistance au cisaillement.

L'étude a montré que toutes les stratégies proposées ont réussi à réduire efficacement le déplacement résiduel dans les murs de cisaillement. Notamment, l'utilisation de trois couches de PRFCS sur les extrémités des murs et l'enveloppement des zones de rotules plastiques ont eu un impact significatif sur l'amélioration de la performance des murs. De plus, l'enveloppement des poutres de couplage et l'augmentation de leur résistance en flexion dans les murs couplés ont réduit efficacement le déplacement résiduel. De plus, les résultats ont mis en évidence que l'intégration de PRFCS dans les MCC était plus efficace que dans les MCI. De plus, il a été observé que, à mesure que la hauteur du mur augmentait, l'efficacité de la méthode proposée pour réduire le déplacement diminuait. Fait intéressant, les MCI à Montréal ont montré une performance presque élastique et n'ont pas nécessité de renforcement. En revanche, les murs de cisaillement affectés par les importants tremblements de terre de Cascadia ont présenté les déplacements résiduels les plus élevés post-séisme.

Mots-clés: Déplacement résiduel, mur de cisaillement couplé, mur de cisaillement simple, composite PRF, lié extérieurement, performance sismique, analyse non linéaire temporelle

Enhancing resilience and self-centering of reinforced concrete single and coupled Shear walls with externally bonded fibre reinforced polymer composites

Ali ABBASZADEH

ABSTRACT

Single shear walls (SSWs) and coupled shear walls (CSWs) are crucial elements in seismic engineering for improving a structure's ability to withstand seismic activity. These structures are carefully designed to withstand the lateral forces of earthquakes while maintaining ductility and providing sufficient stiffness to transmit these forces to the foundation. Moreover, they can dissipate seismic energy by forming plastic hinges under cyclic ground motion loads. Designing effective shear walls requires meticulous attention to detail. A crucial design principle for taller shear walls is ensuring that flexural failure prevails over shear failure. In the design of CSWs, careful attention is given to coupling beams (CBs), which are essential conduits for transferring shear forces between the walls. These beams are engineered to avoid premature shear failure and thereby maintain their integrity and functionality. At the same time, they are strategically designed to accommodate plastic hinge formation at their ends, embodying the concept of a weak beam-strong column.

Although the creation of plastic hinges in shear walls can absorb a significant amount of seismic energy, it can also result in residual displacement in these pivotal components. The lingering effects of these displacements can pose challenges to the structural integrity of buildings after an earthquake. Therefore, to enhance building serviceability and minimize costs related to earthquake damage, it is essential to develop an effective strategy that reduces residual displacements in existing shear walls. This thesis proposes an effective strengthening configuration for shear walls located in Vancouver and Montreal, which represent Canada's western and eastern seismic zones, respectively. The suggested approach is based on the use of Externally Bonded Fiber Reinforced Polymers (EB-FRP) to enhance self-centering capability, therefore minimizing residual displacement in the walls after seismic ground motions.

The permanent displacement within shear walls was gauged by using the Residual Inter-story Drift Ratio (RIDR). Nonlinear Time History Analysis (NLTHA) utilizing RUAUMOKO 2D software was employed to assess RIDR within these walls. To comply with the seismic hazard requirements specified by NBCC 2020, 15 ground motions were selected for Vancouver and 11 for Montreal and then scaled to the required seismic hazard level (2% per 50 years). In each shear wall, the benchmark for residual displacement was established by selecting the average maximum RIDR value. In the following phase, three different strengthening strategies utilizing EB-FRP composites were implemented in the shear walls, and their resulting RIDR values were compared to the control values.
To create prototypes that adhered to the specifications outlined in (NBCC 2020) and (CSA A23.3-19), in the first step, four CSW models of 15 and 20 stories were crafted in Montreal

and Vancouver. The wall piers were strengthened using vertical and horizontal EB-FRP strips to increase their flexural and shear strength. Coupling beams were reinforced with additional FRP wraps and strips to increase their confinement and flexural strength, respectively. In the next step, four SSWs were designed and evaluated with the same height and location. The walls flexural capacity were strengthened with three different configurations of vertical EB-FRP sheets coupled with FRP wraps increasing their shear strength.

The study found that all proposed strategies successfully reduced the residual displacement within the shear walls. Notably, using three layers of EB-FRP on the edge of the walls and wrapping the plastic hinge zones had the most significant impact on improving wall performance. Additionally, wrapping coupling beams and increasing their bending resistance in coupled walls effectively reduced residual displacement. Moreover, the results highlighted that integrating EB-FRP in CSWs was more effective than in SSWs. Additionally, it was observed that as the height of the wall increased, the proposed method's efficacy in reducing displacement decreased. Interestingly, the SSWs in Montreal showed near-elastic performance and did not require retrofitting. Conversely, the shear walls affected by the significant Cascadia earthquakes had the highest residual post-earthquake displacements.

Keywords: Residual displacement, Coupled shear wall, Single shear walls, FRP composite, externally bonded, seismic performance, non-linear time history analysis

TABLE OF CONTENTS

Page

LIST OF TABLES

LIST OF FIGURES

LIST OF ABBREVIATIONS

ACI	American Concrete Institute
ASCE	American Society of Civil Engineers
CB	Coupling Beam
CFRP	Carbon Fiber Reinforced Polymer
CSA	Canadian Standard Association
CSW	Coupled Shear Walls
DC	Degree of Coupling
EB-FRP	Externally Bonded Fiber Reinforced Polymer
FEA	Finite Element Analysis
IDR	Inter-Story Drift Ratio
NBCC	National Building Code of Canada
NLTHA	Nonlinear Time History Analysis
PGA	Peak Ground Acceleration
RC	Reinforced Concrete
RIDR	Residual Inter-Story Drift Ratio
SFRS	Seismic Force Resisting System
SMA	Shape Memory Alloy
SSW	Single Shear Wall

LIST OF SYMBOLS

AI	Axial rigidity
A_{sd}	Area of steel bars in one diagonal group
A_v	Area of the steel stirrups
d	Beam depth
DL	Dead load
DSL	Design snow load
d_v	Effective shear depth of the beam
E_{FRP}	Modulus of elasticity of the FRP sheets
EI	Flexural rigidity
E_s	modulus of elasticity of the steel reinforcing bars
f_c'	Compressive strength of concrete
f_y	Yield strength of steel reinforcements
h	Story height
h_w	Height of the wall
I	Importance factor
I_e	Effective moment of inertia
$K\alpha$	A measure of the relative stiffness of the coupling beams and walls
l_{cg}	Horizontal distance between the centroids of walls in CSWs
l_b	Beam length
LL	Live load
l_u	Clear span of coupling beam

l_w	Wall depth
M	External moment applied to the structure
M_1	Moment resisted by wall 1
M_2	Moment resisted by wall 2
M_v	Factor to account for the effect of higher modes
N	Axial force
P	Axial force resulting from coupling action
R_d	Ductility-related factor
R_o	Overstrength-related factor
$S(T_a)$	Design-spectral-response acceleration at the fundamental period
SL	Snow load
T_a	Fundamental period of vibration
t_{FRP}	Thickness of FRP sheets
V	Shear Strength
V_c	Shear resistance of concrete
V_{FRP}	Shear resistance FRP composites
V_n	Nominal shear strength
V_p	Peak shear force
V_s	Shear resistance of transverse steel reinforcement
V_y	Yield shear force
W	Weight of the building
w_{FRP}	Width of the FRP strip

Δ_p	Displacement at peak load
Δ_u	Ultimate displacement
Δ_y	Yield displacement
ε_{FRPe}	Effective strain of the FRP sheets
ε_s	Steel strain
θ_u	Ultimate rotation angle
θ_y	Yield rotation
μ_d	Displacement ductility
φ_c	Resistance factor for concrete
φ_{FRP}	Resistance factor for FRP
φ_s	Resistance factor for steel

INTRODUCTION

0.1 General

In rapidly urbanizing areas, particularly those susceptible to seismic activities, the need for robust structural integrity in buildings cannot be overstated. As urban landscapes evolve, with high-rises becoming increasingly prevalent, ensuring the stability and safety of these structures through advanced building technologies is paramount. Shear walls, especially pivotal in reinforced concrete (RC) constructions, are instrumental in this endeavor. These walls are strategically integrated into the architectural design to improve the building's ability to withstand lateral loads and stress, enhancing its overall structural response.

Single Shear Walls (SSWs) and Coupled Shear Walls (CSWs) play essential roles in these systems. SSWs act as rigid vertical panels that significantly mitigate building sway and enhance stiffness. In contrast, CSWs, which consist of two RC walls linked by beams, provide increased flexibility and superior energy dissipation during seismic events. This unique configuration allows CSWs to effectively distribute seismic forces across the structure, significantly reducing the risk of failure and ensuring a more balanced load distribution during earthquakes. During seismic events, both SSWs and CSWs are subjected to intense flexural deformation, leading to residual displacements a permanent deformation that remains once the shaking subsides. This phenomenon is critical as it can severely compromise the functionality and safety of the building.

The challenge of managing the seismic impacts brings Fiber-Reinforced Polymer (FRP) composites to the forefront of seismic retrofitting solutions. With their exceptional strength-to-weight ratios and resistance to environmental degradation, FRP composites, particularly when applied as Externally Bonded FRP (EB-FRP), significantly enhance the structural resilience of RC structures. Reinforcing structures with EB-FRP improves ductility, shear, and flexural strength, making them better absorb and dissipate energy during seismic activity. This

approach not only strengthens buildings but also promotes sustainability by reducing the need for new materials and decreasing environmental impact, extending their resilience and life.

The primary impetus for the current study is to numerically evaluate the efficiency of EB-FRP composites in reducing residual displacement in shear walls.

0.2 Problem Statement

One of the primary concerns with shear walls during seismic events is the residual displacement. Such damage can necessitate costly repairs or even lead to the structure's condemnation. In SSWs, residual displacement typically manifests as cracking and inelastic bending. CSWs face additional complexities due to the dynamic interaction between the coupling beams and the wall piers, which may lead to enhanced stresses at these connections.

In Canada, seismic characteristics vary significantly between regions, affecting the response of medium to high-rise structures to earthquakes. Vancouver, located in the western seismic zone, experiences earthquakes with lower frequencies that primarily affect the first vibration mode of buildings. This condition increases the flexural demands on the base of structures. On the other hand, Montreal located in eastern Canada witnesses earthquakes characterized by higher frequencies that significantly affect higher vibration modes. This scenario leads to an increase in stresses in the higher levels of buildings, potentially causing more localized structural damage.

Addressing the challenges of seismic retrofitting in shear walls requires a comprehensive understanding of both the structural vulnerabilities and the advanced materials available for mitigation. FRP composites present significant advantages for the seismic retrofitting of RC structures. By wrapping structural members with EB-FRP, their structural ductility and load-bearing capacity can be increased. Additionally, the application of FRP can be specifically tailored to address vulnerabilities at critical points, such as joints and connections where shear

forces are most concentrated during an earthquake. This targeted strengthening approach is both efficient and cost-effective.

However, the full potential of these composites and the optimal configurations for their application in various seismic scenarios and building types have yet to be thoroughly explored and understood. Thus, this research aims to understand how EB-FRP composites can be optimally utilized to retrofit existing RC buildings with SSWs and CSWs, enhancing their seismic resilience. This involves determining the most effective configurations of EB-FRP applications to minimize residual displacements and improve the overall seismic performance of the walls. The goal is to develop validated retrofitting strategies that are not only cost-effective but also minimally invasive and adaptable to different existing building architectures and seismic intensities.

0.3 Research Objectives

The main objective of this research is to explore the use of EB-FRP to improve the self-centering capacity of the RC bracing systems and hence reduce the residual displacement they experience. Additionally, finding the optimized configuration of EB-FRP that can contribute the most to decreasing residual displacement is a crucial aim of this study, ensuring that the applications are not only practical but also tailored to maximize seismic resilience and structural integrity.

Specific objectives are as follows:

1- To evaluate the changes in the following parameters after the use of EB-FRP in SSWs and in CSWs using nonlinear time history analyses: (i) Residual displacement; (ii) Inter-story drift ratio; (iii) Rotation of coupling beams; (iv) Shear force demand; (v) Bending moment demand; (vi) Effect of earthquake frequency content on residual displacement; (vii) Structural stiffness.

2- To optimize the EB-FRP properties and configuration for SSWs to achieve the lowest residual displacement.

3- To optimize the EB-FRP properties and configuration for CSWs to achieve the lowest residual displacement.

0.4 Methodology

This study was structured around a comprehensive analysis of eight shear wall configurations; four SSWs and four CSWs, each modeled with either 15 or 20 stories. These configurations represented medium to high-rise shear walls found in Montreal and Vancouver, serving as representatives for the Eastern and Western seismic zones in Canada, respectively. The research utilized numerical modeling and simulations to evaluate the effectiveness of EB-FRP composites on these walls under various earthquake scenarios.

For the analysis, a total of fifteen earthquake ground motions for Vancouver and eleven for Montreal were selected to simulate the seismic impact, ensuring a robust evaluation across different seismic scenarios. Each set of ground motions was carefully chosen and scaled to match the design spectrum requirements as outlined in the NBCC 2020 for the respective locations. The series of simulated ground motion histories generated by Atkinson (2009) were utilized.

The shear walls were designed and detailed using the force-based design provisions stipulated in the NBCC 2020 and CSA A23.3-19. RUAUMOKO 2D, a finite element-based program, was employed to perform the nonlinear time history analysis of the shear walls. XTRACT was utilized to model the nonlinear behavior of materials, including detailed representations of material nonlinearity for concrete, FRP composites, and steel, reflecting their actual stress-strain behaviors under seismic loading.

Various configurations of EB-FRP were applied and analyzed across the different shear wall models. Parameters such as FRP location, layering, and configuration were systematically varied to optimize the retrofitting effectiveness.

The residual inter-story drift ratio (RIDR) was established as the primary metric for evaluating residual displacement in the walls. Three strengthening configurations for CSWs and an equal number for SSWs were considered and assessed. The nonlinear analysis compared the results of both unstrengthened and strengthened walls in terms of RIDR, inter-story drift, rotation of coupling beams, shear demand, and bending demand. The reduction in RIDR for each configuration was compared against the original unstrengthened wall's performance, and the most effective configuration was selected based on these comparisons. The most influential ground motion scenario in each city was evaluated based on the severity of the RIDR.

0.5 Research significance

Canada is prone to seismic activity and strong winds, which push structural elements into a non-linear state, leading to residual displacements that may necessitate costly replacements. Therefore, it is crucial to develop effective strategies to mitigate potential hazards and structural damage caused by these natural forces.

Previous investigations into the application of EB-FRP composites have primarily focused on rehabilitating damaged structures or strengthening structures designed according to outdated standards. Furthermore, most studies aimed at increasing structures' self-centering ability have been conducted during the design phase and are not applicable to existing shear walls.

This study specifically focuses on applying EB-FRP composites to enhance self-centering and resilience of existing CSWs and SSWs. The anticipated results will lead to the development of EB-FRP strengthening guidelines and models that promote self-centering, thereby reducing residual displacements. This is especially critical for densely populated cities like Montreal and Vancouver, which are frequently exposed to seismic activities. These advancements will not only prevent the costly replacement and reconstruction of buildings after significant events but also enhance environmental sustainability. By reducing the need to deconstruct and replace concrete elements, this method also decreases CO2 emissions associated with cement production, a significant contributor to global warming.

0.6 Outline of the thesis

This research study is presented across five chapters, beginning with the Introduction and followed by four detailed chapters (Chapters 1-4).

Chapter 1 provides a comprehensive literature review on SSWs and CSWs including their deficiencies, strengthening methods, and self-centering techniques.

Chapter 2 proposes the first published paper in this Ph.D program, titled "Enhancing resilience and self-centering of existing RC coupled and single shear walls using EB-FRP: State-of-the-art review and research needs".

Chapter 3 is devoted to the second published article in this study, based on the results of the numerical evaluation of the proposed method on CSWs. This paper is titled "Resilience of Medium-to-High-Rise Ductile Coupled Shear Walls Located in Canadian Seismic Zones and Strengthened with Externally Bonded Fiber-Reinforced Polymer Composite: Nonlinear Time History Assessment".

Chapter 4 presents the third published paper evaluating the strengthening of SSWs based on numerical results. The paper is titled "The use of externally bonded FRP composites to enhance the seismic resilience of single shear walls: A nonlinear time history assessment."

The final chapter, chapter 5, is focused on providing a concise summary of the research, along with conclusions that encapsulate the findings. Additionally, recommendations for future researchers needs are also provided.

CHAPTER 1

LITERATURE REVIEW

1.1 Shear walls in reinforced concrete buildings

When constructing medium to high-rise reinforced concrete (RC) buildings, it's crucial to ensure that the building can withstand lateral forces such as winds and earthquakes. Shear walls, both single shear walls (SSWs) and coupled shear walls (CSWs), are essential in enhancing the building's resilience to these forces. These components play a significant role in reducing structural damage during such events and limiting the movement and drift within the building framework, thereby minimizing non-structural damage. Choosing between a single shear wall and a coupled shear wall configuration typically depends on the specific architectural needs, expected load conditions, and overall design objectives of the building.

1.1.1 Coupled shear walls

Coupled shear walls (CSWs) have proven to be highly effective in resisting lateral and seismic forces in medium to high-rise buildings. They are designed with two parallel walls connected by coupling beams (CBs), which make them robust and ideal for absorbing energy while providing high lateral stiffness and strength.

The walls connected by CBs are effective due to the moment-resisting mechanism they create. If the joints between the walls and CBs are rigid, the entire length of the walls works together to resist bending moments, which are distributed linearly across the structure. This configuration generates significant tensile and compressive forces in the walls, resulting in a push-pull mechanism that can resist moments. By creating this moment-resisting mechanism and utilizing rigid joints, the walls and CBs interact synergetically to create a strong and effective structure.

CSA A23.3-19 has graded CSWs based on the performance of CBs. They have defined a measure for coupling, known as the Degree of Coupling (DC), with a threshold set at 66%. Walls with a DC lower than this threshold are categorized as partially coupled, while walls with a higher DC are considered coupled walls. DC measures how well the walls interact through the coupling beams to resist overturning forces. A higher degree of coupling indicates that the walls are working together efficiently, sharing the load and reducing the stress on individual walls. According to the CSA A23.3-19, DC is represented as follows:

$$DC = \frac{Pl_{cg}}{M_1 + M_2 + Pl_{cg}} \tag{1.1}$$

Where P is axial push-pull force happening from the coupling action, l_{cg} represents the distance between two walls centroids, $M_1 \, and \, M_2$ are the bending moments at walls foundation. The greater the shear resistance and stiffness of the CBs, the more axial force is generated in the wall piers, leading to higher DC (Chaallal et al., 1996). The CSA A23.3-19 has established guidelines for shear reinforcement in the CBs. Rectangular stirrups can be used as the primary shear resistance elements for beams experiencing factored shear forces below a specified threshold, $0.1(l_u/d)\sqrt{f_c'}$, in which l_u represents beam length, d is the effective depth, and f_c' is concrete compressive strength. These beams are known as conventionally reinforced beams in the literature. However, diagonal shear reinforcement should be implemented for beams subjected to shear forces exceeding this threshold to reduce the risk of brittle shear failure. Providing diagonal rebar near the beam ends improves the hysteretic behavior by preventing sliding shear and by extending the hinging zones away from the wall surface (Paulay, 1974).

Numerous studies have evaluated the shear resistance in CBs during cyclic loading. An experimental evaluation by (Paulay, 1969) on RC beams involved subjecting nearly full-sized deep CBs to static and cyclic loading. Eight CBs, with length-to-height ratios of 1.29 and 1.02, were analyzed. Conventional CBs didn't perform well under seismic pressure. A prominent diagonal crack would appear when they failed, splitting the beam into two triangular portions.

He noted that to avoid diagonal tension failure, excessive stirrup reinforcement must be provided, with stirrups remaining elastic while the flexural reinforcement yields. It was also demonstrated that diagonal cracking significantly reduced CB stiffness to less than 20% of its original value.

In an experimental study on seven-story CSWs by (Santhakumar, 1974), the influence of cracking and variations in CBs stiffness using quasi-static loading on CSWs performance was evaluated. The walls were designed using both conventionally and diagonally reinforced CBs. The study's results indicated that CBs with diagonal reinforcement outperformed conventional reinforcement in several vital aspects. Specifically, the diagonally reinforced CBs exhibited superior stiffness, greater ductility, and enhanced energy dissipation capabilities. Furthermore, the CSWs incorporating these diagonally reinforced CBs demonstrated a significantly higher drift capacity, indicating a greater ability to withstand lateral displacements than CSWs with conventional reinforcement. These findings underscore the advantages of using diagonal reinforcement in CBs to improve the overall performance and resilience of RC CSW structures.

(Tassios et al., 1996) examined how RC CBs behave under cyclic loading, focusing on their performance and ductility. They tested ten scaled-down models with various reinforcement designs and shear ratios of 0.50 and 0.83. The study found that CBs with diagonal reinforcement showed superior performance in rigidity, flexibility, and energy absorption compared to those with traditional reinforcement. It also highlighted the necessity of sufficient stirrup reinforcement to avoid diagonal tension failure and reduce the likelihood of brittle shear failure. Furthermore, the research indicated that the stiffness of the CBs decreased significantly after diagonal cracking, falling to less than 20% of their original stiffness. These findings offered valuable insights into optimizing reinforcement designs to improve the overall performance and resilience of RC CBs in seismic environments, thus contributing to the development of more earthquake-resistant structures.

(Kwan & Zhao, 2002) investigated the cyclic behavior of deep RC CBs with span-to-depth ratios under 2.0. Six half-scale models were tested under reversed cyclic loads using a method

that accurately simulates coupling beam boundary conditions in shear wall structures. Five specimens were conventionally reinforced, and one was diagonally reinforced. The study found that deep conventionally reinforced CBs are more prone to shear failure, especially when additional longitudinal reinforcement increases bending strength and shear demand. However, these beams achieved notable drift ratios of 3.6% to 5.7%. Diagonally reinforced CBs showed improved energy dissipation but did not enhance deformability. The research highlights the importance of adequate stirrup reinforcement to prevent shear-tension failure and maintain ductility in seismic conditions.

(Lehman et al., 2013) conducted an experimental study on the seismic behavior of modern CSWs in mid- to high-rise buildings. Large-scale tests simulated conditions for a midrise building's lower three stories. The coupled wall system showed a complex seismic response, with coupling beams designed to yield under double curvature, transferring shear demands to the wall piers. Damage included CBs yielding, wall pier spalling, and failure at 2.27% drift due to concrete core crushing and longitudinal bar buckling, leading to significant loss of load-carrying capacity. The findings highlight the need for improved design models focusing on reinforcement detailing to enhance seismic performance.

(Ding et al., 2018) developed a mixed beam-shell model for the seismic analysis of RC CSWs. The model combines fiber beam-column elements for boundary elements, layered shell elements for wall piers, and specialized fiber beam-column elements for CBs, addressing various deformation and failure modes. Validation with eight test specimens showed the model's accuracy in predicting structural responses such as beam deformation, base shear, moment distribution, and axial forces in wall piers. Parametric analyses further examined the effects of different degrees of coupling and reinforcement layouts on seismic behavior. The study found that accurately modeling the complex behavior of CBs is crucial for the overall performance of coupled wall systems. This research offered significant insights for improving analytical models and enhancing the seismic design of high-rise buildings.

(Li et al., 2023) assessed a new resilient CSW system with replaceable components in seven, eleven, and fifteen-story buildings. They evaluated seismic fragility and collapse safety using incremental dynamic analysis. The system's design, featuring replaceable dampers in CBs and replaceable corner components in wall piers, aims to localize damage to these parts, enhancing structural resilience. Validated finite element models showed that buildings with the new system had significantly lower collapse probabilities and better seismic performance, with reduced inter-story drift ratios and increased energy dissipation at higher intensities compared to traditional systems. The study highlighted the advantages of replaceable components in improving seismic resilience, reducing damage to primary structural elements, and enabling quick post-earthquake recovery.

(Jafari et al., 2024) analyzed the cyclic behavior and damage patterns of coupled and hybrid-coupled shear walls in high-rise structures. By utilizing numerical models, they examined the impact of varying coupling ratios (CR) and axial stress ratios (ASR) on seismic performance through sixty different scenarios, with CR ranging from 0.2 to 0.5 and ASR from 0.027 to 0.25. The study found that higher coupling ratios led to increased damage along the edges of the shear walls but also improved lateral capacity, stiffness, and energy dissipation, while reducing ultimate drift. RC coupling beams exhibited significant damage but interacted more effectively with the walls, whereas steel beams showed less shear deformation and sustained coupling action for longer durations. Increased ASRs were associated with decreased ductility and lower response modification factors.

1.1.2 Single shear walls

Single shear walls (SSWs) are important structural components commonly utilized in buildings to withstand lateral forces. These walls offer essential rigidity and strength, significantly contributing to the overall stability and integrity of structures. SSWs help prevent excessive deflections and potential structural failures by effectively distributing lateral loads to the foundation. Their simplicity in design and construction makes them a cost-effective solution, suitable for a wide range of architectural layouts. As a crucial component in modern

engineering, SSWs play a vital role in ensuring the safety and resilience of buildings. A literature review on the seismic evaluation of SSWs is provided here.

(Wallace, 1994) introduces a new methodology for the seismic design of SSWs to address the limitations of conservative U.S. code requirements. The study aims to develop a displacement-based approach that links expected building displacements to the required reinforcement details for various SSW cross sections, including rectangular, T-shaped, and barbell-shaped walls. The methodology involves an analytical framework that calculates the necessary transverse reinforcement at the boundaries of SSWs based on building displacement demands. It considers factors like wall cross-sectional area, wall aspect ratio, axial load, and reinforcement ratios to determine strain distributions and required confinement reinforcement. The study concludes that this displacement-based approach offers greater design flexibility and reduces the over-conservatism of current codes, leading to more accurate and resilient designs for buildings with SSWs.

(Hidalgo et al., 2002) created an analytical model to predict the inelastic seismic behavior of SSWs, addressing both flexural and shear failure modes. The aim was to develop a model that accurately estimates the ultimate lateral strength and inelastic deformation demands of SSW buildings during severe earthquakes, thereby improving performance-based design and existing code procedures. The researchers enhanced the larz computer program by adding a shear failure mode model based on experimental data. They used hysteresis models for flexural and shear behaviors, with parameters defined from cyclic tests of shear walls and beams. The study found that the model effectively predicts the inelastic seismic response of SSW, despite operating in two dimensions and not accounting for torsional effects. The model's predictions for lateral strength and deformation closely matched observed behaviors in tested buildings.

(Koduru & Haukaas, 2010) assessed the seismic loss risk of a high-rise building in Vancouver, Canada, using probabilistic models. They developed a seismic loss curve considering various ground motion sources, structural damage, and associated losses, employing a unified reliability analysis to handle uncertainties specific to Vancouver.

Their inelastic dynamic analysis of a finite-element model, featuring RC SSWs, examined crustal, subcrustal, and subduction earthquakes from the Cascadia subduction zone. Monte Carlo simulations with 1,000 samples evaluated seismic fragility and expected losses for each earthquake type. Subduction earthquakes posed the highest monetary loss potential despite low occurrence probability, while crustal and subcrustal earthquakes had higher probabilities but resulted in lower losses. The study concluded that distinct earthquake characteristics are crucial for seismic risk assessments.

(Belletti et al., 2013) investigated the seismic performance of multi-story precast RC buildings with SSWs, focusing on the effectiveness of different modeling approaches for pushover analysis. The purpose of the study was to evaluate and compare the accuracy and applicability of various modeling methods for buildings featuring SSWs with non-rectangular cross-sections, such as U-, L-, and C-shaped walls. The methodology involved analyzing a six-story precast RC building using three different modeling approaches: a shell model (PARC), a distributed plasticity model (fiber element), and a lumped plasticity model (LPA). These models were used to simulate the nonlinear behavior of the structure under seismic loads, with particular attention to the construction details of structural joints connecting the precast SSWs. The findings showed that all three models consistently yielded similar results in terms of earthquake response and failure patterns. The research also emphasizes the significance of thorough modeling of SSWs in precisely evaluating buildings' seismic resilience.

(Liang & Su, 2023) conducted a study combining experimental and theoretical approaches to examine the seismic performance of non-seismically designed SSWs with moderate shear span-to-length ratios (SLR). The research aimed to assess the behavior of these walls under high axial loads, a concern for areas with outdated building standards. The study involved testing four RC shear wall specimens with varying shear-to-flexure strength ratios, SLRs, and axial load ratios (ALRs) under cyclic loading. Digital Image Correlation (DIC) technology was used to evaluate crack patterns and deformation components. Additionally, a new theoretical model that includes stiffness degradation and flexural-shear interaction was developed and validated against experimental data. The findings indicated that non-seismically designed

SSWs with moderate SLRs experience significant shear deformation and stiffness degradation under high axial loads. The proposed model successfully predicted the force-deformation behavior of these walls.

1.1.3 Enhancing resilience and self-centering in shear walls

Seismic resilience is the capability of a structure to endure and recover from the impacts of an earthquake. It includes the ability to absorb and dissipate seismic energy and maintain operational functionality both during and after the event. A resilient structure is designed to minimize damage, shorten downtime, and enable quick repairs, thus ensuring safety and operational continuity. Resilient shear walls are designed to be ductile, allowing them to undergo considerable deformations without losing their load-bearing capacity, which helps prevent sudden and catastrophic failures. Designing shear walls to achieve these resilience goals protects lives and property, thereby mitigating the long-term economic and social effects of seismic events.

Self-centering methods improve the seismic resilience of structures by allowing them to revert to their original position following an earthquake. Unlike conventional systems that may incur significant residual displacements necessitating extensive repairs, self-centering systems aim to minimize or eliminate these permanent deformations. Self-centering systems are divided into two main categories. The first category includes rocking motion techniques: controlled rocking and uncontrolled rocking. Controlled rocking employs post-tensioned (PT) tendons to manage the motion during seismic events. These tendons undergo controlled compression and decompression at specific joints during earthquakes, limiting lateral movement and enabling the building to rock in a controlled manner. This controlled rocking motion enhances the structure's capacity to effectively absorb and dissipate seismic energy. Prior research has explored the potential benefits of incorporating PT elements to enhance the self-centering capabilities of structures (Bedriñana et al., 2022; Marriott et al., 2009). Uncontrolled rocking method relies on the innate self-weight of the structure to induce uncontrolled rocking

movements during seismic events, aiding in energy absorption and dissipation (Chancellor et al., 2014; Zhong & Christopoulos, 2022a).

The second category involves the use of specialized mechanical devices. These devices often integrate Shape Memory Alloys (SMAs) and energy dissipators, which work together to absorb and dissipate seismic energy effectively. By using these methods, structures can return to their original positions after seismic events, minimizing residual deformations and enhancing overall seismic resilience. SMAs lies at the very heart of this ingenious approach. These remarkable materials possess the unique ability to revert to a predefined shape after deformation. Responding to external influences, such as axial deformations, SMAs exhibit memory-like behavior, recovering their original configuration. Integrating SMAs into the structural design significantly enhances adaptability and resilience against seismic events(Qian et al., 2023; Yang et al., 2010). In certain applications, SMAs have been proven to reduce strain by 10% (Lecce, 2014). By harmonizing the energy-absorbing capabilities of dissipators and the shape memory properties of SMAs, this method embodies a comprehensive approach to seismic enhancement. This meticulous integration empowers the structure to adeptly manage seismic energy, minimize deformation, and swiftly return to its original state. Although SMA wires have the potential to be advantageous, they do have some drawbacks, including a lower load-bearing capacity and challenges with securing them properly due to their slick surfaces. Consequently, devices based on SMA are mainly intended for situations involving uniaxial tensile-loading, which restricts their extensive usage (Wang et al., 2020).

(Yang et al., 2017) examined the seismic performance of CSWs enhanced with engineered cementitious composite (ECC) in critical cast-in-place regions. The study aimed to evaluate the effectiveness of using ECC to improve the seismic resilience of CSWs, particularly in the beam-to-wall joints and upper regions of composite coupling beams. The methodology involved testing two half-scale precast CSWs specimens under reversed cyclic loading. One specimen used traditional reinforced concrete, while the other incorporated ECC in key regions. The research assessed various parameters, including failure characteristics, load-displacement hysteresis curves, stiffness degradation, ductility, and energy dissipation

capacity. The results indicated that substituting concrete with ECC in critical regions significantly enhanced the seismic performance of the CSWs. The ECC specimens demonstrated improved load capacity, damage tolerance, ductility, and energy absorption compared to traditional concrete specimens. The findings suggest that using ECC in the cast-in-place beam-to-wall joints and upper regions of composite coupling beams is an effective method to enhance the seismic resilience of the walls.

(Jiang et al., 2023) conducted a study to improve the seismic resilience of CSWs by introducing replaceable CBs and corner components, which are easier to repair after an earthquake. The methodology involved cyclic loading tests on four half-scale specimens: one conventional CSW and three new walls with replaceable components. The new design included a combined damper consisting of a metallic damper and viscoelastic (VE) dampers, installed in the CBs. Replaceable corner components were installed at the bottom of the wall piers to absorb energy during seismic events. The results showed that the new CSWs with replaceable components had superior seismic performance compared to conventional walls. The new walls exhibited higher lateral load-carrying capacity, greater ultimate displacement, and improved energy dissipation.

(Su et al., 2024) evaluated the seismic performance of self-centering hybrid rocking walls (SCRWs) with a curved interface to enhance earthquake resilience. The study addressed local damage issues at rocking wall corners. The methodology involved cyclic loading tests on two SCRW specimens and one monolithic RC shear wall. The SCRW specimens included a precast wall panel with a curved interface, PT tendons, energy dissipation rebars, and shear reinforcements, designed to enhance energy dissipation and maintain self-centering. The results demonstrated that SCRWs with curved interfaces outperformed traditional walls, preventing local crushing at corners and managing stress effectively. The prestressed tendons ensured minimal residual deformation and self-centering. SCRWs showed superior energy dissipation and resilience, concentrating deformations along the interface and minimizing wall damage.

1.2 Deficiencies of existing shear walls and failure modes

The seismic design provisions for SFRS have become considerably more stringent over the last decades. Many existing RC shear walls are designed and detailed using old seismic design provisions, presenting lateral seismic resistance deficiencies (Honarparast & Chaallal, 2021). On the other hand, (Aktan & Bertero, 1985) through numerical and experimental investigations, showed the necessity of making changes and evolution in the old design provisions. In addition, these existing RC structures have gone through decades of service life, including various loadings and solicitations, thereby affecting their lateral resistance. Moreover, many existing RC shear walls are primarily designed for wind loading (Paulay & Priestley, 1992). This demonstrates the keen interest among researchers in assessing the seismic behavior of existing RC structures in recent years. Many studies were performed focusing on the improvement of the shear strength and energy dissipation capacity of the shear walls (Khalil & Ghobarah, 2005; Layssi & Mitchell, 2012), while Some of them focused on flexural strength improvement (Shaheen et al., 2013).

The primary deficiencies related to SSWs and CSWs can be summarized as follows: (i) failure in coupling beams (CBs); (ii) short lap splices; (iii) low ductility; and other deficiencies such as deficient anchorage of the reinforcement and corrosion of reinforced concrete. Investigations clearly show that the presence of these deficiencies in existing SSWs and CSWs can lead to improper seismic performance. Sliding motion in the cracks at the CBs-wall joints, reduction in ductility of walls, diagonal cracks in the CBs, large deformation and residual displacement in shear walls and CBs are among expected improper behaviors (Honarparast & Chaallal, 2019b).

Performance of CBs is highly dependent on their ability to withstand cyclic shear forces, which is determined by their reinforcement detailing. Advantages of using diagonal reinforcement in CBs was proved through numerical and experimental studies (Paulay, 1969; Shiu et al., 1978). To provide flexural and shear resistance, the diagonal reinforcements should run throughout the CB and be embedded into the wall piers. Most modern seismic design guidelines adopted

this configuration detailing. More studies have been done to examine the seismic behavior of CBs with different arrangements of reinforcement (Harries, 1995b; Yun et al., 2008). Also, it is found that the coupling system's behavior is affected by two types of deformations: shear deformations due to small span/depth ratios of the beams and axial deformations due to the beams' sensitivity to relative movements in their built-in support. (Barbachyn et al., 2012; Fortney, 2005; Paulay, 1971; Paulay & Binney, 1974; K.-J. Zhou et al., 2021). In modern design codes, it is recommended to use CSWs with optimized CBs to achieve higher absorption capacity and strength against shear forces. Also, these walls show more resilience against earthquakes. The CBs are exposed to severe cyclic shear deformations when subjected to earthquakes. Hence, one of the most critical issues of CSWs is the brittle failure of the CBs. If this failure is avoided, a tremendous amount of the applied seismic energy will be dissipated by CBs distributed along these walls, thereby increasing the safety of the building. Zhao et al. (Zhao et al., 2004) evaluated a failure characteristic of deep reinforced CBs using the nonlinear finite element method; they showed that using more shear reinforcement in this kind of CBs, although it leads to more shear strength, could also bring on shear sliding and brittle failure

Adequate lap splice of reinforcement is necessary for force transmission in RC structures (see Figure 1.1). Short lap splice can lead to bond deterioration between steel and concrete, resulting in a major reduction of seismic energy dissipation and absorption capacity, brittle shear failure at critical zones, stiffness degradation, and deficiency in ductility (Harajli, 2006). Models of the bond behavior between reinforcing steel and concrete are used to study lap splice behavior. Chemical and mechanical mechanisms govern the bond between rebars and concrete. The mechanical mechanism is related to friction and interlocking between rebars and adjacent concrete, whereas the chemical mechanism is attributed to adhesion between concrete and rebars. Chemical and mechanical mechanisms cause stresses between rebars and concrete medium, and under external loading, the interfacial area between the rebars and concrete develops interfacial stresses. Debonding between rebars and concrete occurs when interfacial stresses exceed bond strength (Shaheen, 2014). Lap splices in the wall's plastic hinging zone can greatly reduce wall ductility during cyclic loads due to the deterioration of the bond between concrete medium and rebars (Aaleti et al., 2013). (Paterson & Mitchell, 2003)

Investigated the behavior of slender shear walls having lap splices within the plastic hinge zone or slightly above. The retrofitting methods include concrete collar addition, headed rebars, and FRP sheets. Due to their aspect ratio greater than two, all the specimens are governed by flexure. The results showed that retrofitting increase the ductility and shear strength and considerably avoid lap splice failure in the shear walls. Other research studies clearly showed the deficiencies in energy dissipation capability, shear, and flexural strength, and ductility of shear walls with inadequate lap splice and put forward the need to retrofit these deficient structural elements, especially in the plastic hinge region (Khalil & Ghobarah, 2005; Shaheen et al., 2013).

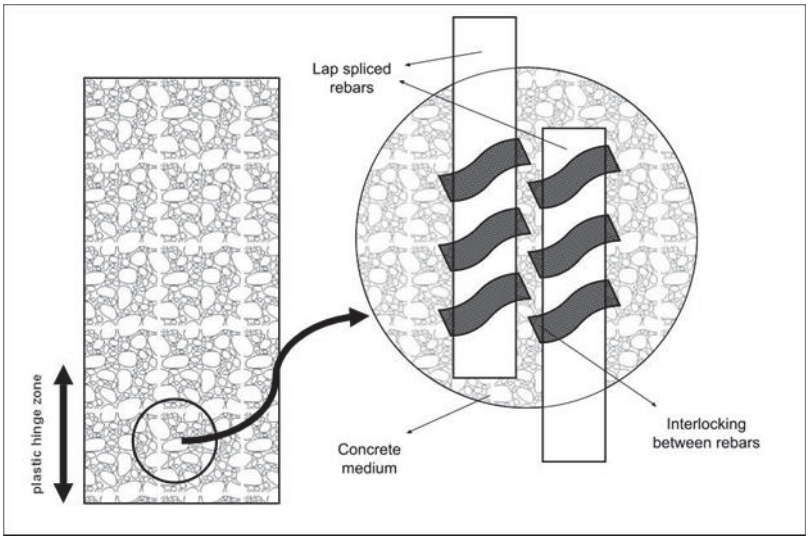

Figure 1.1 Lap splice of reinforcement in RC structures

1.2.1 Failure patterns in shear walls

Numerous studies were conducted to evaluate shear walls' behavior and failure modes in the early 70s and 80s (Cardenas & Magura, 1972; Paulay et al., 1982). (Paulay & Priestley, 1993) First discussed all common failure modes in shear walls. Some of the most common failure modes are as : (i) flexural failure; (ii) shear failure; (iii) rigid action failure.

Flexural failure has received much attention from researchers (O Tang & KL Su, 2014; Yang et al., 2022). Slender RC shear walls with a height-to-length ratio larger than two are typically governed by flexure. In contrast, squat shear walls are governed by shear (Hoult et al., 2018). In this pattern, the initial cracks develop in the tensile wall. As the load increases, more cracks form in the CBs and tensile wall joints. If the load further increases, the cracks propagate along the wall height. This process continues until the complete rupture of the CBs. Also, compressive stress in the bottom corner of the compressive wall could lead to considerable damage in this zone, which can finally lead to rupture (Honarparast, 2018; Subedi, 1991). (Christidis & Karagiannaki, 2021) evaluated the flexural and shear deformation in shear walls through numerical and experimental analysis.

Plastic hinge formation at the shear walls due to flexural yielding is necessary to ensure plastic deformation. Hence, to reach acceptable ductility level, it is vital to avoid shear failure before plastic hinge formation. In this failure pattern, the first cracks form in the CBs and tensile wall joints, but the critical damage in this type of failure is related to the diagonal cracks' development in the middle of CBs and their propagation as the load increases (Beyer et al., 2011). In the early 90s, Ghosh et al. (Ghosh & Markevicius, 1990) conducted extensive studies to improve the shear resistance of shear walls. Later, an analytical model was proposed to evaluate the shear strength of shear walls due to the effects of boundary elements, cyclic loading, and vertical loads (Hwang et al., 2001). (Miao et al., 2022) worked on the effects of the shear-span ratio on the failure mode of shear walls with similar geometrical dimensions. The results showed that the shear-span ratio in shear walls could significantly influence their failure mode, as the higher the shear-span ratio, the lower the shear capacity in walls; also, a considerable increase in this ratio can cause failure mode change from shear failure to the bending failure. More studies in shear failure can be found elsewhere (Hung & Hsieh, 2020; J. Liu et al., 2021; Ni et al., 2019; Park et al., 2015)

An increase in stiffness of CBs can lead to a single overall wall behavior and a rigid action failure. In this pattern, many cracks form in the tensile wall, while no cracks in CBs. Thus, the

failure mode of these rigid overall walls is similar to a simple cantilever beam (Honarparast, 2018; Subedi, 1991).

1.2.2 Ductility, Plastic hinge formation and confinement in shear walls

To investigate the behavior of reinforced concrete structures and especially shear walls, a thorough understanding of ductility, toughness, and resilience is necessary. Ductility refers to a material's ability to withstand a large displacement without failing. The toughness and resilience of material are how well it absorbs energy up to fracture and yield stress, respectively.

The necessity of providing ductility in structures was recognized after catastrophic earthquakes in the early 70s, and many studies were carried out to evaluate ductility in SSWs and CSWs (Allen et al., 1972; Paulay & Goodsir, 1985; Paulay & Santhakumar, 1976; Santhakumar, 1974). It was seen that many modern buildings which were designed according to the last design provisions had been greatly damaged. Therefore, some studies were carried out regarding ductility demand in structures which led to the evolution of design codes. The ductility of RC shear walls is essential to dissipate energy and avoid brittle failure and primarily depends on vertical and transverse reinforcement detailing (Paulay & Santhakumar, 1976). According to the CSA A23.3-19 for ductile and moderately ductile SSWs and CSWs, in which $h_w/\ell_w > 2.0$ and $R_d \geq 2.0$, flexural ductility due to yielding in vertical reinforcement should be considered within the plastic hinge zone. In addition, CSWs, considered as one of the most efficient alternatives in seismic force resisting systems (SFRS), should be protected against disorganized plastic hinge formation. This can be achieved by accurately designing and detailing their CBs. Indeed, CBs must be designed to have high energy dissipation capacity and be ductile to experience flexural yielding well ahead of shear failure and wall yielding. The ductility factor depends very much on deflection or rotation at yield and, therefore, can substantially vary if these yield values change. A study of two CSWs found that conventionally reinforced CBs, despite having a lower ductility factor, experienced greater displacement at failure. This means that large deflection at failure does not mean a higher ductility factor and

yielding deflection should also be evaluated. Since its high value can result in a significant reduction of the ductility factor, the ratio of the ultimate rotation or deflection to those at yield should be used as a quantitative criterion to express the ductility factor (Santhakumar, 1974).

(Tassios et al., 1996) introduced and evaluated other parameters such as displacement, stored energy, and cyclic displacement ductility factor as alternative. For a conventionally reinforced CB they assessed the displacement ductility factor (μ_d) which is equal to $0.85V_{max}$ of conventionally reinforced CB, and the results illustrated the inaccuracy of this parameter. On a second try, they evaluated the stored energy ductility factor (μ_E) which shows acceptable results from the specimen's function. To specify this operator, the zone surrounded by the prime half-cycle (A_{y1} at yield) which represents the cumulated yield energy (E_y) and the one surrounded by the curve of the 3rd cycle (A_{u3} at failure) corresponds to the cumulated ultimate energy (E_U) must be accounted. Since this parameter considers both resistance degradation and plastic deformation capacity, it can be used as a good criterion of specimens' performance. Finally, the cyclic displacement ductility factor ($\mu_{d,p}$) did not show a good capability compared to other parameters. (Kim et al., 2021) Investigated eight RC shear walls to explore the effects of boundary confinement on ductility. Results of the study shows that confinement hoops enhance the deformation ability in the shear walls. They also revealed that, the higher the strength, the greater the deformation ability in shear walls, because concrete failure occurs in compression block before vertical reinforcement yielding.

Modern design provisions require the designers that, through accurate detailing, allow plastic hinging formation in some targeted zones to reach the required ductility and energy dissipation level during a severe earthquake, thereby avoiding collapsing. Commonly, plasticity in SSWs and CSWs first appears at the base of the wall and develops to the top of the walls, and it occurs through cracking and crushing in concrete and yielding and buckling in reinforcement (Basereh, 2021). It should be mentioned that as specified by CSA A23.3-19 the lowest length of the plastic hinge zone must be extended $0.5\ell_w + 0.1h_w$ above the critical section where yielding initiates in the flexural reinforcement. Some studies have shown that the factor influencing most the minimum length of plastic hinge zone in RC shear walls is the dimensions

of the wall (Foroughi & Yüksel, 2019). In CSWs, to attain the ideal energy absorption performance and maintain wall stability, it is required that the plastic hinge formation occurs at the CBs prior to the base of wall piers. It is somehow similar to the weak beam-strong column concept. Hence, CBs feasibly absorb and dissipate energy without disturbing the overall function of the wall and let the wall piers assure gravity load resistance and allow large post-yield deformations before the collapse (Harries, 1995b).

Confinement is another pivotal feature in shear walls playing a key role in lateral load resistance and energy dissipation, which can be achieved through appropriate reinforcement detailing. Its substantial role would be well recognized when the inherent brittle nature of concrete is considered; hence, the ductility of reinforced concrete structures can be improved by proper concrete confinement. As for confinement in RC structures, numerous studies have been conducted in recent years (Ali & El-Salakawy, 2016; Hadhood et al., 2017; Zadeh & Nanni, 2013). Experimental and theoretical investigations carried out on shear walls have demonstrated that confinement of boundary elements through concentration of longitudinal reinforcement in boundary elements can considerably improve shear wall ductility, compressive strength, and energy dissipation capacity (Oesterle et al., 1979; Wallace & Moehle, 1992). Lack of confinement in boundary elements can lead to buckling failure at compression zones (Thomsen & Wallace, 1995). Vertical reinforcement should be tied to avoid flexural buckling failure. Transverse rebars play different roles in RC structures including: (i) shear resistance; (ii) longitudinal reinforcement consolidation; (iii) concrete confinement (Chen, 2005). According to CSA A23.3-19, shear walls within the compression zone must meet the confinement criteria of RC ductile columns.

(Escolano-Margarit et al., 2012) investigated the behavior of two large-scale shear walls: one with a confined region based on ACI-318-11 criteria and the other with no confinement reinforcement. The results showed that confinement reinforcement considerably enhanced the lateral displacement capacity of the shear walls. Further investigations revealed that the lack of confinement in single layer reinforced shear walls leads to concrete damage and a reduction in displacement capacity (Zhang, 2019; Zhang et al., 2018)

1.3 Strengthening of shear walls using EB-FRP

Neglecting the necessary measures, including appropriate retrofitting methods to prevent permanent and critical damage to the RC structures, can lead to damage development in existing buildings during severe seismic forces and will force building owners to replace damaged components and in some cases, the whole structure. This results in increased consumption of cement and subsequently emission of CO2 and irreparable damage to the environment.

The use of externally bonded fiber-reinforced polymer (EB-FRP) to strengthen existing shear walls has gained tremendous popularity worldwide due to its ease of implementation and high efficiency. FRP materials, such as carbon or glass fibers embedded in a polymer matrix, are externally bonded to the surface of shear walls, significantly enhancing their structural performance. This method improves the walls' lateral load-carrying capacity, stiffness, and energy dissipation, addressing issues like shear failure and flexural deficiencies. The application of FRP is minimally invasive, quick to install, and causes less disruption compared to traditional strengthening techniques, making it a preferred solution for retrofitting shear walls.

The specific influence of EB-FRP on mitigating residual displacement of shear walls has not been thoroughly investigated. However, numerous studies have validated the benefits of EB-FRP in improving the structural performance of shear walls under seismic loading, highlighting notable improvements in shear and flexural strength, ductility, and energy dissipation.

(Lombard et al., 2000) conducted a study to assess the efficacy of utilizing externally bonded carbon fiber tow sheets for seismic strengthening and rehabilitation of SSWs. The research aimed to develop and test a new method to enhance the seismic performance of SSWs, especially in older buildings that do not comply with current seismic standards. The methodology involved both experimental and analytical approaches. Four RC shear wall specimens were tested: a control wall, a repaired wall, and two walls strengthened with carbon

fiber sheets. These walls underwent in-plane quasi-static cyclic loading until failure. Additionally, an inelastic analysis model was created to predict the load-deflection behavior of both plain and retrofitted SSWs, considering factors such as wall dimensions, material properties, and reinforcement details. The study found that externally bonded carbon fiber sheets substantially improve the seismic performance of SSWs. The carbon fiber system was effective in restoring initial elastic stiffness, increasing yield load, and enhancing ultimate flexural capacity. The experimental results closely matched the analytical predictions, validating the proposed model. The carbon fiber retrofit method was found to be efficient and less disruptive than traditional techniques, making it a practical option for seismic strengthening and repair of RC shear walls.

(Ko & Sato, 2007) investigated the bond stress-slip relationship between FRP sheets and concrete under cyclic loading conditions. The purpose was to develop a model that accurately describes the bond behavior in FRP-strengthened structures subjected to cyclic loads, which is crucial for ensuring structural integrity during seismic events. The methodology involved testing 54 bond specimens using three types of FRP sheets (aramid, carbon, and polyacetal) with variations in the number of sheet layers and loading hysteresis. Cyclic bond tests were conducted to capture the bond stress-slip relationships, which were then used to develop a model based on the Popovics envelope. This model included seven empirical parameters: maximum bond stress, corresponding slip, curve characteristic constant, unloading stiffness, ultimate slip, friction stress, and negative friction stress. The study found that the developed bond stress-slip model closely matched the experimental results, effectively capturing the bond behavior under cyclic loading.

(Layssi et al., 2012b) examined the seismic behavior of inadequately detailed SSWs before and after retrofitting with EB-FRP composites. The study aimed to assess how effectively EB-FRP wraps could enhance the ductility and shear strength of these deficient walls, which were originally designed under outdated 1960s seismic codes. The research involved constructing and testing four full-scale shear wall specimens subjected to reversed cyclic loading. These walls, representing non-ductile RC construction, had inadequate lap splices and poor

confinement. The retrofitting process included applying a continuous EB-FRP jacket over the potential plastic hinge regions and EB-FRP strips outside these regions to boost shear strength. Findings revealed that the EB-FRP retrofit substantially enhanced the seismic performance of the shear walls. Retrofitted walls showed a 21% increase in flexural strength and achieved a displacement ductility target of 2.0. The EB-FRP wraps effectively postponed premature lap splice failures and increased cumulative energy dissipation by up to 16 times compared to unretrofitted walls. Additionally, the retrofit improved lap splice bond strength, enabling the flexural reinforcement to yield.

(Li et al., 2016) explored the seismic retrofitting of short CBs EB-FRP composites. The study aimed to improve the deformation and energy dissipation capacities of these beams, particularly those with low shear span-to-depth ratios that are prone to brittle shear failure under seismic loading. The methodology involved experimental testing of four large-scale RC CBs with identical geometries and reinforcement layouts but different retrofitting schemes. The researchers evaluated the effects of various EB-FRP arrangements and anchors on seismic performance metrics such as strength, stiffness, ductility, and energy dissipation capacity. The retrofitting schemes included the use of EB-FRP U-wraps and diagonal EB-FRP sheets, with the addition of EB-FRP anchors to delay delamination. The study concluded that EB-FRP composites significantly enhance the seismic performance of CBs. Specifically, EB-FRP U-wraps improve deformation capacity and cumulative energy dissipation without significantly altering beam stiffness. The addition of diagonal EB-FRP sheets increases strength, stiffness, and energy dissipation but also leads to higher stiffness degradation rates. Eb-FRP anchors effectively delay the delamination of U-wraps, improving the overall deformation capacity.

(Sakr et al., 2017a) investigated the behavior of SSWs strengthened with EB-FRP composites, focusing on accurately predicting debonding failures. The purpose was to develop a finite element (FE) model that simulates the interaction between FRP sheets and concrete, accounting for debonding under monotonic loading. Various FRP configurations were analyzed, including cross bracing, lateral strips, and diagonal strips, each applied symmetrically on both sides of the RC walls. These configurations were tested to determine

their impact on the load-carrying capacity, ductility, and energy dissipation of the walls. The study found that different configurations significantly influence the performance of the strengthened walls. For instance, lateral strips were particularly effective in enhancing shear capacity and ductility, while cross-bracing offered the best overall improvement in lateral strength and ductility. The study concluded that the proposed FE models effectively predict the debonding failures and overall behavior of CFRP-strengthened RC shear walls. The results showed that utilizing higher fracture energy values in the adhesive layer significantly enhances the ultimate load capacity and energy dissipation of the shear walls. Additionally, strategic placement of CFRP anchors and partial bonding of CFRP sheets can delay debonding and improve ductility.

(Arabzadeh & Galal, 2017) examined the seismic collapse risk and effectiveness of EB-FRP retrofitting for coupled C-shaped core shear walls. The study aimed to evaluate the inelastic seismic response and torsional sensitivity of these structures and assess how FRP retrofitting can enhance their seismic performance. The researchers performed nonlinear incremental dynamic analysis (IDA) on a 12-story RC building located in Eastern North America, using artificial ground motions. The study tested various FRP configurations, including horizontal FRP wrapping, vertical FRP strips, and X-bracing, to determine their impact on the collapse margin ratio. FRP retrofitting proved to be highly effective, with the study showing that appropriate FRP strengthening schemes could increase the collapse margin ratio by over 60%. This substantial improvement in collapse resistance demonstrates the potential of EB-FRP retrofitting to enhance the seismic resilience of RC shear walls.

(Jin et al., 2024) conducted an experimental investigation to understand the shear contribution of EB-FRP composites in SSWs of different sizes. The primary objective was to determine how structural size and FRP ratio influence the shear performance of FRP-strengthened shear walls. The study involved testing twelve RC shear wall specimens under cyclic horizontal loading. These specimens varied in size (600 mm, 1200 mm, and 1800 mm) and EB-FRP ratios (0.00%, 0.07%, 0.14%, and 0.21%). The FRP configurations included horizontal strips. The tests measured parameters such as failure modes, load-deflection responses, deformation

components, ductility, and energy dissipation. Results indicated that the application of EB-FRP strips significantly enhanced the seismic performance of the shear walls. For instance, specimens with the highest EB-FRP ratio of 0.21% exhibited a 40.3% increase in shear capacity compared to unstrengthened walls. Additionally, the total energy dissipation and ductility coefficients increased substantially, with ductility improving by up to 196.7%. However, it was observed that the effectiveness of EB-FRP in improving shear strength diminished with increasing wall size. Larger specimens showed less pronounced improvements in shear strength and ductility, highlighting a size-dependent efficiency. The study concluded that while CFRP strips effectively enhance the seismic resilience of RC shear walls, their efficiency is influenced by the wall size and CFRP ratio.

1.4 Summary of Conclusions

The key findings from the literature are as follows:

- SSWs and CSWs play a critical role in the seismic performance of buildings, especially in resisting lateral forces during earthquakes. The integration of CBs in CSWs enhances energy dissipation but also introduces challenges related to shear and flexural demands.
- The application of FRP composites, particularly EB-FRP, has been shown to significantly improve the structural performance of RC elements by enhancing their flexural and shear strength. The literature underscores the importance of proper FRP configuration to maximize these benefits.
- The incorporation of self-centering mechanisms, such as rocking systems and mechanical devices like SMAs into RC structures is crucial for minimizing residual displacements after seismic events. These systems help maintain the structural integrity and functionality of buildings post-earthquake.
- Despite the advancements in the application of EB-FRP and self-centering technologies, there remain significant gaps in the optimal design and implementation of these systems. Further research is needed to refine these techniques and to develop guidelines that can be applied to a broader range of structural scenarios, particularly in varying seismic zones.

CHAPTER 2

ENHANCING RESILIENCE AND SELF-CENTERING OF EXISTING RC COUPLED AND SINGLE SHEAR WALLS USING EB-FRP: STATE-OF-THE-ART REVIEW AND RESEARCH NEEDS

Ali Abbaszadeh and Omar Chaallal,

Department of Construction Engineering, École de Technologie Supérieur, Université du Québec, Montréal, QC H3C 1K3, Canada

Paper published in *Journal of Composites Science, Volume 6, Issue 10, Article 301*, October 2022

2.1 Abstract

The primary seismic force resisting system (SFRS) in middle- to high-rise reinforced concrete (RC) building structures often includes coupled shear walls (CSWs) and single shear walls (SSWs). These walls are designed to transfer lateral forces to the foundation and dissipate energy through the development of plastic hinges. The latter lead to residual displacement in these structural components. On the other hand, self-centering systems enable the structures to return to their initial position after severe loading or at least to reduce residual displacement. The objectives of this study were therefore as follows: (i) to review the state of the art on shear wall self-centering techniques and retrofitting methods based on externally bonded fiber-reinforced polymer (EB-FRP); (ii) to evaluate research needs to improve the self-centering ability of shear walls using EB-FRP.

Keywords: Residual displacement, self-centering, coupled shear wall, single shear wall, plastic hinge, FRP composite.

2.2 Introduction

Most RC structures in medium- to high-rise buildings located in seismic and windy zones are made of single and coupled shear walls as lateral force resisting systems. In this regard, it is crucial to find a way to deal with potential hazards and structural damage due to earthquakes, severe wind, and other potential lateral forces. The occurrence of severe earthquakes, even in buildings designed according to the most up-to-date modern building codes and standards, can cause structural elements to enter a nonlinear state and, as a result, experience residual displacements after the events, which can lead to their replacement in severe cases. Therefore, methods to increase the resilience of existing structures and strengthen their weaknesses are essential.

Self-centering systems enable structures experiencing residual displacement to return to their original and upright position after cyclic loading or reduce the residual displacement to the maximum acceptable by the standards, thereby enabling the structure to survive. In recent years, much research has been carried out to develop self-centering systems, although the use of this system cannot be attributed to recent years or even decades because its traces can be seen even in historical buildings left by ancient civilizations. Nevertheless, the ultimate purpose of this study is to use these systems for existing structures.

In the meantime, the application of EB-FRP sheets for strengthening existing RC structures has been well received by researchers in recent decades. Compared to other methods, using FRP sheets offers many advantages such as easy installation, high tensile strength, affordability, high resilience in different weather conditions, and the possibility of use on most structural elements. Moreover, unlike cement and steel, FRP sheets cause less environmental damage because their production generates fewer greenhouse gases. However, FRP laminates have some disadvantages, including lower modulus of elasticity compared to steel, poor long-term dynamic performance (mainly due to debonding of the concrete medium from the FRP sheets), and inadequate fire and heat resistance.

For a better understanding of and approach to the goals of this study, the main sections of this paper are organized as follows:

(i) the role and performance of shear walls in RC buildings.

(ii) the evaluation of strengthening existing RC structures using EB-FRP sheets.

(iii) the review of self-centering methods and their performance in RC buildings.

(iv) conclusion and evaluation of required studies.

Figure 2.1 shows an overview of this research study.

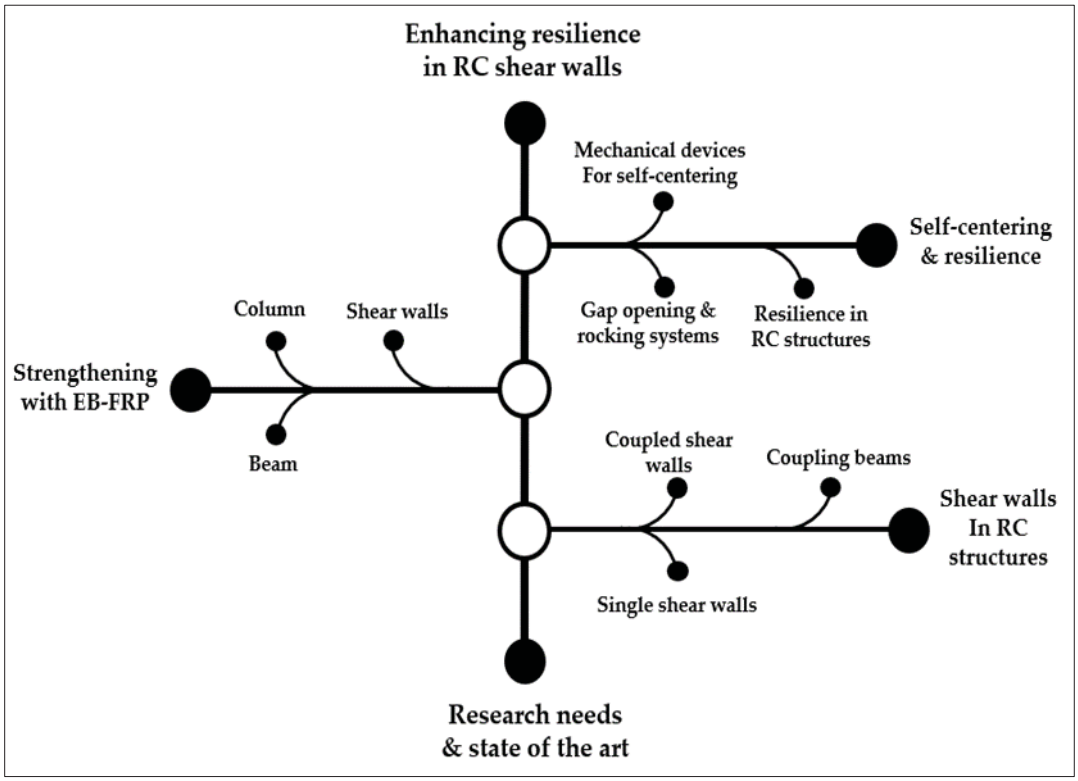

Figure 2.1 Overview of the present research study

2.3 Shear walls in RC structures

Shear walls play a crucial role in a structure's resistance to lateral loads, gravity loads, and severe seismic forces. They prevent structural and non-structural damage by reducing overall displacement and drift in the structure. Two shear wall configurations are often used in

reinforced concrete buildings as lateral load-bearing elements: (i) the single shear wall, and (ii) the coupled shear wall. The behavior of a slender single shear wall (SSW) can be compared to that of a reinforced concrete cantilever beam. These walls can be considered as upright cantilevers, which tolerate tremendous amounts of bending moment, shear force, and compressive force due to lateral and gravity loads respectively (Park & Paulay, 1991). Accordingly, the moment-axial force interaction relationship should be used to determine the strength of the critical section of the shear wall. When assessing the flexural capacity of a shear wall, vertical or flexural reinforcement in the web zone should be considered. As shown in Figure 2.2, when a lateral force is applied to single shear walls, they resist lateral forces by forming moment and shear at the wall base, because the walls are typically considered fixed at the base.

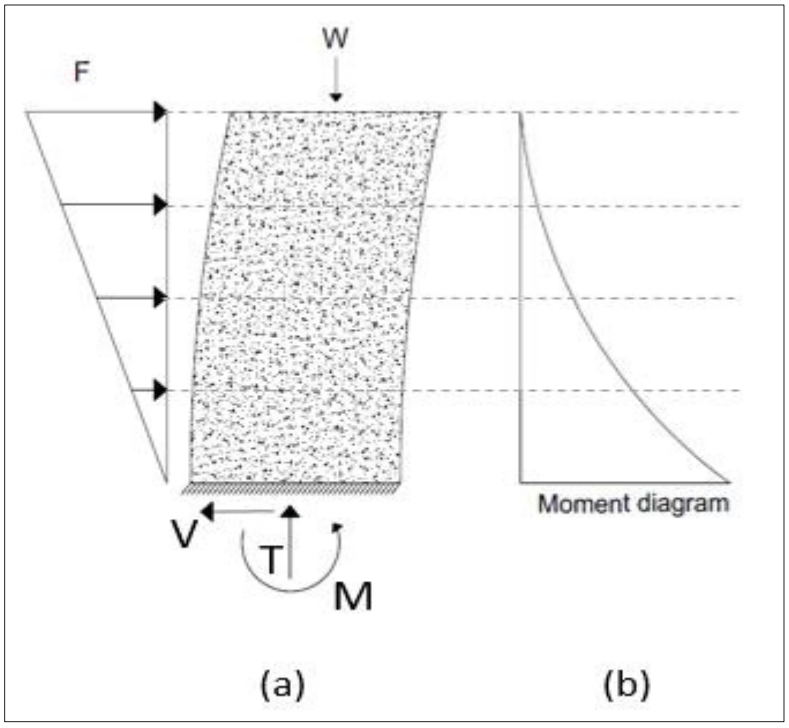

Figure 2.2 (a) wall base reactions (b) bending moment diagram in the fixed base SSWs exposed to lateral force

In the early years, much research was conducted on the amount and configuration of vertical and horizontal reinforcement, wall thickness, concrete strength, and, more recently, the effect

of the location of shear walls on their performance and the interaction of the frame and shear walls in structures. Later, the capacity design method for shear walls was developed (Park & Paulay, 1975). A detailed overview of design requirements and a study on shear walls are available (Paulay & Priestley, 1992). The importance and key role of the size and arrangement of vertical rebars on the ultimate curvature of the shear walls were stated (Cardenas & Magura, 1973). Bertero and Felippa (Bertero & Felippa, 1964) studied the effect of transverse confinement on buckling and ductility capacity. More recently, further research was carried out on the ductility of shear walls (Collins et al., 1993; Cusson & Paultre, 1994). The occurrence of severe earthquakes and the observation of undesirable or unexpected failures in shear walls led to further developments in the design and strengthening of shear walls against seismic loads. In addition, some researchers investigated the effect of a shear wall's thickness on its performance during a severe earthquake (Saatcioglu et al., 2013; Wallace, 2012)

Although single shear walls can perform properly against seismic forces, coupled shear walls (CSW) can be even more efficient due to their coupling system. These walls present many advantageous features such as high lateral stiffness and strength, superior architectural compatibility, and excellent energy dissipation capacity. Generally, CSW systems consist of two walls linked by coupling beams (CB). Fixed joints between the coupling beams and the walls that resist against moments can create an efficient rigid lateral force-resisting system. On the other hand, once a lateral force is applied to a CSW, in addition to the moment and shear force development at the wall piers base, corresponding to shear force formation in the CBs, an axial tension-compression force couple is formed in each wall. This coupling system significantly improves CSWs lateral resistance. Figure 2.3 shows force development in CSWs.

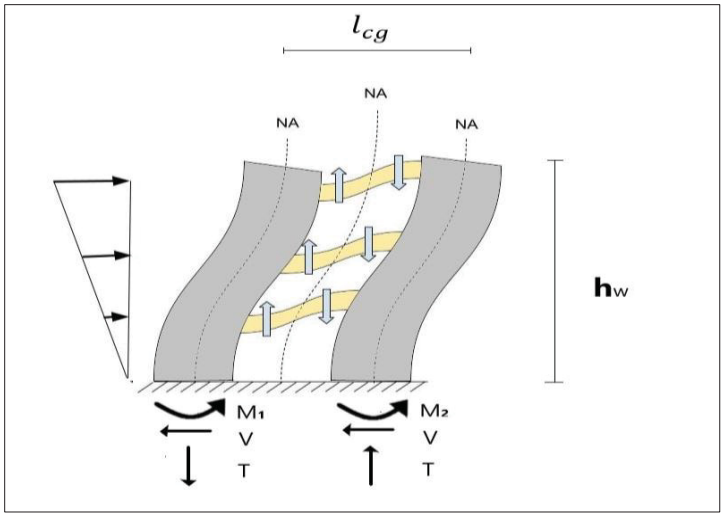

Figure 2.3 Force development in CSW system

Many successful studies have been conducted on CSWs, leading to tremendous development in their design and detailing (Benazza, 2012; McNeice, 2004; Park & Paulay, 1991). These studies showed that the stiffness and geometrical properties of CBs play a crucial role in the performance of these walls during a seismic event. To measure these features in CBs, the National Building Code of Canada (NBCC) has introduced a ratio known as the degree of coupling (DC) as follows:

$$DC = \frac{Pl_{cg}}{M_1 + M_2 + Pl_{cg}} \tag{2.1}$$

where P and l_{cg} represent the value of the tension or compression force arising from the coupling function (in CBs) and the distance between wall centroids respectively; M_1 and M_2 denote the internal moments generated in each wall pier. In addition, (Chaallal et al., 1996) proposed the following formula for DC based on statistical regression correlations between DC and geometric features of CSWs:

$$DC = k\frac{H_b^a}{D_w^b + L_b^c} \tag{2.2}$$

Where H_b and L_b are the coupling beam height and length respectively and D_w is the wall length. Other dimensionless values, including *k*, *a*, *b*, and *c*, can be obtained from Table 2.1.

Table 2.1 Values of k, a, b, and c for Equation 2.1
From Chaallal et al. (1996, p.2)

Number of stories n (1)	k (2)	a (3)	b (4)	c (5)
6	2.976	0.706	0.615	0.698
10	2.342	0.512	0.462	0.509
15	1.697	0.352	0.345	0.279
20	1.463	0.265	0.281	0.190
30	1.295	0.193	0.223	0.106
40	1.190	0.145	0.188	0.059

In Equation 2.2, the author considered γ equal to 0.6 as a coefficient to calculate the moment of inertia (I_e) of walls and CBs (I_e=$\gamma\ I_g$, in which I_g is the uncracked gross section). For other values of γ, including γ_b (for the coupling beams) and γ_w (for the walls), DC can be determined using the following equation (Chaallal et al., 1996) :

$$DC = \frac{(\gamma_b/0.6)^{a/3}}{(\gamma_w/0.6)^{b/3}}\, k\, \frac{H_b^a}{D_w^b L_b^c} \tag{2.3}$$

As an appropriate SFRS, shear walls include many structural considerations and design requirements. Accordingly, in the equivalent static method, the base shear is significantly related to the type of the chosen SFRS. In this regard, NBCC2015 specified some criteria to determine the force at each floor through the distribution of base shear. Equations 2.4, 2.5, and 2.6 calculate the base shear and its maximum and minimum limits:

$$V_{base} = S(T_a) M_v \frac{I_E}{R_d R_o} W \tag{2.4}$$

$$V_{max} = max\left(\frac{2}{3}\frac{S(0.2)M_v I_E W}{R_d R_o}, \frac{S(0.5)M_v I_E}{R_d R_o}\right) \tag{2.5}$$

$$V_{min} = S(4.0)M_v \frac{I_E}{R_d R_o} W \tag{2.6}$$

Where W denotes the total weight of the structure, which encompasses 25% of the snow load (SL) added to the dead load (W=DL+0.25SL). $S(T_a)$ represent the design-spectral-response acceleration at the fundamental period; M_v represents the factor considering higher-mode effects; I_E represents the importance factor. R_d denotes the ductility-related factor, and R_o represents the overstrength-related factor; these values are related to the type of SFRS. Then the force on each floor should be calculated as follows:

$$F_i = (V_{base} - F_t)\frac{W_i h_i}{\sum_{i=1}^{n} W_i h_i} \tag{2.7}$$

Where F_i denotes the force at level i, W_i denotes the weight assigned to the i^{th} story, h_i is the height of the i^{th} story above the base, and F_t is a part of the base shear that should be applied to the highest floor if the period of the structure is greater than 0.7s, to consider the effect of higher modes. F_t is calculated as follows:

$$F_t = 0.07 T_a V_{base} \leq 0.25 V_{base} \tag{2.8}$$

In addition, CSA/A23.3-14 specified some requirements to ensure SSW ductility within and above the plastic hinge zone. In this regard, within the plastic hinge zone of the shear walls, the plastic rotational demand (θ_{id}) should be less than the plastic rotational capacity (θ_{ic}). Equations 2.9 and 2.10 calculate θ_{id} and θ_{ic} respectively:

$$\theta_{id} = \frac{(\Delta_f R_o R_d - \Delta_f \gamma_w)}{(h_w - \ell_w/2)} \geq 0.004 \tag{2.9}$$

where $\Delta_f R_o R_d$ denotes the design displacement and $\Delta_f \gamma_w$ is the elastic portion of the displacement:

$$\theta_{ic} = \left(\frac{\varepsilon_{cu}\ell_w}{2c} - 0.002\right) \tag{2.10}$$

Where c denotes the neutral axis distance (an outermost compression fiber's distance from the neutral axis), given by:

$$c = \frac{P_s + P_n + P_{ns} - \alpha_1 \phi_c f_c' A_f}{\alpha_1 \beta_1 \phi_c f_c' b_w} \tag{2.11}$$

where P_s denotes the axial load at the section, calculated as the sum of factored dead-load, factored live-load, and earthquake-load factors; P_n denotes the earthquake-induced transfer force calculated from the interaction between CSW elements; P_{ns} denotes the nominal net load applied to the segment due to yielding in compression-tension of both concentrated and distributed rebars throughout plastic hinge development; α_1 represents the ratio of middling stress within the compression block to the determined concrete strength; β_1 denotes the ratio of compression block depth to neutral axis depth; b_w represents the wall thickness, and A_f denotes the area of the flange. ε_{cu} should be assumed as 0.0035 except for the compression zone of the wall containing special confinement reinforcement, according to CSA/A23.3-14 requirements. For the CSWs and CBs, θ_{id} should be calculated by Equations 2.12 and 2.13 respectively:

$$\theta_{id} = \frac{\Delta_f R_o R_d}{h_w} \tag{2.12}$$

$$\theta_{id} = \left(\frac{\Delta_f R_o R_d}{h_w}\right) \frac{\ell_{cg}}{\ell_u} \tag{2.13}$$

Where h_w represents height of the wall, ℓ_{cg} denotes the distance between the wall centroids, and ℓ_u represents the length of the clear span.

2.4 FRP composites

All structures may be damaged or eroded due to various factors such as adverse weather conditions, traffic, severe earthquakes, changes in use, and other events. Hence, strengthening existing structures is inevitable because it is often more cost-effective than replacing the entire structure. Various methods have been investigated and proposed to strengthen concrete structures (Al-Mahaidi & Kalfat, 2018; Siddika et al., 2019; Tassios et al., 1996). However, the use of FRP to strengthen existing structures has gained tremendous popularity worldwide due to its ease of implementation and very high efficiency (Fathelbab et al., 2014). The first studies on utilizing FRP composites for the aerospace industry were conducted in the early 60s (Bakis et al., 2002). Later, many numerical and experimental studies demonstrated the effectiveness of the application of FRP composites to rehabilitate RC structures (Rahimi & Hutchinson, 2001; Triantafillou & Plevris, 1992). FRPs can be made of different fiber materials, including carbon, basalt, glass, and aramid fibers, which can be used to retrofit different components of structures (Amran et al., 2018; Siddika et al., 2020). They also feature many other advantages compared to conventional retrofitting methods, including high strength-weight ratio, anti-corrosion properties, resistance to harsh weather conditions, enforceability in under-service intricate structures, and chemical resistance (De Maio et al., 2022; Ou & Zhu, 2015).

2.4.1 Strengthening RC structures using FRP

As a strengthening method for RC structures, FRPs can be used in various forms and configurations, including externally bonded (EB) laminates, anchorage systems, and near-surface mounted (NSM) bars (Mostofinejad & Kashani, 2013; Siddika et al., 2019). EB-FRP is used in various ways to strengthen structures, including side bonding and partial or full wrapping as well as transverse and longitudinal strips on beams and slabs. Nevertheless, debonding of the concrete medium from the FRP sheets is considered as a common drawback

of EB-FRP. To overcome this problem, an anchorage system will help greatly to improve the performance of the strengthened structure (De Maio et al., 2022; Mostofinejad & Kashani, 2013). FRP anchorage, spike anchorage, and mechanical fasteners are some of the anchorage systems used in different strengthening techniques. In addition to the anchorage challenge, FRP composites have some disadvantages, including (i) poor fire and heat resistance; (ii) elastic response up to rupture; (iii) vulnerability during drilling for anchoring; (iv) higher costs compared with traditional strengthening methods (Siddika et al., 2020).

EB-FRP composites can be used to retrofit and repair a wide range of structural deficiencies; however, the type and condition of loading as well as the structural weakness must be carefully established before selecting the appropriate FRP strengthening configuration. Various deficiencies in columns, beams, and shear walls are described in the following subsections, and an overview of different FRP strengthening patterns is shown in Figure 2.4. (Siddika et al., 2020) reviewed RC structure strengthening techniques using FRP composites comprehensively.

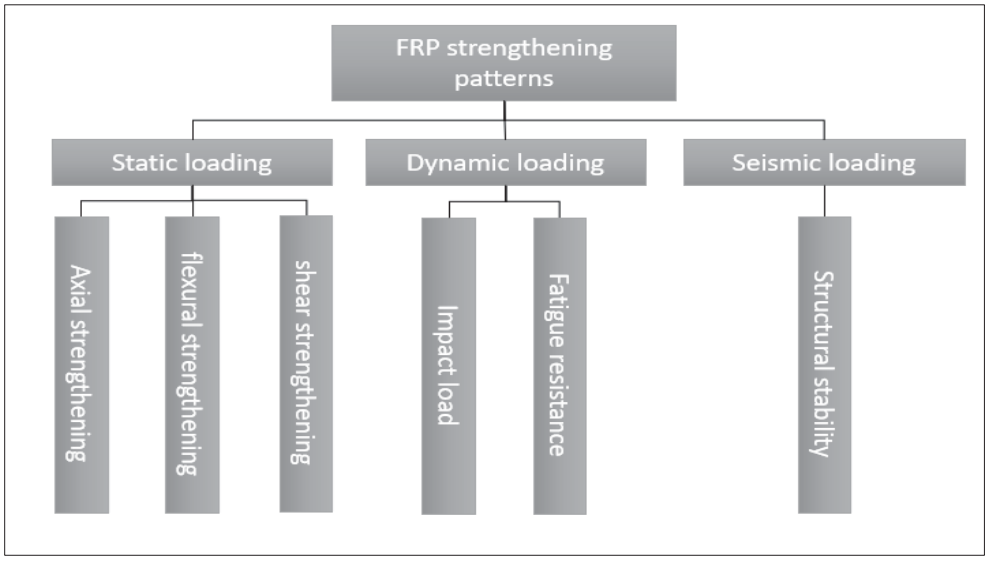

Figure 2.4 FRP strengthening patterns

2.4.1.1 Columns

RC columns might be strengthened due to deficiencies such as (i) poor ductility, compressive, shear, and flexural strength (Shao et al., 2006; Sheikh & Li, 2007; Shin & Jeon, 2022); (ii) lack of lap splice and confinement (Ghosh & Sheikh, 2007; Opabola & Elwood, 2021; Opabola et al., 2021); (iii) poor column-beam connection (Al-Rousan, 2022; Bian et al., 2020).

One of the most prevalent methods of increasing compressive strength in RC structures, especially in columns, is the use of fully wrapped EB-FRP around the perimeter of the element. This can significantly enhance the confinement (lateral pressure) on the column, thereby improving ductility, shear strength, axial strain, and load-carrying capacity (Pham & Hao, 2016; Siddika et al., 2020). Note that confinement by EB-FRP is more effective in circular columns than in rectangular ones due to the larger corner radius of the latter (Bakis et al., 2002). Studies have also showed that the effectiveness of confinement using EB-FRP wrap on circular columns differs from that on a rectangular section. Although axial strength in circular columns is the most influenced by confinement, in rectangular-section columns, confinement primarily enhances concrete strain capacity (De Luca et al., 2009; Wang et al., 2012). (Razavi et al., 2021) conducted tests under axial eccentric cyclic loading in six RC columns: non-strengthened, strengthened with longitudinal EB-FRP sheets, and strengthened with fully wrapped FRP sheets. The results showed that using longitudinal EB-FRP sheets, despite the decrease in ductility, can increase the bearing capacity under high eccentric loads by up to 60%. In contrast, fully wrapped FRP does not improve the bearing capacity, but significantly increases ductility. (Yi et al., 2006) showed that longitudinal and transverse EB-FRP sheets are required for RC columns under eccentric loads to improve ultimate strength and ductility respectively. More studies have been carried out on the behavior of FRP-strengthened RC structures under eccentric axial loads (NoroozOlyaee & Mostofinejad, 2019; Raza, 2021; Torabian & Mostofinejad, 2017; Xu et al., 2021). Moreover, an applied concentric cyclic axial load has been considered by many researchers (Bai et al., 2022; Saljoughian & Mostofinejad, 2018; Zeng et al., 2022).

Poor seismic design can lead to shear-brittle failure before flexural failure in columns (Del Zoppo et al., 2017). Moreover, shear failure is more common in short columns. However, EB-FRP can increase the shear strength of columns and alter shear failure to flexural failure. Using a finite-element model, (Y. Liu et al., 2021) revealed that EB-FRP wrap could improve the shear strength of a damaged column under impact load and alter the failure mode from brittle-shear to ductile-flexural. (Mo et al., 2004) revealed that using FRP sheets considerably increased the ductility and shear capacity of hollow rectangular bridge columns. (Iacobucci et al., 2003) used an FRP jacketing technique to strengthen columns with inadequate seismic design and detailing. The results showed considerable improvement in energy dissipation and ductility. (Kargaran & Kheyroddin, 2022) conducted finite-element analysis and experimental tests on six short RC columns under cyclic lateral displacement to evaluate the effectiveness of the EB-FRP technique in different schemes such as transverse, diagonal, and hybrid. The results revealed that when these techniques were used, the failure mode in columns was altered from shear to flexural, and ductility and energy dissipation improved.

EB-FRP wrap (jacketing) enhances the sectional curvature capacity of an RC column. Taking advantage of this feature and providing an adequate length of EB-FRP wrap in the plastic hinge zone greatly increased the drift capacity of the RC column (Gu et al., 2010). Hence, many studies have taken advantage of the FRP jacketing technique to improve RC column performance (Bedirhanoglu et al., 2022; Saleh et al., 2022). (Parvin & Wang, 2002) conducted a nonlinear finite element analysis on columns retrofitted in the plastic hinge zone, using FRP jackets under axial and cyclic lateral loads. Results revealed that this technique considerably increased ductility and strength, leading to significant delay in stiffness degradation of the RC column.

The importance of column-beam connections is as great as that of other structural components during seismic loading. Even if the beams and columns remain intact, the entire structure can collapse if the column-beam connections fail (Bindhu et al., 2009). One of the most common failures in column-beam joints is shear-brittle failure, which should be avoided through appropriate design and detailing or rehabilitation techniques in existing structures. FRP sheets

can improve the flexural capacity of the connections and decrease joint rotation (Parvin & Granata, 2000). Many studies have been done to evaluate the effectiveness of FRP composites as a beam-column joint strengthening technique (Alhaddad et al., 2021; Tafsirojjaman et al., 2021). (Ghobarah & Said, 2001) showed that using GFRP jacketing in column-beam connections can enhance energy dissipation, shear resistance, and ductility and change shear-brittle failure to flexural failure in joints.

Many buildings experience total structural destruction after a seismic event, mainly due to column failure and shear and flexure deficiencies. Hence, to avoid these incidents, columns should be strengthened. (Ouyang et al., 2017) showed that fully wrapped EB-FRP in columns enhances axial strength and confinement and increases ductility and column failure control. In addition, it greatly enhances energy dissipation capability in columns. (Iacobucci et al., 2003) studied columns strengthened with the fully wrapped EB-FRP technique. The results revealed a 54% improvement in most parameter values and resistance against seismic forces. In addition, it has been shown that using hybrid EB-FRP and NSM techniques considerably increased ductility and load capacity during seismic loading (Seifi et al., 2017). (Murad et al., 2020) evaluated the effect of EB-FRP on the cyclic response of unconfined joints constructed with recycled concrete. The results showed great load-carrying capacity and strength enhancement after strengthening components with FRP. More detailed evaluations on seismic retrofitting of RC connections are presented in recent studies (Davodikia et al., 2021; S. Zhou et al., 2021).

2.4.1.2 Beams

EB-FRP strengthening of RC beams is a widespread method that has shown great effectiveness in practice (Panahi et al., 2021; Phan & Nguyen, 2021). The most common applications of EB-FRP sheets in RC beams can be listed as: (i) shear strengthening (Colajanni & Pagnotta, 2022; El-Ghandour, 2011; Rajendran & Kothapalli, 2022); (ii) flexural strengthening (Chen et al., 2018; Sengun & Arslan, 2022); (iii) fatigue strengthening (Fathi et al., 2022; Guo et al., 2021); (iv) impact strengthening; (v) seismic strengthening.

All RC beams are subjected to bending. Flexural failure mode happens due to exposure to loads that are higher than the flexural capacity of the beam. Depending on the beam type and loading, FRP sheets or laminates with or without anchors can be used to strengthen these elements against bending. Applying unidirectional FRP on the tension side of the element is the most common method of flexural strengthening (Chen et al., 2018; Hadi, 2022; Shannag et al., 2014). (Panahi et al., 2021) evaluated the flexural retrofitting of RC beams with a combination of EB-FRP layers and near-surface mounted FRP rods. The results showed an acceptable increase in flexural capacity, stiffness, ultimate bending moment, and decrease in ductility. (El Ghadioui et al., 2022) investigated the flexural retrofitting of RB members under long-term cyclic loading. Zhang et al. (Zhang et al., 2017) showed that using NSM strips can achieve a 200% gain in flexural resistance. (Attari et al., 2012) showed that using EB-FRP results in a decrease in deflection as well as in the length of bending cracks. Extensive studies have been conducted on the flexural behavior of RC beams strengthened with FRP sheets (Camata et al., 2007; Kumar et al., 2021).

The application of FRP composites as an effective RC beam shear-strengthening method has been evaluated in many studies, which have proved that the orientation of FRP sheets as a significant feature governs its efficiency (Al-Saidy et al., 2010). (Singh, 2013) showed that inclined EB-FRP wrapping is more efficient in enhancing shear capacity. The use of wrapping oriented at 45° could avoid diagonal cracks. Using a hybrid U-wrapped FRP and anchorage system, (Baggio et al., 2014) evaluated the repair of shear cracks caused by a prestressed force. They showed that the increase in load-carrying capacity could reach 82.2%. Numerous researchers also investigated shear strengthening using FRP sheets (Abbasi et al., 2022; Samb et al., 2021; Saribiyik et al., 2021).

Impact load originates from many sources such as moving vehicle load, falling rocks or weights, and explosions. The most probable damage due to this loading pattern is shear failure. Hence, increasing an element's shear capacity is crucial to improving impact strength. (Tang & Saadatmanesh, 2003) argued that EB-FRP on RC beams considerably benefits impact

strength. Their study showed 15% and 96% gain for impact and shear strength respectively. In this context, further research evaluated the impact resistance of RC members strengthened with FRP (Anıl & Yılmaz, 2015; Jin et al., 2021). Although shear strengthening is more common for impact resistance improvement in RC beams, many studies showed that flexural strengthening significantly develops the impact resistance of this component (Kantar & Anil, 2012; Sinh et al., 2022). (Kishi et al., 2020) revealed that flexural strengthening could improve the impact resistance of RC beams. They carried out an experimental evaluation on RC beams strengthened in flexure using both aramid FRP (AFRP) and carbon FRP (CFRP) sheets. The impact load was simulated by a steel weight that was released from different heights, and the increase in the height of the dropping was continued until debonding of FRP and concrete.

A beam exposed to cyclic loading gradually loses its ductility and stiffness, leading to permanent deformation. (Aidoo et al., 2004) showed that using FRP with high tensile strength reduces stress concentration at the cracks in the elements and avoids fatigue in the structure. (Alyousef et al., 2016) showed that because stress flow occurs in the FRP-concrete interface, fatigue control depends entirely on concrete, epoxy resin, and FRP strength. They also revealed that using U-wrapped EB-FRP improved shear capacity and rigidity and decreased crack length under repeated loadings, increasing overall fatigue performance by 62%. (Charalambidi et al., 2016) showed that using EB-FRP in RC beams to increase flexural strength could improve the fatigue resistance of internal steel rebars. Therefore, elastic material can help maintain strength and stiffness against fatigue loading. Meanwhile, it should be considered that FRP-concrete beams may experience fatigue crack propagation due to cyclic loading. Further discussions have been done on the fatigue resistance of FRP-strengthened RC beams (Banjara & Ramanjaneyulu, 2019; James, 2020).

2.4.1.3 Shear walls

Stiffness degradation in shear walls during cyclic loading may alter their efficiency and performance. These concerns have led to the development of various innovative strengthening methods for RC shear walls (Christidis et al., 2016; Li et al., 2013; Petkune et al., 2016).

(Ehsani & Saadatmanesh, 1997) showed that strengthening shear walls with FRP is the most cost-effective technique. However, it can be argued that the functionality of a shear wall strengthened with FRP depends on two major factors: the FRP configuration, and the anchorage pattern between the FRP strips and the shear wall (Altin et al., 2013; Ko & Sato, 2007; Li & Lim, 2010). (Altin et al., 2013) revealed that the configuration using lateral FRP strips featured the best performance among the various FRP configurations to improve lateral displacement and load-carrying capacity.

In another study by (Honarparast & Chaallal, 2019a), two CBs with a span-to-depth ratio equal to two were experimentally evaluated. One was conventionally reinforced and detailed based on NBCC 1941, and the second was diagonally reinforced and detailed based on NBCC 2015 and CSA A23.3 14. The coupling beam dimensions were 500, 250, and 1000 mm in depth, width, and span respectively. Four 20-mm-diameter rebars were used for conventionally reinforced specimens as top and bottom longitudinal reinforcement. The development length, which is vital to calculate the tensile resistance of rebars in the walls, was determined according to NBCC codes. For shear resistance, 10 mm-diameter hooped rebars with 200-mm spacing were used. Six horizontal 10 mm-diameter rebars and 8 diagonal 22 mm-diameter rebars were used for the diagonal reinforcement specimen. Five 10 mm-diameter rebars with 100-mm spacing were used for shear resistance. Both CBs were submitted to reversed cyclic loading. The study revealed that the diagonally reinforced CB outperformed the conventional CB because the load resistance and the energy dissipation in diagonally reinforced CB increased up to 4.4 and 10.2 times respectively. It also showed that stiffness degradation was less in diagonally reinforced CB (4%) than in conventionally reinforced CB (43%). In addition, diagonally reinforced CB featured significantly less pinching in hysteretic loops. According to the results, ataround 138 kN load, the conventional specimen rebars started to yield, and shear cracks due to sliding shear failure emerged at the joint locations in the early stages of reversed cyclic loading. This contrasts with diagonally reinforced CB, where rebars initiated yielding at a load of 495 kN. These results showed the need for seismic rehabilitation of old structures designed and detailed based on old codes and standards. In addition, (Honarparast et al., 2019) evaluated a new method for retrofitting CBs with EB-FRP. To that end, two conventionally

designed RC specimens designed according to NBCC 1941 were considered: one control (unrehabilitated), and one strengthened with EB-FRP. Both were subjected to cyclic loading. A comparison of experimental results revealed a significant improvement in energy dissipation and hysteretic behavior with less stiffness degradation. The results revealed that as the 138 kN load was approached, the rebars in the control specimen started to yield, and shear cracks due to sliding shear failure at the joint locations emerged in the early stages of reversed cyclic loading. For the specimen strengthened with EB-FRP, the load reached 308 kN at the end of reversed cyclic loading, and small cracks appeared near the joints. Debonding of FRP strips at joints also appeared during the load cycles. The hysteretic behavior of the control specimen featured large pinching, stiffness degradation, and loss of energy dissipation capacity. The load-carrying capacity suddenly dropped after the displacement reached 24 mm. In contrast, the rehabilitated specimen did not show any considerable pinching and stiffness degradation before FRP debonding, resulting in a rapid load reduction at the final load cycle. Several schemes for strengthening SSWs and CSWs with EB-FRP are presented in Figure 2.5.

The other critical issue in RC shear wall strengthening with EB-FRP is the premature debonding of FRP sheets, which inhibits the FRP from reaching its strength capacity. As mentioned earlier, epoxy resins are generally used as an adhesive to fix FRP sheets or strips to the concrete surface. However, due to severe cyclic loading, these resins lose their strength and lead to debonding. Hence, research activities are still ongoing to find the best solution to this problem. Studies have also revealed that hybrid application of U-shaped FRP-bonded sheets with a metal anchor is an appropriate technique to avoid premature debonding (Antoniades et al., 2005, 2007).

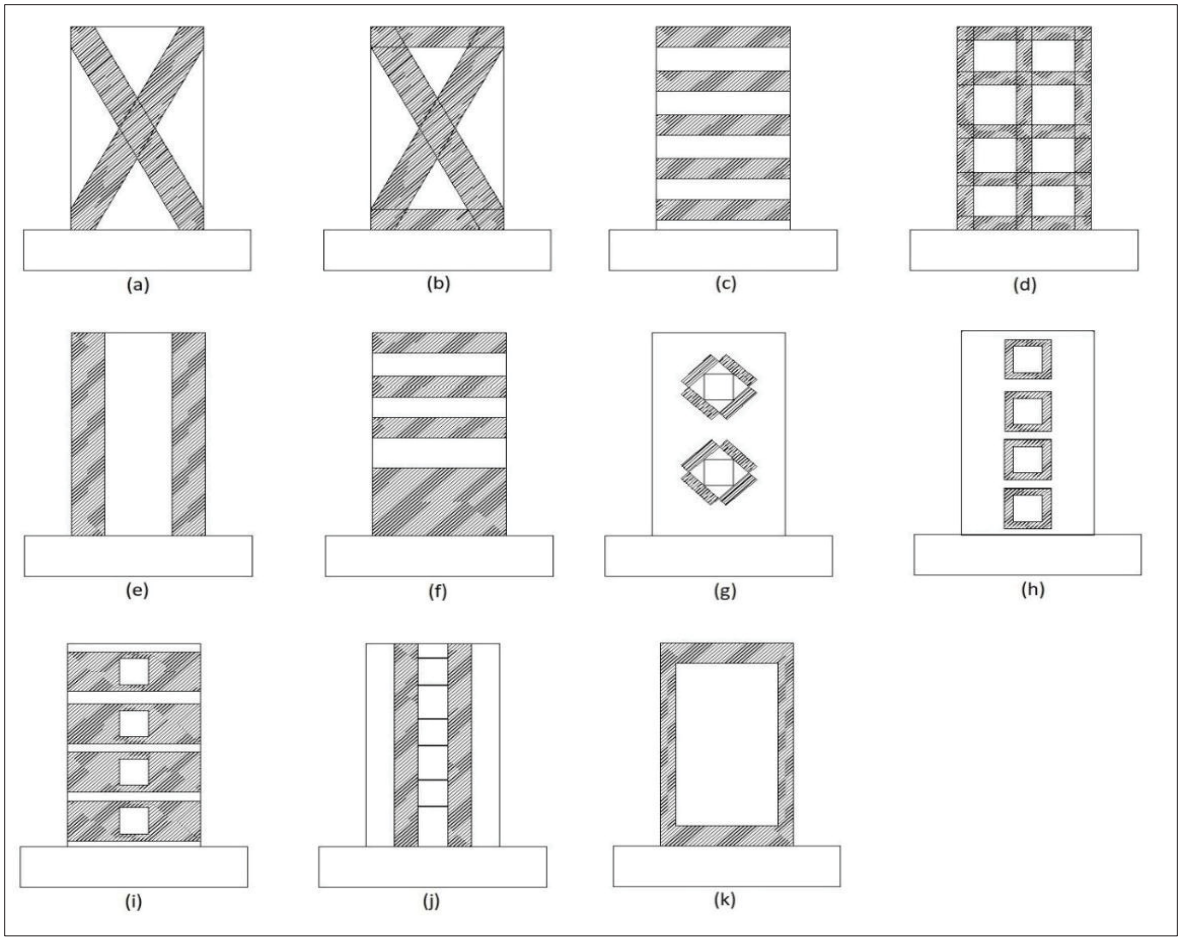

Figure 2.5 Typical schemes of strengthening shear walls with EB-FRP, where (a), (b), (c), and (d) are evaluated by (Sakr et al., 2017b); (e) is evaluated by (Elnady, 2008); (f) is evaluated by (Layssi et al., 2012a); (g), (h), (i), and (j) are evaluated by (Aslani & Kohnehpooshi, 2018); (k) is evaluated by (Arabzadeh & Galal, 2015)

(Sakr et al., 2017b) showed that configuration (c) in the walls, governed by shear failure, has the most satisfactory performance to increase ductility and lateral strength. Nevertheless, pattern (b) has the best performance for the shear walls governed by flexural failure. They also indicated that in diagonal configurations (a,b), bonding overall 50% (from each end) of the diagonal length of FRP sheets is as adequate as complete bonding of FRP sheets. (Elnady, 2008) revealed pattern (e) can improve ductility and energy dissipation and avoid brittle failure in the shear walls. (Layssi et al., 2012a) showed that (i) scheme (f) avoids brittle and side-splitting lap splice failure by providing sufficient confinement in the plastic hinge region; (ii) One layer of fully wrapped FRP within the plastic hinge zone of shear walls can delay the

buckling of flexural rebars and improve shear strength; (iii) This configuration can increase the energy dissipation of the shear walls. (Aslani & Kohnehpooshi, 2018) revealed that configurations (g, h, i, and j) could increase energy dissipation and bearing capacity and decrease residual displacement of the shear walls. They also showed that configurations (g, h) are more effective in the shear walls with central openings, but the pattern (g) cannot be used for large-size openings. (Arabzadeh & Galal, 2015) showed pattern (k) could significantly increase ductility and energy dissipation of the squat shear walls.

2.5 Self-centering and resilience

At high lateral forces, the primary role of shear walls in RC structures is to dissipate a significant amount of energy through plastic hinges that form within the base of the wall and in the CBs of CSWs, as well as through reinforcement yielding. On the other hand, formation of plastic hinges results in residual displacement in SSWs and CSWs (see Figure 6a). Self-centering systems enable structures experiencing residual displacement to return to their original upright positions after cyclic loading or at least to reduce the residual displacement to the maximum acceptable amount, thereby enabling the structure to survive. Typically, hysteretic behavior of an ideal self-centering system is a flag-like shape which features no residual displacement after a cyclic loading (see Figure 2.6 b). The self-centering ability has been studied for many structural components, including columns, frames, walls, and bridge piers. Note that the application of this method is not limited to RC structures (which is the scope of this study), and several studies have been conducted to evaluate self-centering ability in timber, steel, and masonry structures. Various self-centering techniques can be used to restore a structure to its previous state. Two main techniques for creating self-centering in structures are rocking action and use of mechanical devices (Housner, 1963; Zhong & Christopoulos, 2022a). The following subsections are devoted to reviewing the application of these self-centering techniques in RC structures.

2.5.1 Gap opening and rocking systems

In this method, uplifting the whole structure or rocking major structural components can mechanically resist seismic force and decrease damage and residual displacement. When this occurs, structural components remain elastic through a nonlinear softening response. Rocking systems may use either post-tensioned (PT) tendons (controlled rocking) or gain self-weight (uncontrolled rocking) (Chancellor et al., 2014). In controlled rocking systems, structural components are pre-compressed at their surfaces using PT elements. Once the lateral force nullifies the precompression force, the joint section decompresses, and the gap opens. Thereafter, PT elements recover the lost stiffness of the lateral resistance system by forming an axial stiffness. If the strain at the joint overcomes the elastic strain limit of the PT element, then the system may fail (Chancellor et al., 2014) (see Figure 2.6 c). In addition, some hybrid techniques in controlled rocking systems are equipped with dampers or restraining devices (Bedriñana et al., 2022). Numerous research studies on self-centering with unbonded post-tensioning and energy dissipators have also been conducted (Marriott et al., 2009; Sritharan et al., 2015; Zareian et al., 2020). (Holden et al., 2003) showed that using a prestressed concrete system makes it possible to create the necessary force to return the structural element to its initial state. In this case, tendons should be unbonded over a certain length to remain in the elastic range during loading. This process creates the necessary force to deal with large displacement and prevents the formation of plastic hinges at the wall base and consequently residual displacement. Furthermore, because concrete is not bonded to the tendons and the lateral strength system does not rely on the interaction between rebars and concrete to withstand lateral loads, cracks in the concrete are significantly reduced. In addition, the minor damage that may occur in the bottom corners of the walls can be avoided by using foundation-embedded steel mating plates in these areas. Post-tensioning can be used for moment-resisting RC frames as well. This method is also based on a beam-and-column joint gap opening system (Chancellor et al., 2014). In addition, energy dissipator devices located at joints can play a significant role in absorbing seismic loading energy. Such systems can tolerate significant rotation with no loss in load-carrying capacity (Priestley, 1996). Some achievements regarding

the investigation of self-centering of moment-resistance RC frames have also been reported (Buchanan et al., 2011; Cai et al., 2021; Elettore et al., 2021; Priestley, 1996).

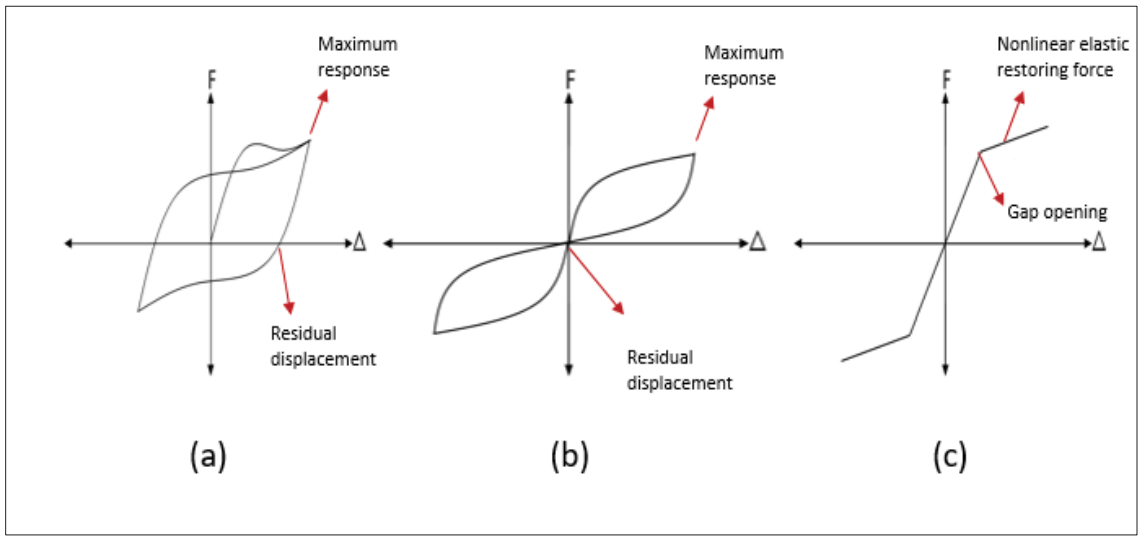

Figure 2.6 (a) Hysteretic behavior of conventional shear walls, (b) typical hysteretic behavior of ideal self-centering systems, and (c)restoring force in rocking and gap opening using PT tendons

In uncontrolled systems, the self-weight of structural components such as beams, slabs, and columns causes moment resistance at the structure's base and thereby lateral resistance for the whole structure (Liu et al., 2022; Zhong & Christopoulos, 2022b). The energy dissipation mechanism in these systems occurs through sliding, impact, and friction between structural components. In the second method, structural components benefit from innovative devices to gain more self-centering and energy dissipation ability. The next subsection briefly discusses one of the most used techniques in this field. Figure 2.7 shows various self-centering systems, which are comprehensively reviewed by (Zhong & Christopoulos, 2022a).

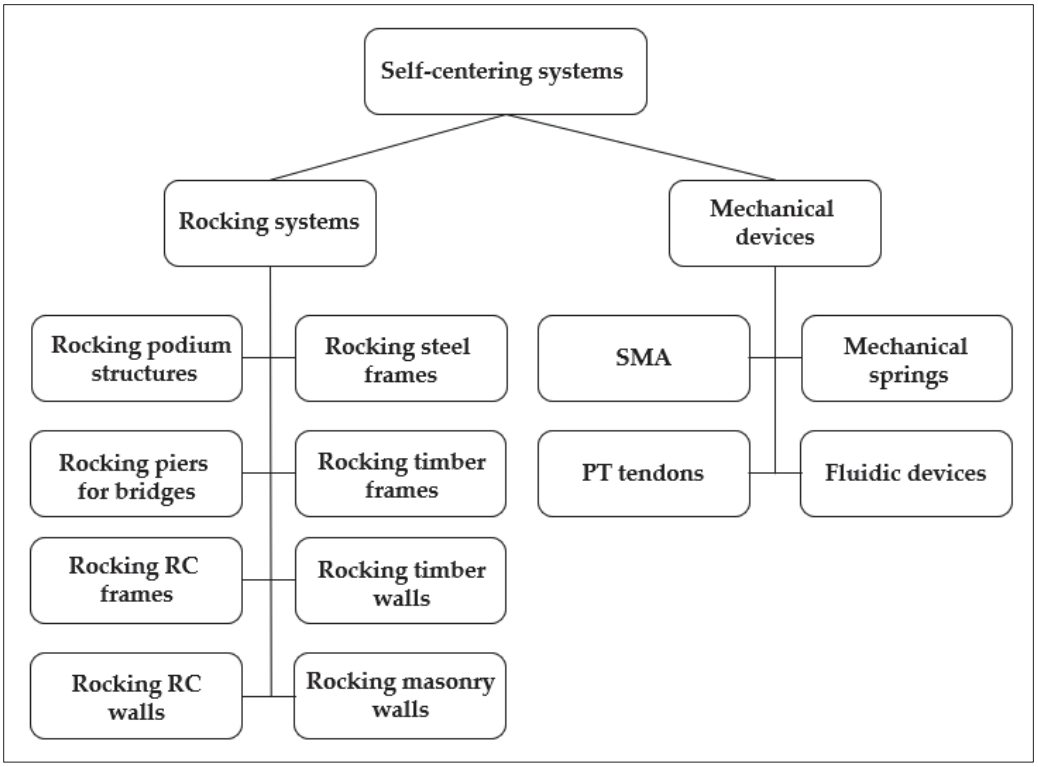

Figure 2.7 Various self-centering systems

2.5.2 Mechanical devices for self-centering

One of the most relevant techniques for self-centering is the use of shape memory alloy (SMA)-based systems. The super-elasticity property of SMA systems leads to the reduction of deformation after unloading. Indeed, SMA systems may recover up to 10% strain in some applications (Lecce, 2014). Therefore, these techniques are widely used in various industries such as medical, mechanical, aerospace, and civil engineering (Chandra, 2001; Speicher et al., 2008). This ability, coupled with its inherent energy dissipation, makes SMA a good choice for self-centering systems. However, SMA wires may present some disadvantages related to their reduced load capacity and challenging anchorage due to their slippery surface. Hence, devices that work based on SMA wires are mostly designed for uniaxial tensile loading cases, which restricts their wide use (Wang et al., 2020). Several research studies have been conducted to develop self-centering systems using SMA technology (Dolce & Cardone, 2006; Yang et al., 2010). (Soares et al., 2021) compared lateral strength, energy dissipation, drift

capacity, and recentering ability of conventionally reinforced and SMA-steel reinforced shear walls. Specimens for both reinforcement types were considered as 10-story shear walls designed for both eastern and western Canadian seismic zones, with similar geometry and reinforcement configuration. All the specimens were evaluated through nonlinear pushover and reverse cyclic finite-element analysis. The results showed similar lateral strength and drift capacity for both steel and hybrid SMA-steel reinforced walls, but the recentering ability of the walls with hybrid SMA-steel reinforcement was significantly higher. However, walls with steel reinforcement had more energy dissipation capacity. Nevertheless, due to the drawbacks and shortcomings of SMA, in many studies, hybrid systems using energy dissipators such as hysteretic, viscous, and frictional dampers are considered (Shook et al., 2008; Yang et al., 2010; Zhu & Zhang, 2008).

Another innovative technique for enhancing self-centering in structures is the application of fluidic devices. These practical devices have the main characteristics of a damper and an internal pressurized fluid action that provide recentering force in a structural component (Zhu et al., 2020). These devices' detailed application and design steps in structures are discussed by (Kitayama & Constantinou, 2016).

2.5.3 Resilience in RC structures

Structural seismic resilience is the ability to undergo large lateral displacements with the minimum level of damage, plastic hinge formation, and residual deformation through inherent self-centering ability or attached self-centering systems. Seismic-resilient structures can dissipate a large amount of energy and rapidly return to their initial position with little permanent deformation, which helps maintain the serviceability of the structures after severe seismic events.

Conventional steel-reinforced shear walls have self-centering ability within elastic deformations. However, as these walls experience large plastic deformations which are followed by concrete crushing, reinforcement yielding, and residual displacement, they

significantly lose their self-centering ability. In this regard, in recent decades, many studies have been carried out to increase self-centering ability and resilience in shear walls.

In ancient buildings, structures benefited from uncontrolled rocking systems in wide columns. These structural components took advantage of their self-weight to form moment resistance and resist lateral forces (Cline, 2010). Such systems are not as common as shear walls in modern buildings due to their poor seismic performance. In contrast, post-tensioned precast RC shear walls as an alternative SFRS showed high efficiency under seismic loads. This method is based on a gap opening system, in which longitudinal PT elements supply a recentering force in precast shear walls after gap opening at the base of the walls. Many studies have illustrated the performance improvement of these lateral force-resisting systems compared to conventional precast RC shear walls (Liu & Zhou, 2022; Smith et al., 2011; Tolou-Kian & Cruz-Noguez, 2022). Some studies have also investigated the use of energy dissipators incorporating PT elements (Aaleti & Sritharan, 2009; Marriott et al., 2009; Wu et al., 2019). This method has also been applied to CSWs, where gap opening formation was considered at the wall base and wall-CB joints. Changes in DC have been investigated, and improvements in ductility, energy dissipation, and strength have been observed (Kurama & Shen, 2004; Kurama et al., 2006).

As another efficient technique, using EB-FRP composites can improve resilience in structures where a large amount of seismic energy can be dissipated through reinforcement yielding and concrete crushing. In contrast, inherent elastic behavior and high strength of FRP composites can provide required self-centering forces and help the structure return to its primary position.

Many studies have evaluated the use of FRP reinforcements to improve blast resilience of concrete structures (Johnson et al., 2021a, 2021b). (Mutalib & Hao, 2011) carried out experimental studies on RC panels strengthened with EB-FRP. The study was conducted on four walls of the same geometrical characteristics, including a non-strengthened wall (w_1), an FRP-strengthened wall with no anchor (w_2), an FRP-strengthened wall with anchors at the boundary (w_3), and an FRP-strengthened wall with distributed anchors (w_4). The results

revealed that using EB-FRP can decrease residual displacement of walls under blast loads. More studies have been carried out on applying FRP bars to achieve seismic-resilient RC structures. (Billah & Alam, 2012) evaluated the hybrid application of SMA and FRP bars in columns to achieve an acceptable level of resilience in RC structures. The study showed improvement in energy dissipation and a significant decrease in residual displacement. The application of FRP bars improved resilience in frames (Fischer & Li, 2003). In this regard, applying EB-FRP sheets can be a beneficial choice for strengthening RC structures to achieve higher resilience and serviceability after seismic events (ElGawady et al., 2010). (Abbass et al., 2020) studied the hybrid application of EB-FRP sheets and SMA to decrease residual displacement of bridge columns. Although many studies have been conducted on applying FRP bars and SMA to achieve more resilient structures, most of them are appropriate for designing new structures. In this regard, EB-FRP sheets can be a good choice for existing complex structures. However, few studies have been dedicated to evaluating this technique's advantages. Figures 2.8 shows an overview of general self-centering systems in RC shear walls.

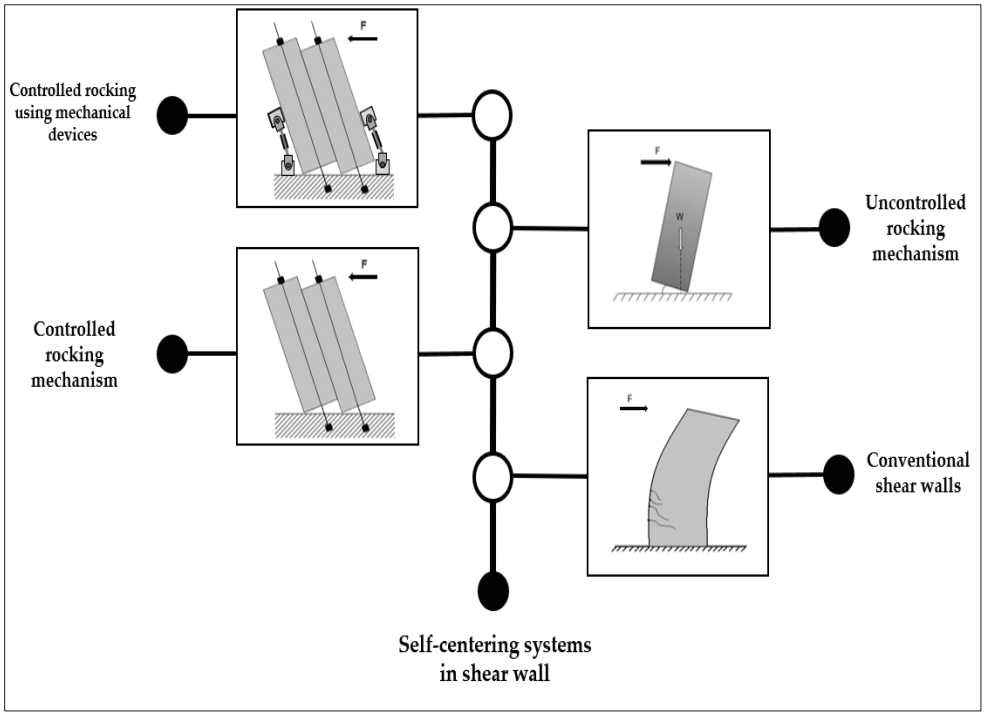

Figure 2.8 General self-centering systems in shear walls

A summary of 74 research studies on the evaluation of different self-centering methods can be found in Table 2.2. The statistical results in this table can contribute to figuring out the areas in which less research has been done so far. The contributions of the various structural components and methods evaluated in these studies are summarized in Figures 2.9 and 2.10 respectively. The statistical analysis underlying Table 2.2 is used in Sections 2.5 and 2.6 to describe the research needs and conclusions in this study.

Table 2.2 Summary of self-centering studies regarding method, structural components, and evaluated parameters. Note: (a) rocking podium structures, (b) rocking piers for bridges, (c) rocking RC frames, (d) rocking RC walls, (e) rocking steel frames, (f) rocking timber frames, (g) rocking timber walls, (h) rocking masonry walls, (i) SMA, (j) springs, (k) PT tendons, (l) fluidic devices, (SR) self-centering capacity or residual displacement, (ED) energy dissipation, (SO) stability and overturning, (St) stiffness, and (DR) other dynamic responses

Study	Method												Structure				Evaluated parameter				
	a	b	c	d	e	f	g	h	i	j	k	l	Column	Frame	Wall	Bridge piers	SR	ED	SO	St	DR
(Drosos & Anastasopoulos, 2014)	✓												✓				✓	✓			
(Drosos & Anastasopoulos, 2015)	✓												✓				✓	✓			
(Makris & Vassiliou, 2013)	✓												✓						✓		
(Mouzakis et al., 2002)	✓												✓				✓				
(Papaloizou & Komodromos, 2009)	✓												✓						✓		
(Dimitrakopoulos & DeJong, 2012)	✓												✓						✓		
(Vassiliou & Makris, 2015)	✓												✓							✓	

Table 2.2 Summary of self-centering studies regarding method, structural components, and evaluated parameters. Note: (a) rocking podium structures, (b) rocking piers for bridges, (c) rocking RC frames, (d) rocking RC walls, (e) rocking steel frames, (f) rocking timber frames, (g) rocking timber walls, (h) rocking masonry walls, (i) SMA, (j) springs, (k) PT tendons, (l) fluidic devices, (SR) self-centering capacity or residual displacement, (ED) energy dissipation, (SO) stability and overturning, (St) stiffness, and (DR) other dynamic responses (cont'd)

Study	Method												Structure				Evaluated parameter				
	a	b	c	d	e	f	g	h	i	j	k	l	Column	Frame	Wall	Bridge piers	SR	ED	SO	St	DR
(Makris & Aghagholizadeh, 2019)	✓												✓								✓
(Ríos-García & Benavent-Climent, 2020)	✓												✓				✓	✓			
(Mander & Cheng, 1997)		✓														✓				✓	
(Cai et al., 2018)		✓														✓	✓			✓	
(Chou & Chen, 2006)		✓									✓						✓	✓			
(Dawood et al., 2012)		✓									✓					✓			✓	✓	
(ElGawady & Dawood, 2012)		✓									✓					✓	✓			✓	
(Guerrini et al., 2015)		✓									✓					✓	✓	✓			
(Hung et al., 2011)		✓														✓					✓
(Ichikawa et al., 2016)		✓									✓					✓		✓			
(Palermo et al., 2007)		✓									✓					✓	✓				
(Nikoukalam & Sideris, 2017)		✓									✓					✓	✓	✓		✓	

Table 2.2 Summary of self-centering studies regarding method, structural components, and evaluated parameters. Note: (a) rocking podium structures, (b) rocking piers for bridges, (c) rocking RC frames, (d) rocking RC walls, (e) rocking steel frames, (f) rocking timber frames, (g) rocking timber walls, (h) rocking masonry walls, (i) SMA, (j) springs, (k) PT tendons, (l) fluidic devices, (SR) self-centering capacity or residual displacement, (ED) energy dissipation, (SO) stability and overturning, (St) stiffness, and (DR) other dynamic responses (cont'd)

Study	Method												Structure				Evaluated parameter				
	a	b	c	d	e	f	g	h	i	j	k	l	Column	Frame	Wall	Bridge piers	SR	ED	SO	St	DR
(Chou & Chen, 2006)		✓									✓					✓	✓	✓			
(Kashani et al., 2018)		✓														✓	✓				
(Motaref et al., 2014)		✓									✓					✓	✓	✓			
(Ou et al., 2007)		✓									✓					✓	✓	✓			
(Xu et al., 2019)		✓									✓					✓	✓	✓			
(Sideris et al., 2014)		✓									✓					✓	✓	✓			
(Salehi et al., 2017)		✓									✓					✓	✓	✓			
(Salehi et al., 2021)		✓									✓					✓	✓	✓			
(Buddika & Wijeyewickrema, 2016)			✓								✓			✓			✓				✓
(Erkmen & Schultz, 2009)				✓							✓				✓		✓				
(Guo et al., 2017)			✓								✓			✓			✓	✓			
(Perez et al., 2013)				✓							✓				✓		✓				
(Kurama, 2000)				✓							✓	✓			✓		✓	✓			
(Morgen & Kurama, 2008)			✓								✓			✓			✓	✓			

Table 2.2 Summary of self-centering studies regarding method, structural components, and evaluated parameters. Note: (a) rocking podium structures, (b) rocking piers for bridges, (c) rocking RC frames, (d) rocking RC walls, (e) rocking steel frames, (f) rocking timber frames, (g) rocking timber walls, (h) rocking masonry walls, (i) SMA, (j) springs, (k) PT tendons, (l) fluidic devices, (SR) self-centering capacity or residual displacement, (ED) energy dissipation, (SO) stability and overturning, (St) stiffness, and (DR) other dynamic responses (cont'd)

Study	Method												Structure				Evaluated parameter				
	a	b	c	d	e	f	g	h	i	j	k	l	Column	Frame	Wall	Bridge piers	SR	ED	SO	St	DR
(Guo et al., 2014)				✓											✓		✓	✓			
(Kurama, 2002)				✓							✓				✓		✓	✓			
(Restrepo & Rahman, 2007)				✓							✓				✓		✓	✓			
(Srithar an et al., 2015)				✓							✓				✓		✓	✓			
(Holden et al., 2003)				✓							✓				✓		✓	✓			
(Kurama & Shen, 2004)				✓							✓				✓		✓		✓		
(Xu et al., 2018)										✓					✓		✓	✓			
(Ricles et al., 2001)					✓									✓			✓			✓	
(Christo poulos et al., 2002)					✓						✓			✓			✓	✓			
(Wang & Filiatrau lt, 2008)					✓						✓			✓			✓	✓			
(Kim & Christop oulos, 2008)					✓						✓			✓			✓	✓		✓	
(Rojas et al., 2005)					✓						✓			✓			✓	✓			
(Roke, 2010)					✓						✓			✓			✓				
(Sause et al., 2010)					✓						✓			✓			✓	✓			

Table 2.2 Summary of self-centering studies regarding method, structural components, and evaluated parameters. Note: (a) rocking podium structures, (b) rocking piers for bridges, (c) rocking RC frames, (d) rocking RC walls, (e) rocking steel frames, (f) rocking timber frames, (g) rocking timber walls, (h) rocking masonry walls, (i) SMA, (j) springs, (k) PT tendons, (l) fluidic devices, (SR) self-centering capacity or residual displacement, (ED) energy dissipation, (SO) stability and overturning, (St) stiffness, and (DR) other dynamic responses (cont'd)

Study	Method												Structure				Evaluated parameter				
	a	b	c	d	e	f	g	h	i	j	k	l	Column	Frame	Wall	Bridge piers	SR	ED	SO	St	DR
(Eatherton & Hajjar, 2014)					✓						✓			✓			✓	✓			
(Eatherton et al., 2014)					✓						✓			✓			✓				
(Wiebe et al., 2013a)					✓						✓			✓			✓	✓			
(Wiebe et al., 2013b)					✓						✓			✓			✓	✓			
(Binder & Christopoulos, 2018)					✓						✓			✓			✓				
(Pollino et al., 2017)					✓						✓			✓			✓				
(Mottier et al., 2018)					✓									✓			✓	✓			
(Mottier et al., 2021)					✓									✓			✓	✓			
(Newcombe et al., 2008)						✓					✓			✓			✓	✓			
(Iqbal et al., 2016)						✓					✓			✓			✓	✓			
(Di Cesare et al., 2017)						✓					✓			✓			✓	✓			✓
(Di Cesare et al., 2020)						✓					✓			✓			✓	✓			
(Ganey et al., 2017)							✓				✓				✓		✓				
(Morodder et al., 2018)							✓				✓				✓		✓	✓			

Table 2.2 Summary of self-centering studies regarding method, structural components, and evaluated parameters. Note: (a) rocking podium structures, (b) rocking piers for bridges, (c) rocking RC frames, (d) rocking RC walls, (e) rocking steel frames, (f) rocking timber frames, (g) rocking timber walls, (h) rocking masonry walls, (i) SMA, (j) springs, (k) PT tendons, (l) fluidic devices, (SR) self-centering capacity or residual displacement, (ED) energy dissipation, (SO) stability and overturning, (St) stiffness, and (DR) other dynamic responses (cont'd)

Study	Method												Structure				Evaluated parameter				
	a	b	c	d	e	f	g	h	i	j	k	l	Column	Frame	Wall	Bridge piers	SR	ED	SO	St	DR
(Sarti et al., 2016)							✓				✓				✓		✓	✓			
(Pei et al., 2019)							✓				✓				✓		✓	✓			
(Loo et al., 2014)							✓								✓		✓	✓			
(Hashemi et al., 2018)							✓								✓		✓	✓			
(Cui et al., 2020)					✓		✓				✓			✓	✓		✓	✓			
(Li et al., 2021)					✓		✓				✓			✓	✓		✓	✓			
(Laursen & Ingham, 2001)								✓			✓				✓		✓	✓			✓
(Rosenboom & Kowalsky, 2004)								✓			✓				✓		✓				
(Wight et al., 2006)								✓			✓				✓		✓	✓			
(Hassanli et al., 2016)								✓			✓				✓		✓				
(Niu & Zhang, 2017)								✓			✓				✓		✓	✓			✓
(Toranzo et al., 2009)								✓							✓		✓	✓			
(Navarro-Gómez & Bonet, 2019)										✓				✓			✓	✓			

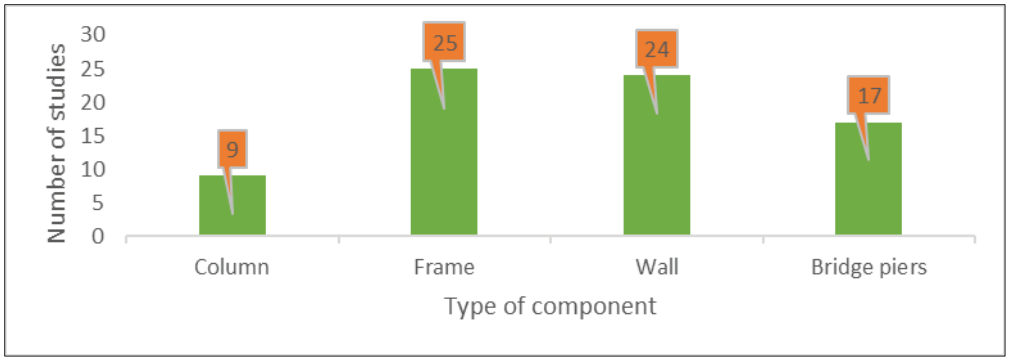

Figure 2.9 Visualization of the summarized research based on the investigated components

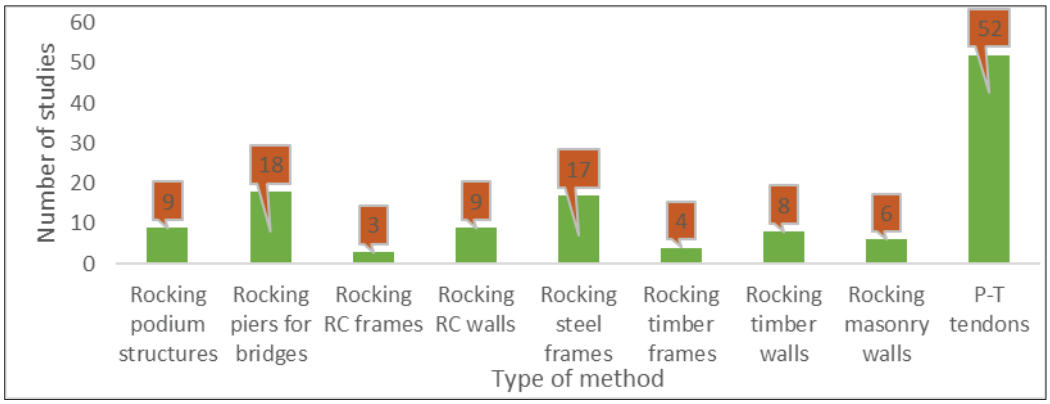

Figure 2.10 Visualization of the summarized research based on the method discussed

2.6 Research needs

This paper has presented a summary of the state of the art of the research dealing with problems related to the stability, strengthening, and resilience of RC structures. It clearly revealed the urgent need to develop a feasible, efficient, and applicable technique to reduce residual displacement and enhance resilience in shear walls. In the last few decades, extensive research has been devoted to FRP and its applications for strengthening RC structures. In parallel, many researchers have evaluated self-centering improvement methods and residual displacement reduction techniques in reinforced concrete structures, specifically shear walls. As shown in Figure 10, most of the research carried out so far has been related to either PT and rocking

methods or systems using mechanical devices, which can only be used in the design of new structures. Considering the excellent performance of EB-FRP in the seismic strengthening of concrete structures and the need to strengthen existing shear walls against large deformations, there is a need to conduct comprehensive research on the use of EB-FRP to increase the self-centering ability of existing RC structures. The exact expression of the required configuration, width, and number of FRP sheets, the mechanical characteristics, and the way to connect FRP to concrete are among the issues that need to be addressed in this research. Some other significant concerns that should be studied are: (i) evaluate the changes in parameters after the use of EB-FRP in SSWs and CSWs, such as displacement and residual displacement, hysteretic behavior, displacement ductility, failure mode, sequence of failure, stiffness degradation, energy dissipation, strength retention, and sequence of hinge formation; (ii) optimize EB-FRP properties and configuration for CSWs and SSWs to achieve the lowest residual displacement. Figure 11 illustrates the parameters that could influence the residual displacement in strengthened shear walls using EB-FRP.

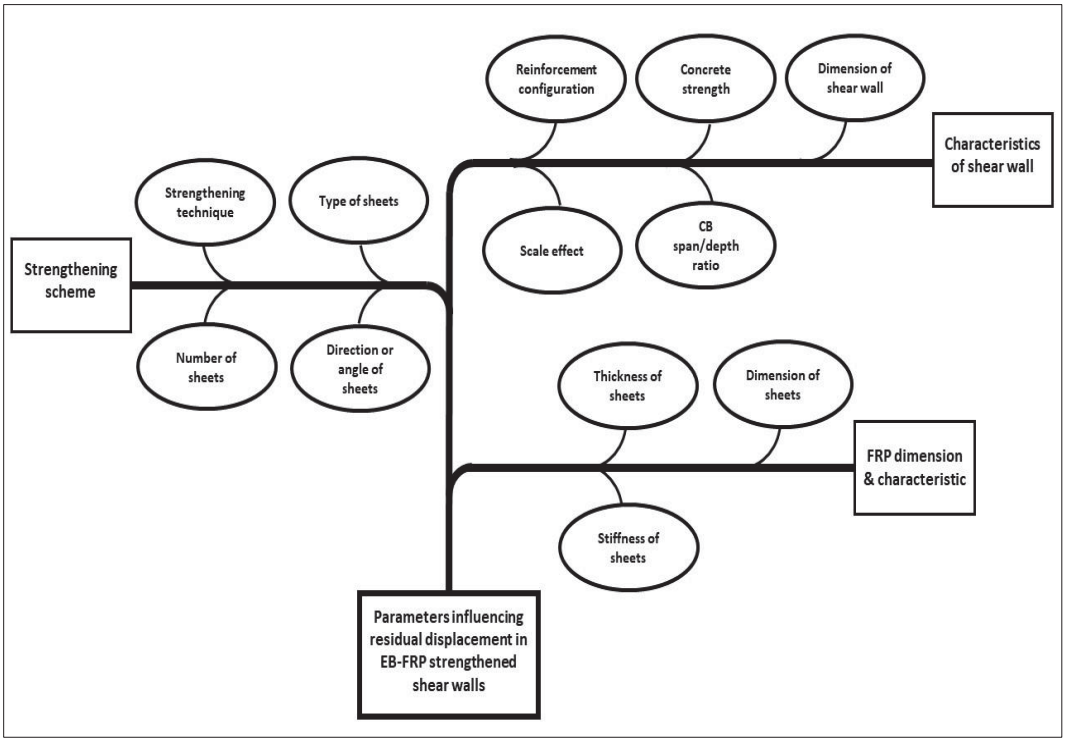

Figure 2.11 Overview of the parameters influencing residual displacement in EB-FRP strengthened shear walls

2.7 Conclusion

This paper has presented the state of the art of self-centering enhancement methods in shear walls and FRP applications for strengthening RC structures. Evaluating their advantages and disadvantages and considering the importance of paying attention to issues such as failure mode and sequence of failure, ductility, energy dissipation, and sequence of hinge formation, the following conclusions were drawn :

- RC structures strengthened with EB-FRP sheets showed outstanding performance in seismic events. This reliable technique can improve RC structures' shear, flexural, axial, fatigue, and impact strength using different configurations such as side bonding, U-wrap, and complete wrapping.
- Most studies have been done to improve self-centering ability in new structures, mainly using PT tendons, SMAs, and other innovative devices. Few studies have focused on self-centering enhancement in existing structures.
- Currently, there are no explicit data on the ability of EB-FRP to enhance the resilience and self-centering ability of existing shear walls; hence, future studies should focus more on evaluating this method's effectiveness.

Accordingly, the authors established a research need to develop methods and techniques to improve the self-centering ability of CSWs and SSWs using EB-FRP. In addition to being cost-effective, these methods will help the environment by preventing the deconstruction and replacement of concrete elements and reducing thereby CO_2 emissions in the environment resulting from cement production. The cement industry is one of the leading causes of global warming, with a share of cement production in global CO_2 emissions of approximately 7%.

CHAPTER 3

RESILIENCE OF MEDIUM-TO-HIGH-RISE DUCTILE COUPLED SHEAR WALLS LOCATED IN CANADIAN SEISMIC ZONES AND STRENGTHENED WITH EXTERNALLY BONDED FIBER-REINFORCED POLYMER COMPOSITE: NONLINEAR TIME HISTORY ASSESSMENT

Ali Abbaszadeh and Omar Chaallal,

Department of Construction Engineering, École de Technologie Supérieur, Université du Québec, Montréal, QC H3C 1K3, Canada

Paper published in *Journal of Composites Science*, *Volume 7, Issue 8, Article 317*, July 2023

3.1 Abstract

Coupled shear walls (CSWs) are structural elements used in reinforced concrete (RC) buildings to provide lateral stability and resistance against seismic and wind forces. When subjected to high levels of seismic loading, CSWs exhibit nonlinear deformation through cracking and crushing in concrete and yielding in reinforcements, thereby dissipating a significant amount of energy, leading to their permanent deformation. Externally bonded fiber-reinforced polymer (EB-FRP) sheets have proven to be effective in strengthening RC structures against various loading and environmental conditions. In addition, their high strength-to-weight ratio makes them an attractive solution as they can be easily applied without significantly increasing the structure's weight. This study investigates the effectiveness of using EB-FRP sheets to reduce residual displacement in CSWs during severe earthquake loadings. Two series of 15-story and 20-story CSWs in Western and Eastern Canadian seismic zones, which serve as representative models for medium- and high-rise structures, were evaluated through nonlinear time history analysis. The numerical simulation of all CSWs and strengthened elements was carried out using the RUAUMOKO 2D software. The findings of this study provided evidence of the effectiveness of EB-FRP sheets in reducing residual deformation in CSWs. Additionally, significant reductions in the rotation of the coupling beams (CBs) and the inter-story drift ratio were observed. The results also revealed that bonding vertical FRP sheets to boundary

elements and confining enhancement by wrapping CBs and wall piers is a very effective configuration in mitigating residual deformations.

Keywords: coupled shear wall; residual displacement; fiber-reinforced polymer; resilience; self-centering; nonlinear time history analysis

3.2 Introduction

The use of coupled shear walls (CSW) in reinforced concrete (RC) buildings has proven to be a highly effective solution for resisting seismic forces. These walls offer increased lateral stiffness and strength and provide efficient seismic energy dissipation. A typical CSW system is composed of two wall piers interconnected by coupling beams (CBs). The role of the coupling beam is to distribute lateral loads evenly between the two wall piers, thereby preventing excessive stress or deformation. In addition, the beam's geometry ensures that shear forces generated by lateral loads are shared in a balanced manner between the two wall piers, enabling the walls to work synergically for an enhanced lateral resistance.

The seismic behavior of CSW systems is significantly impacted by the capacity of the CBs to undergo rotational and vertical deformation during earthquakes. Thus, ensuring adequate rotational ductility in the sections of the CBs is crucial for attaining a ductile performance of the shear walls and enhancing the overall seismic resilience of the system by the dissipation of seismic energy through inelastic deformations (Afefy, 2020). Conventionally reinforced CBs are prone to sliding shear failure at the beam–wall joints. The transverse reinforcements in these beams are typically incapable of resisting the shear forces generated during seismic excitations. Therefore, diagonally reinforced CBs have been developed as a solution (Paulay & Santhakumar, 1976). These beams are designed to resist shear forces and moments, and consist of diagonal bars that run throughout the beam and intersect at its midpoint. Confining stirrups are often utilized to ensure the stability of the diagonal bars under large lateral loads. These stirrups confine the concrete, enhancing its compressive strength, and preventing buckling of the diagonal reinforcements.

RC structures are frequently rehabilitated or strengthened to withstand various factors, including aging, increased loads, design codes and standards changes, and seismic upgrading to ensure their continued safety, serviceability, and durability. In addition, seismic upgrading in areas susceptible to earthquakes is essential to reduce the detrimental impact of seismic activity on structures. The objective of seismic upgrading is to enhance the resistance of the structural system to seismic forces, reduce the possibility of damage through the loading and unloading process (Franchi et al., 2022), and enhance the overall performance of the structure during an earthquake.

FRPs have become increasingly popular due to several key advantages, including their high strength-to-weight ratio, corrosion resistance, ease of installation in complex structures, and cost-effectiveness. The application of EB-FRP sheets has emerged as a promising retrofitting strategy for strengthening and enhancing the seismic performance of RC CSWs. The seismic behavior of CSWs can be improved: (i) by enhancing wall pier capacity via EB-FRP sheets in several ways, such as positioning the sheets parallel to the wall axis (Arabzadeh & Galal, 2015, 2017; Elnady, 2008) or perpendicular to the wall axis (Sakr et al., 2017b), wrapping the wall sections along the height, especially in the potential plastic hinge zones (Arabzadeh & Galal, 2015; Layssi et al., 2012b), and implementing X-bracing on the wall surface (Arabzadeh & Galal, 2017; El-Sokkary & Galal, 2013; Sakr et al., 2017b); (ii) by applying FRP sheets to CBs by bonding the sheets perpendicular to the CB axis (Lavorato et al., 2018), installing diagonal strips on both sides (Honarparast & Chaallal, 2019b; Honarparast et al., 2019), and fully wrapping (Arabzadeh & Galal, 2017) or U-wrapping (El-Sokkary, 2023; Fathalla et al., 2022). Note that the number of bonded FRP layers is a crucial factor in reaching the effectiveness of these strengthening schemes. In a study by (Arabzadeh & Galal, 2017), the impact of FRP retrofitting of a 12-story coupled C-shaped RC core system was evaluated. The authors modified a previously proposed wide-column model to capture the inelastic torsional behavior. Additionally, the authors introduced a simplified spring model to reflect the effect of FRP retrofitting. The nonlinear incremental dynamic analysis results showed that using EB-FRP strengthening can significantly enhance the collapse resistance of RC core wall systems by

more than 60%. (Layssi et al., 2012b) evaluated the impact of fully wrapping the plastic hinge zone of shear walls having poorly lap-spliced details using FRP. The results showed that this technique led to a remarkable improvement in terms of both energy dissipation and displacement ductility, and prevented brittle failure by privileging yielding of the primary flexural reinforcements in the walls. (Honarparast et al., 2019) investigated a new method for strengthening CBs using EB-FRP sheets. They tested two CB specimens, one control and the other reinforced with FRP, designed according to the NBCC 1941 code. The specimens were subjected to cyclic loading and compared in terms of energy dissipation and hysteretic behavior. The control specimen showed the yielding of rebars and shear cracks at joint locations during loading, while the strengthened model exhibited improved load-carrying capacity before FRP debonding. In addition, the control specimen showed significant pinching, stiffness degradation, and loss of energy dissipation capacity. In contrast, the strengthened specimen showed limited pinching and stiffness degradation before the rapid load reduction at the final load cycle.

The ineffectiveness of equivalent elastic force methods of analysis and design in addressing the destructive consequences of earthquakes was revealed after several major earthquake events, such as the Northridge earthquake in 1994 and the Kobe earthquake in 1995 (Pecker, 2008). As a result, the need for more accurate methods for evaluating seismic demand on structures became evident, as these methods consider both geometrical and material nonlinearities. Currently, the nonlinear time history (NLTH) analysis method is widely used and recognized as the most accurate method for assessing the response of structures subjected to severe seismic excitation (Wu, 2014). The seismic performance of CSWs has been evaluated through the conduct of several nonlinear analyses in recent years (El-Sokkary, 2023; Honarparast & Chaallal, 2019b; McNeice, 2004). Some researchers have examined the improvement in nonlinear responses of structures retrofitted with EB-FRP. (Honarparast & Chaallal, 2019b) evaluated the seismic performance of old-designed (NBCC 1941) and modern-designed (NBCC 2015) 20-story CSWs located in Vancouver. They assessed the effectiveness of EB-FRP retrofitting on the seismic response of old-designed CSWs. Nonlinear time history analyses were carried out using RUAUMOKO 2D and simulated earthquake

records. The retrofitting scheme employed in this study consisted of applying vertical and horizontal EB-FRP sheets on the wall piers to enhance their flexural and shear capacities, respectively. Additionally, to improve the seismic performance of the conventionally reinforced CBs, diagonal EB-FRP sheets were attached to both faces of the CBs. The results illustrated that the application of the EB-CFRP retrofitting technique significantly improved the seismic performance of the old CSWs, as evidenced by the reduction in story displacement, inter-story drift, wall curvature, and improved CB rotation. (El-Sokkary, 2023) conducted a nonlinear time history analysis to evaluate the effectiveness of U-wrap EB-FRP sheets as a retrofitting method for increasing the rotational ductility of concrete beams (CBs) in 10-story and 15-story buildings. CBs were modeled using the lumped plastic method, in which an elastic beam with two plastic springs at each end represents the CB. The results indicated that adding one, two, or three layers of U-wrap FRP improved the CBs' ductility to limited, moderate, and ductile levels, respectively. Furthermore, the inter-story drift capacity of the 10- and 15-story buildings were improved by up to 277% and 203%, respectively, through the FRP retrofit of the CBs. Boivin and Paultre (Boivin & Paultre, 2010) evaluated the seismic performance of a 12-story ductile concrete core wall in an office building in Montreal, which consisted of a cantilever and a coupled wall system. The primary purpose of this study was to evaluate the shortcomings and underestimation of previous Canadian codes and standards concerning the seismic design of shear walls. The study confirmed the underestimation of the capacity design shear envelope, because of an underestimation of the NBCC spectral response acceleration and a deficiency in the capacity design method.

Despite the extensive research conducted in nonlinear analysis of retrofitted CSWs, a significant gap still exists in the literature regarding the reduction of residual displacement and improvement in the resilience and self-centering ability of CSWs. Residual displacement refers to a structure's permanent deformation or displacement after a seismic event. In the case of CSWs, residual displacement occurs due to the formation of plastic hinges in the wall piers and CBs. The magnitude of residual displacement can significantly impact the safety and functionality of a structure, as well as the need for costly repairs, maintenance, or replacement (Ye et al., 2008). (Bruneau & Reinhorn, 2006) comprehensively discussed seismic resilience

in structures and defined different concepts (social and physical) for resilience. They established limits for the inter-story drift in structures during nonlinear responses to measure seismic resilience. They showed that retrofitting structures can affect fragility and performance boundary levels, and neglecting seismic retrofitting can lead to structural failure and collapse. Accordingly, the notion of seismic resilience in structures is associated with the capacity of the structure to endure substantial lateral displacements with minor damage (plastic hinge formation) and residual deformation. This capability can be achieved either through the natural self-centering properties of the structure or through the use of attached self-centering systems. It is worth noting that improving the resilience and strength of structures is crucial, not only for direct costs like repairing damage or lives lost from seismic hazards but also for considering indirect costs. These additional costs include disruptions to the structure's function, damages to the surrounding area, and impacts on other networks, like roads and utilities. It is essential to prevent a chain reaction of problems occurring when a structure fails due to a seismic event. More discussions in this regard can be found elsewhere (Adey et al., 2004; Brookshire et al., 1997; Forcellini, 2019). Also, implementing seismic retrofitting reduces the necessity for demolishing and renovating buildings. This, in turn, leads to a decrease in cement consumption, which is beneficial for the environment as cement production generates a significant amount of greenhouse gas emissions, contributing to global warming (de Oliveira et al., 2022).

The self-centering ability of structures refers to their capability to return to almost their original position after a seismic event without significant permanent deformation (Abbaszadeh & Chaallal, 2022). This advantage can be improved through two prevalent methods, namely: (i) rocking motion that enhances mechanical resistance by uplifting the whole structure or significant structural components, and (ii) the use of mechanical devices that incorporate energy dissipators and shape memory alloys (SMAs) (Abbaszadeh & Chaallal, 2022). A rocking motion is achieved through either post-tensioned (PT) tendons, which results in controlled rocking, or self-weight, which results in uncontrolled rocking (Chancellor et al., 2014). Controlled rocking systems utilize pre-compressed PT elements at the surface of the structural components. When lateral forces negate the pre-compression forces, the joint section

decompresses, creating a gap. The PT elements then regain the lost stiffness of the lateral resistance system through axial stiffness. Failure may occur if the strain at the joint surpasses the elastic strain limit of the PT element. The effectiveness of using PT elements in the self-centering improvement of structures has been investigated in previous research studies (Abbaszadeh & Chaallal, 2022; Bedriñana et al., 2022; Holden et al., 2003; Marriott et al., 2009).

SMAs, on the other hand, reduce deformation after unloading due to their super-elasticity property. It has been demonstrated that the use of SMAs can decrease the strain by 10% in specific applications (Lecce, 2014), and, due to their inherent capacity for energy dissipation, SMAs are considered a viable option for self-centering methods. Despite their potential benefits, SMA wires feature certain drawbacks, such as a reduced load-bearing capacity and difficulties in anchoring them properly due to their slippery surfaces. As a result, SMA-based devices are primarily designed for uniaxial tensile-loading situations, thereby limiting their widespread application (Wang et al., 2020). The use of SMAs and energy dissipators for enhancing the self-centering capability of structures has been studied previously in several research investigations (Qian et al., 2023; Soares et al., 2021; Yang et al., 2010). Moreover, some research studies have examined the feasibility of integrating mechanical equipment, such as friction and viscous dampers, disk springs, and energy-dissipating devices (Chancellor et al., 2014; Naeem & Kim, 2018; Noureldin et al., 2021). The outcomes of these investigations have confirmed the effectiveness of these devices in improving the self-centering capacity of steel and RC structures. However, the use of these devices is not widespread due to architectural limitations.

Furthermore, the literature has explored other methods to mitigate residual displacement in shear walls. (Shen et al., 2022) conducted a study to assess the effectiveness of CFRP grids in reducing residual deformation in shear walls with varying failure modes, taking into account the aspect ratio and reinforcement ratio. (Song et al., 2020) performed experiments to evaluate the cyclic behavior of a hybrid approach combining CFRP grids and steel in six large-scale

shear walls. (Zhao et al., 2019) demonstrated that CFRP bars are an effective alternative to low-yield strain steel bars in reducing residual deformation in RC shear walls.

In the current literature on self-centering systems, research has focused primarily on improving the self-centering properties and reducing residual displacement in newly designed and detailed structures. Although some studies have explored the application of mechanical equipment such as dampers and disk springs to increase self-centering in existing steel and RC frames, research on reducing residual displacement in existing CSWs is limited. This has been the leading momentum to implementing a novel approach by focusing on reducing residual displacement in existing CSWs by applying EB-FRP sheets. This research fills a gap in the current understanding of self-centering systems, and offers a unique contribution to improving seismic performance in existing structures. Accordingly, this study aims to examine the efficiency and performance of various configurations of EB-FRP sheets in reducing residual displacement in existing CSWs and their impact on seismic parameters, including CB rotation, shear force and bending moment demand, and inter-story drift. To this end, a comprehensive evaluation of 20-story and 15-story CSWs in Montreal and Vancouver is conducted using advanced RUAUMOKO 2D software. The evaluation includes nonlinear time history analyses and a curated selection of 15 ground motions for Vancouver and 11 for Montreal. The CSWs are tested under various scenarios, including three strengthening configurations and non-strengthened conditions. The analysis results effectively visualize the impacts of the strengthening schemes on the parameters assessed.

3.3 Canadian Seismic Design Provisions for Ductile Walls

3.3.1 Force-Based Design Provisions

The force-based design technique is currently the prominent approach used in the seismic design provisions of Canada for RC shear walls. This method calculates the internal forces and stresses that develop within a structure due to applied loads, based on the elastic design spectrum. Nevertheless, these values are subsequently adjusted by reduction factors, which

include those related to overstrength (R_o) and ductility (R_d), to account for the structure's inelastic behavior (Sadeghian, 2018). According to the National Building Code of Canada (NBCC20), the equivalent plastic seismic shear force at the base of building shall be calculated, as given in Equation 3.1 :

$$V_{base} = S(T_a)M_v \frac{I_E}{R_d R_o} W \tag{3.1}$$

In Equation 3.1, T_a represents the fundamental period of the structure, and $S(T_a)$ = the design spectral response acceleration corresponding to T_a and is based on a 2% probability of exceedance in 50 years. The factor that accounts for higher mode effects is represented by M_v, while the importance factor is denoted by I_E. The weight of the structure, represented by *W*, can be calculated as the sum of the dead load and 25% of the snow load (*W = DL + 0.25SL*).

The precise classification of walls is crucial in determining the accurate value of the ductility-related force modification factor, R_d, as CSWs are defined for a higher amount of it. When considering a wall with openings that are proportionately small compared with the height of the wall and are surrounded by upper and lower solid and rigid segments, the behavior of the wall can be classified as that of a cantilever single shear wall. Determining whether these segments possess sufficient stiffness to treat the wall as a single entity is a complex task. To address this issue, a concept known as the degree of coupling (*DOC*) should be computed, as given in Equation 3.2.

$$DOC = \frac{Pl_{cg}}{M_1 + M_2 + Pl_{cg}} \tag{3.2}$$

where l_{cg} = the span between two walls from center to center; M_1 *and* M_2 = the moments at the base of each wall; and *P* = axial force developing from the coupling action. *DOC* is a measure of the contribution of tension–compression forces in wall piers, originating from the shear in coupling beams, to the base overturning moment resistance. When this parameter

approaches one, the CSW behaves more like a cantilever shear wall. The Canadian Standards Association (CSA) A23.3-19 categorizes CSWs based on their DOC; those with a DOC greater than 66% are classified as coupled walls, and those with a DOC less than 66% are partially coupled. For ductile shear walls, NBCC20 defines the ductility-related factor (R_d) and overstrength-based factor (R_o), as given in Table 3.1.

Table 3.1 Ductility-related factors (R_d) and overstrength-based factors (R_o)

Type of Ductile Wall	**Force Modification Factor**	
Coupled wall	R_d = 4	R_o = 1.7
Partially coupled wall	R_d = 3.5	R_o = 1.7
Shear wall	R_d = 3.5	R_o = 1.6

Thereafter, V_{base} is to be distributed between the floors corresponding to their weight and height, as given in Equation 3.3.

$$F_i = (V_{base} - F_t)\frac{W_i h_i}{\sum_{i=1}^{n} W_i h_i} \tag{3.3}$$

In Equation 3.3, F_i = the force at floor *i*. If the period of a structure exceeds 0.7 s, it is necessary to consider the impact of higher modes. In such cases, a portion of the base shear, denoted by F_t, should be allocated to the top floor of the building and should be computed, as given in Equation 3.4. W_i = the weight given to the i^{th} floor, and h_i = the height of the i^{th} floor over the base level.

$$F_t = 0.07 T_a V_{base} \leq 0.25 V_{base} \tag{3.4}$$

To ensure the accuracy and reliability of the design of medium-to-high-rise buildings for seismic events, it is necessary to conduct equivalent static and dynamic analyses. Equivalent static analysis is a convenient method for the preliminary design and estimation of seismic

loads. Nevertheless, it is unable to account for the dynamic behavior of structures. Instead, it allocates forces in an ascending manner along the structure's height, relying on the first dynamic vibration mode. This may result in floors experiencing a more significant applied force due to other modes. Conversely, dynamic analysis offers a more precise depiction of buildings' actual behavior during seismic events. However, the base shear calculated through dynamic analysis needs to be calibrated by equivalent static analysis.

In the linear analysis of RC structures, it should be noted that the concrete undergoes cracking as the lateral load increases, which reduces the initial stiffness and other sectional properties. On the other hand, the general response of concrete is nonlinear. Therefore, to account for the average cracking effect in various element types, CSA A23.3-19 suggests the reduction factors presented in Table 3.2.

Table 3.2 Section effective properties for linear dynamic analysis suggested by CSA A23.3-19

Element	**Property**	**Effective Property**
Diagonally reinforced CB	Moment of inertia	$I_e = 0.25I_g$
	Shear area	$A_{ve} = 0.45A_g$
Wall	Flexural stiffness	$EI_e = \alpha_w \mathrm{E} I_g$
	Axial stiffness	$EA_{xe} = \alpha_w \mathrm{E} A_g$

In Table 3.2, I_e and I_g represent the effective and the gross section moment of inertia, respectively. A_{ve}, A_{xe}, and A_g represent the effective shear cross section, the effective axial cross section, and the gross area of section, respectively. For ductile CSWs, the value of α_w can be considered 0.5 at the initial stage of analysis (Canada & Association, 2016).

3.3.2 Capacity Design Provisions

It has been widely recognized that it is not cost-effective for structures to resist seismic forces while remaining within the elastic domain. Therefore, the seismic-resistant design of structures relies on the ability to dissipate energy with minimal loss of strength during multiple cyclic loading (Paulay & Santhakumar, 1976). To guarantee sufficient ductility, resistance, and stiffness in CSWs, the CSA A23.3-19 implements capacity design principles. This approach allows designers to control the plastic mechanism of the shear walls by incorporating overstrength in specific structural elements. The primary structural stability elements, wall piers, must be designed to have sufficient stiffness to ensure that the structure's overall stability is not compromised by incoming loads. Conversely, coupling beams (CBs) must be designed to absorb and dissipate the seismic energy by forming plastic hinges at designated zones.

In order to achieve the aims of capacity design provisions for CSWs, it is essential to adhere to three fundamental principles: (i) wall piers need specific reinforcement detailing in the potential plastic hinge region (i.e., the base of wall piers) to ensure large plastic deformation without significant strength loss (Canada & Association, 2016); (ii) the CSWs should be designed and detailed so that flexural yielding occurs at the end of CBs prior to the base of the wall piers (e.g., weak beam–strong column in frames); and (iii) the inelastic rotational capacity of both CBs and wall piers (within the plastic hinge region) must exceed their corresponding rotational demand.

Inelastic rotational demand (θ_{id}) in wall piers shall be calculated using Equation 3.5.

$$\theta_{id} = \frac{\Delta_f R_o R_d}{h_w} \tag{3.5}$$

In Equation 3.5, based on the linear analysis, Δ_f is the factored displacement and h_w denotes wall height.

Inelastic rotational capacity (θ_{ic}) in wall piers can be calculated using Equation 3.6.

$$\theta_{ic} = \left(\frac{\varepsilon_{cu}\ell_w}{2c} - 0.002\right) \tag{3.6}$$

where ε_{cu} = 0.0035 except for the compression zone of the wall with different confinement details, ℓ_w = length of CSW, and c = depth of neutral axis.

Also, (CSA) A23.3-19 recommends Equation 3.7 to calculate the height of the plastic hinge region, h_p, in wall piers.

$$h_p = 0.5\ell_w + 0.1h_w \tag{3.7}$$

Then, the inelastic rotational demand in CBs can be calculated using Equation 3.8.

$$\theta_{id} = \left(\frac{\Delta_f R_o R_d}{h_w}\right)\frac{\ell_{cg}}{\ell_u} \tag{3.8}$$

In Equation 3.8, ℓ_u = the length of the beam clear span, and ℓ_{cg} = the length between the wall piers' centroids. Furthermore, the inelastic rotational capacity of diagonally reinforced CBs shall be considered 0.04.

In compliance with capacity design provisions, it should be noted that the combined effects of gravity and seismic loads generate axial forces in CSWs. Seismic loads induce shears in the diagonal reinforcement of the CBs, which subsequently act as axial loads on the corresponding wall piers' sections. Therefore, each section should be able to resist the sum of the shear forces required to yield the coupling beams above the section. Additionally, in designing each section of wall piers, it is imperative to ensure that the factored bending moment resistance exceeds the bending moment arising from both the nominal resistance of the coupling beams acting into the corresponding sections and the applied bending moment of the wall piers. Accordingly, the wall over-strength factor, , γ, as given in Equation 3.9, should be applied to the factored wall moments at each level (Honarparast & Chaallal, 2019b).

$$\gamma = \frac{\sum V_n}{\sum V_f} \tag{3.9}$$

Where $\sum V_n$ = the sum of the nominal shear resistance of CBs, and $\sum V_f$ = the total factored shear in CBs due to lateral loading above the corresponding level.

More details and design requirements of CSWs, including restriction in compressive strength of concrete, lap splice length, concentrated and distributed reinforcements, maximum span/depth ratio of CBs, the minimum number of diagonal reinforcements, length of diagonal reinforcement anchorage in wall piers, hoop spacing in diagonal reinforcements, and plastic hinge specific requirements, are discussed in CSA A23.3-19.

3.4 Details and Geometry of the Case Study

This study evaluated two series of 20-story and 15-story buildings located in Montreal and Vancouver. The buildings under investigation feature RC structures with SFRS made of four CSWs in North–South (N–S) and two CSWs in West–East (W–E) directions. However, as the buildings may experience ground motion acceleration in both directions, this study primarily evaluates the seismic demand in the N–S direction. The shear walls of this structure are uninterrupted from the base to the top level, and they are relied upon to resist all lateral loads. Additionally, all floor plans are symmetrical, with no level variations. This creates regularity in both the plan and elevation of the structure. All four CSWs have CBs between floors level with a 2.0 m clear span, 400 mm width, and the same reinforcement layout in the corresponding level, connected at each end to a 3.25 m length wall pier with constant geometry along the building height. The floor dimension is 23 m by 35 m, and has a 200 mm thick concrete slab with compressive strength, f_c', of 30 MPa, and steel reinforcement yield strength, f_y, of 400 MPa. All floors have a 3.5 m height, resulting in a total height of 52.5 m and 70 m for 15-story and 20-story CSWs, respectively. Figure 3.1 presents the plan view and 2D layout of CSWs.

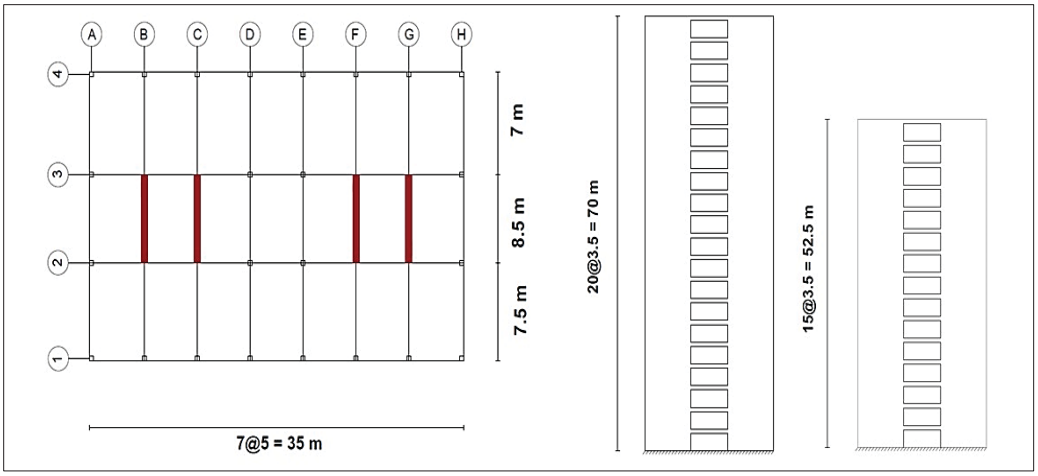

Figure 3.1 Plan view and 2D layout of CSWs

During the design phase, the first step involved the computation of lateral forces using Equations 3.1 and 3.3. Subsequently, a linear dynamic analysis was performed using SAP2000 software v19.0.0 to obtain the design forces in the CBs and wall piers. Finally, the CSWs were designed following standard specifications, utilizing the internal forces that were previously calculated. A similar building is discussed in (Honarparast & Chaallal, 2022). Also, a step-by-step guide for the design and detailing of shear walls can be found in concrete design handbook. Figure 3.2 illustrates the reinforcement layout in wall piers and CBs; specific details and quantities are provided in Tables 3.3 and 3.4.

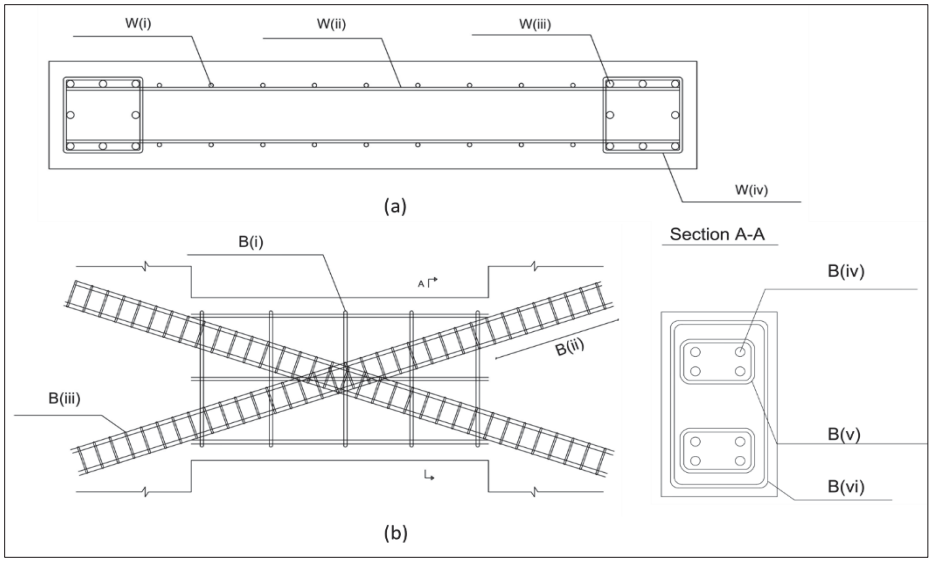

Figure 3.2 Reinforcement layout in (a) wall piers, and (b) CBs

Table 3.3 Reinforcement details of wall piers

		W (i) (mm)	**W (ii) (mm)**	**W (iii) (mm)**	**W (iv) (mm)**	**Section Dimension (mm)**
West	20-story	15M @200	10M @200	8M 30 in PH region 8M 25 out of PH region	10M @150	8250 × 400
	15-story	10M @200	10M @250	4M 25 in PH region 4M 20 out of PH region	10M @200	8250 × 400
East	20-story	15M @200	10M @250	6M 25 in PH region 6M 20 out of PH region	10M @150	8250 × 400
	15-story	10M @200	10M @250	4M 20 in PH region 4M 15 out of PH region	10M @200	8250 × 400

Table 3.4 Reinforcement details of coupling beams

		B (i) (mm)	**B (ii) (mm)**	**B (iii) (mm)**	**B (iv) (mm)**	**B (v) (mm)**	**B (vi) (mm)**	**Section Dimension (mm)**
West	20-story	10M @250	1500 mm stories 1–7 1300 mm stories 8–16 850 mm stories 17–20	10M @80	25M stories 1–7 20M stories 8–16 15M stories 17–20	10M @100	10M @200	750 × 400
	15-story	10M @250	1300 mm stories 1–5 850 mm stories 6–10 700 mm stories 11–15	10M @100	20M stories 1–5 15M stories 6–10 10M stories 11–15	10M @150	10M @250	750 × 400
East	20-story	10M @250	1100 mm stories 1–5 950 mm stories 6–13 700 mm stories 14–20	10M @100	25M stories 1–5 20M stories 6–3 15M stories 14–20	10M @100	10M @200	750 × 400
	15-story	10M @250	900 mm stories 1–4 750 mm stories 5–10 700 mm stories 11–15	10M @120	20M stories 1–4 15M stories 5–10 10M stories 11–15	10M @150	10M @250	750 × 400

3.5 Seismic Strengthening of CSWs with EB-FRP Sheets

Severe cyclic loading and rotational demand in CSWs may cause considerable damage, followed by local or global residual displacements in SFRS. Three failure modes can be differentiated in diagonally reinforced CSWs, namely flexural, shear, and rigid action failure. The areas most susceptible to damage under these modes include the extreme tensile edges of the wall piers' base and compressive corners of the wall piers' base, as well as CBs and walls joints (Afefy, 2020). To ensure adequate seismic resistance of CSWs, CBs should exhibit sufficient strength and flexibility to absorb seismic energy over plastic action. The inevitable collapse of the CSWs occurs when there is a shear failure of the CBs, and, subsequently, the compression wall piers are crushed. However, it should be emphasized that excessive strength of CBs should be avoided since this can negatively affect the overall performance of CSWs (Manohar & Madhekar, 2015). Consequently, seismic strengthening of vulnerable areas of

CSWs using EB-FRP sheets can effectively improve their seismic performance (Mohammadi et al., 2007). Nevertheless, the seismic retrofitting of shear walls should promote a flexural failure over a fragile shear failure (Committee, 2017).

3.5.1 Provisions for the Design of EB-FRP Sheets

The common failure mode in RC structures strengthened using EB-FRP strips is by debonding (Teng et al., 2002). In seismic applications, physical testing is required to validate anchorage systems' effectiveness in providing resistance against debonding failure. ACI 440.2 R-17 recommends that flexural FRP strips be fully wrapped with FRP sheets, particularly in regions where plastic hinge formation is expected. This wrapping technique can significantly improve the seismic performance of FRP-strengthened structures by enhancing debonding failure resistance in flexural-strengthening FRP sheets and considering the stress reversal effect for shear-strengthening FRP sheets.

To prevent debonding failure, ACI 440.2 R-17 recommends a limitation on the effective strain, ε_{fd}, of FRP sheets beyond which debonding may occur, as expressed in Equation 3.10.

$$\varepsilon_{fd} = 0.41\sqrt{\frac{f_c'}{nE_f t_f}} \leq 0.9\,\varepsilon_{fu} \tag{3.10}$$

in which ε_{fu} = FRP sheet design rupture strain; f_c' = compressive strength of concrete; n and E_f represent number of FRP layers and modulus of elasticity of FRP sheets, respectively; and t_f = thickness of FRP sheets. Also, FRP sheets' contribution to the bending, M_{nf}, in rectangular RC beams can be calculated using Equation 3.11.

$$M_{nf} = \psi_f A_f f_{fe}\left(d_f - \frac{\beta_1 c}{2}\right) \tag{3.11}$$

where ψ_f is the FRP reduction factor (equal to 0.85 for flexure and 0.95 for shear fully wrapped sections); A_f is the area of EB-FRP sheet; f_{fe} and d_f are effective stress and depth in the FRP,

respectively; and β_1 and c are the ratio of depth of the equivalent rectangular stress block to depth of the neutral axis, and the distance from the extreme compression fiber to the neutral axis, respectively.

Using fully wrapped EB-FRP sheets when practically possible is the optimal method for the shear strengthening of RC beams (Committee, 2017). In this study, the CBs are placed at the height between the floors, and all four sides are accessible. Thus, a fully wrapped configuration to enhance the shear capacity of CBs is employed. Additionally, FRP sheets' contribution to the shear, V_f, in rectangular RC beams can be calculated using Equation 3.12.

$$V_f = \frac{A_{fv} f_{fe} (sin\,\alpha + cos\,\alpha) d_{fv}}{S_f} \tag{3.12}$$

Where A_{fv} = area of EB-FRP sheets; α = angle between the main axis of the FRP strips and the horizontal axis of the beam (equal to 90 degrees); d_{fv} = effective depth of EB-FRP sheets; and S_f = axis-to-axis space between the EB-FRP sheets.

3.5.2 Strengthening Schemes

This study aims to increase the resilience and self-centering capabilities of the CSWs and minimize their residual displacement using EB-FRP sheets. To that end, strengthening configurations are proposed to improve the seismic behavior of CBs and wall piers by increasing their load-carrying capacity and strengthening regions susceptible to cracking caused by cyclic earthquake loading. Finally, the effectiveness of different configurations is compared to determine the most efficient strengthening scheme.

Three different strengthening schemes, in addition to the plain CSWs in Montreal and Vancouver, were evaluated, encompassing a total of eight CSWs (see Figure 3.3). In the first scheme, labelled S1-CSW, a vertical layer of FRP sheets was applied across the entire width of wall piers to improve their in-plane flexural capacity. Moreover, the wall piers and CBs were completely wrapped with a single layer of EB-FRP to promote shear strength, ductility,

and rotational capacity. In the second scheme, labelled S2-CSW, vertical layers were applied in a structured manner. Two layers of vertical FRP were incorporated in the first 15% of the wall pier's length from each edge, followed by one layer in the subsequent 15% of the wall length. Also, similarly to S1-CSW, CBs and wall piers were wholly wrapped with a single layer of EB-FRP. In the third configuration, labelled S3-CSW, three layers of vertical FRP within the first 15% of the wall pier's length from each edge were applied, followed by a single layer of FRP sheets wrapping the entire wall pier and an additional layer within the plastic hinge region. To enhance the flexural resistance of the CBs, a single layer of EB-FRP sheets was applied on the top and bottom sides. Finally, complete wrapping of the CBs was carried out to improve their ductility and rotational capacity. The non-strengthened walls were considered control walls and labelled C-CSW. The manufacturer's mechanical properties of CFRP sheets are summarized in Table 3.5.

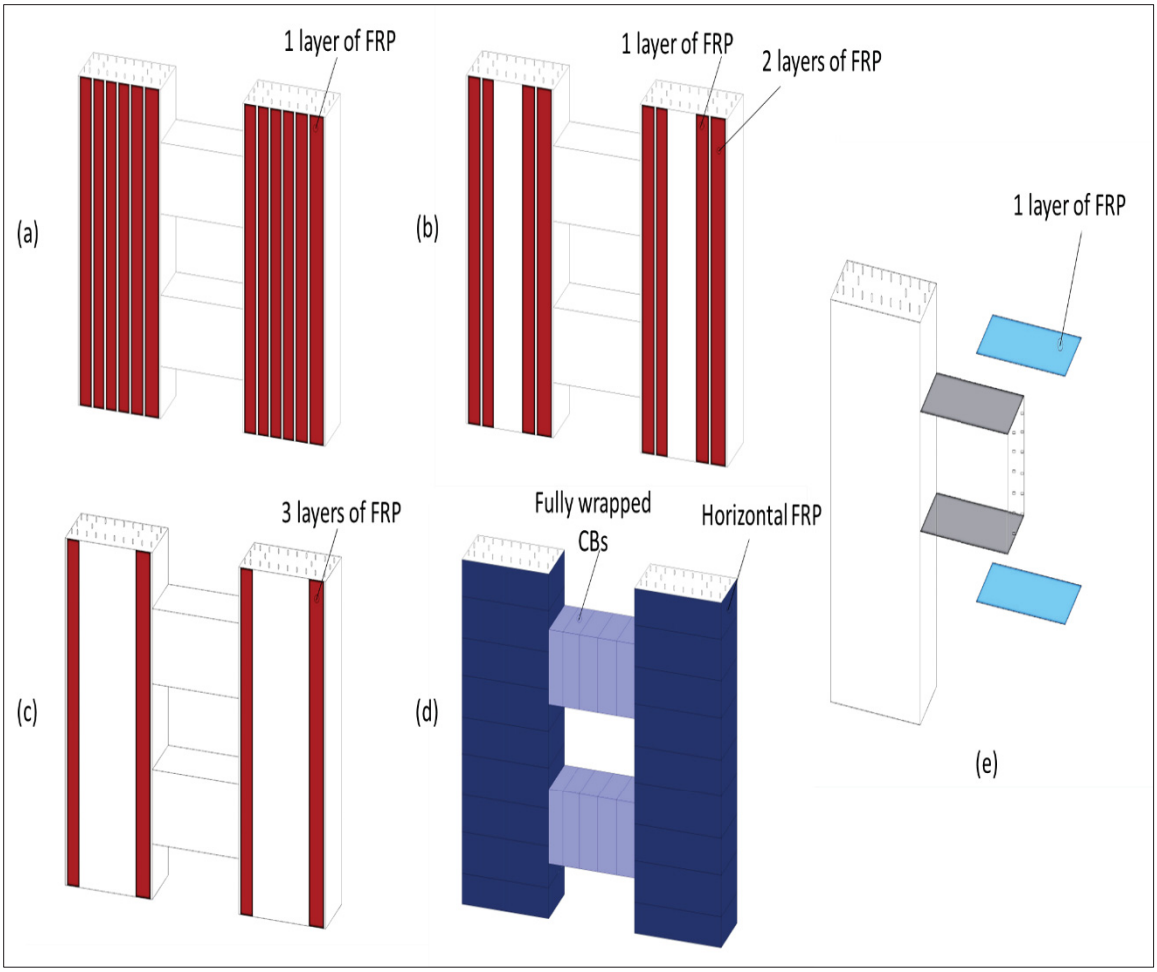

Figure 3.3 Strengthening schemes: (a) wall piers in S1-CSW; (b) wall piers in S2-CSW; (c) wall piers in S3-CSW; (d) FRP wrapping of wall piers and coupling beams in all schemes; and (e) coupling beams' flexural strengthening in S3-CSW

Table 3.5 Manufacturer's mechanical properties of CFRP sheets

Ultimate tensile strength (MPa)	1355
Tensile modulus, W_{frp} (MPa)	115,700
Elongation at break (%)	0.95
Thickness per ply (mm)	1.3

3.6 Nonlinear Time History Analysis

The use of nonlinear time history (NLTH) analysis for the performance-based seismic design of RC buildings is gaining popularity in the United States (C.A.O, 2016). The implementation of the NLTH method, as described in the User's Guide—NBC 2015 (NRCC, 2015), entails the utilization of a nonlinear model of the structure that incorporates its suitable and efficient cross-sectional characteristics, and subjecting it to a set of seismic records, whether they are synthetic or natural. In addition, these records should be scaled to fit the design spectrum.

3.6.1 CSWs Assumptions for Nonlinear Analysis

In the current study, the nonlinear time history analysis of CSWs was conducted using a finite element method (FEM)-based computer program RUAUMOKO 2D (Carr, 2004). This software was developed at the University of Canterbury in New Zealand to evaluate properly the time history response of frame-like structures to ground motions.

3.6.1.1 Member Modeling

To model the complex behavior of CSWs, several analysis techniques are available in the literature, including the continuous medium, finite element, and equivalent frame methods (Harries, 1995a); the last was considered for this study. The equivalent frame method (EFM) is widely used for analyzing CSWs. It transforms the original CSW system into a simplified frame model with comparable properties. In the EFM, the CSW system is divided into interconnected frames consisting of vertical columns and horizontal beams. In this context, the wall piers are represented by the vertical columns with axial rigidity, AE, and flexural rigidity, EI, which correspond to the actual wall piers, whereas the horizontal beams represent the CBs with fitting structural properties and rigid arms at each end. These arms are utilized to ensure that the correct rotations and displacements are achieved, thereby fulfilling the requirement for plane wall sections to remain planar (Smith & Coull, 1991). RUAUMOKO offers multiple members to model frame-type elements. Typically, beam or beam–column finite elements are used to model slender shear walls. Nonetheless, in the case of CSWs, the coupling action

between walls results in significant shifts in the axial force in wall piers during cyclic loading. Therefore, modeling these elements as beam–column members is necessary to capture their behavior accurately. Thus, a quadratic beam–column member was chosen to model wall piers. Moreover, choosing a beam–column member to model the wall is logical as per the regulations stated in CSA A23.3-19. According to this standard, all the shear walls with $\frac{h_w}{\ell_w} \geq 2$ must be considered flexural shear walls, and these types of walls are designed to withstand in-plane lateral forces through flexural action and act practically like RC beams.

CBs were analyzed using a one-component (Giberson) beam model (Giberson, 1969) comprising an elastic beam that incorporates two rigid links, with rotational springs at each end to concentrate all nonlinear deformations. It was considered that the span of the rigid end block was half the depth of the member (Jury, 1978). A double curvature shape is formulated for the elastic beam, and thus a hysteretic model may determine the moment–rotation loading history of each hinge (Boivin, 2006). While the interaction between the axial yield and moment–curvature yield in beam members can be disregarded, the axial force affects the member's yield moment in a beam–column member (Carr, 2008). Therefore, the yielding surface of the moment–axial interaction diagram should be defined to account for the combined effects of bending and axial forces in wall piers. To overcome the computational complexities of nonlinear sectional analysis, the Xtract software v2.6.0 was utilized for both FRP-strengthened and control members to obtain control points of the yielding surfaces. This software can accurately compute moment–axial interaction and moment–curvature diagrams for each section. To consider the materials' nonlinearity, nonlinear stress–strain curves of materials were defined. The bilinear model with strain hardening was used for steel reinforcement, while the model introduced by (Mander et al., 1988) was used for reinforcement-confined and unconfined concrete. Lastly, the linear elastic behavior of EB-FRP sheets was defined using the manufacturing properties of the FRP materials. Moreover, FRP wrapping can increase concrete's ultimate strain, improving curvature, and rotational and load-carrying capacity. Hence, for FRP-confined members, the Lam and Teng model (Lam & Teng, 2003) was utilized to account for capacity improvement of concrete. Both the quadratic beam–column and the one-component (Giberson) beam have been identified and used in previous

studies to model CSWs (Honarparast & Chaallal, 2019b; McNeice, 2004; Zhijun, 2006). Additionally, as all the diaphragms are considered to be rigid and have sufficient thickness to develop diaphragm effects, the lumped mass model was implemented for all buildings, and the relative horizontal movement of nodes on the same level was disregarded (Boivin & Paultre, 2010; Choi & Kim, 2014; Dong, 2003). (Vecchio & Collins, 1986) demonstrated that transverse cracking significantly impacts the compression behavior of cracked concrete, leading to substantial softening effects. Thus, the ductility-based model, proposed in RUAUMOKO using experimental test data presented by (McNeice, 2004), was utilized to model strength degradation in CSWs during cyclic loading. Moreover, to consider geometric nonlinearity, the large displacement approach was employed. This approach updates the nodal coordinates and member stiffnesses at each time step to account for changes in axial forces and geometry, making analyzing structures undergoing large displacements possible (Zhijun, 2006) . Figure 3.4 depicts member modeling and node numbering of CSWs evaluated in this study.

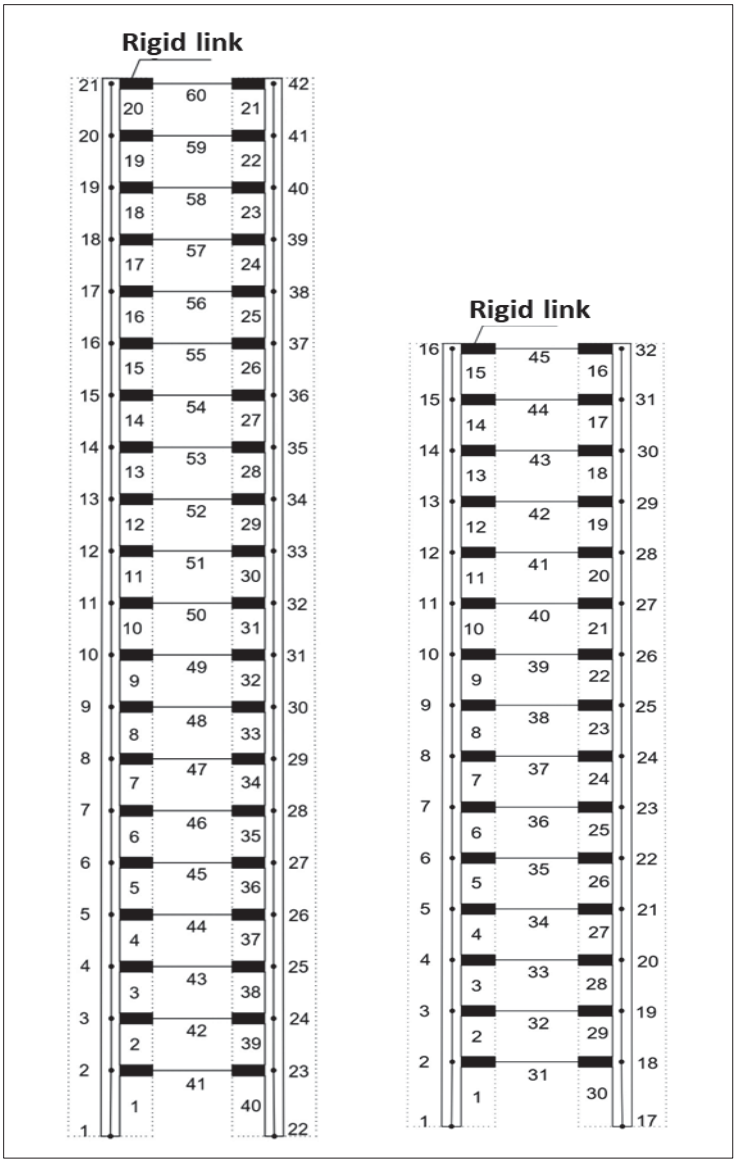

Figure 3.4 Member modeling and node numbering of
20-story and 15-story CSWs in RUAUMOKO

3.6.1.2 Damping Modeling

Choosing an appropriate damping model in NLTH is paramount for achieving accurate results. In many studies, the Rayleigh damping model has been considered (Arabzadeh & Galal, 2017; Boivin & Paultre, 2010; Dong, 2003). This model considers the linear proportional combination of the stiffness and mass matrices. As the stiffness matrix changes throughout the

nonlinear analysis, the damping matrix is updated at each time step. Equation 3.13 expresses the Rayleigh damping matrix, denoted as *C*:

$$C = \alpha M + \beta K \tag{3.13}$$

where *M* = mass matrix, *K* = stiffness matrix, and α and β are coefficients calculated using Equation 3.14.

$$\begin{Bmatrix} \alpha \\ \beta \end{Bmatrix} = 2\frac{\omega_i \omega_j}{w_j^2 - w_i^2} \begin{bmatrix} \omega_j & -\omega_i \\ -\frac{1}{\omega_j} & \frac{1}{\omega_i} \end{bmatrix} \begin{Bmatrix} \xi_i \\ \xi_j \end{Bmatrix} \tag{3.14}$$

where $(\xi_i, \xi_{j)}$ and (ω_i, ω_j) are the damping ratio (given damping/critical damping) and circular natural frequency (rad/s) for *i*th and *j*th modes, respectively. Once the damping ratio of the two modes is provided, the damping matrix can be computed using Equation 3.13. The damping ratio in the other vibration mode, ξ_n, of the structure can be calculated using Equation 3.15.

$$\xi_n = \frac{1}{2}\left(\frac{\alpha}{\omega_n} + \beta\omega_n\right) \tag{3.15}$$

As demonstrated by Equation 3.15 and Figure 3.5, the damping ratio for modes with a frequency lower than ω_i displays a significant increase and is proportional to the mass. Conversely, the damping ratio for modes with a frequency greater than ω_j exhibits a consistently increasing trend, and, at higher frequencies, the threshold limit is solely proportional to the stiffness. It should be noted that the modes falling within the frequency ranges of ω_i and ω_j exhibit slightly lower damping ratios, consequently resulting in more conservative results. This highlights the importance of appropriate selection of damping ratio and two corresponding modes in Equation3.14. It is suggested to choose the first mode (fundamental mode) of the structure and one of the higher modes corresponding to ω_i and ω_j,

respectively. This approach ensures that most of the modes that significantly impact the structure's response are within the same range of damping ratio (Dong, 2003; Hall, 2006; Petrini et al., 2008). It also satisfies the requirements of reducing the mass-portion damping term to avoid unrealistic high values of damping forces in nonlinear analysis using the initial stiffness damping model (Hall, 2006). Thus, in this study, initial stiffness Rayleigh damping with 5% critical damping was utilized for modes 1 and 10. Similar assumptions can be found in the literature (Arabzadeh & Galal, 2017; Honarparast & Chaallal, 2019b).

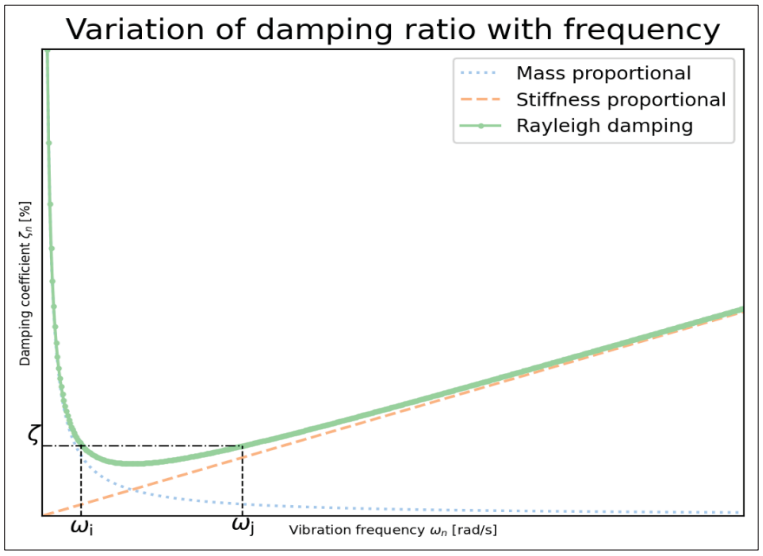

Figure 3.5 Rayleigh damping model

3.6.1.3 Hysteresis Modeling

Repeated cyclic loading beyond the yield point tends to reduce the stiffness of RC elements due to concrete cracking and steel reinforcement plastic behavior. Various hysteretic models replicate the response of RC structures to cyclic loading. However, few models can accurately simulate the feature deterioration and actual behavior of members exposed to significant loading reversal cycles. Hence, selecting a suitable hysteretic model for reproducing the inelastic response of structural members is a critical step in NLTH. To that end, RUAUMOKO 2D offers multiple hysteresis models to characterize the plastic response of RC elements under dynamic excitations.

The modified bilinear Takeda model (Otani, 1974) is considered in this study to replicate the stiffness degradation of control and strengthened CBs. The model is widely used because of its adaptability to a broad spectrum of hysteresis responses of RC members. The coefficients α and β control this model's elastic–perfectly plastic loading and unloading response. Also, the Q-HYST stiffness degrading model (Saiidi & Sozen, 1979b) is used for the nonlinear flexural response of wall piers (see Figure 3.6). The general characteristic of this model is similar to the modified Takeda, in which β is equal to zero. Both hysteresis rules have been previously employed in other studies and have demonstrated their ability to model the inelastic behavior of RC members accurately under cyclic loading conditions (Arabzadeh & Galal, 2017; Benazza, 2012; Boivin, 2006). Moreover, the values of α and β are obtained from experimental data presented by (Zhijun, 2006) and (McNeice, 2004).

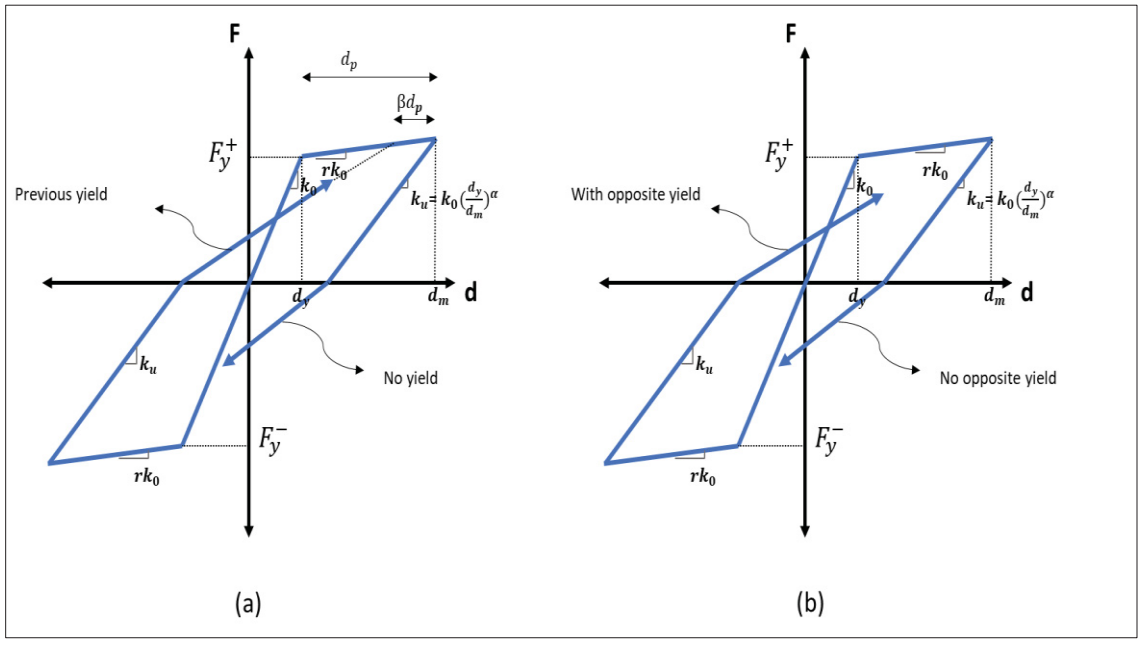

Figure 3.6 Hysteresis rules used in RUAUMOKO: (a) modified bilinear Takeda model; and (b) Q-HYST model

3.7 Ground Motion Selection and Scaling

The Geological Survey of Canada provides the probabilistic-based assessment of earthquake occurrence and intensity level as seismic hazard models for various cities, which are then utilized to develop Canada's seismic design provisions. The last (6th) generation of seismic hazard models was recently provided for NBCC 2020. The seismic hazards are represented as a fraction of gravity by (i) the spectral acceleration, Sa, parameter corresponding to the period ranges of 0.2, 0.5, 1.0, 2.0, 5.0, and 10.0 s (contributing to form the uniform hazard spectrum (UHS) for each city), and (ii) peak ground acceleration, PGA, and velocity, PGV; all for the probability of 0.000404 per annum (2%/50 years) (Adams et al., 2019). Therefore, when choosing ground motion time histories, they must align with the specific tectonic conditions, anticipated ground motion magnitudes, and distances at the building site to comply with the projected level of seismic hazard. Alternatively, as outlined by NBCC, the ground motion time histories should adhere to the UHS corresponding to the building site. Note that the seismic hazard level related to class C shows a significant increase in NBCC 2020 compared with NBCC 2015, as shown in Figure 3.7.

The de-aggregation of the seismic hazard analysis is necessary to determine primary magnitude–distance pairs that dominate the seismic hazard level of a given city (McGuire, 1995). In eastern Canada, Montreal in a region characterized by moderate-to-high seismicity levels resulting from crustal earthquakes, having anticipated earthquakes with high frequencies and short duration (Atkinson, 1996; Tremblay & Atkinson, 2001). Two distinct M–R scenarios of earthquakes dominate the seismic hazard level in Montreal (Adams et al., 2019; Adams & Atkinson, 2003). The first scenario comprises earthquakes with a magnitude of six (M6) occurring at fault distances (R) of 10–30 km, and is compatible with the short-period portion of the UHS, while the second, with a magnitude of seven (M7) occurring at R = 15–100 km, is compatible with the long-period portion of the UHS (Atkinson, 2009). On the contrary, in western Canada, crustal and in-slab events (generating moderate-to-high earthquakes) contribute to hazards at low-to-intermediate periods (Adams & Atkinson, 2003). Additionally, Cascadian subduction events (megathrust earthquakes), characterized by magnitudes greater

than eight (M > 8), account for long-period motion hazards. Although Cascadian events are far from densely populated regions (typically more than 100 km), these events are usually of long duration, which may cause significant damage to structures that are loaded beyond their elastic capacity (Atkinson, 2009). Accordingly, three scenarios of earthquakes with (i) M = 6.5 and 10 < R < 30; (ii) M = 7.5 and 15 < R < 100; and (iii) M = 9 and 100 < R < 200 were used for analysis of shear walls in western Canada.

Only a few time histories are available for earthquakes in eastern Canada, and the magnitudes and distance of these earthquakes are inconsistent with the abovementioned seismic hazard levels. Thus, simulated ground motion time histories for soil site class C, developed by (Atkinson, 2009), are used in this study. As per the NBCC guidelines, it is imperative to have at least five time histories for each suite to conduct a dynamic analysis. Furthermore, a minimum of eleven earthquakes across all suites is required to perform the analysis. In this regard, NLTH is performed in eastern and western Canada, with the selection of 11 and 15 time histories, respectively. Figure 8 shows response spectra for scaled ground motions in both sites. The mean value of all analyses is then utilized as the nonlinear dynamic response of the structure. The earthquake selection and scaling was performed as requested by NBCC guidelines, using the method suggested by (Tremblay et al., 2015b). For each suite, 45 simulated accelerograms were created by Atkinson. The ideal records were selected by calculating the ratio of the target spectral amplitude to the spectral amplitude of the records in each suite. The chosen records must have mean values between 0.5 and 2 and the lowest standard deviation. Tables 3.6 and 3.7 summarize selected ground motion characteristics, including peak ground acceleration (PGA), durations, M–R scenarios, period range, and event types.

Table 3.6 Selected ground motions' description (Vancouver)

Scenario	Rec. No.	M	R (km)	PGA (g)	Duration (s)	Period Range (s)	Event Type
1	West 1	6.5	8.8	0.475	49.30	0.2–0.8	Crustal
	West 2	6.5	11.2	0.483	49.30		
	West 3	6.5	10.8	0.503	49.30		
	West 4	6.5	12.3	0.497	53.63		
	West 5	6.5	14.6	0.559	53.63		
2	West 6	7.5	16.4	0.391	102.02	0.3–1.5	In-slab
	West 7	7.5	18.1	0.430	102.02		
	West 8	7.5	21.6	0.351	102.02		
	West 9	7.5	35.7	0.289	93.39		
	West 10	7.5	48.4	0.423	93.39		
3	West 11	9	112.4	0.137	309.42	1–4	Cascadia subduction
	West 12	9	112.4	0.132	309.42		
	West 13	9	156.7	0.173	309.42		
	West 14	9	156.7	0.146	309.42		
	West 15	9	200	0.167	309.42		

Table 3.7 Selected ground motions' description (Montreal)

Scenario	Rec. No.	M	R (km)	PGA (g)	Duration (s)	Period Range (s)	Event Type
1	East 1	6	10.7	0.322	43.59	0.2–1	Crustal
	East 2	6	12.8	0.645	43.59		
	East 3	6	20.8	0.423	43.59		
	East 4	6	21.6	0.451	47.53		
	East 5	6	26.3	0.301	47.53		
2	East 6	7	13.8	0.478	51.12	0.5–2.42	Crustal
	East 7	7	20.6	0.410	51.12		
	East 8	7	50.3	0.308	51.12		
	East 9	7	62.6	0.331	57.35		
	East 10	7	95.5	0.248	57.35		
	East 11	7	94.2	0.299	57.35		

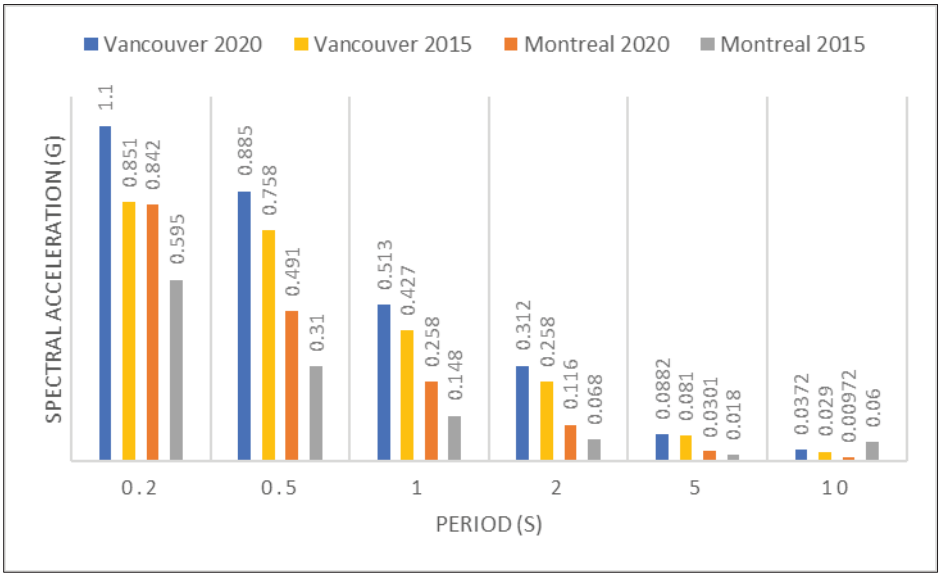

Figure 3.7 Comparison of seismic hazard values of 2% probability in 50 years in site class C in Vancouver and Montreal

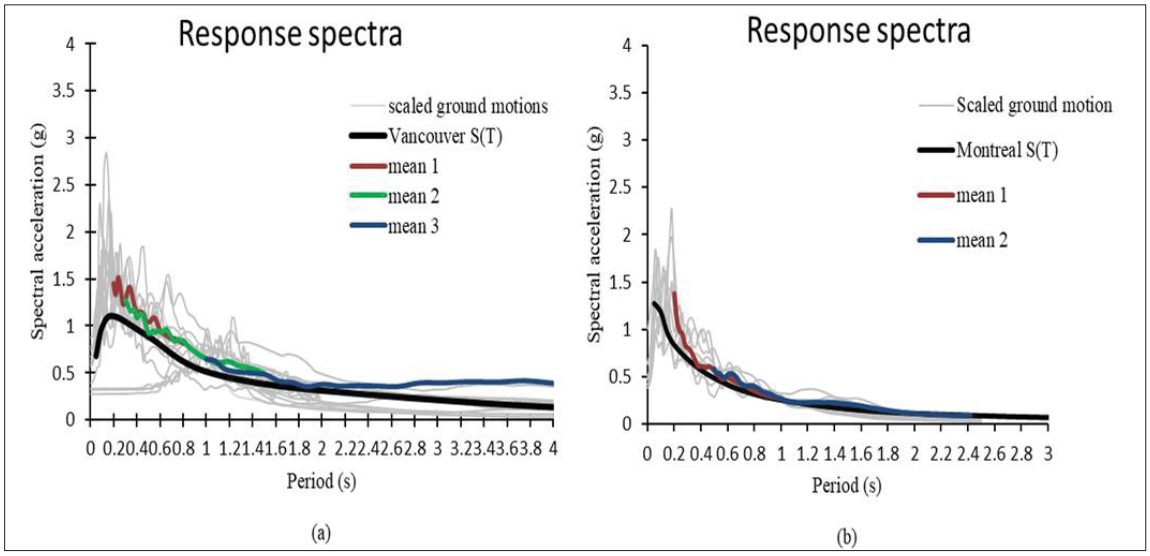

Figure 3.8 Response spectra for scaled ground motions: (a) Vancouver; and (b) Montreal

3.8 Results and Discussion

This study evaluates the effectiveness of various configurations of EB-FRP sheets in reducing residual displacement and enhancing self-centering in two sets of medium- (15 stories) and high-rise (20 stories) CSWs, located in Montreal and Vancouver. Nonlinear time history analysis was employed, with the shear walls designed and detailed according to NBCC 2020 and CSA A23.3-19 requirements. Results of the study are presented and analyzed in terms of the following parameters: inter-story drift ratio (IDR), residual inter-story drift of shear walls (RIDR) rotation of CBs, and bending moment and shear force of wall piers.

3.8.1 Residual Inter-Story Drift Ratio

The inter-story drift ratio is the horizontal displacement between two adjacent floors divided by the story height, and is subject to a maximum limit of 2.5%, as prescribed by NBCC 2020. This parameter is the most significant factor contributing to structural damage in shear walls during earthquakes. On the other hand, the primary aim of the present study is to assess the

effectiveness of using EB-FRP sheets to minimize the residual displacement and enhance the self-centering capacity of CSWs. However, establishing specific criteria for restricting residual displacement in RC structures remains a topic of ongoing discussion and debate within the engineering community. While ASCE 7-22 does provide a guideline for limiting the maximum residual inter-story drift ratio (RIDR) in buildings exceeding 73 m in height to 1%, there are currently no other universally accepted standards in place. Accordingly, the RIDR will be deemed the focal point of this article, and the present section presents the outcomes of the NLTH for the given indicators. Moreover, the findings unveil a significant variation in the walls' response between the eastern and the western regions of Canada, which can be attributed to the distinctive levels of seismicity and ground motion sources in these areas.

3.8.1.1 Western Canada

The graphical representation of Figure 3.9 illustrates the IDR domains of 20-story CSWs for fifteen different time histories. Each story is denoted by a pair of vertical solid lines, with the first representing the minimum IDR value obtained through NLTH analysis and the second representing the maximum. The red box indicates the mean value of all responses. The results indicate that the highest mean value of the C-CSW was observed in the 5th story, with a remarkable value of 1.31%, predominantly influenced by Cascadia events (M9). Notably, the impact of these events was more pronounced in the 20-story CSWs, as the dominant period in these ground motions is close to the natural period of high-rise structures. However, the application of EB-FRP resulted in a notable decrease in the peak IDR, specifically, a 13, 18, and 27% reduction in S1-CSW, S2-CSW, and S3-CSW, respectively. Moreover, it was found that strengthening schemes can mitigate the fluctuation of the mean IDR across the height of the wall. Additionally, the upper floors (60–70% of the wall height) may experience a second PH due to the higher mode effect, as shown in Figure 3.9.

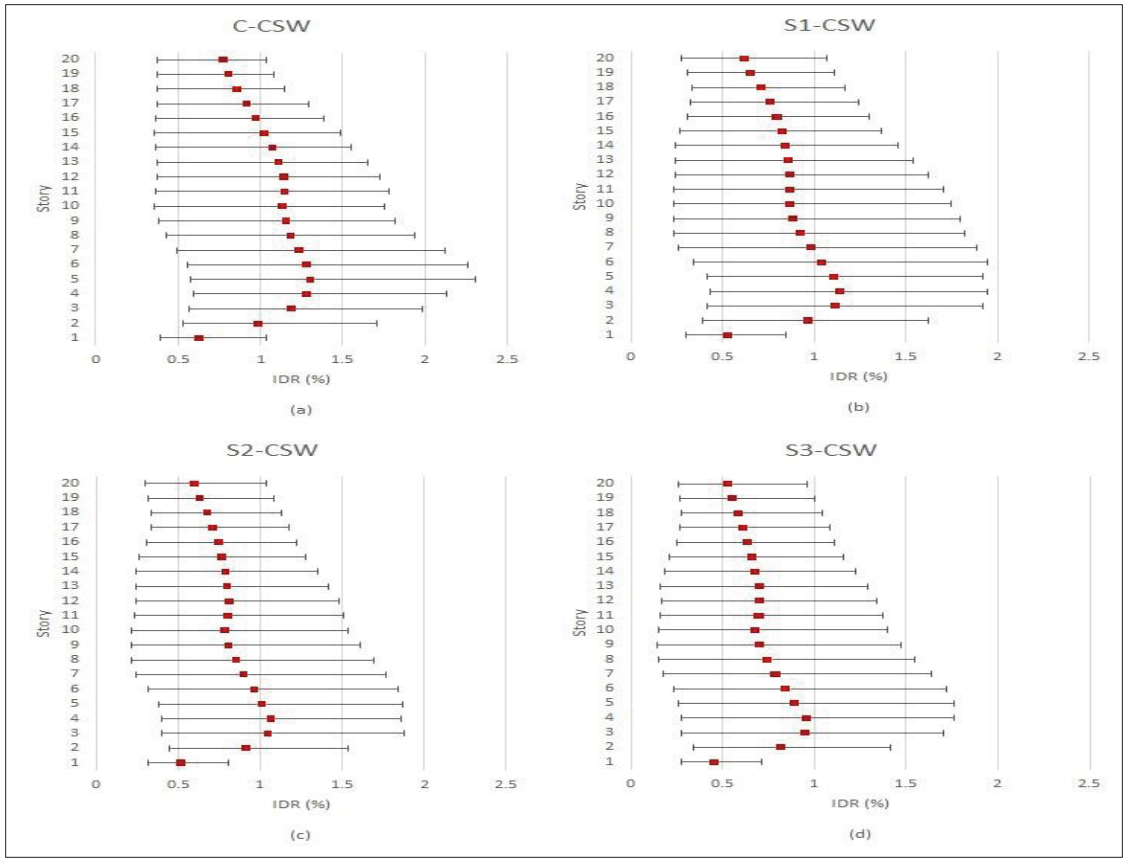

Figure 3.9 Inter-story drift ratio domains of 20-story CSWs in Vancouver: (a) original CSW (C-CSW); (b) first strengthening configuration (S1-CSW); (c) second strengthening configuration (S2-CSW); and (d) third strengthening configuration (S3-CSW)

This reduction results in a significant decrease in the residual inter-story drift ratio (RIDR). The RIDR distribution in a 20-story C-CSW subjected to fifteen ground motions is depicted in Figure 3.10 (a). It is observed that, similarly to the IDR, scenario (iii) (M9) was dominant for the highest obtained values. In the C-CSW, among all ground motions, the maximum RIDR was found to be 1.48% for time history number 13, while the minimum value occurred in time history number 3, with a value of 0.04%. Such a finding highlights the impact of low-frequency ground motions on high-rise structures, leading to heightened stimulation of the first vibration mode of the wall and consequent escalation of the flexural demand at the lower levels. This escalation can lead to an expansion of more bending cracks along the wall, concrete crushing at the base of the wall piers, and, consequently, more residual deformation in the CSW.

Nevertheless, Figure 3.10 (b) indicates that implementing EB-FRP sheets results in a significant reduction of the RIDR in the C-CSW. The results revealed a 41%, 34%, and 20% reduction in the peak RIDR in S3-CSW, S2-CSW, and S1-CSW, respectively. The observed self-centering ability improvement can be attributed to the superior efficiency of vertical EB-FRP sheets in increasing the flexural strength and stiffness of wall piers, with the magnitude of impact positively correlated with the proximity to the edge. Additionally, confinement of CBs and walls with FRP wrapping can increase shear strength, load-carrying capacity, and ductility of the CSW to avoid shear failure due to flexural overstrength in the base of the wall. The significance of the aforementioned issue lies in the fact that the plastic hinge formation at the base of the wall, resulting from resonance in the first mode of vibration, leads to an increase in shear force in the wall due to the influence of higher modes. As such, it becomes imperative to enhance the shear strength of the wall to avoid any possibility of brittle shear failure. However, previous studies have shown that cantilever single shear walls are more sensitive to this issue (Adebar et al., 2015).

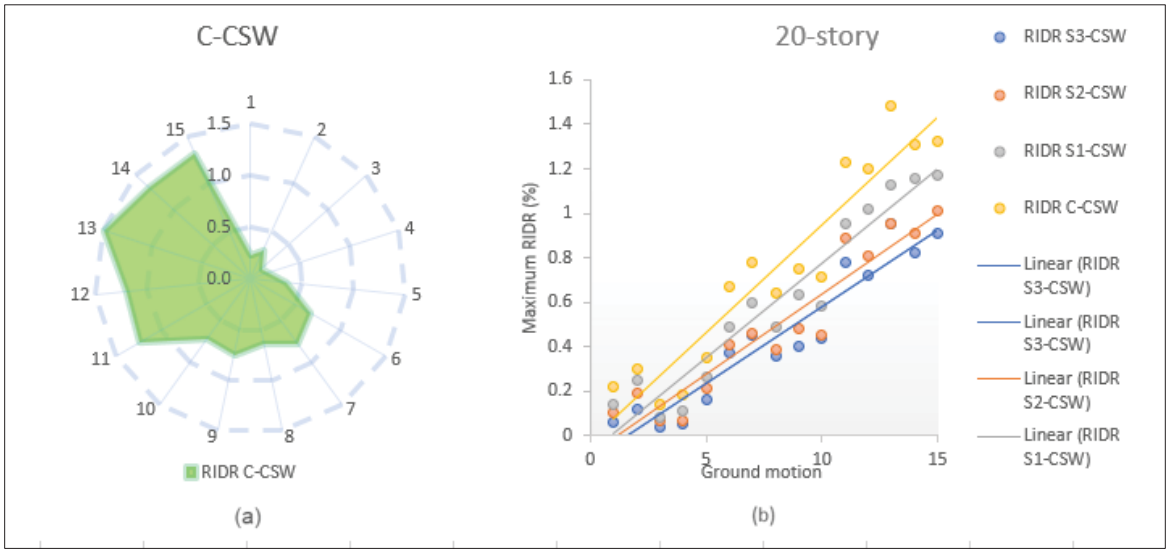

Figure 3.10 Maximum residual inter-story drift ratio in a 20-story CSW in Vancouver: (a) the RIDR distribution in the C-CSW subjected to all ground motions; and (b) reduction of the RIDR in the C-CSW using 3 strengthening configurations

The effectiveness of strengthening configurations was notably more pronounced in the medium-rise CSW. In a 15-story CSW, the implementation of EB-FRP sheets reduced the peak IDR by 39, 26, and 19% in S3-CSW, S2-CSW, and S1-CSW, respectively. Additionally, the impact of higher modes was less pronounced on shorter CSWs. Furthermore, the effect of EB-FRP strengthening on the increase in shear wall stiffness was inversely proportional to the wall height, which is in agreement with previous research by (Arabzadeh & Galal, 2015) . Notably, S3-CSW demonstrated the capacity to decrease the maximum RIDR by up to 53%, while S2-CSW and S1-CSW showed a decrease of 40% and 25%, respectively. Figures 3.11 and 3.12 show the IDR domains of a 15-story CSW, and the maximum RIDR in a 15-story CSW, respectively.

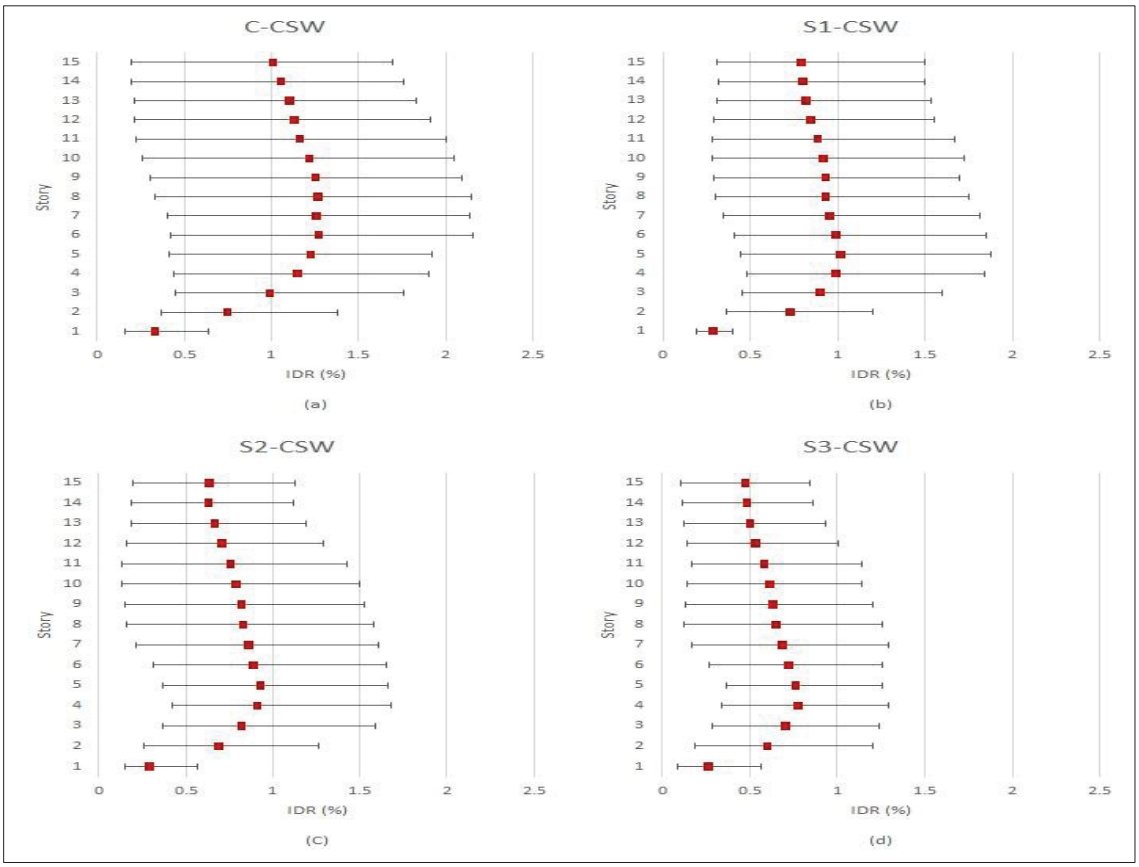

Figure 3.11 Inter-story drift ratio domains of a 15-story CSW in Vancouver: (a) original CSW (C-CSW); (b) first strengthening configuration (S1-CSW); (c) second strengthening configuration (S2-CSW); and (d) third strengthening configuration (S3-CSW)

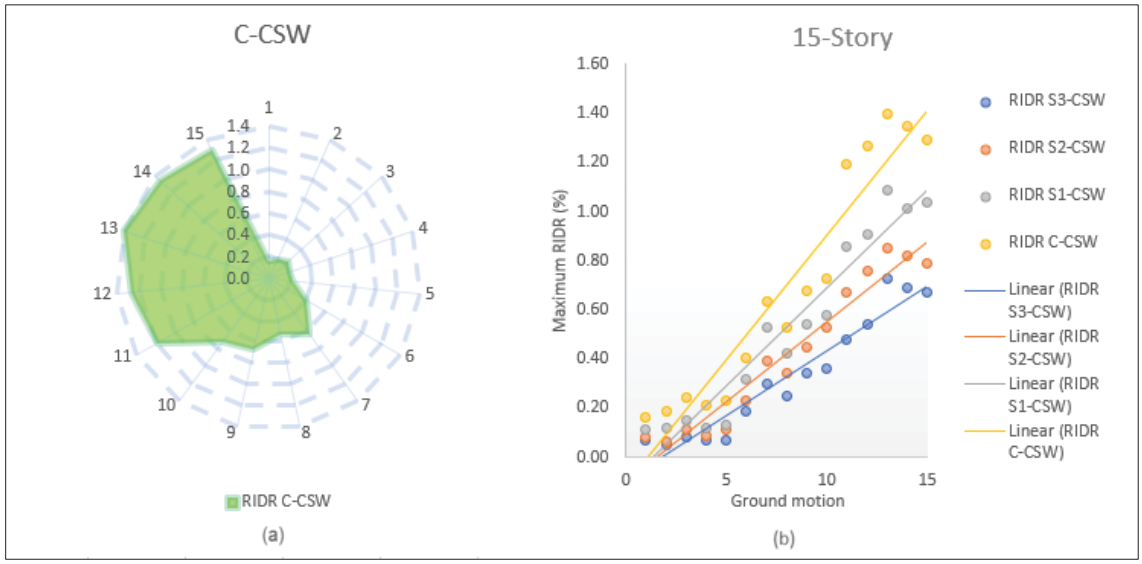

Figure 3.12 Maximum residual inter-story drift ratio in a 15-story CSW in Vancouver: (a) the RIDR distribution in the C-CSW subjected to all ground motions; and (b) reduction of the RIDR in the C-CSW using 3 strengthening configurations

3.8.1.2 Eastern Canada

Despite having less seismic activity compared with western Canada, the eastern region of Canada is abundant in high-frequency ground motions that can intensify the effect of higher modes. This observation was substantiated by the outcome of NLTH analysis for a 20-story CSW located in Montreal, where the probability of the formation of the second PH was noted to be significant in stories 14–16. However, the average IDR for these walls was significantly lower than for the corresponding walls in Vancouver, which are exposed to low-frequency Cascadia (M9) ground motions. The peak mean IDR value was dominated by (M7) events and occurred in stories 2–4 at approximately 0.29%, whereas the mean IDR was around 0.27% in stories 14–16. The proposed strengthening configurations reduced the peak mean IDR by 20, 14, and 10% in S3-CSW, S2-CSW, and S1-CSW, respectively. Additionally, similarly to the response experienced in western Canada, the strengthening measures led to a decline in the fluctuations of mean IDR values across the wall height. Figure 3.13 shows the IDR domains of a 20-story CSW in Montreal.

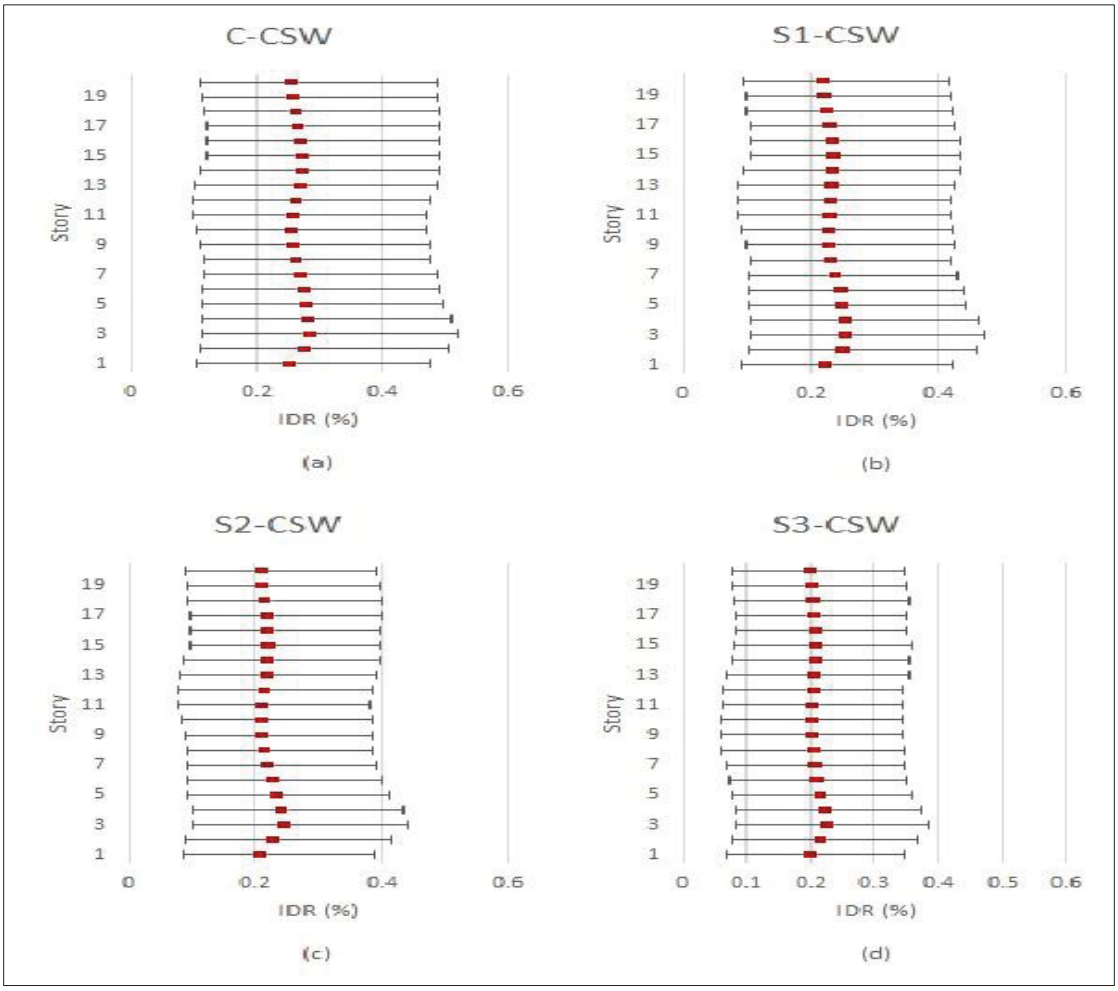

Figure 3.13 Inter-story drift ratio domains of a 20-story CSW in Montreal: (a) original CSW (C-CSW); (b) first strengthening configuration (S1-CSW); (c) second strengthening configuration (S2-CSW); and (d) third strengthening configuration (S3-CSW)

As a result of the shortage of low-frequency ground motions and a low seismicity level in the eastern region of Canada, flexural demand in the walls is much lower; thereby, residual displacement in CSWs in that area was significantly lower than that observed in the western zone. However, due to the geometric configuration of CSWs, the lateral displacement is primarily inelastic, as will be explained in the subsequent section. Consequently, even with significantly low movements, some residual displacement occurs in CSWs in eastern Canada,

dominated mainly by (M7) events with lower frequency content. Figure 3.14 (a) shows the RIDR distribution among all ground motions.

Figure 3.14 (b) illustrates that the peak mean RIDR within the 20-story C-CSW structure was measured at 0.09%. S3-CSW could lower this value by 29%, compared with 26% and 14% for S2-CSW and S1-CSW, respectively. Nonetheless, given the minimal RIDR values exhibited by these walls, it is not deemed reasonable to use any strengthening technique to reduce residual displacement within the eastern Canadian region.

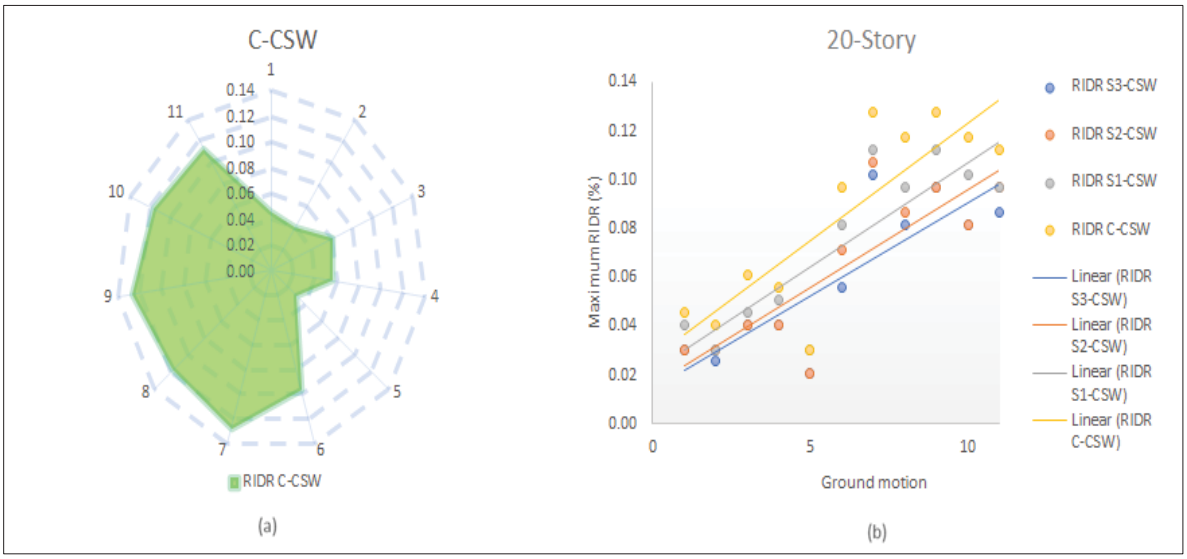

Figure 3.14 Maximum residual inter-story drift ratio in a 20-story CSW in Montreal: (a) the RIDR distribution in the C-CSW subjected to all ground motions; and (b) reduction of RIDR in the C-CSW using 3 strengthening configurations

The findings of the present study indicate that the suggested strengthening configurations are more effective in reducing the IDR of a 15-story CSW than that of a 20-story CSW. Specifically, the maximum IDR reduction in S3-CSW was 26%, which is more effective than the corresponding configuration implemented in the 20-story CSW. The peak mean IDR reductions for S2-CSW and S1-CSW were 19% and 14%, respectively. Furthermore, the impact of higher modes was found to be less pronounced in the 15-story CSW.

It is worth noting that S3-CSW exhibited the highest level of effectiveness in reducing the maximum RIDR across all configurations, with a reduction of 34%. In comparison, the maximum RIDR reduction achieved by S2-CSW was 28%, while the least effective configuration was S1-CSW, which resulted in a 19% reduction in the peak RIDR. Figures 3.15 and 3.16 show the IDR domains of a 15-story CSW, and the maximum RIDR in a 15-story CSW, respectively.

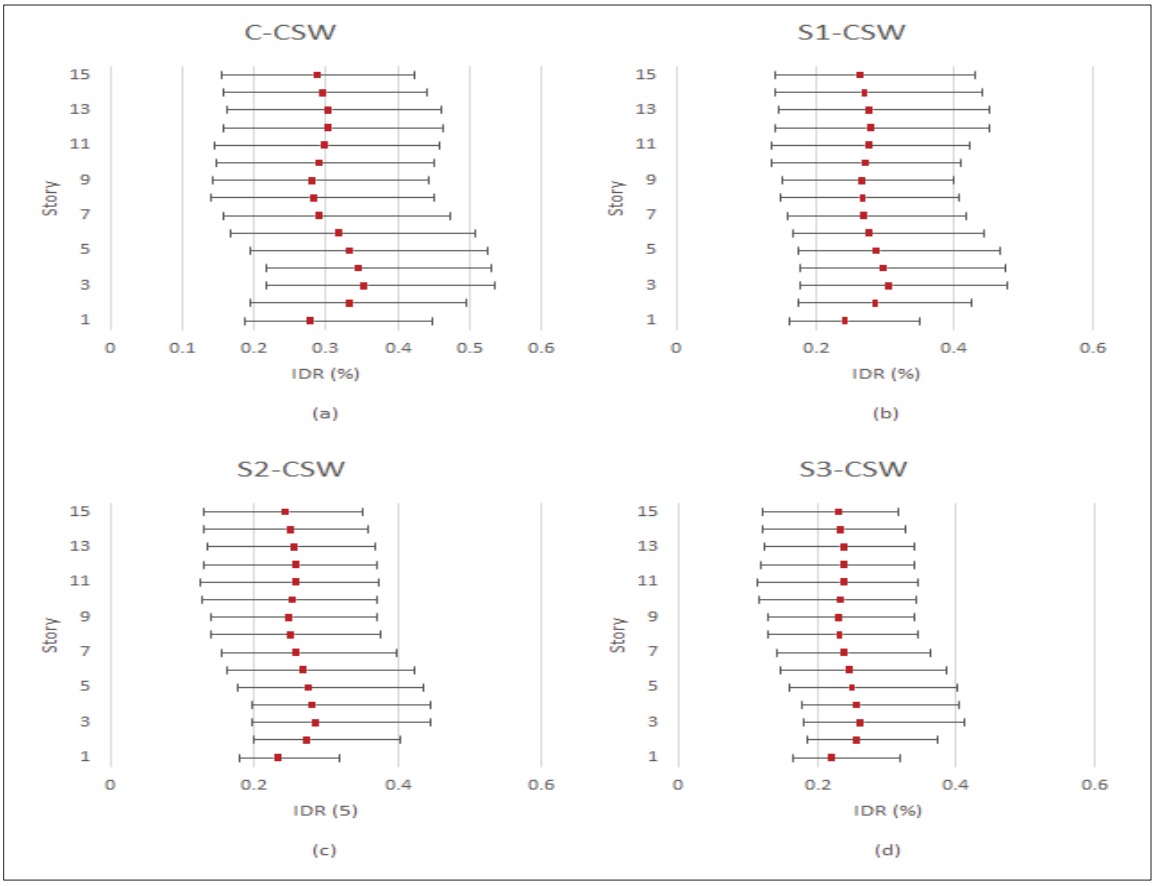

Figure 3.15 Inter-story drift ratio domains of a 15-story CSW in Montreal: (a) original CSW (C-CSW); (b) first strengthening configuration (S1-CSW); (c) second strengthening configuration (S2-CSW); and (d) third strengthening configuration (S3-CSW)

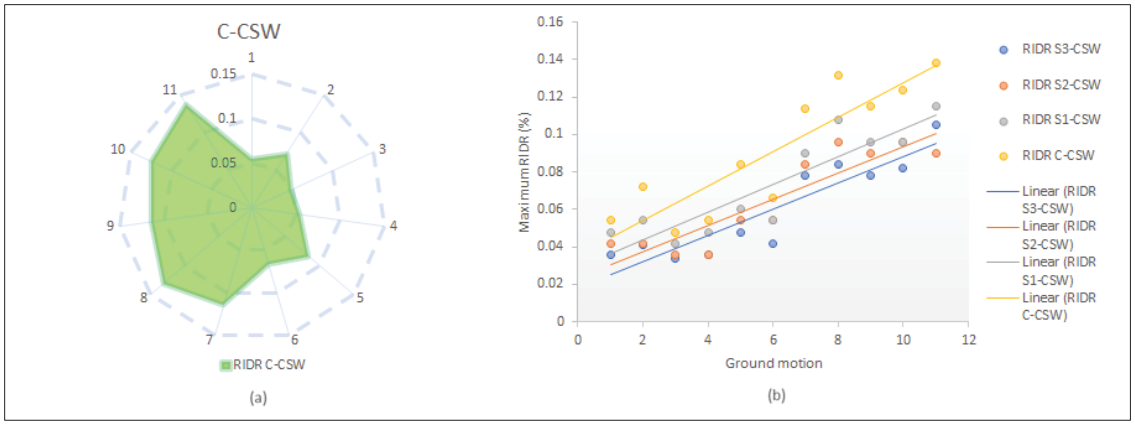

Figure 3.16 Maximum residual inter-story drift ratio in a 15-story CSW in Montreal: (a) the RIDR distribution in the C-CSW subjected to all ground motions; and (b) reduction of the RIDR in the C-CSW using 3 strengthening configurations

3.8.2 Beam Rotation

The total horizontal movement of CSWs includes both elastic and inelastic displacement. However, the elastic portion of displacement is deemed negligible due to the reverse bending in CBs, as suggested in CSA A23.3-19. On the other hand, a CB's rotation is determined by the difference between the rotation of the wall piers and the floor. Additionally, the rotation of the wall piers in relation to the maximum rotation of CBs is much more effective than the floor rotation, leading (White & Adebar, 2004) to suggest disregarding the floor rotation in the critical wall slope for simplification purposes. Consequently, a noteworthy similarity exists between the shape of the mean IDR envelope of CSWs and the mean maximum rotation of the CBs' envelope.

3.8.2.1 Western Canada

As clearly shown in Figure 3.17 (a), EB-FRP sheets have demonstrated a significant ca-pacity to reduce the rotation of CBs in a 20-story CSW. While the maximum CB rotation in the C-CSW was measured as 0.02, falling below the capacity limit outlined before, it is noteworthy that S3-CSW displayed a 31% reduction in peak mean CB rotation. Similarly, S2-CSW and

S1-CSW experienced a 23% and 17% decrease, respectively. These findings suggest that the proposed strengthening configurations are an efficient solution for limiting CB rotation in high-rise CSWs in western Canada. The data indicate that the effectiveness of strengthening configurations on a 15-story CSW was notably more pronounced. Specifically, the peak mean CB rotation was reduced by 41% in S3-CSW, while 27% and 20% reductions were observed in S2-CSW and S1-CSW, respectively. In addition, Figure 3.17 (b) shows that the impact of higher modes on the rotation envelope of CBs is less significant in the 15-story CSW than in the 20-story CSW. Again, these findings prove that EB-FRP strengthening strategies are more effective in medium-rise buildings.

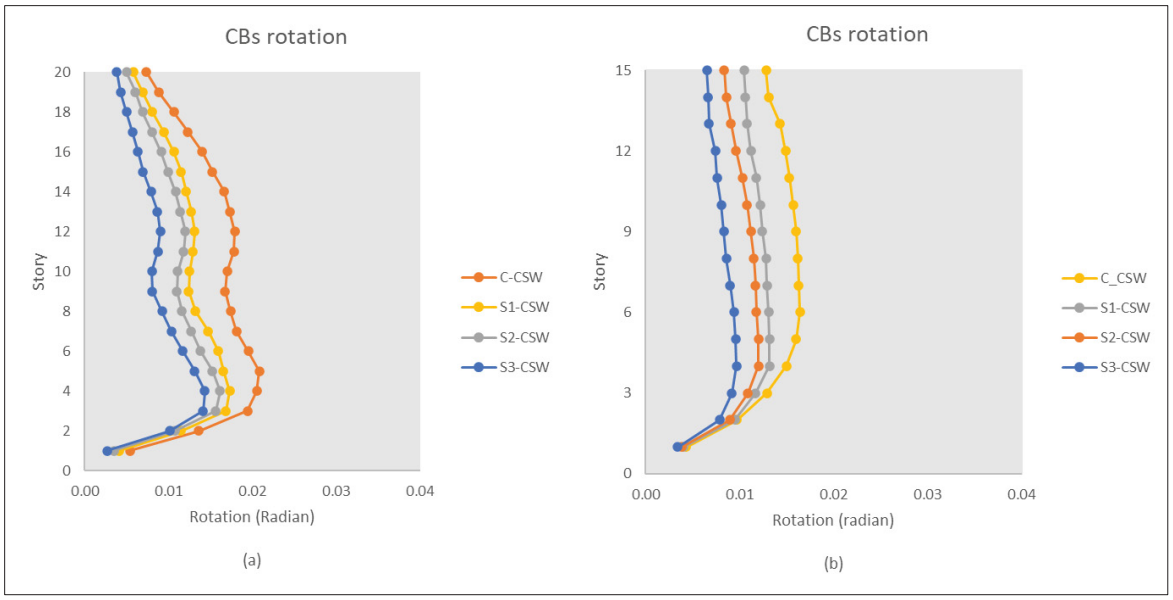

Figure 3.17 Mean coupling beam rotation in: (a) a 20-story CSW in Vancouver; and (b) a 15-story CSW in Vancouver

3.8.2.2 Eastern Canada

As previously explained, a strong correlation exists between the rotation of CBs and the IDR in CSWs. Also, the inherent high-frequency ground motions and lower seismic intensity in eastern Canada contribute to a lower IDR of CSWs in Montreal than their counterparts in

Vancouver. Consequently, the study's findings reveal that the rotation of CBs in CSWs located in Montreal is significantly lower than that in Vancouver's corre-sponding CSWs.

In the C-CSW of Montreal, the peak value of the mean CB rotation envelope was 0.005, while in S1-CSW, S2-CSW, and S3-CSW, there was a reduction of 10%, 15%, and 20%, respectively. In addition, as depicted in Figure 3.18 (a), the impact of higher modes was more pronounced in a 20-story CSW, with the second peak being experienced in higher stories. In the case of a 15-story CSW, as shown in Figure 3.18 (b), the most effective strengthening configuration was S3-CSW, which led to a peak CB rotation reduction of 29%, compared with 22% and 16% for the S2-CSW and S1-CSW schemes, respectively.

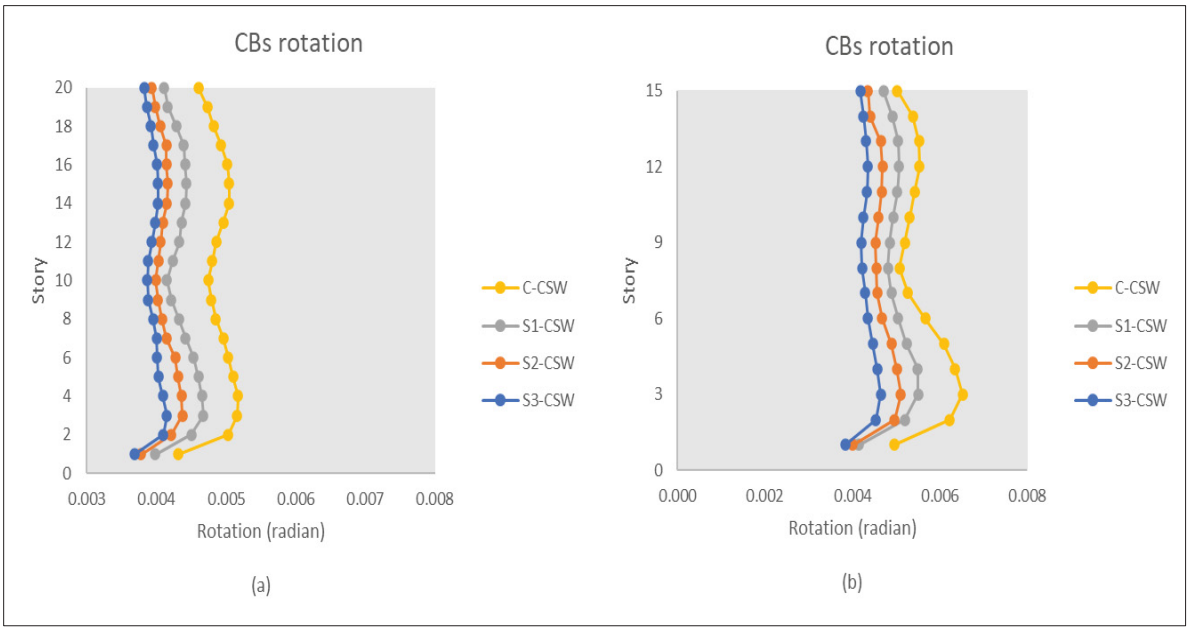

Figure 3.18 Mean coupling beam rotation in: (a) a 20-story CSW in Montreal; and (b) a 15-story CSW in Montreal

3.8.3 Shear Demand in Wall Piers

The shear demand in wall piers was also evaluated as another critical factor. The findings of NLTH analysis revealed that, while the implementation of EB-FRP sheets can lead to a decrease in the IDR and rotation in CSWs, it may also result in an increase in the base shear demand of these walls in both eastern and western Canada.

Figure 3.19 illustrates the normalized mean story shear demand envelopes in all specimens, with the horizontal axis normalized by mean base shear demand in the C-CSW and the vertical axis normalized by building height. The NLTH analysis of a 20-story CSW located in Vancouver revealed that using EB-FRP sheets in S3-CSW in-creased the base shear demand by up to 16%. The mean base shear in S2-CSW and S1-CSW increased by 11% and 8%, respectively. Similarly, results for the 15-story CSW in this city showed a 22%, 15%, and 11% increase in S3-CSW, S2-CSW, and S1-CSW, re-spectively.

In the case of the 20-story CSW in Montreal, the use of EB-FRP sheets resulted in a 20%, 15%, and 12% increase in the base shear demand in S3-CSW, S2-CSW, and S1-CSW, respectively, while, in the 15-story CSW, the increase was 28%, 23%, and 19%, respec-tively. Table 8 shows the base shear demand in all specimens.

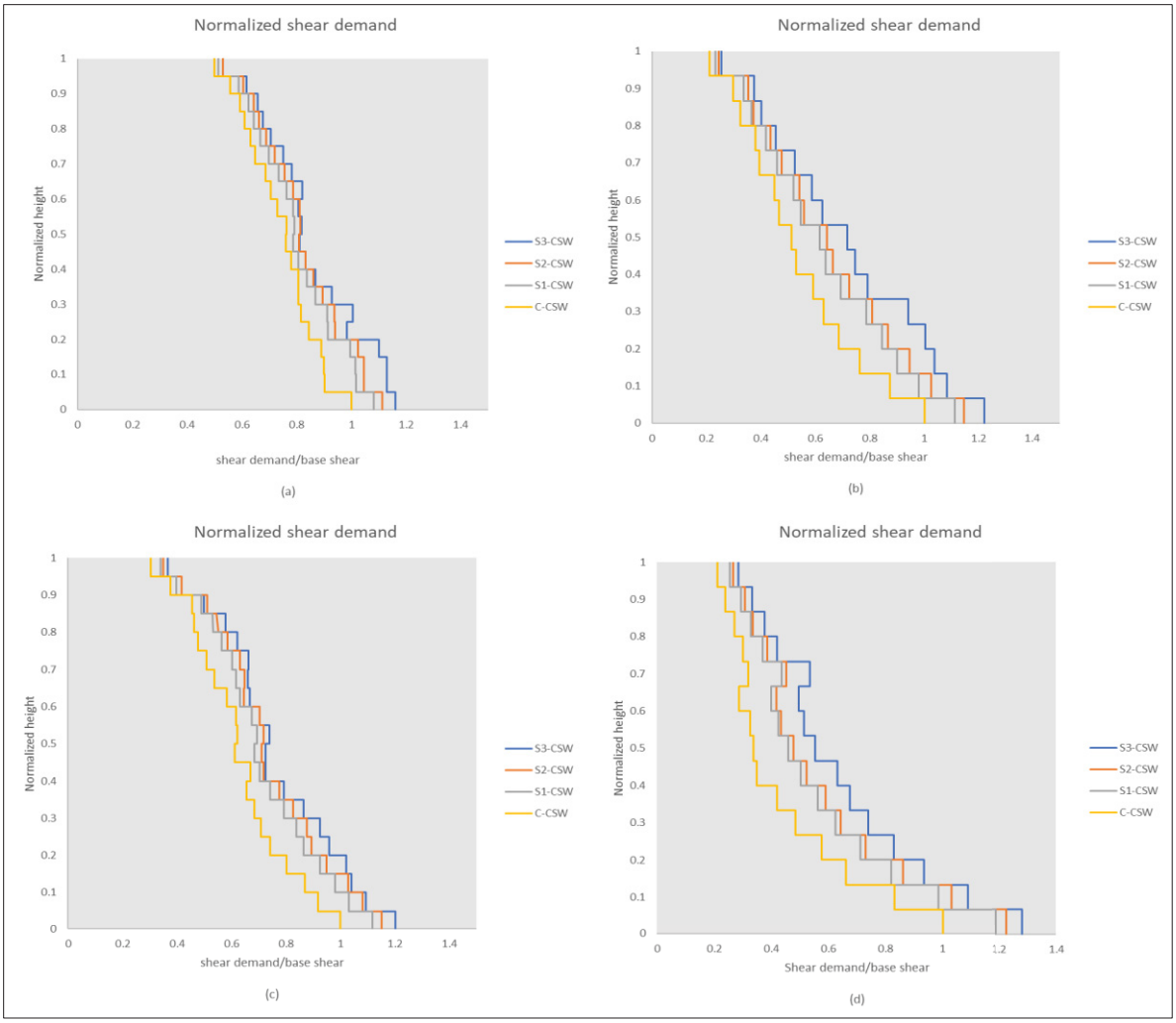

Figure 3.19 Normalized shear demand in CSWs: (a) a 20-story located in Vancouver; (b) a 15-story located in Vancouver; (c) a 20-story located in Montreal; and (d) a 15-story located in Montreal

Table 3.8 Base shear demand in all specimens

		Base Shear Demand (kN)			
		S3-CSW	**S2-CSW**	**S1-CSW**	**C-CSW**
Vancouver	20-story	1126	1081	1048	969
	15-story	736	691	670	603
Montreal	20-story	1158	1110	1077	963
	15-story	633	606	588	494

The frequency content of ground motions can significantly impact shear demand in buildings, mainly through higher modes' excitation (Sadeghian, 2018). However, the rise in the base shear demand of CSWs due to the application of EB-FRP sheets can be attributed to two factors: (i) a decrease in the CSW vibration period due to an increase in stiffness; and (ii) an improvement in post-yield stiffness in strengthened members due to the confinement effect and flexural improvement caused by vertical and horizontal EB-FRP sheets. This effect has also been observed elsewhere (Arabzadeh & Galal, 2017; El-Sokkary et al., 2013; Honarparast & Chaallal, 2022).

3.8.4 Bending Moment Demand in Wall Piers

The use of vertical EB-FRP sheets enhanced the bending capacity of CSWs. However, the strengthening configurations could increase the bending demand in wall piers. This is illustrated in Figure 3.20, which shows the normalized mean bending moment demand across all specimens in the NLTH analysis. The 15-story CSW in Montreal exhibited the most significant influence, with an 18% increase in demand for S3-CSW, and a 13% and 9% increase for S2-CSW and S1-CSW, respectively. Similarly, the 20-story CSW in Montreal experienced a 13%, 11%, and 7% increase in demand for the same configurations. In contrast, the CSWs in Vancouver showed less influence, with the 20-story S3-CSW, S2-CSW, and S1-CSW experiencing increases of 11%, 7%, and 3%, respectively, and the 15-story CSW

showing a 16%, 11%, and 8% increase in S3-CSW, S2-CSW and S1-CSW, respectively. Table 3.9 shows the base bending moment demand in all specimens.

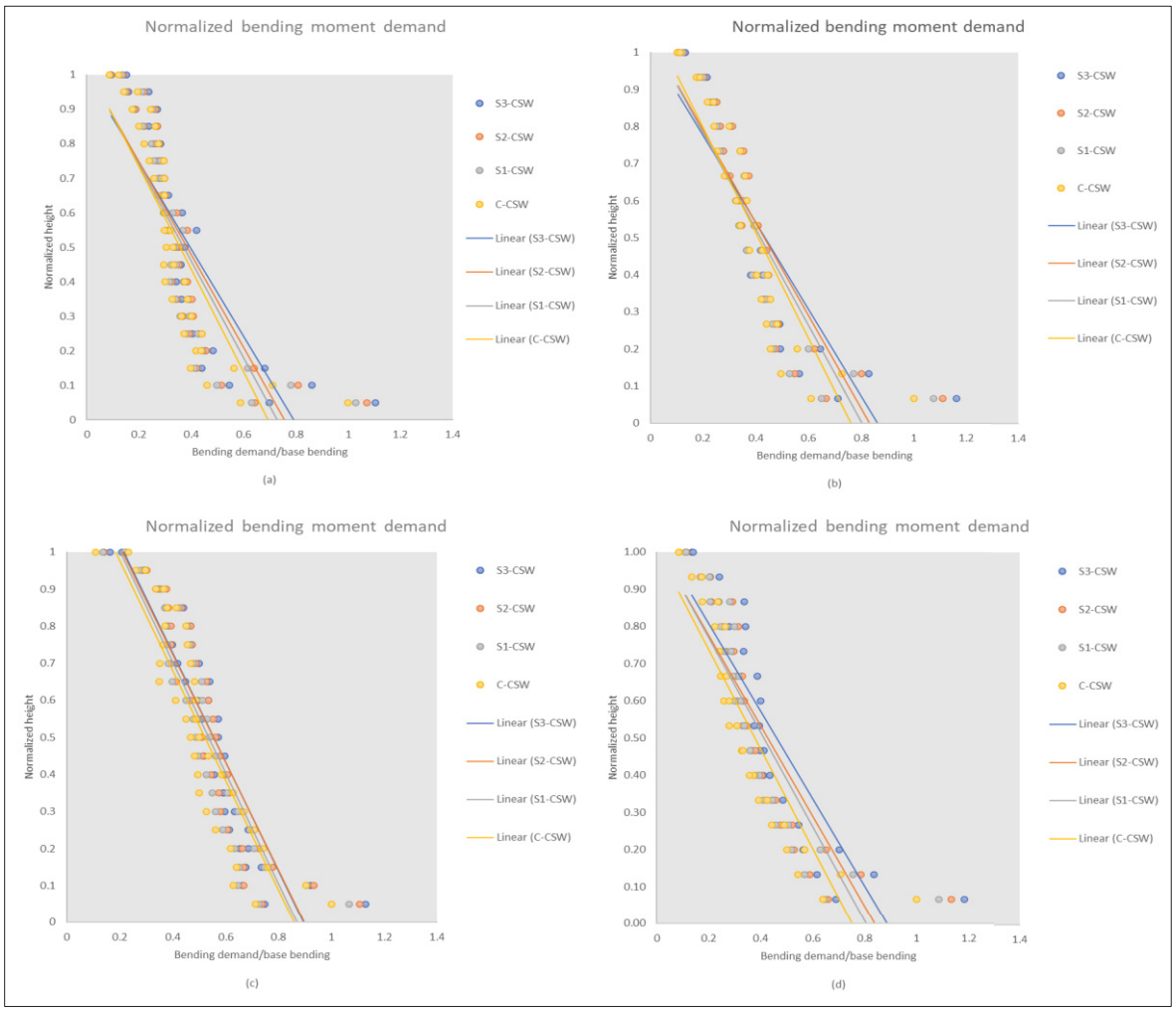

Figure 3.20 Normalized bending moment demand in CSWs: (a) a 20-story located in Vancouver; (b) a 15-story located in Vancouver; (c) a 20-story located in Montreal; and (d) a 15-story located in Montreal

Table 3.9 Base bending moment demand in all specimens

		Base Bending Moment (kN.m)			
		S3-CSW	**S2-CSW**	**S1-CSW**	**C-CSW**
Vancouver	20-story	5346	5181	4972	4843
	15-story	3729	3564	3454	3212
Montreal	20-story	2806	2754	2651	2486
	15-story	2134	2046	1958	1804

3.9 Conclusions

The present study aimed to assess the effectiveness of EB-FRP sheets in reducing residual displacement of medium-to-high-rise CSWs in Vancouver and Montreal, rep-resenting western and eastern Canadian seismic zones, respectively. All CSWs were de-signed and detailed according to CSA A23.3-19 and NBCC20. Three distinct strength-ening schemes were considered for each CSW, and 2D nonlinear time history analysis using RUAUMOKO software was conducted for all RC CSWs, strengthened and un-strengthened. Based on the seismic hazard de-aggregation results, fifteen and eleven ground motions were chosen and scaled to the target spectrum for Vancouver and Montreal, respectively. Consequently, a total of 208 nonlinear time history analyses were carried out to evaluate the impact of EB-FRP sheets on various parameters of CSWs. On the basis of the results, the following conclusions can be drawn:

1. EB-FRP sheets are a viable option for reducing the RIDR in existing modern CSWs (14–53%). The proposed strengthening schemes were evaluated, and it was found that S3-CSW was the most effective in decreasing the RIDR in CSWs. However, it was also observed that the efficiency of the proposed configurations decreased as the height of the shear walls increased. Notably, the RIDR in western Canada was significantly higher compared with eastern Canada.

2. The predominant cause of the RIDR among CSWs in western Canada can be attributed to Cascadia events, compared with other seismic sources. Apart from their long duration, which could induce structural fatigue, the low frequency of such events could result in resonance in high-rise buildings with longer vibration periods.

3. Based on the behavior of 15-story and 20-story CSWs in eastern Canada, it is not deemed reasonable nor cost-effective to apply EB-FRP sheets on the CSWs in this region due to their predominantly elastic behavior and absence of significant residual dis-placement. Nonetheless, it was observed that, for the eastern CSWs, higher modes had an impact, displaying the potential formation of a second plastic hinge in the upper stories (60–70% of the wall height).

4. The S3-CSW performed better in reducing the IDR and CB rotation. This can be attributed to the higher flexural strength resulting from the three layers of vertical EB-FRP sheets, coupled with the confinement caused by the FRP wrapping. Moreover, the horizontal FRP sheets enhanced the shear strength of CSWs, thereby preventing brittle shear failure. The fully wrapped FRP sheets also increased the debonding failure resistance of vertical FRP sheets, which further contributed to the system's overall effectiveness. Also, the research findings indicate the effectiveness of using EB-FRP sheets in mitigating the fluctuation of the IDR cross height of CSWs.

Applying EB-FRP sheets to CSWs resulted in a slight increase in base shear and bending moment demand. Among the various strengthening schemes employed, it was observed that S3-CSW had the highest impact on increasing the shear force and bending moment demand in CSWs. This increase was found to be more pronounced in the CSWs located in eastern Canada, attributable to the relatively larger share of EB-FRP sheets in the overall stiffness of the reinforced walls compared with western Canada. However, the improvement in the shear and bending resistance of CSWs due to the EB-FRP sheets far outweighed the increase in demand.

CHAPTER 4

THE USE OF EXTERNALLY BONDED FRP COMPOSITES TO ENHANCE THE SEISMIC RESILIENCE OF SINGLE SHEAR WALLS: A NONLINEAR TIME HISTORY ASSESSMENT

Ali Abbaszadeh and Omar Chaallal,

Department of Construction Engineering, École de Technologie Supérieur, Université du Québec, Montréal, QC H3C 1K3, Canada

Paper published in *Journal of Composites Science*, *Volume 8, Issue 6, Article 229,* July 2023

4.1 Abstract

In medium to high-rise buildings, single shear walls (SSWs) are often used to resist lateral force due to wind and earthquakes. They are designed to dissipate seismic energy mainly through plastic hinge zones at the base. However, they often display large post-earthquake deformations that can give rise to many economic and safety concerns within buildings. Hence, the primary objective of this research study is to minimize residual deformations in existing SSWs located in the Western and Eastern seismic zones of Canada, thereby enhancing their resilience and self-centering capacity. To that end, four SSWs of 20 and 15 stories, located in Vancouver and Montreal, were meticulously designed and detailed per the latest Canadian standards and codes. The study assessed the impact of three innovative strengthening schemes on the seismic response of these SSWs through 2D Nonlinear Time History (NLTH) Analysis. All three strengthening schemes involved the application of Externally Bonded Fiber Reinforced Polymer (EB-FRP) to the shear walls. Accordingly, a total of 208 NLTH analyses were conducted to assess the effectiveness of all strengthening configurations. The findings unveiled that the most efficient technique for reducing residual drift in SSWs involved applying three layers of vertical FRP sheets to the extreme edges of the wall, full FRP wrapping the walls, and full FRP wrapping of the plastic hinge zone. Nevertheless, it is noteworthy that implementing these strengthening schemes may lead to an increase in bending moment and base shear force demands within the walls.

Keywords: Single shear walls; permanent deformation; FRP sheets; self-centering; Canadian seismic zones; nonlinear time history analysis; resilience

4.2 Introduction

Single Shear Walls (SSWs) are widely used in earthquake-resistant building designs because they are easy to build, cost-effective, and can add rigidity to high-rise buildings. These walls are subjected to different forces, such as axial forces from the gravity loads of the upper floors and shear force and bending moment resulting from the lateral forces applied to them. Based on the type of loading and response of tall SSWs, they can be modeled as cantilever beams, and their seismic response is governed by the bending moment. Modern design codes allow the shear walls to exhibit nonlinear behaviors, enabling them to undergo substantial distortions to absorb considerable amounts of energy effectively. The National Building Code of Canada (NBCC20) mandates precise reinforcement detailing for shear walls with ductile properties to fulfill this role. Plastic hinges formed at the base of shear walls can cause permanent deformations in this Seismic Force Resisting System (SFRS).

Recent studies have focused on improving seismic resilience of structures. In a study conducted by (Bruneau & Reinhorn, 2006), they examined the resilience of structures to seismic events, focusing on both social and structural dimensions of resilience. They defined structural seismic resilience as the capability of structures to experience significant deformation without major residual displacement. They established specific thresholds for inter-story drift within nonlinear responses, which act as indicators of seismic resilience. The research also highlights how retrofitting affects the vulnerability and performance thresholds of buildings, pointing out the severe risks of structural collapses and failures without seismic retrofitting. One method to enhance resilience is by increasing the structure's strength and stiffness through high-resistance materials or larger dimensions, although this can be expensive and pose architectural challenges. Alternatively, structures can gain self-centering capabilities through either the inherent properties of the materials used or by incorporating attached self-centering systems (Abbaszadeh & Chaallal, 2023).

Self-centering systems encompass two primary approaches. The first approach is categorized as (i) controlled rocking, which utilizes post-tensioned tendons for controlled motion (Bedriñana et al., 2022); (ii) uncontrolled rocking, which relies on the structure's self-weight for uncontrolled movement during seismic events (Zhong & Christopoulos, 2022a). In the second approach, specialized mechanical devices combining Shape Memory Alloys (SMAa) with energy dissipators can absorb and diffuse seismic energy (Naeem & Kim, 2018; Noureldin et al., 2021). Figure 4.1 illustrates the self-centering mechanisms that are frequently discussed in seismic-related literature.

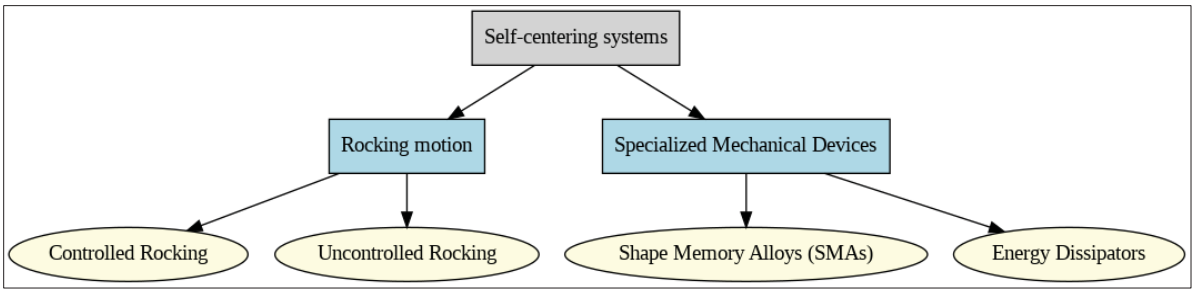

Figure 4.1 Self-centering mechanisms are frequently discussed in seismic literature

The seismic resilience of structures is also crucial in masonry structures. Some studies have explored resilience and collapse dynamics in masonry structures. (Fortunato et al., 2018) presented a new method to analyze masonry failures using a variational approach that accommodates discontinuities in crack formations. This method accurately predicts load-bearing capabilities and failure modes under various loads. Their work, demonstrated through computational simulations, offers essential insights into maintaining and preserving historical masonry buildings. Advanced methodologies for enhancing the seismic resilience of structures involve integrating contemporary high-performance materials, utilizing sophisticated analytical instruments to evaluate structural susceptibilities, and strategically applying retrofitting procedures to address shortcomings within pre-existing systems. To that end, the use of Fiber Reinforced Composites (FRP) features many advantages, encompassing an exceptional strength-to-weight ratio, inherent resistance to corrosion, easy incorporation

within intricate architectural frameworks, and economic viability (Abbaszadeh & Chaallal, 2023; GangaRao et al., 2006). This technique consists of bonding FRP sheets onto the external surfaces of the shear walls, consequently bolstering their load-bearing capacity (Deng et al., 2018), ductility (El-Sokkary et al., 2013), flexural capacity (Altin et al., 2013), shear strength (Huang et al., 2020), and energy dissipation mechanisms (Sakr et al., 2017b). (El-Sokkary et al., 2013) assessed the effectiveness of using Externally Bonded Fiber Reinforced Polymer (EB-FRP) in 8-story SSWs subjected to various seismic time histories representing the design spectrum of Montreal as a representative of the eastern Canadian seismic zone. The plain wall exhibited a second plastic hinge zone in the upper stories (6th) due to the effect of higher vibration modes. EB-FRP strips were used to increase flexural and shear strength in upper levels, while the wall base was confined to develop ductility. The strengthening scheme resulted in a significant reduction in wall rotation (up to 28%), a strain decrease in steel rebars, and an increase in demand for shear force and bending moment. (Deng et al., 2018) demonstrated that fully wrapping shear walls, especially at the base where plastic hinges are expected to form, can enhance damaged shear walls' load-carrying capacity and ductility. (Cruz-Noguez et al., 2015) investigated the advantages of using horizontal EB-FRP sheets and showed a considerable increase in shear strength, ductility, and energy dissipation with this strengthening configuration. They argued that implementing horizontal EB-FRP can improve its seismic behavior even if the wall does not require shear strengthening. (El-Sokkary & Galal, 2013) increased the flexural capacity of shear walls using 200 mm width EB-FRP strips on both sides of the wall. Horizontal FRPs were used to follow the ductile seismic design philosophy and prevent brittle shear failure, resulting in an 80% improvement in flexural capacity. Other studies also confirmed the effectiveness of using vertical EB-FRP to improve the flexural strength of SSWs (Khalil & Ghobarah, 2005; Sakr et al., 2017b)

Some studies have investigated the impact of using EB-FRP on the energy dissipation capacity of shear walls (El-Sokkary, 2023; El-Sokkary et al., 2013). The findings by (Cruz-Noguez et al., 2015) indicated that increasing the number of FRP layers, especially those oriented both vertically and horizontally, significantly enhances the energy dissipation and ductility of RC shear walls. Also, including horizontal FRP reinforcement is crucial, as it prevents premature

shear failures and maintains structural integrity even after initial FRP debonding. These insights highlight the importance of optimizing FRP layers' quantity and orientation to maximize the energy dissipation capacity and seismic resilience of RC shear walls.

Previous studies showed that deploying EB-FRP sheets amplifies the lateral resistance of shear walls against seismic forces and avoids the need for substantial structural reinforcement and reconstruction caused by severe seismic loadings, streamlining the overall upgrading process. However, no research study in the literature directly evaluates the decrease in the residual displacement of SSWs strengthened with EB-FRP sheets. A study on innovative methods to reduce residual displacement in coupled shear walls (CSWs) by (Abbaszadeh & Chaallal, 2023) found that using fully wrapped FRP and vertical layers of EB-FRP can reduce inter-story drift, beam rotation, and residual inter-story drift in the walls located in Canadian seismic zones. In addition, various research studies have investigated alternative techniques for reducing residual deformation in shear walls, such as CFRP grids (Shen et al., 2022), hybrid CFRP grids-steel (Song et al., 2020), and CFRP bars (Zhao et al., 2019). Nevertheless, there has been no emphasis on reducing residual displacement and increasing resilience and self-centering in pre-existing SSWs by employing EB-FRP sheets.

This has been the main impetus to investigate the effectiveness of different EB-FRP sheet configurations in reducing inter-story drift in existing SSWs in terms of pivotal seismic indicators encompassing residual inter-story drift, shear force, bending moment, and inter-story drift. Accordingly, the total of 208 Nonlinear Time-History (NLTH) analysis via RUAUMOKO 2D software is utilized to thoroughly assess 20-story and 15-story SSWs located in seismic zones of Vancouver and Montreal. The walls are subjected to different magnitude-distance ground motion scenarios corresponding to each city's uniform hazard spectrum (UHS). Various strategies are used to test the SSWs' behavior, encompassing an unstrengthen SSW and three SSWs strengthened with innovative EB-FRP configurations. The nonlinear response of the shear wall is determined by analyzing the mean value of all shear wall responses to the selected ground motions. Each wall in Vancouver was evaluated using 15 ground motions, while 11 ground motions were used for the walls located in Montreal. The

analysis outcomes clearly illustrate the influence of the strengthening schemes on the assessed variables.

After the introduction, the study is explained through a series of focused sections. Section 4.3 begins our exploration by examining the design standards that govern the construction of ductile shear walls. Section 4.4 provides detailed insights into the architectural and seismic design specifics of the analyzed buildings. In Section 4.5, we delve into the strategic application of FRP composites to bolster the structural resilience of shear walls. Section 4.6 outlines the analytical methods employed to simulate the seismic response of these reinforced structures. Section 4.7 evaluates the impact of FRP reinforcements, focusing on their effectiveness in reducing residual displacement of shear walls. The paper concludes with Section 4.8, which highlights the most important discoveries.

4.3 Seismic design of ductile SSW according to standards

According to CSA A23.3-19 the factored shear force at the base of SSWs should be calculated using either the equivalent static force procedure or dynamic analysis specified in NBCC20. The base shear force must be increased to account for flexural overstrength and plastic effects of higher modes. The final base shear force is used to calculate the internal forces and stress of structural components following the force-based design technique. The dynamic analysis method required by NBCC20 assumes the linear behavior of structural materials and relies on the response of vibration modes to evaluate seismic performance. The foundational assumptions underlying this approach can be outlined as follows: (i) The seismic response of a structure during an earthquake can be represented as a linear combination of distinct vibration modes inherent to the structure; (ii) The periodicity of structural vibrations within each vibration mode remains constant throughout the seismic event. Given that the maximum responses across various vibration modes do not coincide during an earthquake, predicting these maximum responses within different structural members is imperative. Accomplishing this necessitates the utilization of statistical methodologies that amalgamate the peak responses derived from different vibration modes. Moreover, these methods must account for potential

interaction effects stemming from diverse responses originating from other vibration modes. In this context, the Square Root of the Sum of Squares (SRSS) and the Complete Quadratic Combination (CQC) methods are two viable approaches for estimating the comprehensive structural response. These methods enable aggregating responses from different modes, providing a holistic understanding of structural behavior during a seismic event.

When using the equivalent static method, the base shear value must be reduced to account for the structure's plastic behavior by applying overstrength (R_o) and ductility-related (R_d) factors (see Table 4.1). Therefore, NBCC20 introduced Equation 4.1 to determine equivalent static base shear force (based on the seismic hazard of 2% probability/50years).

$$V_{base} = S(T_a)M_v \frac{I_E}{R_d R_o} W \tag{4.1}$$

Where T_a is the structures' fundamental period, and $S(T_a)$ is the design spectral response acceleration. I_E and M_v represent the importance and higher mode effects factors respectively. *W* represents the structures' weight that can be determined by Equation 4.2.

$$W = DL + 0.25SL \tag{4.2}$$

Where *DL* is dead load and *SL* represent snow load.

Table 4.1 R_d and R_o in different types of SSWs

Type of SFRS	Force modification factor

Ductile SSW	R_d = 3.5	R_o = 1.6
Moderately ductile SSW	R_d = 2	R_o = 1.4
Conventional SSW	R_d = 1.5	R_o = 1.3

The factored shear force should be raised to consider flexural overstrength, γ_w, since rebars located vertically in the plastic hinge zone may experience high tension stresses due to strain hardening. Therefore, to increase safety against brittle shear failure in ductile SSWs, flexural overstrength is determined by employing a stress of 1.25 f_y in the vertical rebars (f_y is the yield strength of steel rebars) (Adebar et al., 2014) . This is particularly important for components with significant force reduction factors. For ductile SSWs, flexural overstrength coefficient may be calculated by the ratio of the probable bending moment to the factored bending moment (Canada & Association, 2016). In multi-degree of freedom SSWs, shear force in the first vibration mode does not increase after flexural yielding occurs in the plastic hinge zone. However, it significantly increases in higher vibration modes as the level of ground motion intensity rises (Adebar et al., 2015). Hence, the CSA A23.3-19 requires modifying the factored base shear force to account for the plastic effect of higher modes. Table 4.2 displays the corresponding coefficients.

Table 4.2 Coefficient for plastic effects of higher modes

$T_a \leq T_L$	$T_a \geq T_U$
1.0	$1.0+0.25\left(\frac{R_o R_d}{\gamma_w} - 1.0\right) \leq 1.5$ and ≥ 1.0

Where T_L and T_U shall be calculated according to Table 4.3.

Table 4.3 Calculation of T_L and T_U

	T_L	T_U

S(0.2)/S(2.0) < 10.0	0.5 s	1.0 s
S(0.2)/S(2.0) ≥ 10.0	0.2 s	0.5 s

Where S(T) is the design spectral acceleration and is presented for different periods by NBCC20. When a lateral load is applied, the RC component loses its initial stiffness due to cracking and crushing on the tension side of the concrete. CSA A23.3-19 required employing sectional properties reduction factors to address the nonlinear behavior of concrete in the linear analysis of RC members. Table 4.4 displays sectional properties reduction factors.

Table 4.4 Proposed sectional effective properties for linear analysis

Element	Property	Effective property
Wall	Flexural stiffness	$EI_e = \alpha_w EI_g$
	Axial stiffness	$EA_{xe} = \alpha_w EA_g$

Where A_g= areas' gross section, E= concretes' modulus of elasticity, A_{xe}= effective axial cross section, I_g= gross section moment of inertia, I_e = effective moment of inertia, and α_w can be regarded as 0.5 for ductile SSWs, as suggested elsewhere(Canada & Association, 2016). Per capacity-design method regulations, the CSA A23.3-19 offers a framework for establishing a well-designed zone at the base of SSWs to manipulate the formation of plastic hinges. This designated zone must exhibit uniformity concerning cross-section area, reinforcement detailing, and concrete strength. Notably, designing structures to experience elastic behavior during seismic events can prove uneconomical. By forming the plastic zones within SSWs, a substantial amount of energy dissipation becomes achievable without incurring significant strength deterioration.

The computation of the top displacement of SSWs can be straightforwardly derived by multiplying the total rotation at the base of the shear walls with the wall's height, h_w. Furthermore, research investigations have demonstrated a correlation between the rotational capacity of shear walls and critical factors such as the height of the plastic hinge zone, the

ultimate compressive strain of concrete, ε_{cu}, and the ultimate tensile strain of rebars, ε_{smax}, within the plastic hinge zone (Adebar et al., 2005). Considering this, CSA A23.3-19 mandates that to ensure the ductile performance of SSWs, the inelastic rotational capacity of the shear wall within the plastic hinge zone must surpass the inelastic rotational demand. Inelastic rotational demand in SSWs could be calculated as presented in Equation 4.3.

$$\theta_{id} = \left(\frac{\Delta_f R_o R_d \ - \Delta_f \gamma_w}{h_w - \frac{\ell_w}{2}} \right) \geq 0.004 \tag{4.3}$$

where Δ_f is the factored walls' top displacement. Accordingly, $\Delta_f R_o R_d$ represents design wall displacement, and $\Delta_f \gamma_w$ is the elastic portion of the wall displacement. The Inelastic rotational capacity of the wall is presented in Equation 4.4.

$$\theta_{ic} = \left(\frac{\varepsilon_{cu} \ell_w}{2c} - 0.002 \right) \leq 0.025 \tag{4.4}$$

where c is the depth of neutral axis. It should be noted that within the plastic hinge zone, the flexural rebars' plastic curvature and plastic tension strain change in a linear manner from the maximum level (which is at the point where the first yielding occurs) to zero. However, the plastic tension strain and curvature can be considered uniform at the maximum level to ease wall deformation calculation (Bohl, 2006).

4.4 An overview of the studied building

The present study evaluated specifically two sets of buildings with 20-story and 15-story configurations located in Vancouver and Montreal, site class C. As seen in Figure 4.2, these buildings solely rely on SSWs as their SFRS in both primary axes and have four SSWs in North-South (N-S) direction and two SSWs in West-East (W-E) direction. Regarding the vulnerability of structures to ground motion acceleration from different angles, the principal objective of this investigation was to evaluate the seismic implications along the North-South

axis. The vertical distance between the floors has been set to 3.5 meters, leading to a total height of 70 meters, and 52.5 meters for 20-story and 15-story SSWs, respectively. As seen in Figure 2, the buildings have a symmetrical 21m by 40 m dimension and 200 mm-thick RC slabs. The concrete compressive strength, f_c', and the steel rebar yield strength, f_y, are assumed to be 30 MPa and of 400 MPa, respectively.

The first phase of the study involved designing and detailing SSWs. The base shear was determined through an equivalent static method. This was followed by executing a linear dynamic analysis using SAP2000 software version 19.0.0. The resulting base shear from the dynamic analysis was then scaled with the base shear obtained from the equivalent static method, as per the provisions of the NBCC20. Similar procedure and design guide can be found elsewhere (Abbaszadeh & Chaallal, 2023; Canada & Association, 2016). Figure 4.2 illustrates the plan view, Figure 4.3 shows the reinforcement configuration and Table 4.5 the reinforcement detailing.

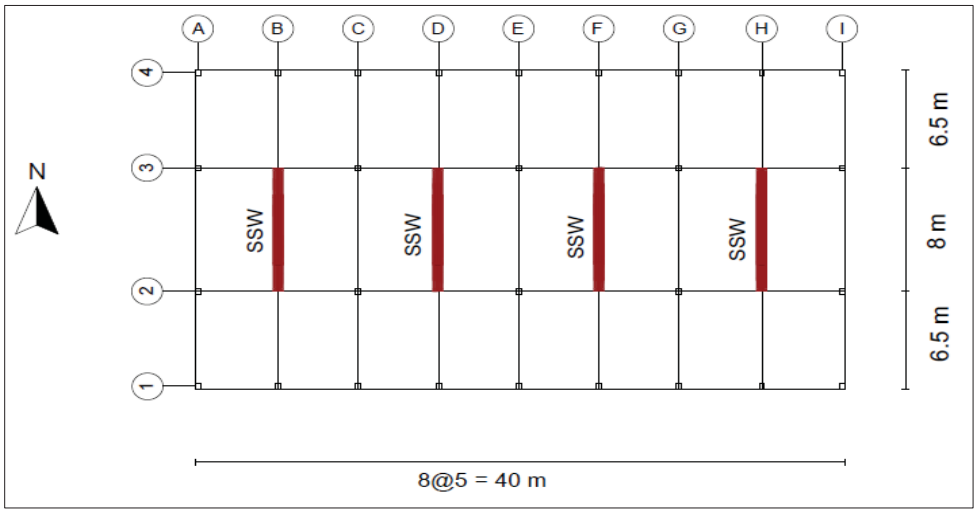

Figure 4.2 Plan view of the studied building

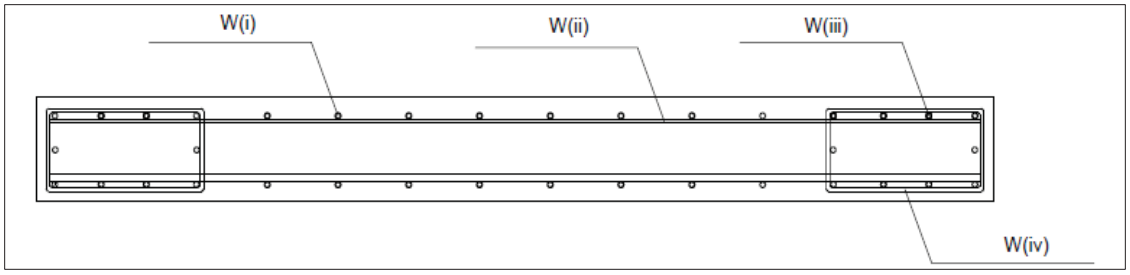

Figure 4.3 Reinforcement configuration of shear walls

Table 4.5 Reinforcement details of shear walls

		W (i) (mm)	**W (ii) (mm)**	**W (iii) (mm)**	**W (iv) (mm)**	**Section Dimension (mm)**
West	20-story	15M @200	15M @150 15M @200	2x10 30M in PH region 2x10 25M out of PH region	10M @150 10M @200	8000*450
	15-story	10M @200	15M @200 15M @250	2x8 25M in PH region 2x8 20M out of PH region	10M @200 10M @250	8000*400
East	20-story	15M @200	15M @200 15M @250	2x8 25M in PH region 2x8 20M out of PH region	10M @200 10M @250	8000*450
	15-story	10M @200	15M @200 15M @250	2x8 20M in PH region 2x8 15M out of PH region	10M @200 10M @250	8000*400

4.5 Seismic improvement of SSWs using EB-FRP sheets

As discussed in previous sections, ductile shear walls are susceptible to plastic hinge formation at the wall base due to excessive bending and flexural demands experienced during cyclic loads. These loads can lead to reinforcement yielding and concrete crushing at the wall base,

which are the primary causes of permanent deformation in these walls. Additionally, higher mode effects can lead to excessive shear force demands for taller shear walls.

On the other hand, ACI 440.2 R-17 introduces specific strengthening configurations using EB-FRP composites to address these weaknesses in SSWs. The guideline specifies using vertical EB-FRP composites for flexural strengthening, horizontal EB-FRP for shear strengthening, and wrapping FRP for confinement improvement and avoiding debonding failure. Accordingly, this study has adopted its proposed strengthening configurations based on a combination of the schemes suggested by ACI 440.2 R-17 to find an effective configuration for reducing residual deformation in SSWs.

Incorporating vertical EB-FRP sheets to enhance the flexural resistance of SSWs poses a primary concern with regard to FRP debonding, owing to the concrete's vulnerability in tension (Ceroni et al., 2008). Several studies have recommended resorting to diverse anchorage systems to forestall the premature debonding of EB-FRP (Grelle & Sneed, 2013; Mostafa & Razaqpur, 2013). Despite this, the execution of experimental examinations to authenticate the effectiveness of these systems during seismic events limits their application. As a reliable solution, ACI 440.2 R-17 has put forward the utilization of fully wrapped FRP in regions prone to debonding, particularly in plastic hinge zones (Abbaszadeh & Chaallal, 2023; Committee, 2017). In analytical procedures, according to Equation 4.5, ACI requires designers to restrict the effective strain of FRP sheets, ε_{fd}, to avoid debonding failure.

$$\varepsilon_{fd} = 0.41\sqrt{\frac{f_c'}{nE_f t_f}} \leq 0.9\,\varepsilon_{fu} \tag{4.5}$$

In Equation 4.5, f_c' and n denote concrete compressive strength and the number of FRP layers, respectively; E_f and t_f are modulus of elasticity and thickness of FRP sheets, respectively; ε_{fu} represents rupture strain of FRP composites.

This study considered three unique schemes aimed at fortifying vulnerable flexural and compressive cracking regions within medium-to high-rise SSWs. The primary goal is to

enhance the seismic resilience of these crucial SFRS. The present study comprehensively assesses and interprets the effectiveness of these schemes in reducing residual deformation in SSWs. Also, it is crucial to prevent brittle shear failure prior to yielding of bending moment reinforcement.

Consequently, as a means of enhancing the load-carrying capacity, ductility, and shear strength of SSWs, fully wrapped FRP has been implemented. This implementation is primarily aimed at improving the resistance against debonding failure in accordance with the recommendations of the ACI. Moreover, the issue of concrete crushing due to high compressive strain in the plastic hinge zone is a formidable challenge in slender SSWs during cyclic events. However, this challenge can be addressed through additional confinement and complete wrapping of the shear wall base. In the first retrofitting scheme, hereinafter R1-SSW, vertical FRP layers were added to both surfaces of the SSW to enhance the bending capacity of the shear wall in addition to the FRP wrapping. In the second configuration, R2-SSW, from both vertical edges, the first 15% of SSW's length on both faces was fully covered by two layers of vertical EB-FRP, followed by one layer of vertical EB-FRP in the adjacent 15% from base to the top of walls. In the third proposed scheme, R3-SSW, three layers of vertical EB-FRP were attached to the first 15% of the length of SSW from vertical edges on both sides. An additional layer of FRP wrapping was also used in its plastic hinge zone. A similar retrofitting configuration in coupled shear walls has been previously used elsewhere (Abbaszadeh & Chaallal, 2023). In this research study, with the unreinforced wall being referred to as the control wall and labeled as C-SSW, a total of 16 distinct SSWs were evaluated. Also, FRP sheets with tensile strength of 1355 MPa, tensile modulus of 115,700 MPa, and thickness of 1.3 mm were used. The impact of concrete cracking on the bonding behavior of EB-FRP composites is not considered. Figure 4.4 shows the different configurations considered in this study.

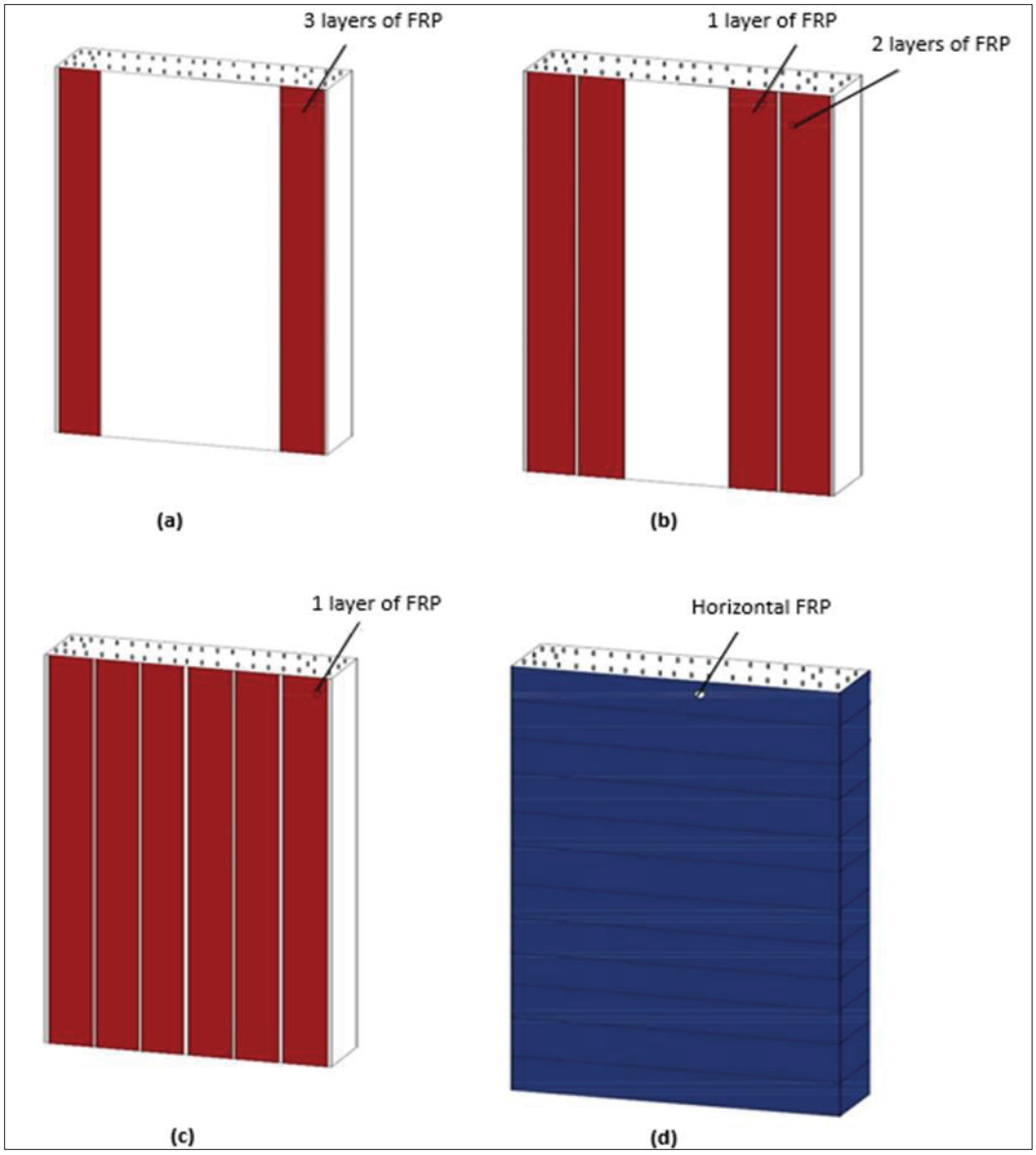

Figure 4.4 Different strengthening schemes used in this study: (a) R3-SSW; (b) R2-SSW; (c) R1-SSW; (d) FRP wrapping of shear walls

4.6 Nonlinear Time History Analysis of SSWs

The NLTH analysis technique is widely acknowledged as one of the most accurate and practical approaches for evaluating the behavior of structures under cyclic seismic forces.

Therefore, NLTH analysis using RUAUMOKO 2D software has been carried out in this study following provisions of Structural commentaries (NRCC, 2015).

4.6.1 Model assumptions

The slender walls considered in this study can withstand the forces induced by ground motions through flexural action, akin to the resilience displayed by cantilevered RC beams. In particular, the analysis of shear deformation should consider a linear elastic approach as specified by capacity design regulations that pertain to ductile shear walls (Boivin & Paultre, 2010). RUAUMOKO 2D software, a finite element-based computational tool, boasts an expansive array of beam and beam-column components expressly designed to simulate flexural frame-like components. The plastic behavior of these components is based on the Giberson one-component model (Giberson, 1969). In this model, the inelastic tendencies occur only at both ends, while the central elastic portion remains unaffected. Beam-column members have a significant advantage as they can handle both axial loads and bending moments, which is a critical factor in assessing the performance of shear walls during seismic events. Therefore, quadratic beam-column members were used in the centroid of both strengthened and control shear walls to model them in this study. Figure 4.5 displays the modeling of SSWs assessed in this investigation.

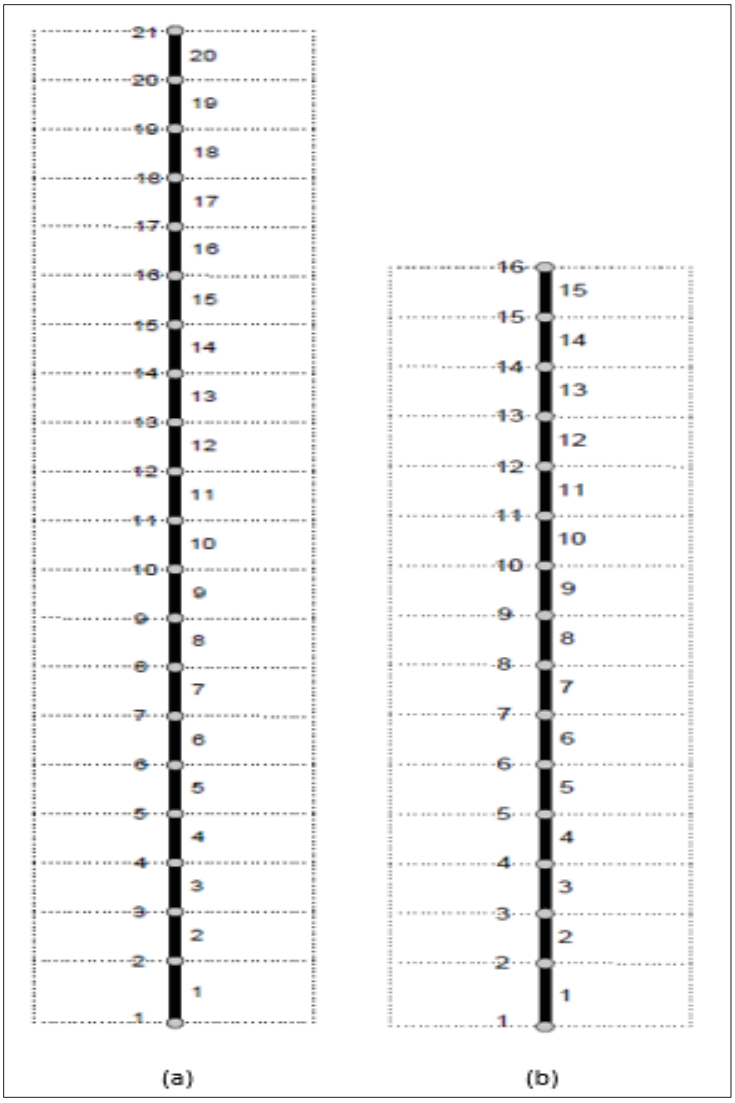

Figure 4.5 Member and node modeling of: (a) 20-story shear wall; (b) 15-story shear wall

In addition to the advantages mentioned above, plastic hinges on both ends of this member allow the wall to experience plastic response throughout its height during the NLTH analysis. This insight is even more critical when considering the impact of higher modes on tall shear walls, which can create a second set of plastic hinges in the upper levels (Dezhdar, 2012). However, it is important to acknowledge that the selection of member height can affect the model. This is because inelastic behavior is confined to the ends of the components, neglecting potential distributed plasticity. Quadratic beam-column members have previously been used

to model shear walls (Abbaszadeh & Chaallal, 2023; Honarparast & Chaallal, 2019b). In order to address the impacts of axial forces and bending moments in SSWs, Xtract software v2.6.0 was employed to create the interaction graph. The linear elastic response of the FRP materials bonded to the RC members was determined by their manufacturing attributes. To model reinforcing rebars' nonlinear response, a bilinear model with strain hardening was considered. For confined and unconfined concrete, the model presented by (Mander et al., 1988) was applied, while the (Lam & Teng, 2003) model was utilized to view curvature enhancement in concrete with FRP confinement. While this study focuses primarily on the nonlinear sectional properties of reinforced concrete (RC) members, it is acknowledged that the seismic performance of concrete structures is heavily influenced by the material properties used in construction. Key factors, including the type and quality of aggregates, cement grade, and specific mix design, are fundamental in shaping the structures' ductility, strength, and energy dissipation capacities. Notably, the response of aggregates under dynamic loads is critical for understanding the integrity and cracking behavior during seismic events. Further details on these aspects are extensively discussed in existing literature (Sherzer et al., 2022). Also, the lumped mass model was employed due to the assumption that all floors are rigid and thick to produce diaphragm effects. This model assumes that the whole mass of the building is consolidated at the nodes. The mass matrix will only be affected by nodal weights, M_i, on the diagonal elements, and typically, the elements related to rotational degrees of freedom are considered to be zero. So each diagonal element only corresponds to one translational degree of freedom of the lumped mass. Equation 4.6 represents lumped mass matrix, M, in an n-story SSW.

$$M = \begin{bmatrix} M_1 & \square & \square & \square & \square \\ \square & M_2 & \square & \square & \square \\ \square & \square & \ddots & \square & \square \\ \square & \square & \square & M_{n-1} & \square \\ \square & \square & \square & \square & M_n \end{bmatrix} \tag{4.6}$$

The ductility-based model, using the data suggested by (McNeice, 2004), simulated the decay in RC concrete strength caused by ground motion loading. Furthermore, the large displacement

technique was used in order to account for geometric nonlinearity. This method involves updating the nodal coordinates and component stiffnesses during each time step to accommodate axial forces and geometry changes. This enables the analysis of structures experiencing significant displacements (Zhijun, 2006).

This study used the Q-HYST hysteresis model (Saiidi & Sozen, 1979a) for the nonlinear response of strengthened and control SSWs to the ground motions. An experimental constant, α, controls the unloading stage of Q-HYST, which is adopted from the experimental studies available in the literature (McNeice, 2004). The stiffness degradation in this model is controlled by Equation 4.7.

$$K_u = K_o \left(\frac{d_y}{d_m}\right)^{\alpha} \tag{4.7}$$

where, K_u, is the degraded stiffness through unloading stage, K_o is the initial stiffness in loadings stage, d_y and d_m are yielding and ultimate displacement. This hysteresis model has been used in other investigations and has shown its capability to replicate the plastic response of RC components under seismic loading (Honarparast & Chaallal, 2019b).

4.6.2 Damping assumptions

NLTH is a step-by-step systematic approach for solving the fundamental equation of motion (Equation 4.8) of a given structure.

$$M\,(\ddot{X}_{(t)} + \ddot{u}_{(t)}) + C\dot{X}_{(t)} + KX_{(t)} = 0 \tag{4.8}$$

where, $\ddot{X}_{(t)}$, $\dot{X}_{(t)}$, and $X_{(t)}$ denote, acceleration, velocity, and displacement of the structure respectively; M represents mass matrix; C and K denote damping and stiffness matrices; and $\ddot{u}_{(t)}$ represents ground acceleration.

Choosing an appropriate damping model is crucial to correctly evaluate a structure's nonlinear behavior. Rayleigh model expressed in Equation 4.9, is a highly adopted technique in the literature due to its ability and is used in this study.

$$C = \alpha M + \beta K \tag{4.9}$$

In Equation 4.9, α and β are constant damping factors proportional to mass and stiffness matrices. For a structure with several degrees of freedom in each vibration mode with vibration frequency, ω_i, the damping ratio, ξ_i, can be calculated using Equation 4.10.

$$\xi_i = \frac{1}{2}\left(\frac{\alpha}{\omega_i} + \beta\omega_i\right) \tag{4.10}$$

As per Equation 4.10, at low frequencies, damping proportional to mass is dominant, while at high frequencies, damping proportional to stiffness is dominant.

In the Rayleigh damping model, selecting two vibration modes along with their corresponding damping ratios is standard practice. In typical applications involving time-domain operations, Rayleigh damping is commonly employed to impart damping characteristics that exhibit a notably diminished sensitivity to frequency variations. Despite the inherent frequency-dependent nature attributed to Rayleigh damping, its parameters can be judiciously chosen within a specific range, aiming to mitigate the extent of frequency-related influences to the greatest extent achievable. On the other hand, selecting very low frequencies (proportional to the mass matrix) results in excessive damping force, which is unsuitable for NLTH analysis. These modes should be chosen strategically to provide an appropriate and balanced representation of the system's damping behavior across the frequency spectrum (different vibration modes) (Hall, 2006). This ensures that the damping ratios are not skewed towards particular frequency ranges, preventing the issues mentioned earlier with excessive damping at low frequencies. Accordingly, this research study employed the Rayleigh damping technique, which incorporated a critical damping rate of 5% for modes 1 and 10. This

methodology has been previously detailed and used elsewhere (Abbaszadeh & Chaallal, 2023; Honarparast & Chaallal, 2022).

4.6.3 Selection and scaling of the ground motions

All selected ground motions for NLTH analysis must conform to the designated characteristics that correspond to their site-specific seismic hazard level. These characteristics include fault distance to the building site, Magnitude, and fault plate tectonic state. In Canada, design seismic hazard levels are periodically updated by NBCC as a function of peak ground acceleration, PGA, peak ground velocity, PGV, and spectral accelerations, Sa, for six distinguishing vibration periods. Currently, NBCC20 is tracking the 6th generation of the seismic hazard model (Adams et al., 2019), based on a 2% probability of exceedance in 50 years. This version exhibits a considerable increase in the hazard level of site category C (pertaining to building sites in this research) compared to the last version, as depicted in Figure 4.6.

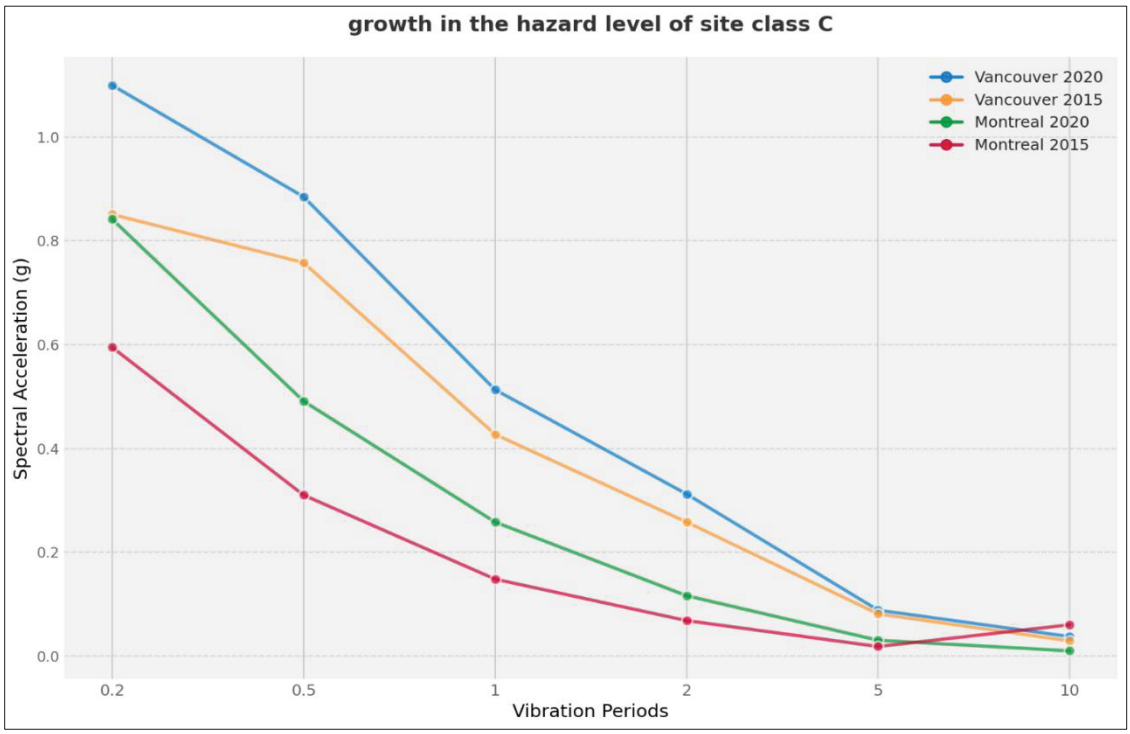

Figure 4.6 Growth in the hazard level of site category C

Ground motions have profound differences in the cities in western Canadian and eastern Canadian seismic zones. As a matter of fact, ground motions in Montreal have higher frequency content than ground motions in Vancouver (Tremblay & Atkinson, 2001) In contrast, Vancouver has typical earthquakes with longer durations specially due to the Cascadian earthquake's occurrence ($M > 8$) on Canada's west coast (Atkinson, 2009). Accordingly, in order to accurately ascertain the magnitude-distance (M-R) scenarios of ground motions that align with the hazard level of a given city, it is imperative to perform a de-aggregation of the seismic hazard analysis pertaining to the aimed city. The findings of the de-aggregation analysis indicate that in the case of Vancouver, three distinct hazard M-R scenarios must be taken into consideration. Similarly, for Montreal, two scenarios need to be accounted for (Adams et al., 2019; Adams & Atkinson, 2003).

Because of the deficiency of ground motions conforming with the seismic hazard level of eastern Canada, artificial earthquakes developed by (Atkinson, 2009) are utilized in this research study. The process of choosing and scaling time histories was carried out in line with NBCC guidelines, utilizing the technique recommended by Tremblay et al. (Tremblay et al., 2015a). Per the guidelines outlined by the Structural commentaries (N.R.C.C, 2015), it is required that a minimum of five ground motions be selected for each scenario, with a total of no less than eleven ground motions per city. As such, eleven ground motions have been chosen from the aforementioned source for the city of Montreal, while fifteen ground motions have been selected for Vancouver as detailed in Tables 4.6 and 4.7, respectively. The response spectra for the scaled time histories are presented in Figure 4.7, depicting Montreal and Vancouver.

Table 4.6 Description of selected earthquakes in Montreal

Scenario	Rec. No.	PGA (g)	Duration (s)	Period range (s)	Event type
M = 6 10 < R < 30	East 1	0.322	43.59	0.2-1	crustal
	East 2	0.645	43.59		
	East 3	0.423	43.59		
	East 4	0.451	47.53		
	East 5	0.301	47.53		
M = 7 15 < R < 100	East 6	0.478	51.12	0.5-2.42	crustal
	East 7	0.410	51.12		
	East 8	0.308	51.12		
	East 9	0.331	57.35		
	East 10	0.248	57.35		
	East 11	0.299	57.35		

Table 4.7 Description of selected earthquakes in Vancouver

Scenario	Rec. No.	PGA (g)	Duration (s)	Period range (s)	Event type
M = 6.5 10 < R < 30	West 1	0.475	49.30	0.2-0.8	crustal
	West 2	0.483	49.30		
	West 3	0.503	49.30		
	West 4	0.497	53.63		
	West 5	0.559	53.63		
M = 7.5 15 < R < 100	West 6	0.391	102.02	0.3-1.5	In-slab
	West 7	0.430	102.02		
	West 8	0.351	102.02		
	West 9	0.289	93.39		
	West 10	0.423	93.39		
M=9 100 < R < 200	West 11	0.137	309.42	1-4	Cascadia subduction
	West 12	0.132	309.42		
	West 13	0.173	309.42		
	West 14	0.146	309.42		
	West 15	0.167	309.42		

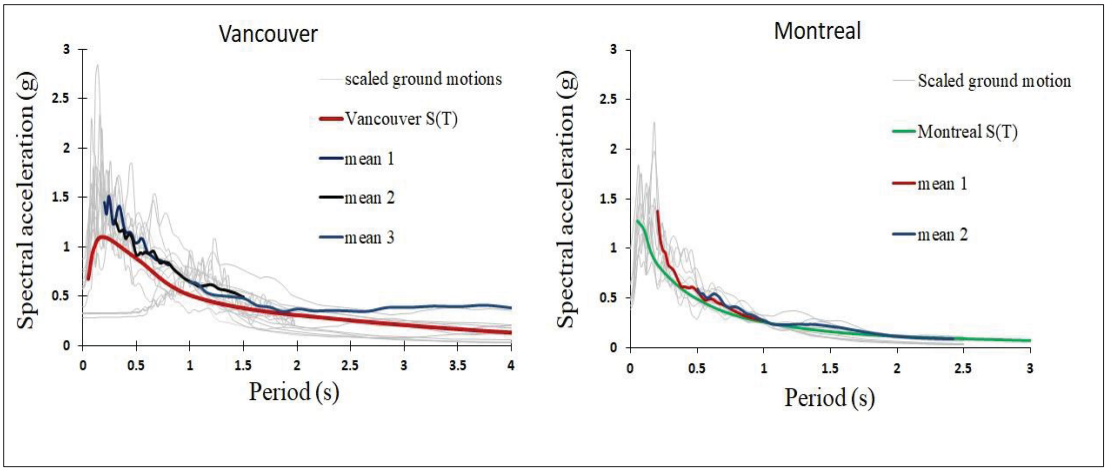

Figure 4.7 Response spectra for scaled ground motions

Figure 4.8 illustrates variations in earthquake record content for different ground motion scenarios.

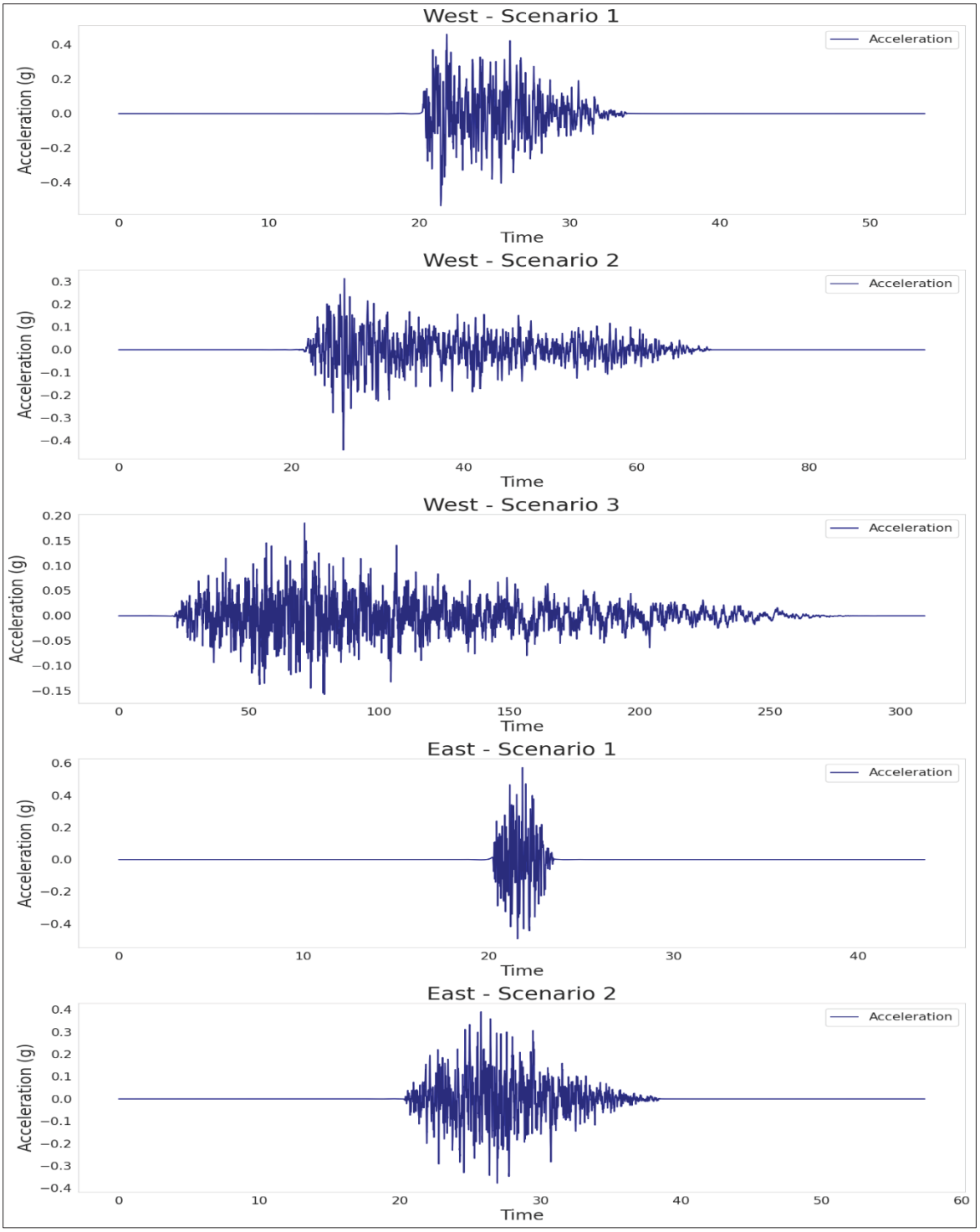

Figure 4.8 Variation in earthquake record content for different ground motion scenarios

4.7 Interpretation of the Results

The present study aimed to evaluate the efficiency of using EB-FRP sheets in enhancing the seismic resilience of SSWs by decreasing the residual displacement. This was achieved by means of nonlinear time history analysis of different strengthening schemes of 20 and 15-story SSWs located in Western and Eastern Canadian seismic zones. The study also discusses the influence of applied strengthening schemes on inter-story drift ratio (IDR), shear force demand, and bending moment demand in shear walls. Nevertheless, assessing residual displacement in reinforced concrete structures is a contentious issue intricately linked to the specific aim under examination (Abbaszadeh & Chaallal, 2023). In this regard, ASCE-7-22 used IDR as a metric to evaluate structures' self-centering capability and restricted residual inter-story drift ratio (RIDR) in structures taller than 73 meters to 1%. Hence, this study capitalized on the RIDR as a metric to assess the effectiveness of proposed reinforcement strategies in reducing residual displacement in SSWs.

4.7.1 Inter-Story Drift Ratio (IDR)

The NBCC20 regulations restrict IDR demand to 2.5%. However, in seismic zones with low-frequency ground motions, the IDR profiles of RC shear walls can diverge from the one derived through linear analysis due to concentrated plastic rotation at the base. Thus, a thorough assessment of IDR is crucial to anticipate unexpected demands.

4.7.1.1 Walls in Vancouver

The NLTH analysis results for a 20-story SSW in Vancouver reveal a significant influence of ground motion frequency content (across various scenarios) on the IDR. Figure 4.9 displays the mean peak IDR values for different scenarios and strengthening schemes. Notably, the dominant events driving the flexural response of SSWs in this region are Cascadia subduction events (M9). These events are characterized by their low-frequency content and extended durations, capable of exciting the wall's first vibration mode. While the peak mean IDR for this scenario did not exceed the 2.5% limit, it still stood at approximately twice the peak mean IDR

envelope value of all ground motions. Additionally, the influence of higher modes becomes evident in the M6.5 scenario, where ground motions exhibit higher frequencies and there is possibility for second plastic hinge in the upper levels. Meanwhile, results show that using EB-FRP sheets could decrease peak IDR in this wall up to 8, 11, and 17% in R1-SSW, R2-SSW, and R3-SSW, respectively.

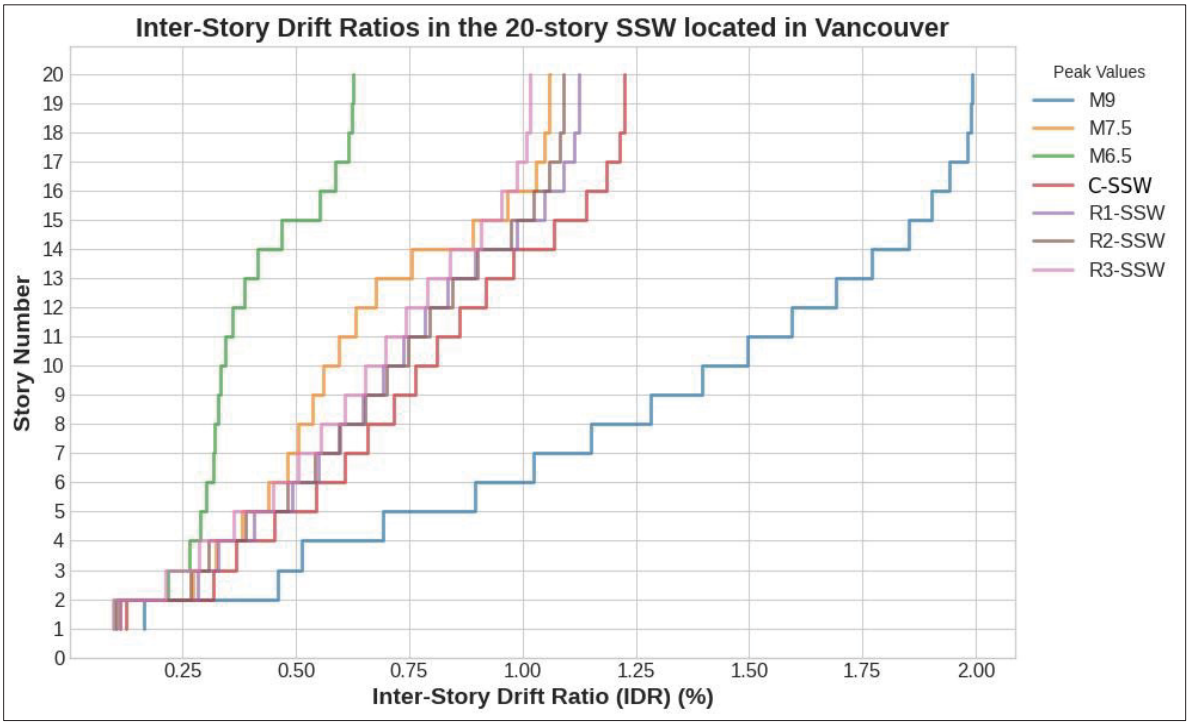

Figure 4.9 Mean peak IDR values for different scenarios and strengthening schemes in 20 story SSW located in Vancouver

The efficiency of strengthening configurations demonstrated a more significant impact in the 15-story SSW, where the maximum reduction in R3-SSW reached 28%. This comparison with the R3-SSW in the 20-story wall indicates that the effectiveness of implementing EB-FRP sheets in shear walls diminishes as the height of the walls increases. Also, shorter SSWs displayed a comparatively lower sensitivity to the effects of higher modes. Similar findings have been reported elsewhere (Abbaszadeh & Chaallal, 2023). Additionally, the suggested strengthening schemes resulted in a reduction of IDR by up to 18% in R2-SSW and 13% in

R1-SSW. Figure 4.10 illustrates mean peak IDR in the 15-story SSW located in Vancouver for different scenarios.

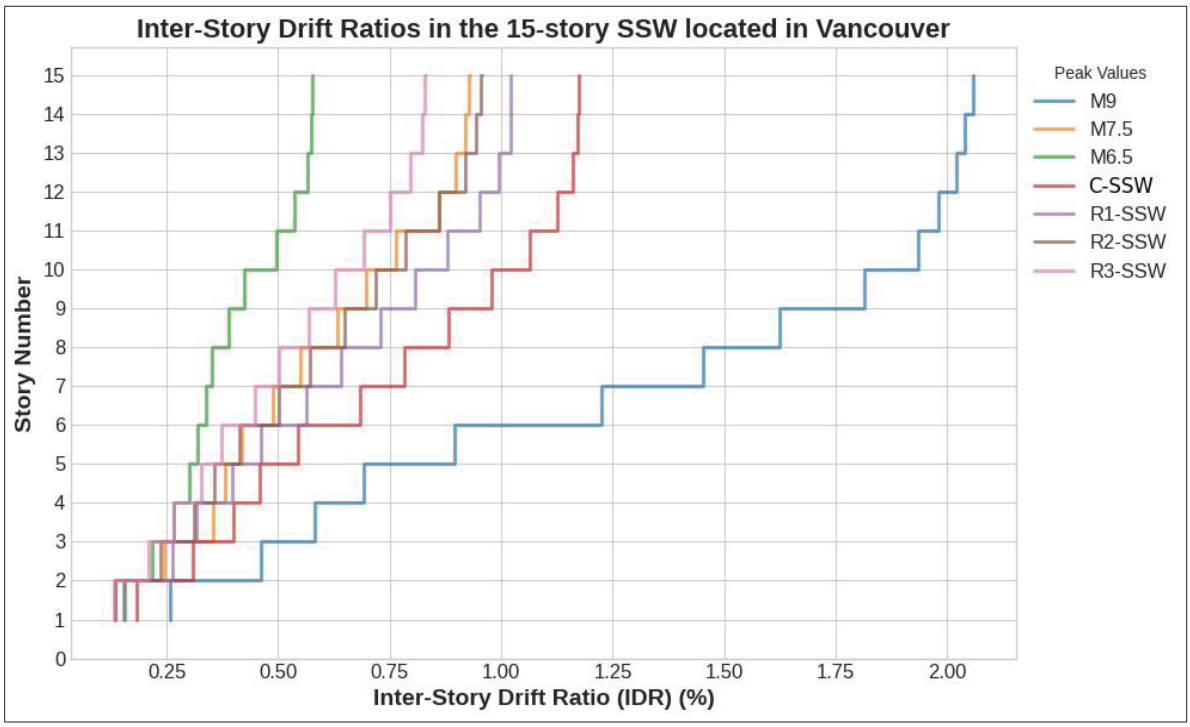

Figure 4.10 Mean peak IDR values for different scenarios and strengthening schemes in 15-story SSW located in Vancouver

4.7.1.2 Walls in Montreal

While Western Canada does experience low-frequency seismic events with longer durations, Montreal, on the other hand, does not encounter such low-frequency seismic events. Notably, the results of NLTH analysis revealed a reduced IDR in a 20-story SSW in Montreal compared to a corresponding wall in Vancouver due to the lower seismic activity level. As illustrated in Figure 4.11, both the M6 and M7 scenarios observed in Montreal highlight the impact of higher modes on the wall structure, which could potentially result in the development of a secondary plastic hinge at upper levels. This phenomenon is observed within the wall's 60% to 70% height range. However, due to this region's relatively low seismic activity, the flexural demands on these walls are lower than their capacity. Nonetheless, the likelihood of secondary plastic hinge

formation at upper levels increases in taller walls where the higher frequency effect becomes more pronounced. The NLTH analysis results of IDR revealed that both M7 and M6 scenarios in 20-story SSWs reflect the effects of higher modes, but the M7 was the prevailing scenario in Montreal, where the wall experienced an average peak IDR of approximately 0.25%, while the mean peak IDR for all ground motions stood at around 0.23%. Furthermore, the implementation of strengthening schemes demonstrated the potential to reduce IDR in this wall by margins up to 5%, 8%, and 13% in R1-SSW, R2-SSW, and R3-SSW, respectively. Furthermore, the use of the proposed strengthening configurations can decrease the fluctuations in the mean IDR envelope within this wall.

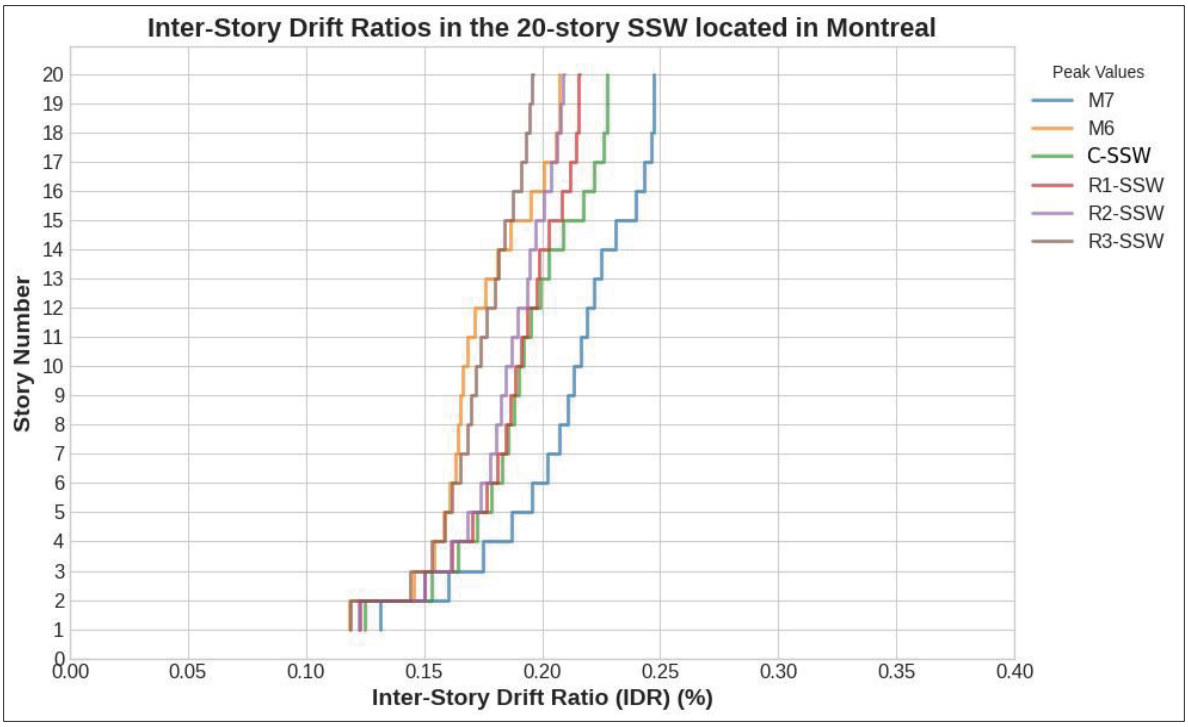

Figure 4.11 Mean peak IDR values for different scenarios and strengthening schemes in 20-story SSW located in Montreal

The NLTH analysis results indicate that higher modes' influence on the 15-story wall is relatively limited compared to the taller shear wall. Although forming a second plastic hinge between levels 9 and 12 appears possible in M6 events, the ground motion intensity in this scenario falls significantly below the wall's flexural capacity. Conversely, the M7 scenario

emerges as the dominant event for this wall, exhibiting a maximum IDR of approximately 0.53% (see Figure 4.12). However, this value is considerably lower than the NBCC20 limit for ductile shear walls. Furthermore, the findings suggest that the recommended strengthening strategies are more effective in reducing the IDR of a 15-story wall than a 20-story one. Notably, the S3-CSW configuration achieved the most significant IDR reduction, reaching 21%, while mean IDR decreases of 12% and 9% were observed for the S2-CSW and S1-CSW configurations, respectively.

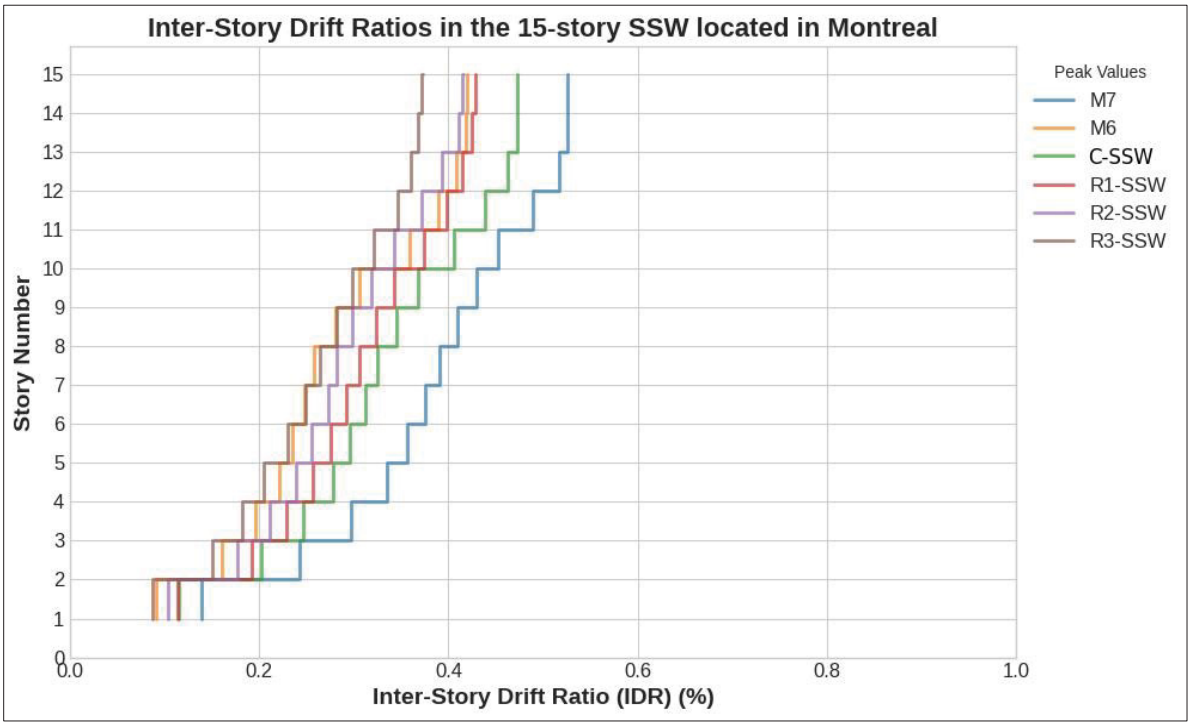

Figure 4.12 Mean peak IDR values for different scenarios and strengthening schemes in 15-story SSW located in Montreal

4.7.2 Residual displacement of walls

4.7.2.1 Walls in Vancouver

The presence of severe ground motions characterized by low frequencies and prolonged durations in Western Canada resulted in significant residual displacements in SSWs within this region. As shown in Figure 4.13, the findings revealed that the maximum RIDR in a 20-story SSW occurred during earthquake 14, wherein the wall experienced a notable 1.36% RIDR. Figure 4.14 also shows the RIDR values of 15-story shear wall for all ground motions in Vancouver. This heightened residual value can be attributed to the extended duration of Cascadia events, leading to structural fatigue due to a substantial number of loading and unloading cycles. Furthermore, in addition to the Cascadia events (M9), In-slab events (M7.5) exhibited a noteworthy level of RIDR. This can be attributed to the significant energy generated by these events in lower vibration modes, resulting in substantial flexural forces at the base of the shear walls, consequently leading to notable residual displacements.

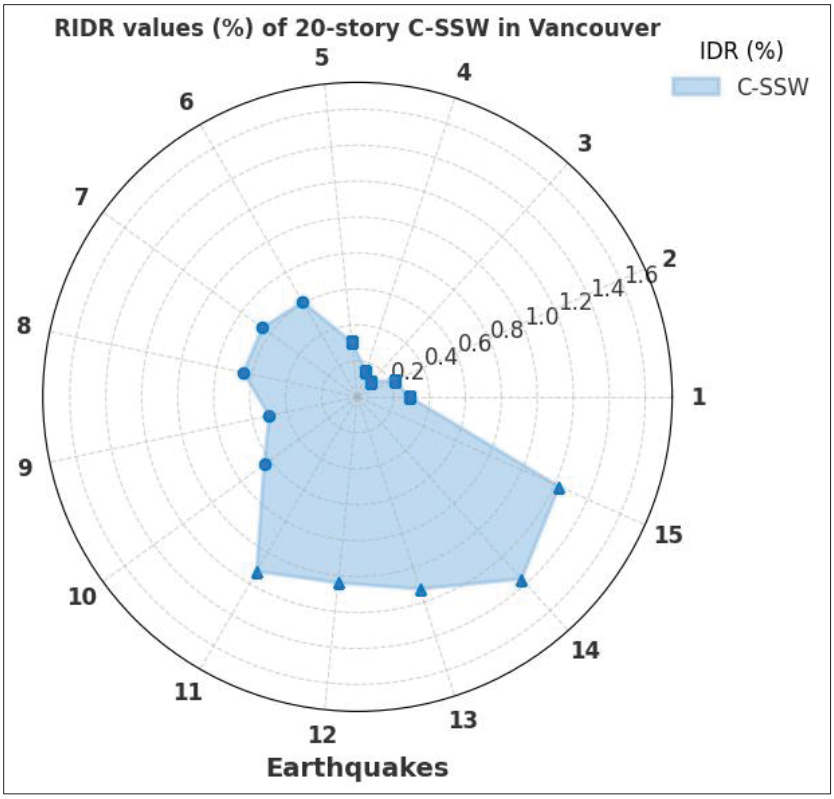

Figure 4.13 Maximum RIDR in 20-story C-SSW for different scenarios located in Vancouver

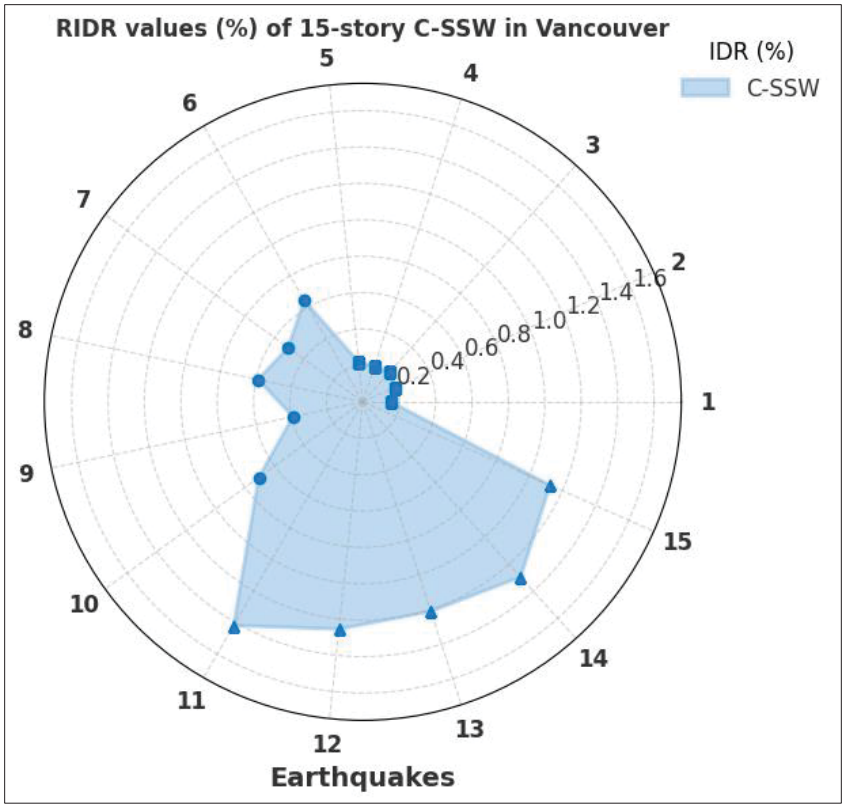

Figure 4.14 Maximum RIDR in 15-story C-SSW for different scenarios located in Vancouver

The proposed strengthening strategies yielded significant reductions in RIDR for both 20-story and 15-story shear walls, with the 15-story wall experiencing a more pronounced effect. According to the results, R3-SSW achieved a remarkable 39% reduction in RIDR for the 15-story wall, compared to a 22% reduction in the 20-story wall. This disparity can be attributed to the greater efficiency of EB-FRP in enhancing stiffness in shorter walls, a trend that previous studies have corroborated (Abbaszadeh & Chaallal, 2023; Arabzadeh & Galal, 2015).

Furthermore, R2-SSW demonstrated substantial reductions of up to 29% in the 15-story wall and 14% in the 20-story wall. In contrast, R1-SSW had a comparatively milder impact on reducing RIDR, resulting in reductions of 15% for the 15-story shear wall and 8% for the 20-story shear wall. Figures 4.15 and 4.16 illustrate reduction in RIDR due to strengthening schemes, for all ground motions in 20-story and 15-story SSWs, respectively.

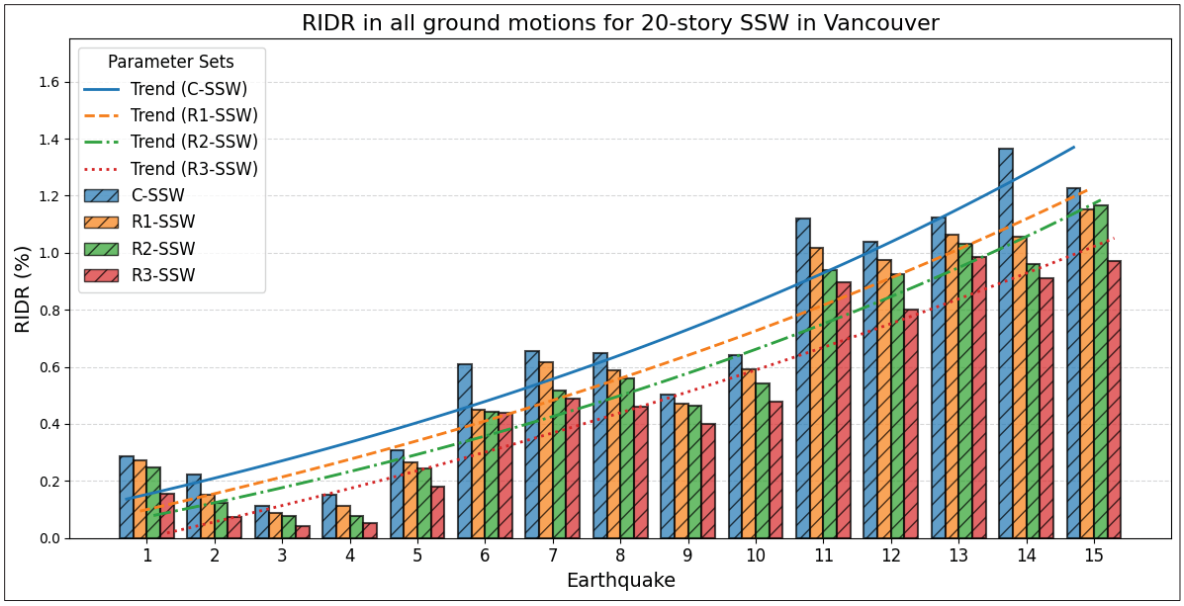

Figure 4.15 Reduction of RIDR in 20-story SSW due to strengthening schemes, in all scenarios

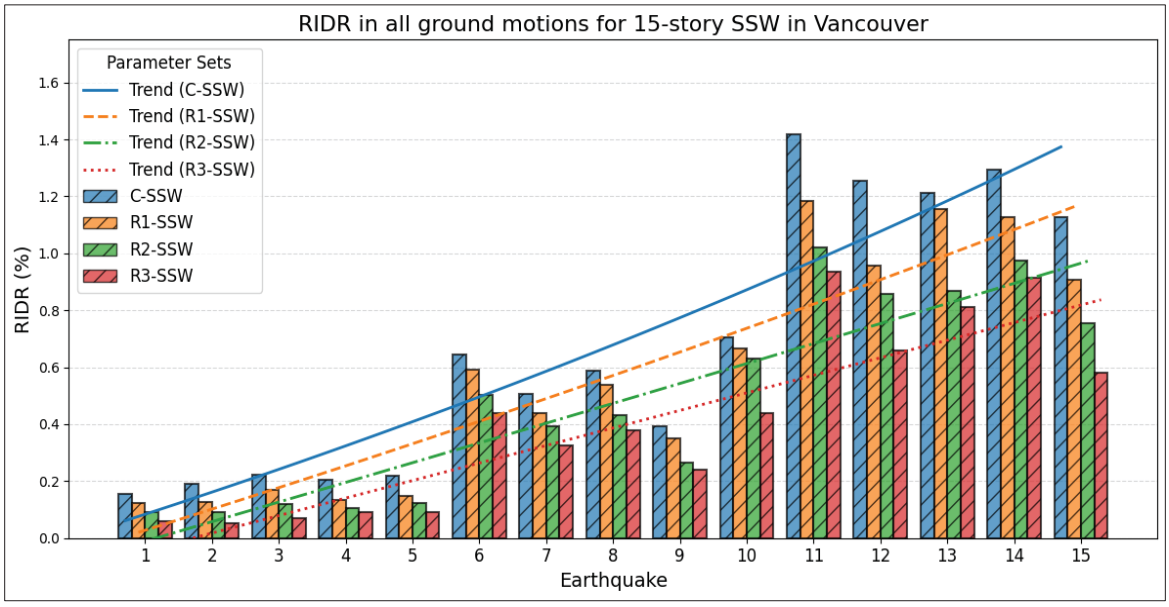

Figure 4.16 Reduction of RIDR in 15-story SSW due to strengthening schemes, in all scenarios

4.7.2.2 Walls in Montreal

The findings reveal a notable reduction in wall damage within Eastern Canada, attributed to their reduced susceptibility to destruction owing to their exposure to high-frequency, low-magnitude earthquakes incapable of inducing substantial flexural strains in structures (see Figure 4.17 and 4.18). The prevalence of higher-frequency seismic waves in these areas allocates a more significant proportion of seismic energy to the higher vibration mode range, thereby diminishing the likelihood of plastic hinge formation at the base of the walls.

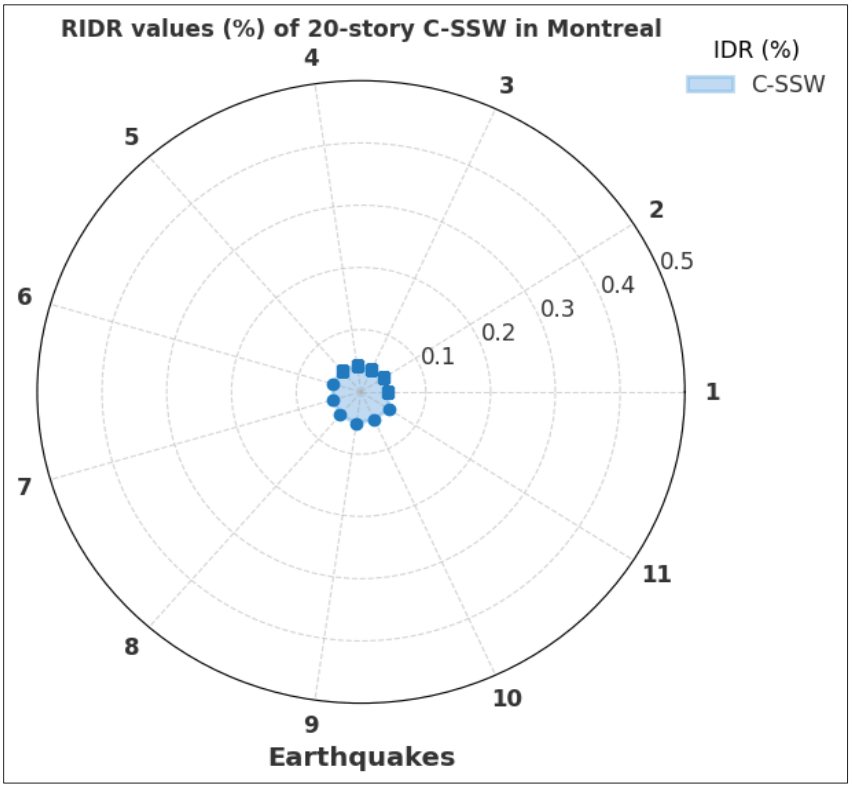

Figure 4.17 Maximum RIDR in 20-story C-SSW for different scenarios located in Montreal

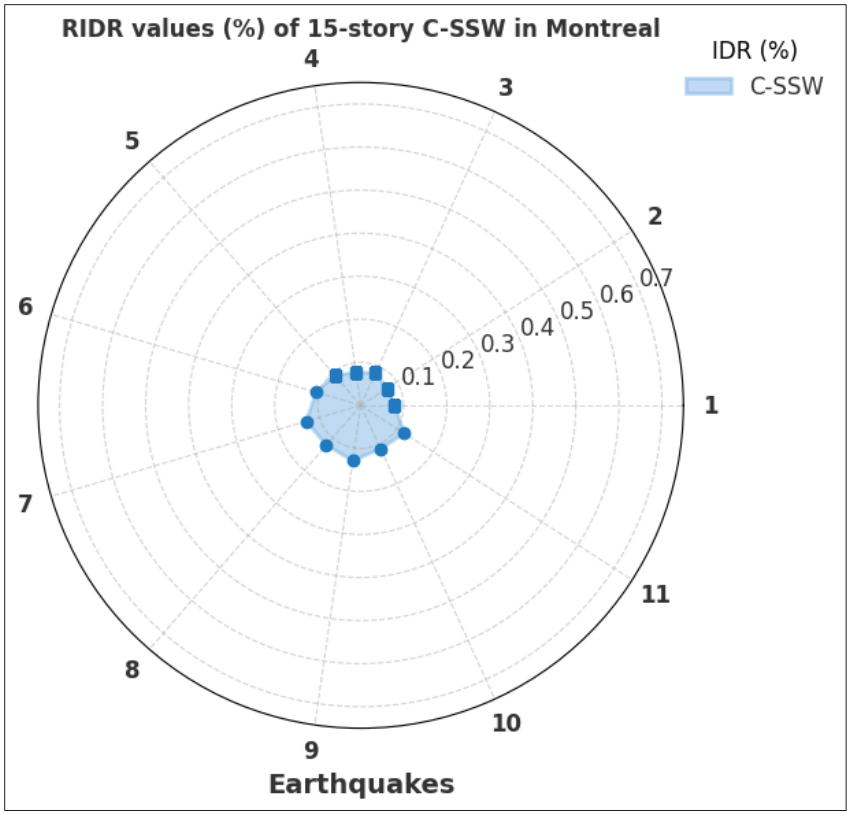

Figure 4.18 Maximum RIDR in 15-story C-SSW for different scenarios located in Montreal

As shown in Figure 4.19, the residual displacements of a 20-story SSW in Montreal remain remarkably low when subjected to seismic-dominant scenarios. In contrast, the 15-story SSW exhibits slightly higher residual displacements compared to its taller counterpart (refer to Figure 4.20). Nevertheless, these values remain significantly lower than those observed in the corresponding wall located in Vancouver. In the case of the 15-story SSW in Montreal, denoted as R1-SSW, R2-SSW, and R3-SSW, the application of EB-FRP sheets resulted in RIDR reductions of 31%, 49%, and 66%, respectively. However, it is worth noting that the seismic behavior of the 20-story SSW appears to be predominantly elastic, making the use of EB-FRP sheets in this wall less justifiable. Previous studies have also demonstrated that high-rise slender shear walls in Eastern Canadian seismic zones tend to exhibit predominantly elastic responses to ground motions.

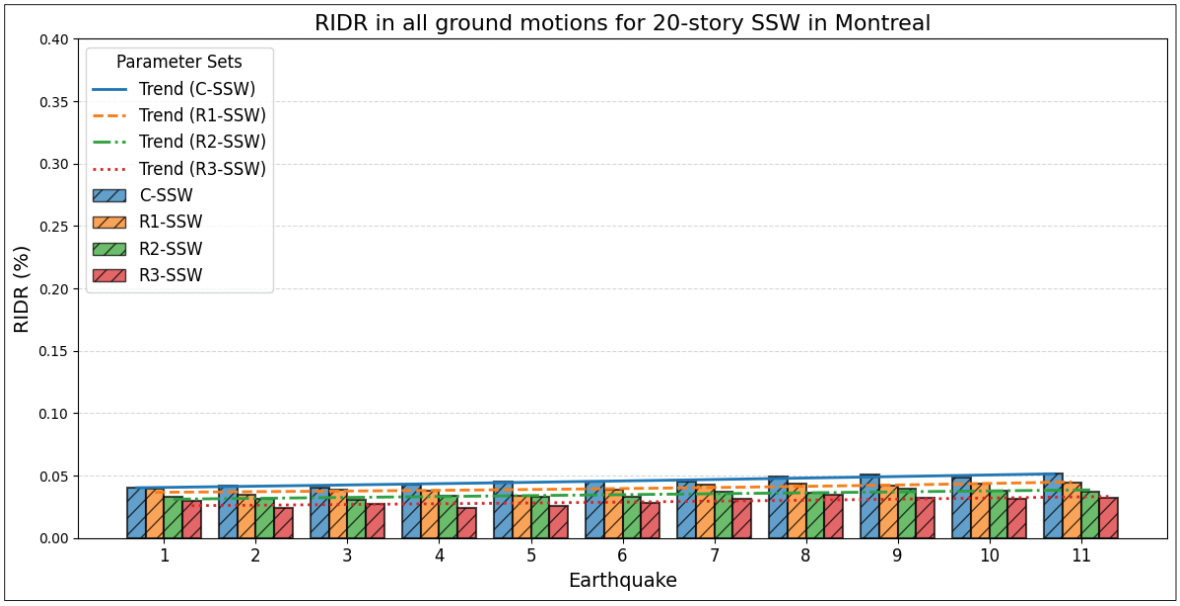

Figure 4.19 Reduction of RIDR in 20-story SSW due to strengthening schemes, in all scenarios

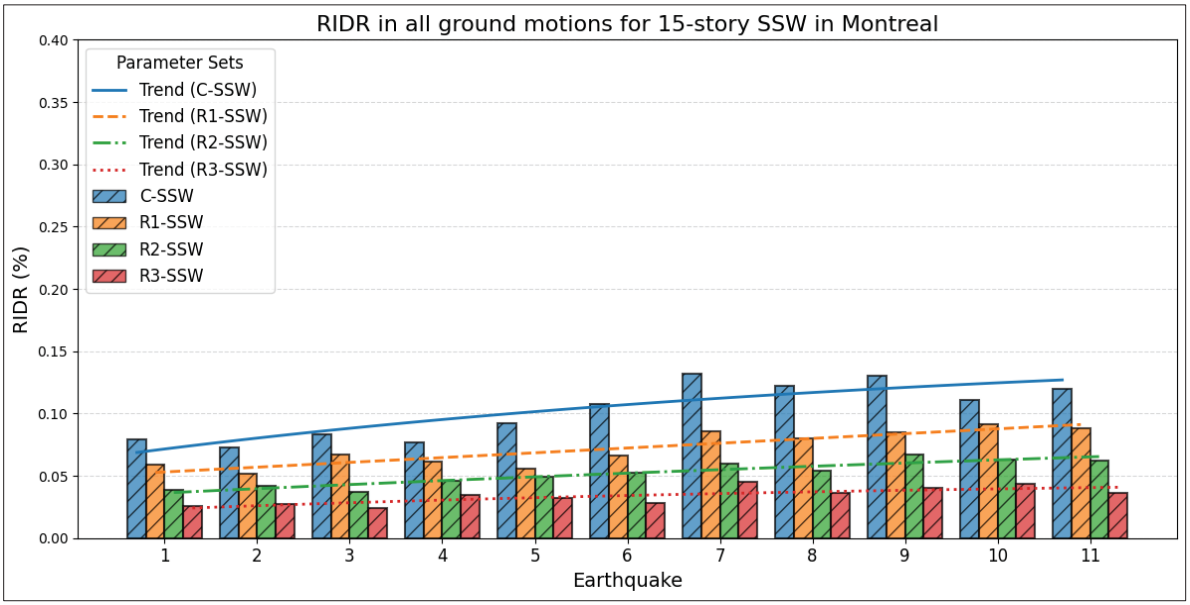

Figure 4.20 Reduction of RIDR in 15-story SSW due to strengthening schemes, in all scenarios

4.7.3 Shear force demand

In the case of ductile shear walls, it is essential for flexural failure to prevail as the primary mode of failure. Any flexural demand escalation may result in an elevated shear demand on the walls. Therefore, this study sought to assess potential alterations in shear force demands resulting from implementing strengthening schemes. Analyzing the mean base shear force demand for FRP-strengthened shear walls in response to ground motions revealed that while the application of EB-FRP sheets has the potential to mitigate residual displacement and drift in these walls, it may also result in an increased demand for base shear in all seismic scenarios. The variations in shear force demand resulting from the implementation of the suggested strengthening strategies are depicted in Figure 4.21 and Figure 4.22 for the shear walls in Vancouver and Montreal, respectively. To enhance comprehension, the shear force demands have been normalized against the base shear force demand in the control wall (C-SSW), and the vertical axis has been scaled relative to the height of the walls.

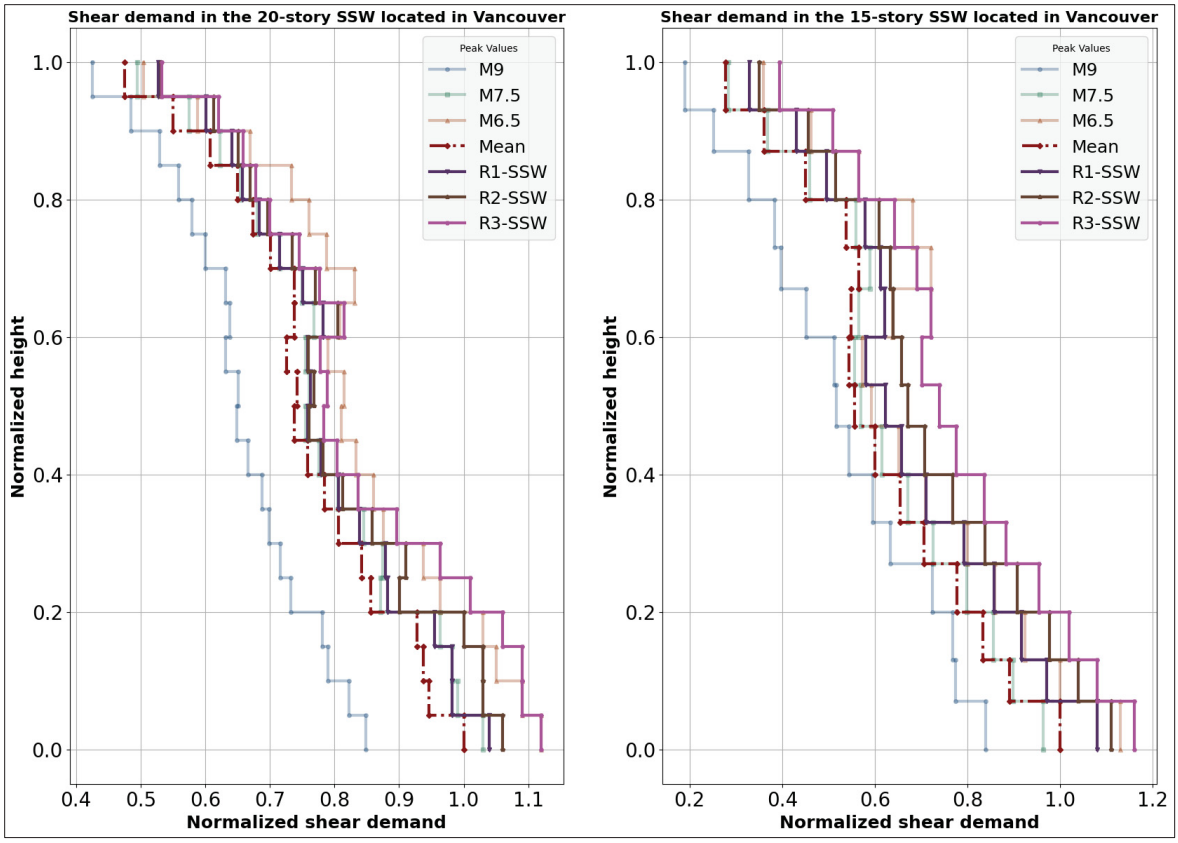

Figure 4.21 Shear demand in the 20-story and 15-story SSWs located in Vancouver due to different scenarios

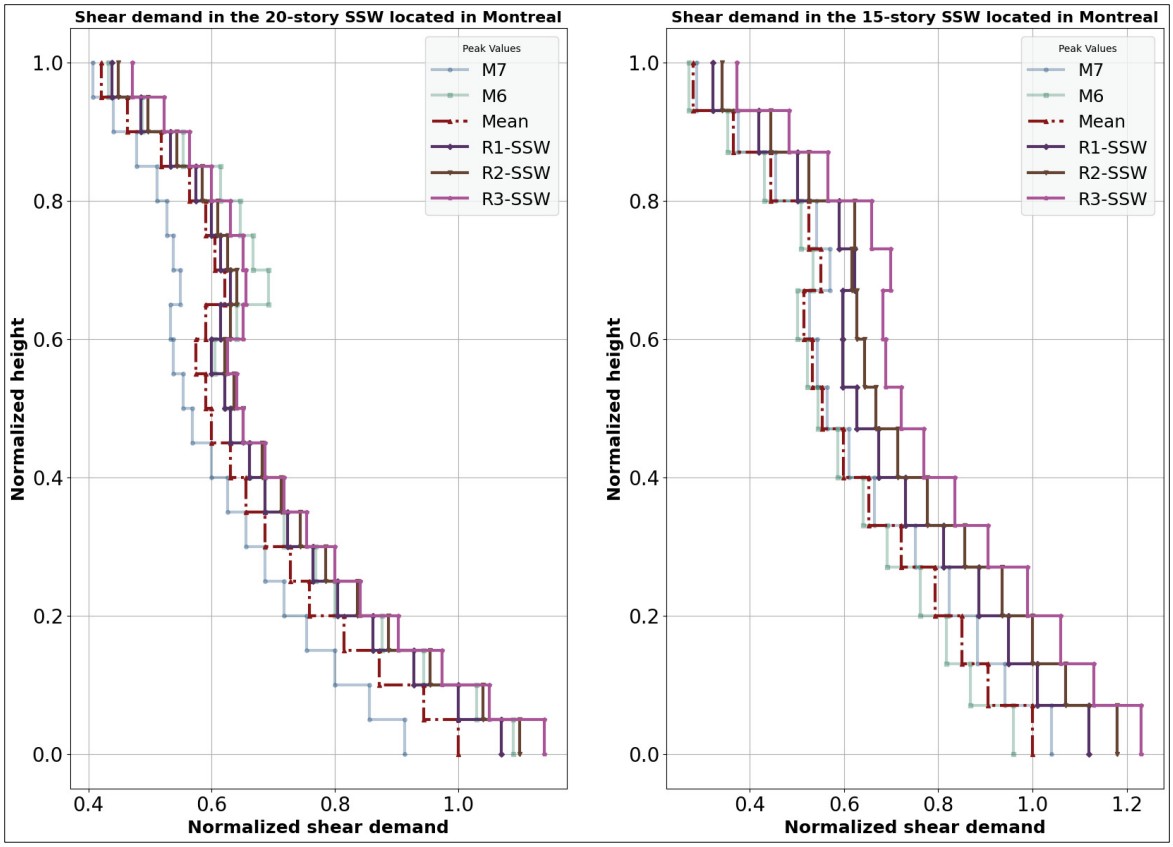

Figure 4.22 Shear demand in the 20-story SSWs located in Montreal due to different scenarios

In line with earlier sections, separate illustrations depict the mean response envelopes for all scenarios. Notably, for walls situated in Vancouver, a conspicuous disparity emerges between the shear demand resulting from the M9 scenario and ground motions featuring higher frequency content. This observed phenomenon, where the base shear demand in the M9 scenario is lower than in the other scenarios, may be attributed to the plastic effects induced by higher vibration modes, a topic addressed in greater detail elsewhere (Adebar et al., 2015). Furthermore, this dissimilarity is accentuated in taller shear walls, underscoring the greater sensitivity of taller shear walls to higher modes. In the meantime, the findings have revealed that applying strengthening strategies leads to an increase in the base shear force requirements for SSWs. As an illustrative example, in the 20-story SSW located in Vancouver, namely R1-SSW, R2-SSW, and R3-SSW, the use of these methods resulted in an increase of respectively 4%, 6%, and 12% in the base shear demand. Similarly, for a 15-story shear wall, the increments

were 8%, 11%, and 16%. The increase in shear demand due to the implementation of EB-FRP composites can be attributed to two key factors. Firstly, it arises from the confinement effect and flexural strengthening, which effectively enhances the post-yield stiffness in these structural elements. Secondly, adopting strengthening schemes reduces the structural vibration period, collectively leading to an amplified shear demand on the walls (Abbaszadeh & Chaallal, 2023; Arabzadeh & Galal, 2017; El-Sokkary et al., 2013; Honarparast & Chaallal, 2022). In Eastern Canada, the 20-story wall, denoted as R1-SSW, R2-SSW, and R3-SSW, experienced increases in base shear demand by 7%, 10%, and 14%, respectively. Similarly, in its base shear demand, the 15-story SSW experienced increases up to 12%, 18%, and 23%. It is important to emphasize that the additional shear capacity due to horizontal EB-FRPs exceeds the shear demand increase within the walls.

4.7.4 Bending moment demand

Despite the enhanced flexural capacity, the strengthening strategies amplified the bending moment demand in all specimens. In this context, the 15-story SSW located in Vancouver exhibited a 4% increase in bending moment demand at its base level under the R1-SSW scheme. On the other hand, the R2-SSW and R3-SSW configurations featured a 6% and 9% rise in bending moment demands for the same wall, respectively. As scenarios with higher frequency content (M6.5 and M7.5) were considered, the upper stories experienced more significant bending. In contrast, the lower stories bore the brunt of significant bending moments due to Cascadia events (M9). This phenomenon was more pronounced in taller walls, possibly attributable to the heightened influence of higher modes, which tend to be more pronounced in high-rise structures. Furthermore, when applying EB-FRP sheets, the 20-story wall demonstrated a relatively minor increase in bending moment demands. Under the R1-SSW, R2-SSW, and R3-SSW schemes, the wall experienced increases of 3%, 4%, and 7%, respectively.

In Eastern Canada, the influence of higher modes was more pronounced in the 20-story wall, particularly in the upper levels, where the disparity in bending moment demand caused by M6

and M7 was more conspicuous. However, the M7 scenario remained dominant in the lower levels in both shear walls. In Montreal, the 15-story wall with the R3-SSW strengthening scheme experienced the highest increase in base bending demand, recording an 11% rise. Comparatively, the increases in R2-SSW and R1-SSW were 6% and 4%, respectively. Additionally, in the case of the 20-story shear wall, there were increases of 9%, 6%, and 4% observed in R3-SSW, R2-SSW, and R1-SSW, respectively. Figure 4.23 and Figure 4.24 show the variation in bending moment demand in shear walls located in Vancouver and Montreal, respectively. In these Figures, bending moments are normalized with respect to base bending moment in C-SSW.

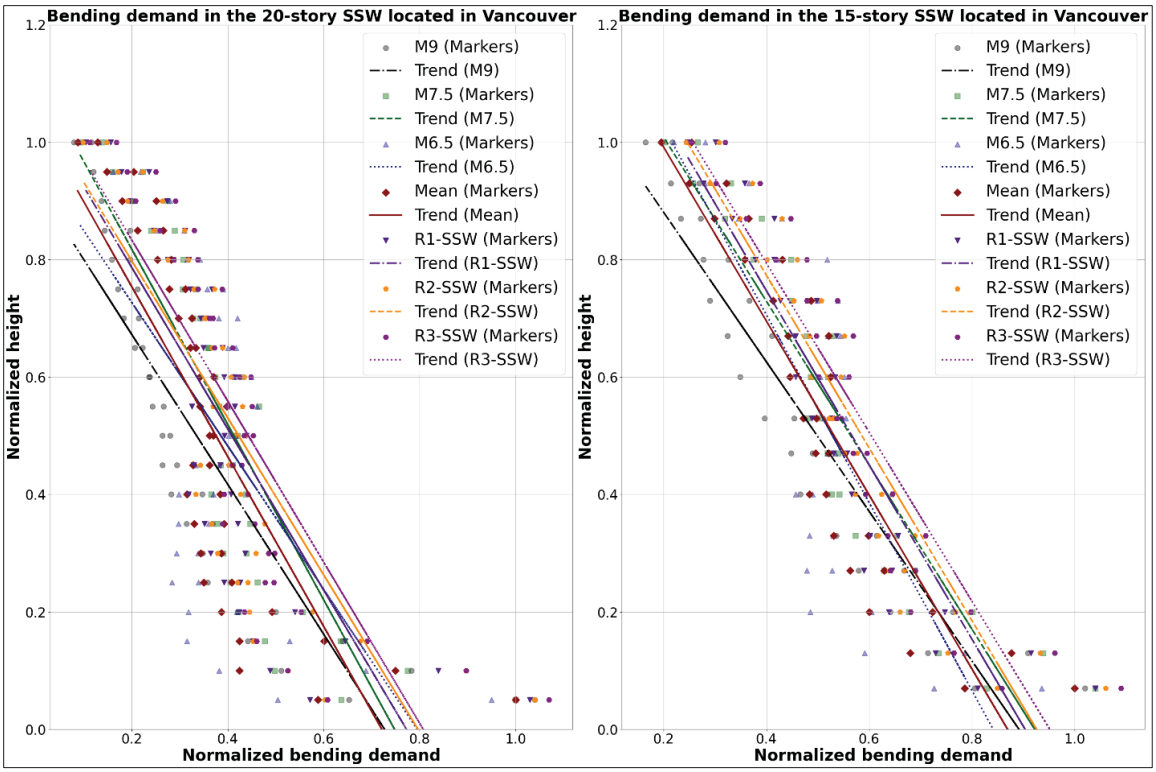

Figure 4.23 Bending demand in the 15-story SSWs located in Vancouver due to different scenarios

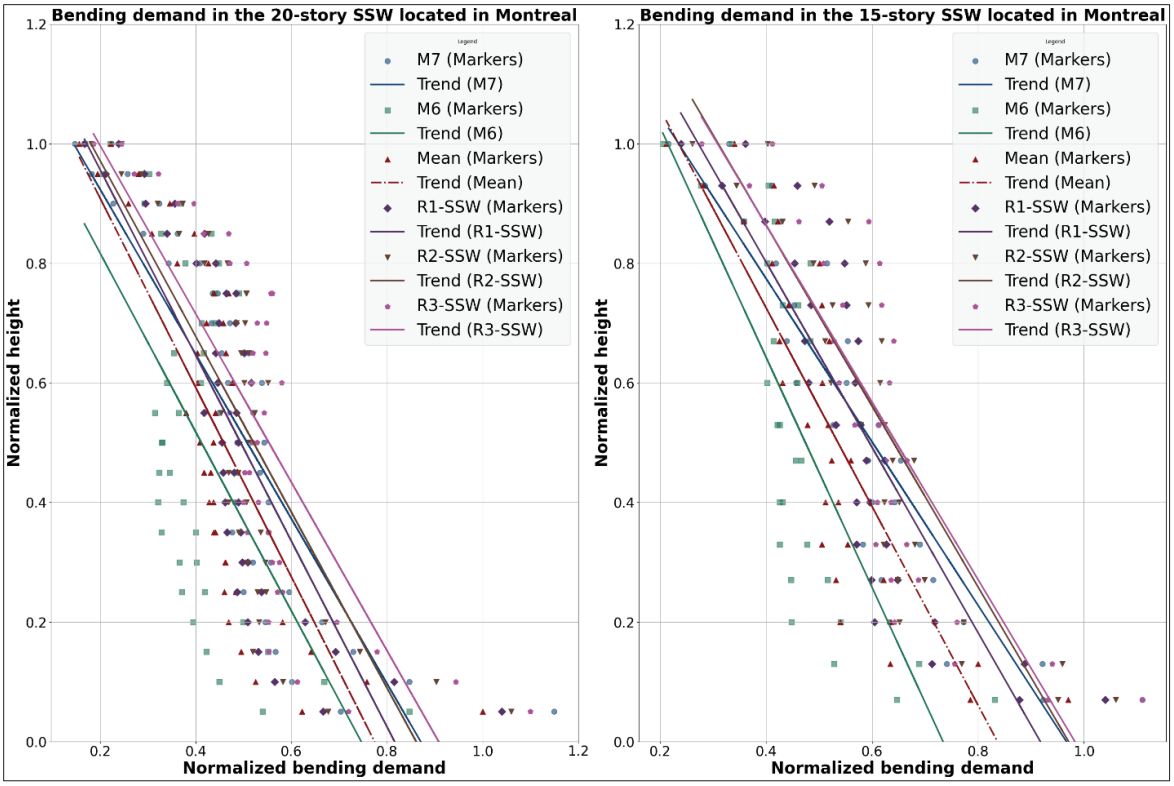

Figure 4.24 Bending demand in the 20-story SSWs located in Montreal due to different scenarios

Although these increases did not exceed the shear and bending capacity of the shear walls in this study, excessive increases could pose problems. Therefore, it is crucial to check the force demand increase in buildings within the practical implications of the proposed method. Increased base shear demands can lead to higher stress levels in existing foundations and connections, potentially necessitating additional strengthening measures. Similarly, increased bending moments require careful consideration of the existing reinforcement to prevent failures. Strategic decision-making processes are essential to ensure that these increased demands do not compromise structural integrity or result in economic inefficiencies. (Lifshitz Sherzer et al., 2024) emphasized the need for a comprehensive assessment of safety and economic aspects in seismic retrofitting, highlighting the importance of balancing enhanced seismic performance with retrofitting cost.

Building owners must consider the cost of the proposed strengthening method. Decisions should be based on: 1- the cost of strengthening versus the benefit of enhanced resilience; if

the main objective is to decrease residual displacement, this may take priority despite the costs; 2- the cost-effectiveness of the strengthening given the increased demands; and 3- the building's importance, determining how much investment is necessary and whether the proposed method satisfies the requirements. By integrating these considerations into strategic decision-making, we can achieve a balance between enhanced seismic resilience and maintaining safety and economic viability in existing structures.

4.8 Conclusions

The current investigation has assessed a novel approach for mitigating residual deformations in newly designed existing slender medium to high-rise ductile shear walls. The primary technique employed to achieve this objective involved applying FRP sheets bonded to the shear wall surfaces. Within this investigation, four walls were designated as control specimens. These control specimens consisted of two 20-story and two 15-story walls, one of each located in Montreal and Vancouver, serving as representatives of Eastern and Western Canadian seismic zones. Three innovative strengthening configurations were devised for these walls, and their response to scaled ground motions was comprehensively assessed through 2-dimensional Nonlinear Time History Analysis. The following conclusions can be drawn:

- The proposed configurations affectively reduced shear wall drift by a range of 8% to 28%, with the R3-SSW scheme featuring the highest performance level. However, the efficiency of EB-FRP sheets in SSWs diminishes as the wall height increases.
- Cascadia subduction earthquakes, with a magnitude of M9, pose a unique challenge in Western Canada due to their low-frequency characteristics, which can excite the first vibration mode of SSWs and elevate flexural demands within the walls. Furthermore, their prolonged duration results in many loading and unloading cycles, ultimately leading to structural fatigue. Consequently, these seismic events influence the seismic behavior of shear walls in Vancouver, contributing to a substantial portion of the residual drift in western walls (1.42%).
- The proposed strengthening schemes led to a significant reduction in RIDR (from 8% to 66%) within shear walls. Among the various configurations tested, R3-SSW

emerged as the top performer. This outcome underscores the effectiveness of enhancing shear walls by bolstering concrete compressive capacity, curbing crack propagation originating from substantial bending moments at the wall base and mitigating concrete crushing in wall corners—a significant contributor to ductile slender wall failures. Furthermore, the use of vertical EB-FRP sheets at the extremities of the walls enhances flexural stiffness by harnessing their substantial tensile strength and limiting flexural cracks in the boundary elements of the walls.

- Given the relatively low to medium intensity of ground motions experienced in Eastern Canada, these seismic events did not induce significant residual deformations in slender shear walls. Maximum permanent drift deformations observed are 0.13% in 15-story walls and less than 0.05% in 20-story walls. Particularly in taller shear walls within this region, the seismic response tends to remain predominantly elastic. Suggesting that their strengthening may not be required.
- The limited efficiency of R1-SSW and R2-SSW indicates that incorporating vertical EB-FRP sheets in the central portion of wall lengths is not as beneficial compared to the outer edges of the walls.
- Using EB-FRP sheets increases base shear demand within the walls, ranging from 4% to 23%. In Western Canada, the shear demand is predominantly influenced by scenarios of M7.5 and M6.5 due to the plastic effects of higher modes in SSWs. Additionally, as wall height increases, the impact of higher modes on base shear demand becomes more pronounced.
- The additional shear capacity provided by horizontal EB-FRPs exceeds the increased shear demand within the walls. However, while these methods enhance shear capacity beyond the increased demand, it is essential to evaluate their cost-effectiveness. The main objective of this study is to propose an effective method to reduce residual displacement in shear walls. It is crucial to consider the rationale behind this practice. The proposed method can be effective if the primary goal is to minimize residual displacement. However, if the objective is to reduce post-earthquake maintenance and repair costs, a cost-effectiveness analysis may be necessary to fully assess the benefits

of the implemented strategies. Further discussion on this topic can be found elsewhere (Egbelakin & Wilkinson, 2008; Egbelakin et al., 2014).

- The proposed strengthening configurations elevates the bending moment demand within shear walls by 3% to 13%. As wall height increases, the influence of strengthening schemes on flexural demand tends to decrease.
- Future research should focus on several key areas to optimize the use of FRP in seismic retrofitting. Exploring alternative materials that might offer similar benefits at reduced costs or improved performance could provide valuable insights. Additionally, investigating hybrid strengthening methods that combine FRP with other retrofitting techniques could lead to innovations in seismic resilience strategies. Finally, long-term durability studies under cyclic loading conditions are crucial to understand the longevity and performance of FRP-strengthened structures over time.
- The impact of ground motion characteristics on NLTH analysis has been found to be profound. Factors such as tectonic conditions, ground motion magnitudes, source-to-site distances, and soil type play critical roles. The frequency content and ground motion duration, shaped by these factors, dictate the structure's response to seismic waves. Consequently, cities with similar frequency content and ground motion durations as Montreal and Vancouver are expected to exhibit similar NLTH responses. However, further studies are required to evaluate the precise effects of other features of ground motions and tectonic conditions on the nonlinear response of buildings in cities with similar seismic activities.
- The selected number of ground motions, while representative, may not encompass the full range of possible seismic events. The selection and scaling procedure, though consistent with NBCC guidelines, introduces another layer of approximation that can influence the accuracy of the nonlinear time history analysis. This becomes especially important when the study clearly demonstrates the impact of ground motion frequency content.

Future experimental studies are required to validate the numerical findings through real-world verification of the bonding behavior between EB-FRP composites and shear walls, accurately

capture the hysteretic behavior under seismic loads, and confirm the overall performance and effectiveness of the strengthening schemes beyond modeling accuracy.

CONCLUSION

This thesis has extensively investigated the enhancement of resilience and self-centering capabilities in RC SSWs and CSWs through the application of EB-FRP composites. The primary purpose of this research was to address residual displacements that occur in shear walls following seismic events, which can compromise structural integrity and necessitate costly repairs and replacements. By conducting comprehensive NLTHA and evaluating various strengthening configurations, the study aimed to identify the most effective strengthening configuration for reducing residual displacements and improving the overall seismic performance of these critical structural components.

This study is divided into two phases to address the unique challenges and characteristics of CSWs and SSWs separately. Each phase focuses on understanding and optimizing the seismic performance of these distinct types of shear walls under different configurations and conditions.

Phase 1 – CSWs: For CSWs, the study utilized NLTHA with the RUAUMOKO 2D software to simulate seismic impacts. Ground motions specific to Vancouver and Montreal were selected to reflect their unique seismic profiles. Two models of CSWs were designed for each city, representing medium to high-rise buildings with 15 to 20 stories. The CSWs were strengthened with vertical and horizontal EB-FRP strips to enhance their flexural and shear strength, and additional FRP wraps were used on coupling beams to improve their confinement and flexural resistance. The features evaluated in this phase included RIDR, inter-story drift ratio, rotation of coupling beams, shear force demand, and bending moment demand.

The conclusions related to Phase 1 can be summarized as follows:

1. The study demonstrated that all proposed EB-FRP strengthening configurations effectively reduced residual displacements in CSWs.

2. Applying three layers of EB-FRP at the edges of the walls and wrapping the plastic hinge zones significantly improved the performance of CSWs.
3. Wrapping coupling beams and enhancing their flexural resistance were particularly effective strategies for reducing residual displacements.
4. EB-FRP sheets are a viable option for reducing the RIDR in existing modern CSWs, with reductions ranging from 14% to 53%. However, the effectiveness of these configurations diminished with increasing wall height.
5. Among the proposed strengthening schemes, the S3-CSW configuration was the most effective in decreasing RIDR in CSWs.
6. The RIDR in western Canada was notably higher compared to eastern Canada, primarily due to the influence of Cascadia events, which have long durations that can induce structural fatigue and low frequencies that can cause resonance in high-rise buildings with longer vibration periods.
7. For 15-story and 20-story CSWs in eastern Canada, applying EB-FRP sheets is neither reasonable nor cost-effective due to their mostly elastic behavior and lack of significant residual displacement.
8. Despite this, higher modes in eastern CSWs showed the potential for forming a second plastic hinge in the upper stories (60%–70% of the wall height).
9. The S3-CSW configuration also excelled in reducing inter-story drift ratio (IDR) and coupling beam rotation due to the enhanced flexural strength from three layers of vertical EB-FRP sheets and the confinement provided by FRP wrapping.
10. Horizontal FRP sheets improved the shear strength of CSWs, preventing brittle shear failure and increasing resistance to debonding failure of vertical FRP sheets, enhancing overall system effectiveness.
11. The study indicated the effectiveness of EB-FRP sheets in stabilizing IDR variations across the height of CSWs.
12. Applying EB-FRP sheets to CSWs resulted in a slight increase in base shear and bending moment demand.
13. Among various strengthening schemes, the S3-CSW configuration had the highest impact on increasing shear force and bending moment demand, more pronounced in

eastern CSWs due to the greater contribution of EB-FRP sheets to overall wall stiffness compared to western Canada. However, the improvements in shear and bending resistance due to EB-FRP sheets significantly outweighed the increase in demand.

Phase 2 – SSWs: For SSWs, four models of SSWs were designed and evaluated, matching the heights and locations of the CSWs. The flexural capacity of the walls was enhanced using three different configurations of vertical EB-FRP sheets coupled with FRP wraps to increase shear strength. The features evaluated in this phase included RIDR, inter-story drift ratio, shear force demand, and bending moment demand.

The conclusions related to Phase 2 can be summarized as follows:

1. The proposed strengthening schemes significantly reduced the residual inter-story drift ratio (RIDR) in shear walls, achieving reductions between 8% and 66%. The configuration with three layers of vertical EB-FRP sheets at the edges and horizontal FRP wraps was the most effective, enhancing flexural stiffness and minimizing flexural cracks in boundary elements by utilizing the tensile strength of vertical EB-FRP sheets. However, the limited effectiveness of configurations with fewer layers or central placement of EB-FRP sheets suggests that placing vertical EB-FRP sheets in the central portion of wall lengths is less beneficial compared to positioning them at the outer edges.
2. In Eastern Canada, where ground motions are of relatively low to medium intensity, significant residual deformations in slender shear walls were not observed. Maximum permanent drift deformations were 0.13% in 15-story walls and less than 0.05% in 20-story walls, indicating that strengthening may not be necessary for taller shear walls in this region as their seismic response remains predominantly elastic. However, Cascadia subduction earthquakes, especially those with a magnitude of M9, pose a major challenge in Western Canada. These low-frequency events can excite the first vibration mode of SSWs, increasing flexural demands and resulting in substantial residual drift (1.42%) due to prolonged loading cycles and structural fatigue.

3. Applying EB-FRP sheets increased the base shear demand within the walls by 4% to 23%, with a more pronounced effect in Western Canada due to higher mode effects in M7.5 and M6.5 scenarios. Additionally, the strengthening configurations elevated bending moment demand by 3% to 13%.

Despite the significant findings and contributions of this research, several limitations should be acknowledged:

- The study relied mainly on numerical simulations using finite element method. While these tools provide valuable insights, they are subject to limitations related to the accuracy of material models and assumptions made during the simulation process. The results might differ when applied to real-world scenarios due to factors not captured in the simulations.
- The performance of EB-FRP composites can vary significantly based on the quality of materials, manufacturing processes, and installation techniques. The study assumes ideal material and FRP-concrete bonding properties, but in practice, these can be affected by various factors, which were not considered in this research.
- The study focused on 15-story and 20-story buildings with specific structural configurations. The conclusions drawn may not be applicable to taller buildings or structures with significantly different geometries or load distributions.

Based on the findings of this research, some design requirements can be made to enhance the resilience and self-centering capabilities of RC shear walls using EB-FRP composites:

- To prevent overstrength effects and brittle shear failure in structures due to flexural resistance enhancement, it is necessary to ensure that shear resistance is also adequately enhanced. This can be achieved by incorporating additional shear reinforcement, such as FRP wraps or diagonal EB-FRP in critical areas like coupling beams and wall piers. Proper attention to shear capacity is crucial to avoid premature shear failure and to maintain the ductility of the structure.

- Given the variability in seismic characteristics across different regions, it is crucial to conduct site-specific seismic evaluations when designing EB-FRP retrofits. The selection of ground motions for analysis should reflect the local seismicity, ensuring that the design is robust under the most likely seismic events for the region.
- The success of EB-FRP retrofitting depends heavily on the quality of application. It is recommended that stringent quality control measures be implemented during the installation process, including proper surface preparation, adhesive application, and curing conditions, to ensure that the composites achieve their design performance.
- Continued research into the long-term performance of EB-FRP systems is recommended, particularly in real-world applications. Additionally, the installation of monitoring systems in retrofitted buildings can provide valuable data on the actual performance of these systems during seismic events, providing thereby improved designs and retrofits for the future.

The research study has successfully demonstrated that EB-FRP composites significantly enhance the seismic resilience and self-centering capabilities of both CSWs and SSWs. The proposed strengthening configurations offer practical solutions for mitigating seismic risks, ensuring the safety, functionality, and longevity of buildings in earthquake-prone regions. These advancements will not only improve structural resilience but also contribute to environmental sustainability by reducing the need for extensive material replacements and minimizing CO2 emissions associated with concrete production.

RECOMMENDATIONS

According to the investigation carried out in this thesis, the following recommendations for potential future studies can be drawn:

1. It is recommended that full-scale experimental tests be conducted to validate the numerical results.
2. Long-term durability studies should be undertaken to evaluate the performance of EB-FRP strengthened structures under various environmental conditions and cyclic loads. Understanding how these materials perform over time will provide insights into their reliability and future maintenance needs in real-world applications.
3. Comprehensive cost-benefit analyses are suggested to evaluate the economic viability of EB-FRP retrofitting strategies. This analysis should consider installation costs, long-term maintenance, and potential savings from reduced earthquake damage and repair needs.
4. Research may explore alternative materials that could offer similar or superior benefits at lower costs or with enhanced performance characteristics. Advances in material science might lead to more efficient and cost-effective seismic retrofitting solutions.
5. It is suggested that detailed studies be conducted on how different ground motion characteristics, such as frequency content, duration, and intensity, affect the seismic performance of EB-FRP strengthened shear walls. This will help refine design guidelines and ensure retrofitting strategies are tailored to specific seismic environments.
6. Wrapping FRP composites in the plastic hinge zone of shear walls can significantly enhance the ultimate compressive strain of the concrete and increase the overall ductility of the structure. It is recommended that future studies explicitly evaluate the ductility and energy dissipation increase in shear walls due to this configuration and study the possible relocation of the plastic hinge zone in shear walls accordingly.
7. It is recommended that research be extended to different types and heights of buildings and structural configurations to determine the effectiveness of EB-FRP strengthening

methods in a broader range of applications. This can help in developing versatile retrofitting solutions for diverse building stock.

REFERENCES

Aaleti, S., Brueggen, B. L., Johnson, B., French, C. E., & Sritharan, S. (2013). Cyclic response of reinforced concrete walls with different anchorage details: Experimental investigation. *Journal of structural engineering, 139*(7), 1181-1191.

Aaleti, S., & Sritharan, S. (2009). A simplified analysis method for characterizing unbonded post-tensioned precast wall systems. *Engineering Structures, 31*(12), 2966-2975.

Abbasi, A., Benzeguir, Z. E. A., Chaallal, O., & El-Saikaly, G. (2022). FE modelling and simulation of the size effect of RC T-beams strengthened in shear with externally bonded FRP fabrics. *Journal of Composites Science, 6*(4), 116.

Abbass, A., Attarnejad, R., & Ghassemieh, M. (2020). Seismic assessment of RC bridge columns retrofitted with near-surface mounted shape memory alloy technique. *Materials, 13*(7), 1701.

Abbaszadeh, A., & Chaallal, O. (2022). Enhancing resilience and self-centering of existing RC coupled and single shear walls using EB-FRP: State-of-the-art review and research needs. *Journal of Composites Science, 6*(10), 301.

Abbaszadeh, A., & Chaallal, O. (2023). Resilience of medium-to-high-rise ductile coupled shear walls located in canadian seismic zones and strengthened with externally bonded fiber-reinforced polymer composite: Nonlinear time history assessment. *Journal of Composites Science, 7*(8), 317.

Abbaszadeh, A., & Chaallal, O. (2024). The Use of Externally Bonded Fibre Reinforced Polymer Composites to Enhance the Seismic Resilience of Single Shear Walls: A Nonlinear Time History Assessment. *Journal of Composites Science, 8*(6), 229.

Adams, J., Allen, T., Halchuk, S., & Kolaj, M. (2019). Canada's 6th Generation Seismic Hazard Model, as Prepared for the 2020 National Building Code of Canada. 12th Can. Conf. *Earthquake Engineering*.

Adams, J., & Atkinson, G. (2003). Development of seismic hazard maps for the proposed 2005 edition of the National Building Code of Canada. *Canadian Journal of Civil Engineering, 30*(2), 255-271.

Adebar, P., Dezhdar, E., & Yathon, J. (2015). Accounting for higher mode shear forces in concrete wall buildings: 2014 CSA A23. 3. The 11th Canadian Conference on Earthquake Engineering,

Adebar, P., Mutrie, J., & DeVall, R. (2005). Ductility of concrete walls: the Canadian seismic design provisions 1984 to 2004. *Canadian Journal of Civil Engineering, 32*(6), 1124-1137.

Adebar, P., Mutrie, J. G., Devall, R., & Mitchell, D. (2014). Seismic design of concrete shear wall buildings: new requirements of csa standard A23. 3–.

Adey, B., Hajdin, R., & Brühwiler, E. (2004). Effect of common cause failures on indirect costs. *Journal of Bridge Engineering, 9*(2), 200-208.

Afefy, H. M. (2020). Seismic retrofitting of reinforced-concrete coupled shear walls: A review. *Practice Periodical on Structural Design and Construction, 25*(3), 03120001.

Aidoo, J., Harries, K. A., & Petrou, M. F. (2004). Fatigue behavior of carbon fiber reinforced polymer-strengthened reinforced concrete bridge girders. *Journal of Composites for Construction, 8*(6), 501-509.

Aktan, A. E., & Bertero, V. V. (1985). RC structural walls: seismic design for shear. *Journal of structural engineering, 111*(8), 1775-1791.

Al-Mahaidi, R., & Kalfat, R. (2018). Methods of structural rehabilitation and strengthening. In *Rehabilitation of concrete structures with fiber-reinforced polymer* (pp. 7-13). Elsevier.

Al-Rousan, R. Z. (2022). Cyclic behavior of alkali-silica reaction-damaged reinforced concrete beam-column joints strengthened with FRP composites. *Case Studies in Construction Materials, 16*, e00869.

Al-Saidy, A., Al-Harthy, A., Al-Jabri, K., Abdul-Halim, M., & Al-Shidi, N. (2010). Structural performance of corroded RC beams repaired with CFRP sheets. *Composite Structures, 92*(8), 1931-1938.

Alhaddad, M. S., Binyahya, A. S., Alrubaidi, M., & Abadel, A. A. (2021). Seismic performance of RC buildings with Beam-Column joints upgraded using FRP laminates. *Journal of King Saud University-Engineering Sciences, 33*(6), 386-395.

Ali, M. A., & El-Salakawy, E. (2016). Seismic performance of GFRP-reinforced concrete rectangular columns. *Journal of Composites for Construction, 20*(3), 04015074.

Allen, C., Jaeger, L., & Fenton, V. (1972). Ductility in reinforced concrete shear walls. *Special Publication, 36*, 97-118.

Altin, S., Anil, Ö., Kopraman, Y., & Kara, M. E. (2013). Hysteretic behavior of RC shear walls strengthened with CFRP strips. *Composites Part B: Engineering, 44*(1), 321-329.

Alyousef, R., Topper, T., & Al-Mayah, A. (2016). Effect of FRP wrapping on fatigue bond behavior of spliced concrete beams. *Journal of Composites for Construction, 20*(1), 04015030.

American Concrete Institute (ACI) Committee 318. (2011). Building Code Requirements for Structural Concrete (ACI 318-11) and Commentary (ACI 318R-11). Farmington Hills, MI: ACI.

American Society of Civil Engineers ASCE/SEI 7-22; (2022). Minimum Design Loads and Associated Criteria for Buildingsand Other Structures. ASCE: Reston, VA, USA.

Amran, Y. M., Alyousef, R., Rashid, R. S., Alabduljabbar, H., & Hung, C.-C. (2018). Properties and applications of FRP in strengthening RC structures: A review. Structures,

Anıl, Ö., & Yılmaz, T. (2015). Low velocity impact behavior of shear deficient RC beam strengthened with cfrp strips. *Steel and Composite Structures, 19*(2), 417-439.

Antoniades, K. K., Salonikios, T. N., & Kappos, A. J. (2005). Tests on seismically damaged reinforced concrete walls repaired and strengthened using fiber-reinforced polymers. *Journal of Composites for Construction, 9*(3), 236-246.

Antoniades, K. K., Salonikios, T. N., & Kappos, A. J. (2007). Evaluation of hysteretic response and strength of repaired R/C walls strengthened with FRPs. *Engineering Structures, 29*(9), 2158-2171.

Arabzadeh, H., & Galal, K. (2015). Effectiveness of FRP wraps for retrofitting of existing RC shear walls. Proceeding of the 11th Canadian Conference on Earthquake Engineering, Victoria, BC, Canada,

Arabzadeh, H., & Galal, K. (2017). Seismic collapse risk assessment and FRP retrofitting of RC coupled C-shaped core walls using the FEMA P695 methodology. *Journal of Structural Engineering, 143*(9), 04017096.

Aslani, K., & Kohnehpooshi, O. (2018). Structural behavior of FRP-strengthened reinforced concrete shear walls with openings using finite element method. *Advances in Structural Engineering, 21*(7), 1072-1087.

Atkinson, G. M. (1996). The high-frequency shape of the source spectrum for earthquakes in eastern and western Canada. *Bulletin of the seismological society of America, 86*(1A), 106-112.

Atkinson, G. M. (2009). Earthquake time histories compatible with the 2005 National building code of Canada uniform hazard spectrum. *Canadian Journal of Civil Engineering, 36*(6), 991-1000.

Attari, N., Amziane, S., & Chemrouk, M. (2012). Flexural strengthening of concrete beams using CFRP, GFRP and hybrid FRP sheets. *Construction and Building Materials, 37*, 746-757.

Baggio, D., Soudki, K., & Noel, M. (2014). Strengthening of shear critical RC beams with various FRP systems. *Construction and Building Materials, 66*, 634-644.

Bai, Y.-L., Zhang, Y.-F., Jia, J.-F., Mei, S.-J., Han, Q., & Dai, J.-G. (2022). Simplified plasticity damage model for large rupture strain (LRS) FRP-confined concrete. *Composite Structures, 280*, 114916.

Bakis, C. E., Bank, L. C., Brown, V., Cosenza, E., Davalos, J., Lesko, J., Machida, A., Rizkalla, S., & Triantafillou, T. (2002). Fiber-reinforced polymer composites for construction-state-of-the-art review. *Journal of Composites for Construction, 6*(2), 73-87.

Banjara, N. K., & Ramanjaneyulu, K. (2019). Investigations on behaviour of flexural deficient and CFRP strengthened reinforced concrete beams under static and fatigue loading. *Construction and Building Materials, 201*, 746-762.

Barbachyn, S. M., Kurama, Y. C., & Novak, L. C. (2012). Analytical evaluation of diagonally reinforced concrete coupling beams under lateral loads. *ACI Structural Journal, 109*(4), 497.

Basereh, S. (2021). *Seismic Retrofit of Reinforced Concrete Shear Walls Using Selective Weakening and Self-Centering* State University of New York at Buffalo].

Bedirhanoglu, I., Ilki, A., & Triantafillou, T. C. (2022). Seismic Behavior of Repaired and Externally FRP-Jacketed Short Columns Built with Extremely Low-Strength Concrete. *Journal of Composites for Construction, 26*(1), 04021068.

Bedriñana, L. A., Tani, M., Kono, S., & Nishiyama, M. (2022). Evaluation of the Seismic Performance of Unbonded Post-Tensioned Precast Concrete Walls with Internal and External Dampers. II: Design Criteria and Numerical Research. *Journal of Structural Engineering, 148*(8), 04022106.

Belletti, B., Damoni, C., & Gasperi, A. (2013). Modeling approaches suitable for pushover analyses of RC structural wall buildings. *Engineering Structures, 57*, 327-338.

Benazza, T. (2012). *Non-linear behavior of coupled shear wall systems under seismic events* PhD thesis), University of Quebec, Montreal].

Bertero, V. V., & Felippa, C. (1964). Discussion of "Ductility of Concrete" by HEH Roy and MA Sozen. Proceedings of the international Symposium on flexural mechanics of reinforced concrete', ASCE-ACI, Miami,

Beyer, K., Dazio, A., & Priestley, N. (2011). Shear deformations of slender reinforced concrete walls under seismic loading. *ACI Structural Journal, 108*, 167-177.

Bian, J., Cao, W., Zhang, Z., & Qiao, Q. (2020). Cyclic loading tests of thin-walled square steel tube beam-column joint with different joint details. Structures,

Billah, A. M., & Alam, M. S. (2012). Seismic performance of concrete columns reinforced with hybrid shape memory alloy (SMA) and fiber reinforced polymer (FRP) bars. *Construction and Building Materials, 28*(1), 730-742.

Binder, J., & Christopoulos, C. (2018). Seismic performance of hybrid ductile‐rocking braced frame system. *Earthquake Engineering & Structural Dynamics, 47*(6), 1394-1415.

Bindhu, K., Sukumar, P., & Jaya, K. (2009). Performance of exterior beam-column joints under seismic type loading. *ISET Journal of Earthquake Technology, 46*(2), 47-64.

Bohl, A. G. (2006). *Plastic hinge length in high-rise concrete shear walls* University of British Columbia].

Boivin, Y. (2006). *Assessment of the seismic performance of a 12-storey ductile concrete shear wall system designed according to the NBCC 2005 and the CSA A23. 3 2004 standard*. Université de Sherbrooke.

Boivin, Y., & Paultre, P. (2010). Seismic performance of a 12-storey ductile concrete shear wall system designed according to the 2005 National building code of Canada and the 2004 Canadian Standard Association standard A23. 3. *Canadian Journal of Civil Engineering, 37*(1), 1-16.

Brookshire, D. S., Chang, S. E., Cochrane, H., Olson, R. A., Rose, A., & Steenson, J. (1997). Direct and indirect economic losses from earthquake damage. *Earthquake Spectra, 13*(4), 683-701.

Bruneau, M., & Reinhorn, A. (2006). Overview of the resilience concept. Proceedings of the 8th US national conference on earthquake engineering,

Buchanan, A. H., Bull, D., Dhakal, R., MacRae, G., Palermo, A., & Pampanin, S. (2011). Base isolation and damage-resistant technologies for improved seismic performance of buildings.

Buddika, H. S., & Wijeyewickrema, A. C. (2016). Seismic performance evaluation of posttensioned hybrid precast wall-frame buildings and comparison with shear wall-frame buildings. *Journal of structural engineering, 142*(6), 04016021.

C.A.O. (2016). Concrete Design Handbook, 4th ed. Ottawa, ON, Canada. *(No Title)*.

Cai, X., Pan, Z., Zhu, Y., Gong, N., & Wang, Y. (2021). Experimental and numerical investigations of self-centering post-tensioned precast beam-to-column connections with steel top and seat angles. *Engineering Structures, 226*, 111397.

Cai, Z.-K., Wang, Z., & Yang, T. (2018). Experimental testing and modeling of precast segmental bridge columns with hybrid normal-and high-strength steel rebars. *Construction and Building Materials, 166*, 945-955.

Camata, G., Spacone, E., & Zarnic, R. (2007). Experimental and nonlinear finite element studies of RC beams strengthened with FRP plates. *Composites Part B: Engineering, 38*(2), 277-288.

Canada, C. A. o., & Association, C. S. (2016). *Concrete Design Handbook, 4th Edn*. Cement Association of Canada

Canada, C.A.O.; Association, C.S. (2016) Concrete Design Handbook, 4th ed.; Cement Association of Canada: Ottawa, ON, Canada.

Canadian Standards Association (CSA). (2014). Design of Concrete Structures for Buildings. Standard CAN-A23.3-14, CSA, Rexdale, ON, Canada.

Canadian Standards Association (CSA). (2019). Design of Concrete Structures for Buildings. Standard CAN-A23.3-19, CSA, Rexdale, ON, Canada.

Cardenas, A., & Magura, D. (1973). Strength of High-Rise Shear Walls-Rectangular Cross Section. In: Response of Multistory Concrete Structures to Lateral Forces. *ACI Publication SP-36, American Concrete Institute, Detroit, MI*.

Cardenas, A. E., & Magura, D. D. (1972). Strength of high-rise shear walls-rectangular cross section. *Special Publication, 36*, 119-150.

Carr, A. (2004). RUAUMOKO, Computer program library. *Department of Civil Engineering, University of Canterbury, Christchurch, New Zealand*

Carr, A. J. (2008). Ruaumoko manual, Volume 2: User manual for the 2-dimensional version Ruaumoko2D. *University of Canterbury, Christchurch, NZ*.

Ceroni, F., Pecce, M., Matthys, S., & Taerwe, L. (2008). Debonding strength and anchorage devices for reinforced concrete elements strengthened with FRP sheets. *Composites Part B: Engineering, 39*(3), 429-441.

Chaallal, O., Gauthier, D., & Malenfant, P. (1996). Classification methodology for coupled shear walls. *Journal of Structural Engineering, 122*(12), 1453-1458.

Chancellor, N. B., Eatherton, M. R., Roke, D. A., & Akbaş, T. (2014). Self-Centering seismic lateral force resisting systems: high performance structures for the city of tomorrow. *Buildings, 4*(3), 520-548.

Chandra, R. (2001). Active shape control of composite blades using shape memory actuation. *Smart materials and structures, 10*(5), 1018.

Charalambidi, B. G., Rousakis, T. C., & Karabinis, A. I. (2016). Analysis of the fatigue behavior of reinforced concrete beams strengthened in flexure with fiber reinforced polymer laminates. *Composites Part B: Engineering, 96*, 69-78.

Chen, W., Pham, T. M., Sichembe, H., Chen, L., & Hao, H. (2018). Experimental study of flexural behaviour of RC beams strengthened by longitudinal and U-shaped basalt FRP sheet. *Composites Part B: Engineering, 134*, 114-126.

Chen, X. Y. (2005). Effect of confinement on the response of ductile shear walls.

Choi, K.-S., & Kim, H.-J. (2014). Strength demand of hysteretic energy dissipating devices alternative to coupling beams in high-rise buildings. *International Journal of High-Rise Buildings, 3*(2), 107-120.

Chou, C. C., & Chen, Y. C. (2006). Cyclic tests of post‐tensioned precast CFT segmental bridge columns with unbonded strands. *Earthquake Engineering & Structural Dynamics, 35*(2), 159-175.

Christidis, K. I., & Karagiannaki, D. (2021). Evaluation of flexural and shear deformations in medium rise RC shear walls. *Journal of Building Engineering, 42*, 102470.

Christidis, K. I., Vougioukas, E., & Trezos, K. G. (2016). Strengthening of non-conforming RC shear walls using different steel configurations. *Engineering Structures, 124*, 258-268.

Christopoulos, C., Filiatrault, A., Uang, C.-M., & Folz, B. (2002). Posttensioned energy dissipating connections for moment-resisting steel frames. *Journal of structural engineering, 128*(9), 1111-1120.

Cline, E. H. (2010). *The Oxford Handbook of the Bronze Age Aegean*. Oxford University Press.

Colajanni, P., & Pagnotta, S. (2022). RC beams retrofitted by FRP oriented in any direction: Influence of the effectiveness factors. *Engineering Structures, 266*, 114589.

Collins, M. P., Mitchell, D., & MacGregor, J. G. (1993). Structural design considerations for high-strength concrete. *Concrete international, 15*(5), 27-34.

Committee, A. (2017). Guide for the design and construction of externally bonded FRP systems for strengthening concrete structures (ACI 440.2 R-17). *American Concrete Institute, Farmington Hills, MI*.

Cruz-Noguez, C. A., Lau, D. T., Sherwood, E. G., Hiotakis, S., Lombard, J., Foo, S., & Cheung, M. (2015). Seismic behavior of RC shear walls strengthened for in-plane bending using externally bonded FRP sheets. *Journal of Composites for Construction, 19*(1), 04014023.

Cui, Y., Shu, Z., Zhou, R., Li, Z., Chen, F., & Ma, Z. (2020). Self‐centering steel–timber hybrid shear wall with slip friction dampers: Theoretical analysis and experimental investigation. *The Structural Design of Tall and Special Buildings, 29*(15), e1789.

Cusson, D., & Paultre, P. (1994). High-strength concrete columns confined by rectangular ties. *Journal of structural engineering, 120*(3), 783-804.

Davodikia, B., Saghafi, M. H., & Golafshar, A. (2021). Experimental investigation of grooving method in seismic retrofit of beam-column external joints without seismic details using CFRP sheets. Structures,

Dawood, H., ElGawady, M., & Hewes, J. (2012). Behavior of segmental precast posttensioned bridge piers under lateral loads. *Journal of Bridge Engineering, 17*(5), 735-746.

De Luca, A., Matta, F., Nanni, A., Nardone, F., Lignola, G., & Prota, A. (2009). Experimental evaluation of full-scale FRP-confined reinforced concrete columns. 2nd Asia-Pacific Conference on FRP in Structures, APFIS 2009,

De Maio, U., Greco, F., Leonetti, L., Blasi, P. N., & Pranno, A. (2022). An investigation about debonding mechanisms in FRP-strengthened RC structural elements by using a cohesive/volumetric modeling technique. *Theoretical and Applied Fracture Mechanics, 117*, 103199.

de Oliveira, L. B., de Azevedo, A. R., Marvila, M. T., Pereira, E. C., Fediuk, R., & Vieira, C. M. F. (2022). Durability of geopolymers with industrial waste. *Case Studies in Construction Materials, 16*, e00839.

Del Zoppo, M., Di Ludovico, M., Balsamo, A., Prota, A., & Manfredi, G. (2017). FRP for seismic strengthening of shear controlled RC columns: Experience from earthquakes and experimental analysis. *Composites Part B: Engineering, 129*, 47-57.

Deng, K., Pan, P., Shen, S., Wang, H., & Feng, P. (2018). Experimental study of FRP-reinforced slotted RC shear walls under cyclic loading. *Journal of Composites for Construction, 22*(4), 04018017.

Dezhdar, E. (2012). *Seismic response of cantilever shear wall buildings* University of British Columbia].

Di Cesare, A., Ponzo, F. C., Lamarucciola, N., & Nigro, D. (2020). Experimental seismic response of a resilient 3-storey post-tensioned timber framed building with dissipative braces. *Bulletin of Earthquake Engineering, 18*(15), 6825-6848.

Di Cesare, A., Ponzo, F. C., Nigro, D., Pampanin, S., & Smith, T. (2017). Shaking table testing of post-tensioned timber frame building with passive energy dissipation systems. *Bulletin of Earthquake Engineering, 15*(10), 4475-4498.

Dimitrakopoulos, E. G., & DeJong, M. J. (2012). Revisiting the rocking block: closed-form solutions and similarity laws. *Proceedings of the Royal Society A: Mathematical, Physical and Engineering Sciences, 468*(2144), 2294-2318.

Ding, R., Tao, M.-X., Nie, X., & Mo, Y. (2018). Analytical model for seismic simulation of reinforced concrete coupled shear walls. *Engineering Structures, 168*, 819-837.

Dolce, M., & Cardone, D. (2006). Theoretical and experimental studies for the application of shape memory alloys in civil engineering.

Dong, P. (2003). Effect of varying hysteresis models and damage models on damage assessment of r/c structures under standard design level earthquakes obtained using a new scaling method.

Drosos, V., & Anastasopoulos, I. (2014). Shaking table testing of multidrum columns and portals. *Earthquake Engineering & Structural Dynamics, 43*(11), 1703-1723.

Drosos, V. A., & Anastasopoulos, I. (2015). Experimental investigation of the seismic response of classical temple columns. *Bulletin of Earthquake Engineering, 13*(1), 299-310.

Eatherton, M. R., & Hajjar, J. F. (2014). Hybrid simulation testing of a self‐centering rocking steel braced frame system. *Earthquake Engineering & Structural Dynamics, 43*(11), 1725-1742.

Eatherton, M. R., Ma, X., Krawinkler, H., Deierlein, G. G., & Hajjar, J. F. (2014). Quasi-static cyclic behavior of controlled rocking steel frames. *Journal of structural engineering, 140*(11), 04014083.

Egbelakin, T., & Wilkinson, S. (2008). Factors affecting motivation for improved seismic retrofit implementation. Australian Earthquake Engineering Conference (AEES),

Egbelakin, T., Wilkinson, S., & Ingham, J. (2014). Economic impediments to successful seismic retrofitting decisions. *Structural Survey, 32*(5), 449-466.

Ehsani, M. R., & Saadatmanesh, H. (1997). Fiber composites: an economical alternative for retrofitting earthquake-damaged precast-concrete walls. *Earthquake Spectra, 13*(2), 225-241.

El-Ghandour, A. (2011). Experimental and analytical investigation of CFRP flexural and shear strengthening efficiencies of RC beams. *Construction and Building Materials, 25*(3), 1419-1429.

El-Sokkary, H. (2023). Nonlinear behaviour of FRP-retrofitted RC coupled shear walls. Structures,

El-Sokkary, H., & Galal, K. (2013). Seismic behavior of RC shear walls strengthened with fiber-reinforced polymer. *Journal of Composites for Construction, 17*(5), 603-613.

El-Sokkary, H., Galal, K., Ghorbanirenani, I., Léger, P., & Tremblay, R. (2013). Shake table tests on FRP-rehabilitated RC shear walls. *Journal of Composites for Construction, 17*(1), 79-90.

El Ghadioui, R., Wagner, J., Klein, J., Proske, T., Curbach, M., & Graubner, C. A. (2022). RC members with a flexural ‐ strengthening layer of CFRP textile ‐ reinforced concrete under monotonic and cyclic long ‐ term loading. *Structural Concrete, 23*(2), 939-953.

Elettore, E., Freddi, F., Latour, M., & Rizzano, G. (2021). Design and analysis of a seismic resilient steel moment resisting frame equipped with damage-free self-centering column bases. *Journal of Constructional Steel Research, 179*, 106543.

ElGawady, M., Endeshaw, M., McLean, D., & Sack, R. (2010). Retrofitting of rectangular columns with deficient lap splices. *Journal of Composites for Construction, 14*(1), 22-35.

ElGawady, M. A., & Dawood, H. M. (2012). Analysis of segmental piers consisted of concrete filled FRP tubes. *Engineering Structures, 38*, 142-152.

Elnady, M. (2008). *Seismic rehabilitation of RC structural walls* Ph. D. Thesis].

Erkmen, B., & Schultz, A. E. (2009). Self-centering behavior of unbonded, post-tensioned precast concrete shear walls. *Journal of Earthquake Engineering, 13*(7), 1047-1064.

Escolano-Margarit, D., Klenke, A., Pujol, S., & Benavent-Climent, A. (2012). Failure mechanism of reinforced concrete structural walls with and without confinement. Proceedings of the Fifteenth World Conference on Earthquake Engineering,

Fathalla, E., Rajapakse, R., & Mihaylov, B. I. (2022). Modeling the shear behavior of deep beams strengthened with FRP sheets. *Engineering Structures, 260*, 114232.

Fathelbab, F. A., Ramadan, M. S., & Al-Tantawy, A. (2014). Strengthening of RC bridge slabs using CFRP sheets. *Alexandria Engineering Journal, 53*(4), 843-854.

Fathi, A., El-Saikaly, G., & Chaallal, O. (2022). On Bond-slip of EB-FRP/Concrete Interface in Shear Under Fatigue Loading: Review and Synthesis of Experimental Studies and Models. *Journal of Civil Engineering and Construction, 11*(1), 1-19.

Fischer, G., & Li, V. C. (2003). Intrinsic response control of moment-resisting frames utilizing advanced composite materials and structural elements. *Structural Journal, 100*(2), 166-176.

Forcellini, D. (2019). A new methodology to assess indirect losses in bridges subjected to multiple hazards. *Innovative Infrastructure Solutions, 4*(1), 10.

Foroughi, S., & Yüksel, S. B. (2019). Investigation of Displacement Behavior of Reinforced Concrete Shear Walls with Different Plastic Hinge Relationships. *Uluslararası Doğu Anadolu Fen Mühendislik ve Tasarım Dergisi, 1*(2), 196-211.

Fortney, P. J. (2005). *The next generation of coupling beams*. University of Cincinnati.

Fortunato, A., Fabbrocino, F., Angelillo, M., & Fraternali, F. (2018). Limit analysis of masonry structures with free discontinuities. *Meccanica, 53*, 1793-1802.

Franchi, A., Napoli, P., Crespi, P., Giordano, N., & Zucca, M. (2022). Unloading and reloading process for the earthquake damage repair of ancient Masonry columns: The case of the Basilica di Collemaggio. *International Journal of Architectural Heritage, 16*(11), 1683-1698.

Ganey, R., Berman, J., Akbas, T., Loftus, S., Daniel Dolan, J., Sause, R., Ricles, J., Pei, S., Lindt, J. v. d., & Blomgren, H.-E. (2017). Experimental investigation of self-centering cross-laminated timber walls. *Journal of structural engineering, 143*(10), 04017135.

GangaRao, H. V., Taly, N., & Vijay, P. (2006). *Reinforced concrete design with FRP composites*. CRC press.

Ghobarah, A., & Said, A. (2001). Seismic rehabilitation of beam-column joints using FRP laminates. *Journal of Earthquake Engineering, 5*(01), 113-129.

Ghosh, K. K., & Sheikh, S. A. (2007). Seismic upgrade with carbon fiber-reinforced polymer of columns containing lap-spliced reinforcing bars. *ACI Materials Journal, 104*(2), 227.

Ghosh, S., & Markevicius, V. P. (1990). Design of earthquake resistant shearwalls to prevent shear failure.

Giberson, M. F. (1969). Two nonlinear beams with definitions of ductility. *Journal of the Structural Division, 95*(2), 137-157.

Grelle, S. V., & Sneed, L. H. (2013). Review of anchorage systems for externally bonded FRP laminates. *International Journal of Concrete Structures and Materials, 7*, 17-33.

Gu, D.-S., Wu, G., Wu, Z.-S., & Wu, Y.-F. (2010). Confinement effectiveness of FRP in retrofitting circular concrete columns under simulated seismic load. *Journal of Composites for Construction, 14*(5), 531-540.

Guerrini, G., Restrepo, J. I., Massari, M., & Vervelidis, A. (2015). Seismic behavior of posttensioned self-centering precast concrete dual-shell steel columns. *Journal of structural engineering, 141*(4), 04014115.

Guo, T., Xu, Z., Song, L., Wang, L., & Zhang, Z. (2017). Seismic resilience upgrade of RC frame building using self-centering concrete walls with distributed friction devices. *Journal of structural engineering, 143*(12), 04017160.

Guo, T., Zhang, G., & Chen, C. (2014). Experimental study on self-centering concrete wall with distributed friction devices. *Journal of Earthquake Engineering, 18*(2), 214-230.

Guo, X., Wang, Y., Huang, P., & Shu, S. (2021). Fatigue behavior of RC beams strengthened with FRP considering the influence of FRP-concrete interface. *International Journal of Fatigue, 143*, 105977.

Hadhood, A., Mohamed, H. M., & Benmokrane, B. (2017). Experimental study of circular high-strength concrete columns reinforced with GFRP bars and spirals under concentric and eccentric loading. *Journal of Composites for Construction, 21*(2), 04016078.

Hadi, S. (2022). Full-scale experimental evaluation of flexural strength and ductility of reinforced concrete beams strengthened with various FRP mechanisms. Structures,

Hall, J. F. (2006). Problems encountered from the use (or misuse) of Rayleigh damping. *Earthquake engineering & structural dynamics, 35*(5), 525-545.

Harajli, M. H. (2006). Effect of confinement using steel, FRC, or FRP on the bond stress-slip response of steel bars under cyclic loading. *Materials and structures, 39*(6), 621-634.

Harries, K. A. (1995a). *Seismic design and retrofit of coupled walls using structural steel* McGill University]. Montreal, Canada.

Harries, K. A. (1995b). Seismic design and retrofit of coupled walls using structural steel.

Hashemi, A., Zarnani, P., Masoudnia, R., & Quenneville, P. (2018). Experimental testing of rocking cross-laminated timber walls with resilient slip friction joints. *Journal of structural engineering, 144*(1), 04017180.

Hassanli, R., ElGawady, M. A., & Mills, J. E. (2016). Experimental investigation of in-plane cyclic response of unbonded posttensioned masonry walls. *Journal of structural engineering, 142*(5), 04015171.

Hidalgo, P., Jordan, R., & Martinez, M. (2002). An analytical model to predict the inelastic seismic behavior of shear-wall, reinforced concrete structures. *Engineering Structures, 24*(1), 85-98.

Holden, T., Restrepo, J., & Mander, J. B. (2003). Seismic performance of precast reinforced and prestressed concrete walls. *Journal of structural engineering, 129*(3), 286-296.

Honarparast, S. (2018). *Nonlinear behaviour of coupled shear walls strengthened with externally bonded carbon fibre reinforced polymer composite under seismic loadings* École de technologie supérieure].

Honarparast, S., & Chaallal, O. (2019a). Experimental seismic performance evaluation of coupling beams: comparison of old with modern codes. *Journal of Earthquake Engineering*, 1-16.

Honarparast, S., & Chaallal, O. (2019b). Non-linear time history analysis of reinforced concrete coupled shear walls: Comparison of old design, modern design and retrofitted with externally bonded CFRP composites. *Engineering Structures, 185*, 353-365.

Honarparast, S., & Chaallal, O. (2021). Experimental seismic performance evaluation of coupling beams: comparison of old with modern codes. *Journal of Earthquake Engineering, 25*(11), 2269-2284.

Honarparast, S., & Chaallal, O. (2022). Seismic performance of coupled shear walls designed according to old and new codes and retrofitted with Eb-CFRP composites. *Journal of Earthquake Engineering, 26*(4), 1875-1898.

Honarparast, S., El-Saikaly, G., & Chaallal, O. (2019). Externally bonded carbon fiber–reinforced polymer composites for seismic retrofit of reinforced concrete coupling beams designed according to old codes. *Advances in Structural Engineering, 22*(6), 1412-1425.

Hoult, R., Goldsworthy, H., & Lumantarna, E. (2018). Plastic hinge length for lightly reinforced rectangular concrete walls. *Journal of Earthquake Engineering, 22*(8), 1447-1478.

Housner, G. W. (1963). The behavior of inverted pendulum structures during earthquakes. *Bulletin of the seismological society of America, 53*(2), 403-417.

Huang, Z., Shen, J., Lin, H., Song, X., & Yao, Y. (2020). Shear behavior of concrete shear walls with CFRP grids under lateral cyclic loading. *Engineering Structures, 211*, 110422.

Hung, C.-C., & Hsieh, P.-L. (2020). Comparative study on shear failure behavior of squat high-strength steel reinforced concrete shear walls with various high-strength concrete materials. Structures,

Hung, H. H., Liu, K. Y., Ho, T. H., & Chang, K. C. (2011). An experimental study on the rocking response of bridge piers with spread footing foundations. *Earthquake Engineering & Structural Dynamics, 40*(7), 749-769.

Hwang, S.-J., Fang, W.-H., Lee, H.-J., & Yu, H.-W. (2001). Analytical model for predicting shear strengthof squat walls. *Journal of structural engineering, 127*(1), 43-50.

Iacobucci, R. D., Sheikh, S. A., & Bayrak, O. (2003). Retrofit of square concrete columns with carbon fiber-reinforced polymer for seismic resistance. *Structural Journal, 100*(6), 785-794.

Ichikawa, S., Matsuzaki, H., Moustafa, A., ElGawady, M. A., & Kawashima, K. (2016). Seismic-resistant bridge columns with ultrahigh-performance concrete segments. *J. Bridge Eng, 21*(9), 04016049.

Imbsen Software Systems, 2002, Release Notes of XTRACT v 2.6.2—Cross Sectional Xs Structural Analysis of Components.

Iqbal, A., Pampanin, S., & Buchanan, A. H. (2016). Seismic performance of full-scale post-tensioned timber beam-column connections. *Journal of Earthquake Engineering, 20*(3), 383-405.

Jafari, A., Beheshti, M., Shahmansouri, A. A., & Bengar, H. A. (2024). Cyclic response and damage status of coupled and hybrid-coupled shear walls. Structures,

James, V. R. (2020). *Fatigue Behaviour of CFRP Strengthened Reinforced Concrete Beams* Faculty of Engineering and the Built Environment].

Jiang, H., Li, S., Bolander, J. E., & Kunnath, S. K. (2023). Seismic performance of a new type of coupled shear wall with replaceable components: experimental Validation. *Journal of Earthquake Engineering, 27*(4), 810-832.

Jin, L., Lan, Y., Zhang, R., & Du, X. (2021). Numerical analysis of the mechanical behavior of the impact-damaged RC beams strengthened with CFRP. *Composite Structures, 274*, 114353.

Jin, L., Zhang, B., Chen, F., Miao, L., & Du, X. (2024). Experimental investigation on the size-dependent CFRP shear contribution in CFRP-strengthened RC shear wall. *Engineering Structures, 307*, 117800.

Johnson, J., Xu, M., & Jacques, E. (2021a). Predicting the self-centering behavior of hybrid FRP-steel reinforced concrete beams under blast loading. *Engineering Structures, 247*, 113117.

Johnson, J., Xu, M., & Jacques, E. (2021b). Self-Centering Hybrid GFRP-Steel Reinforced Concrete Beams for Blast Resilience. *Journal of structural engineering, 147*(7), 04021099.

Jury, R. D. (1978). *Seismic Load Demands on Columns of Reinforced Concrete Multistorey Frames: A Report Submitted in Partial Fulfilment of the Requirements for the Degree of Master of Engineering at the University of Canterbury,* University of Canterbury]. Christchurch, New Zealand.

Kantar, E., & Anil, Ö. (2012). Low velocity impact behavior of concrete beam strengthened with CFRP strip. *Steel and Composite Structures, An International Journal, 12*(3), 207-230.

Kargaran, A., & Kheyroddin, A. (2022). Experimental and numerical investigation of seismic retrofitting of RC square short columns using FRP composites. *European Journal of Environmental and Civil Engineering, 26*(10), 4619-4642.

Kashani, M. M., Gonzalez-Buelga, A., Thayalan, R. P., Thomas, A. R., & Alexander, N. A. (2018). Experimental investigation of a novel class of self-centring spinal rocking column. *Journal of Sound and Vibration, 437*, 308-324.

Khalil, A., & Ghobarah, A. (2005). Behaviour of rehabilitated structural walls. *Journal of Earthquake Engineering, 9*(3), 371-391.

Kim, H.-J., & Christopoulos, C. (2008). Friction damped posttensioned self-centering steel moment-resisting frames. *Journal of structural engineering, 134*(11), 1768-1779.

Kim, S.-H., Lee, E.-K., Kang, S.-M., Park, H.-G., & Park, J.-H. (2021). Effect of boundary confinement on ductility of RC walls. *Engineering Structures, 230*, 111695.

Kishi, N., Komuro, M., Kawarai, T., & Mikami, H. (2020). Low-velocity impact load testing of RC beams strengthened in flexure with bonded FRP sheets. *Journal of Composites for Construction, 24*(5), 04020036.

Kitayama, S., & Constantinou, M. C. (2016). Design and analysis of buildings with fluidic self-centering systems. *Journal of structural engineering, 142*(11), 04016105.

Ko, H., & Sato, Y. (2007). Bond stress–slip relationship between FRP sheet and concrete under cyclic load. *Journal of Composites for Construction, 11*(4), 419-426.

Koduru, S., & Haukaas, T. (2010). Probabilistic seismic loss assessment of a Vancouver high-rise building. *Journal of Structural Engineering, 136*(3), 235-245.

Kumar, J. D., Sharma, A. S., & Devi, K. S. (2021). Study on flexural behaviour of RC beam strengthened with FRP. Journal of Physics: Conference Series,

Kurama, Y. C. (2000). Unbonded post-tensioned precast concrete walls with supplemental viscous damping. *ACI Structural Journal, 97*(4), 648-658.

Kurama, Y. C. (2002). Hybrid post-tensioned precast concrete walls for use in seismic regions. *PCI journal, 47*(5), 36-59.

Kurama, Y. C., & Shen, Q. (2004). Posttensioned hybrid coupled walls under lateral loads. *Journal of structural engineering, 130*(2), 297-309.

Kurama, Y. C., Weldon, B. D., & Shen, Q. (2006). Experimental evaluation of posttensioned hybrid coupled wall subassemblages. *Journal of structural engineering, 132*(7), 1017-1029.

Kwan, A., & Zhao, Z.-Z. (2002). Cyclic behaviour of deep reinforced concrete coupling beams. *Proceedings of the Institution of Civil Engineers-Structures and Buildings, 152*(3), 283-293.

Lam, L., & Teng, J. G. (2003). Design-oriented stress–strain model for FRP-confined concrete. *Construction and Building Materials, 17*(6-7), 471-489.

Laursen, P. T., & Ingham, J. M. (2001). Structural testing of single-storey post-tensioned concrete masonry walls. *The Masonry Society Journal, 19*(1), 69-82.

Lavorato, D., Bergami, A. V., Fiorentino, G., Fiore, A., Santini, S., & Nuti, C. (2018). Experimental tests on existing RC beams strengthened in flexure and retrofitted for shear by C-FRP in presence of negative moments. *International Journal of Advanced Structural Engineering, 10*, 211-232.

Layssi, H., Cook, W. D., & Mitchell, D. (2012a). Seismic response and CFRP retrofit of poorly detailed shear walls. *Journal of Composites for Construction, 16*(3), 332.

Layssi, H., Cook, W. D., & Mitchell, D. (2012b). Seismic response and CFRP retrofit of poorly detailed shear walls. *Journal of Composites for Construction, 16*(3), 332-339.

Layssi, H., & Mitchell, D. (2012). Experiments on seismic retrofit and repair of reinforced concrete shear walls. Proceedings of the 6th International Conference on FRP Composites in Civil Engineering (CICE),

Lecce, L. (2014). *Shape memory alloy engineering: for aerospace, structural and biomedical applications*. Elsevier.

Lehman, D. E., Turgeon, J. A., Birely, A. C., Hart, C. R., Marley, K. P., Kuchma, D. A., & Lowes, L. N. (2013). Seismic behavior of a modern concrete coupled wall. *Journal of Structural Engineering, 139*(8), 1371-1381.

Li, B., & Lim, C. L. (2010). Tests on seismically damaged reinforced concrete structural walls repaired using fiber-reinforced polymers. *Journal of Composites for Construction, 14*(5), 597-608.

Li, B., Qian, K., & Tran, C. T. N. (2013). Retrofitting earthquake-damaged RC structural walls with openings by externally bonded FRP strips and sheets. *Journal of Composites for Construction, 17*(2), 259-270.

Li, S., Jiang, H., & Kunnath, S. K. (2023). Seismic assessment of a new resilient coupled shear wall. *Engineering Structures, 277*, 115476.

Li, X., Liu, L., Lv, H.-L., & Sha, S.-Y. (2016). Seismic retrofit of short RC coupling beams using CFRP composites. *Magazine of Concrete Research, 68*(5), 260-270.

Li, Z., Chen, F., He, M., Zhou, R., Cui, Y., Sun, Y., & He, G. (2021). Lateral performance of self-centering steel–timber hybrid shear walls with slip-friction dampers: Experimental investigation and numerical simulation. *Journal of structural engineering, 147*(1), 04020291.

Liang, K., & Su, R. K. L. (2023). Experimental and theoretical study on seismic behavior of non-seismically designed shear walls with moderate shear span-to-length ratios. *Journal of Building Engineering, 76*, 107213.

Lifshitz Sherzer, G., Urlainis, A., Moyal, S., & Shohet, I. M. (2024). Seismic Resilience in Critical Infrastructures: A Power Station Preparedness Case Study. *Applied Sciences, 14*(9), 3835.

Liu, H., Huang, Y., & Qu, Z. (2022). A discretely damped SDOF model for the rocking response of freestanding blocks. *Earthquake Engineering and Engineering Vibration*.

Liu, J., Li-yue, M., Dong, L., & Xiu-li, D. (2021). Influence of axial compression ratio on size effect of RC shear wall under shear failure: meso-scale simulation. *工程力学, 38*(9), 26-35.

Liu, Y., Dong, A., Zhao, S., Zeng, Y., & Wang, Z. (2021). The effect of CFRP-shear strengthening on existing circular RC columns under impact loads. *Construction and Building Materials, 302*, 124185.

Liu, Y., & Zhou, W. (2022). Numerical modeling to predict seismic performance of the post-tensioned self-centering concrete shear walls. *Bulletin of Earthquake Engineering, 20*(2), 1057-1086.

Lombard, J., Lau, D. T., Humar, J. L., Foo, S., & Cheung, M. S. (2000). Seismic strengthening and repair of reinforced concrete shear walls. Proc., 12th World Conf. on Earthquake Engineering,

Loo, W. Y., Kun, C., Quenneville, P., & Chouw, N. (2014). Experimental testing of a rocking timber shear wall with slip‐friction connectors. *Earthquake Engineering & Structural Dynamics, 43*(11), 1621-1639.

Makris, N., & Aghagholizadeh, M. (2019). Effect of supplemental hysteretic and viscous damping on rocking response of free-standing columns. *Journal of Engineering Mechanics, 145*(5), 04019028.

Makris, N., & Vassiliou, M. F. (2013). Planar rocking response and stability analysis of an array of free‐standing columns capped with a freely supported rigid beam. *Earthquake Engineering & Structural Dynamics, 42*(3), 431-449.

Mander, J. B., & Cheng, C.-T. (1997). Seismic resistance of bridge piers based on damage avoidance design. In *Seismic resistance of bridge piers based on damage avoidance design* (pp. 109-109).

Mander, J. B., Priestley, M. J., & Park, R. (1988). Theoretical stress-strain model for confined concrete. *Journal of structural engineering, 114*(8), 1804-1826.

Manohar, S., & Madhekar, S. (2015). *Seismic design of RC buildings*. Springer.

Marriott, D., Pampanin, S., & Palermo, A. (2009). Quasi‐static and pseudo‐dynamic testing of unbonded post‐tensioned rocking bridge piers with external replaceable dissipaters. *Earthquake engineering & structural dynamics, 38*(3), 331-354.

McGuire, R. K. (1995). Probabilistic seismic hazard analysis and design earthquakes: closing the loop. *Bulletin of the seismological society of America, 85*(5), 1275-1284.

McNeice, D. (2004). Performance-based design of a 30-storey coupled wall structure. *MSCE Thesis. University of South Carolina*.

Miao, L., Jin, L., Li, D., Du, X., & Zhang, B. (2022). Effect of shear-span ratio and vertical reinforcement ratio on the failure of geometrical-similar RC shear walls. *Engineering Failure Analysis*, 106407.

Mo, Y. L., Yeh, Y.-K., & Hsieh, D. (2004). Seismic retrofit of hollow rectangular bridge columns. *Journal of Composites for Construction, 8*(1), 43-51.

Mohammadi, H., Esfahani, M., & Riyazi, M. (2007). Behavior of coupling beams strengthened with carbon fiber reinforced polymer sheets. *International Journal of Engineering, 20*(1), 49-58.

Morgen, B. G., & Kurama, Y. C. (2008). Seismic response evaluation of posttensioned precast concrete frames with friction dampers. *Journal of structural engineering, 134*(1), 132-145.

Moroder, D., Smith, T., Dunbar, A., Pampanin, S., & Buchanan, A. (2018). Seismic testing of post-tensioned Pres-Lam core walls using cross laminated timber. *Engineering Structures, 167*, 639-654.

Mostafa, A., & Razaqpur, A. G. (2013). CFRP anchor for preventing premature debonding of externally bonded FRP laminates from concrete. *Journal of Composites for Construction, 17*(5), 641-650.

Mostofinejad, D., & Kashani, A. T. (2013). Experimental study on effect of EBR and EBROG methods on debonding of FRP sheets used for shear strengthening of RC beams. *Composites Part B: Engineering, 45*(1), 1704-1713.

Motaref, S., Saiidi, M. S., & Sanders, D. (2014). Shake table studies of energy-dissipating segmental bridge columns. *Journal of Bridge Engineering, 19*(2), 186-199.

Mottier, P., Tremblay, R., & Rogers, C. (2018). Seismic retrofit of low‐rise steel buildings in Canada using rocking steel braced frames. *Earthquake Engineering & Structural Dynamics, 47*(2), 333-355.

Mottier, P., Tremblay, R., & Rogers, C. (2021). Shake table test of a two‐story steel building seismically retrofitted using gravity‐controlled rocking braced frame system. *Earthquake Engineering & Structural Dynamics, 50*(6), 1576-1594.

Mouzakis, H., Psycharis, I., Papastamatiou, D., Carydis, P., Papantonopoulos, C., & Zambas, C. (2002). Experimental investigation of the earthquake response of a model of a marble classical column. *Earthquake Engineering & Structural Dynamics, 31*(9), 1681-1698.

Murad, Y., Al Bodour, W., & Ashteyat, A. (2020). Seismic retrofitting of severely damaged RC connections made with recycled concrete using CFRP sheets. *Frontiers of Structural and Civil Engineering, 14*(2), 554-568.

Mutalib, A. A., & Hao, H. (2011). Numerical analysis of FRP-composite-strengthened RC panels with anchorages against blast loads. *Journal of Performance of Constructed Facilities, 25*(5), 360-372.

N.R.C.C, N. R. C. o. C. (2015). *Structural commentaries (user's guide—NBC 2015: Part 4 of Division B)*. National Research Council of Canada.

Naeem, A., & Kim, J. (2018). Seismic performance evaluation of a spring viscous damper cable system. *Engineering Structures, 176*, 455-467.

National Building Code of Canada (NBCC). (1941). Institute for Research in Construction, National Research Council of Canada, Ottawa, Ont. .

National Building Code of Canada (NBCC). (2015). Institute for Research in Construction, National Research Council of Canada, Ottawa, Ont. .

National Building Code of Canada (NBCC). (2019). Institute for Research in Construction, National Research Council of Canada, Ottawa, Ont. .

Navarro-Gómez, A., & Bonet, J. L. (2019). Improving the seismic behaviour of reinforced concrete moment resisting frames by means of SMA bars and ultra-high performance concrete. *Engineering Structures, 197*, 109409.

Newcombe, M., Pampanin, S., Buchanan, A., & Palermo, A. (2008). Section analysis and cyclic behavior of post-tensioned jointed ductile connections for multi-story timber buildings. *Journal of Earthquake Engineering, 12*(S1), 83-110.

Ni, X., Cao, S., Liang, S., Li, Y., & Liu, Y. (2019). High-strength bar reinforced concrete walls: Cyclic loading test and strength prediction. *Engineering Structures, 198*, 109508.

Nikoukalam, M., & Sideris, P. (2017). Resilient bridge rocking columns with polyurethane damage-resistant end segments and replaceable energy-dissipating links. *Journal of Bridge Engineering, 22*(10), 04017064.

Niu, L., & Zhang, W. (2017). Experimental study on a self-centering earthquake-resistant masonry pier with a structural concrete column. *Advances in Materials Science and Engineering, 2017*.

NoroozOlyaee, M., & Mostofinejad, D. (2019). Slenderness effects in circular RC columns strengthened with CFRP sheets using different external bonding techniques. *Journal of Composites for Construction, 23*(1), 04018068.

Noureldin, M., Memon, S. A., Gharagoz, M., & Kim, J. (2021). Performance-based seismic retrofit of RC structures using concentric braced frames equipped with friction dampers and disc springs. *Engineering Structures, 243*, 112555.

NRCC. (2015). *Structural commentaries (user's guide—NBC 2015: Part 4 of division B)*. National Research Council Canada (NRCC).

O Tang, T., & KL Su, R. (2014). Shear and flexural stiffnesses of reinforced concrete shear walls subjected to cyclic loading. *The Open Construction & Building Technology Journal, 8*(1).

Oesterle, R., Aristizabal-Ochoa, J., Fiorato, A., Russell, H., & Corley, W. (1979). Earthquake resistant structural walls-tests of isolated walls-phase II. *Construction Technology Laboratories, Portland Cement Association*.

Opabola, E. A., & Elwood, K. J. (2021). Seismic assessment of reinforced concrete columns with short lap splices. *Earthquake Spectra, 37*(3), 1726-1757.

Opabola, E. A., Elwood, K. J., & Liel, A. B. (2021). Evaluation of seismic performance of as‐built and retrofitted reinforced concrete frame structures with LAP splice deficiencies. *Earthquake Engineering & Structural Dynamics, 50*(12), 3138-3159.

Otani, S. (1974). *SAKE: A computer program for inelastic response of R/C frames to earthquakes.* In *Civil Engineering Studies SRS-413* University of Illinois.

Ou, Y.-C., Chiewanichakorn, M., Aref, A. J., & Lee, G. C. (2007). Seismic performance of segmental precast unbonded posttensioned concrete bridge columns. *Journal of structural engineering-New York, N.Y., 133*(11), 1636.

Ou, Y., & Zhu, D. (2015). Tensile behavior of glass fiber reinforced composite at different strain rates and temperatures. *Construction and Building Materials, 96*, 648-656.

Ouyang, L.-J., Gao, W.-Y., Zhen, B., & Lu, Z.-D. (2017). Seismic retrofit of square reinforced concrete columns using basalt and carbon fiber-reinforced polymer sheets: A comparative study. *Composite Structures, 162*, 294-307.

Palermo, A., Pampanin, S., & Marriott, D. (2007). Design, modeling, and experimental response of seismic resistant bridge piers with posttensioned dissipating connections. *Journal of structural engineering, 133*(11), 1648-1661.

Panahi, M., Zareei, S. A., & Izadi, A. (2021). Flexural strengthening of reinforced concrete beams through externally bonded FRP sheets and near surface mounted FRP bars. *Case Studies in Construction Materials, 15*, e00601.

Papaloizou, L., & Komodromos, P. (2009). Planar investigation of the seismic response of ancient columns and colonnades with epistyles using a custom-made software. *Soil Dynamics and Earthquake Engineering, 29*(11-12), 1437-1454.

Park, H.-G., Baek, J.-W., Lee, J.-H., & Shin, H.-M. (2015). Cyclic loading tests for shear strength of low-rise reinforced concrete walls with grade 550 MPa bars. *ACI Structural Journal, 112*(3), 299.

Park, R., & Paulay, T. (1975). *Reinforced concrete structures*. John Wiley & Sons.

Park, R., & Paulay, T. (1991). *Reinforced concrete structures*. John Wiley & Sons.

Parvin, A., & Granata, P. (2000). Investigation on the effects of fiber composites at concrete joints. *Composites Part B: Engineering, 31*(6-7), 499-509.

Parvin, A., & Wang, W. (2002). Concrete columns confined by fiber composite wraps under combined axial and cyclic lateral loads. *Composite Structures, 58*(4), 539-549.

Paterson, J., & Mitchell, D. (2003). Seismic retrofit of shear walls with headed bars and carbon fiber wrap. *Journal of structural engineering, 129*(5), 606-614.

Paulay, T. (1969). *The coupling of shear walls* University of Canterbury]. Christchurch, New Zealand.

Paulay, T. (1971). Coupling beams of reinforced concrete shear walls. *Journal of the Structural Division, 97*(3), 843-862.

Paulay, T. (1974). Some seismic aspects of coupled shear walls. Proceedings, 5th World Conference on Earthquake Engineering,

Paulay, T., & Binney, J. (1974). Diagonally reinforced coupling beams of shear walls. *Special Publication, 42*, 579-598.

Paulay, T., & Goodsir, W. J. (1985). The ductility of structural walls. *Bulletin of the new zealand society for earthquake engineering, 18*(3), 250-269.

Paulay, T., & Priestley, M. (1993). Stability of ductile structural walls. *Structural Journal, 90*(4), 385-392.

Paulay, T., Priestley, M., & Synge, A. (1982). Ductility in earthquake resisting squat shearwalls. Journal Proceedings,

Paulay, T., & Priestley, M. N. (1992). Seismic design of reinforced concrete and masonry buildings.

Paulay, T., & Santhakumar, A. R. (1976). Ductile behavior of coupled shear walls. *Journal of the Structural Division, 102*(1), 93-108.

Pecker, A. (2008). *Advanced earthquake engineering analysis* (Vol. 494). Springer Science & Business Media.

Pei, S., van de Lindt, J. W., Barbosa, A. R., Berman, J. W., McDonnell, E., Daniel Dolan, J., Blomgren, H.-E., Zimmerman, R. B., Huang, D., & Wichman, S. (2019). Experimental seismic response of a resilient 2-story mass-timber building with post-tensioned rocking walls. *Journal of structural engineering, 145*(11).

Perez, F. J., Pessiki, S., & Sause, R. (2013). Experimental Lateral Load Response of Unbonded Post-Tensioned Precast Concrete Walls. *ACI Structural Journal, 110*(6).

Petkune, N., Donchev, T., Hadavinia, H., Limbachiya, M., & Wertheim, D. (2016). Performance of pristine and retrofitted hybrid steel/fibre reinforced polymer composite shear walls. *Construction and Building Materials, 117*, 198-208.

Petrini, L., Maggi, C., Priestley, M. N., & Calvi, G. M. (2008). Experimental verification of viscous damping modeling for inelastic time history analyzes. *Journal of Earthquake Engineering, 12*(S1), 125-145.

Pham, T. M., & Hao, H. (2016). Review of concrete structures strengthened with FRP against impact loading. Structures,

Phan, V.-T., & Nguyen, D.-D. (2021). Efficiency of flexural strengthening RC beams using fiber reinforced polymer materials. *Materials Today: Proceedings, 38*, 2584-2589.

Pollino, M., Slovenec, D., Qu, B., & Mosqueda, G. (2017). Seismic rehabilitation of concentrically braced frames using stiff rocking cores. *Journal of structural engineering, 143*(9), 04017080.

Priestley, M. (1996). The PRESSS program—current status and proposed plans for phase Ill. *PCI journal, 4*(2), 22-40.

Qian, H., Wang, X., Li, Z., & Zhang, Y. (2023). Experimental study on re-centering behavior and energy dissipation capacity of prefabricated concrete frame joints with shape memory alloy bars and engineered cementitious composites. *Engineering Structures, 277*, 115394.

Rahimi, H., & Hutchinson, A. (2001). Concrete beams strengthened with externally bonded FRP plates. *Journal of Composites for Construction, 5*(1), 44-56.

Rajendran, S. C., & Kothapalli, N. (2022). Influence of FRP on the shear behaviour of RC rectangular beam elements. *Materials Today: Proceedings*.

Raza, A. (2021). Structural behavior of GFRP-reinforced circular HFRC columns under concentric and eccentric loading. *Arabian Journal for Science and Engineering, 46*(5), 4239-4252.

Razavi, M., Mostofinejad, D., & Eftekhar, M. (2021). Behavior of RC columns and those strengthened with FRP composite under an innovative reversing cyclic eccentric axial loading. *Engineering Structures, 241*, 112438.

Restrepo, J. I., & Rahman, A. (2007). Seismic performance of self-centering structural walls incorporating energy dissipators. *Journal of structural engineering, 133*(11), 1560-1570.

Ricles, J. M., Sause, R., Garlock, M. M., & Zhao, C. (2001). Posttensioned seismic-resistant connections for steel frames. *Journal of structural engineering, 127*(2), 113-121.

Ríos-García, G., & Benavent-Climent, A. (2020). New rocking column with control of negative stiffness displacement range and its application to RC frames. *Engineering Structures, 206*, 110133.

Rojas, P., Ricles, J., & Sause, R. (2005). Seismic performance of post-tensioned steel moment resisting frames with friction devices. *Journal of structural engineering, 131*(4), 529-540.

Roke, D. A. (2010). *Damage-free seismic-resistant self-centering concentrically-braced frames*. Lehigh University.

Rosenboom, O. A., & Kowalsky, M. J. (2004). Reversed in-plane cyclic behavior of posttensioned clay brick masonry walls. *Journal of structural engineering, 130*(5), 787-798.

Saatcioglu, M., Palermo, D., Ghobarah, A., Mitchell, D., Simpson, R., Adebar, P., Tremblay, R., Ventura, C., & Hong, H. (2013). Performance of reinforced concrete buildings during the 27 February 2010 Maule (Chile) earthquake. *Canadian Journal of Civil Engineering, 40*(8), 693-710.

Sadeghian, A. (2018). *Seismic deformations of taller Reinforced Concrete shear walls located in eastern Canada* Ecole Polytechnique, Montreal (Canada)].

Saiidi, M., & Sozen, M. A. (1979a). *Simple and complex models for nonlinear seismic response of reinforced concrete structures*.

Saiidi, M., & Sozen, M. A. (1979b). Simple and complex models for nonlinear seismic response of reinforced concrete structures. *Civil Engineering Studies SRS-465*.

Sakr, M. A., El-Khoriby, S. R., Khalifa, T. M., & Nagib, M. T. (2017a). Modeling of RC shear walls strengthened by FRP composites. *Struct. Eng. Mech, 61*(3), 407-417.

Sakr, M. A., El-Khoriby, S. R., Khalifa, T. M., & Nagib, M. T. (2017b). Modeling of RC shear walls strengthened by FRP composites. *Structural Engineering and Mechanics, 61*(3), 407-417.

Saleh, E., Tarawneh, A., Almasabha, G., & Momani, Y. (2022). Slenderness limit of FRP-confined rectangular concrete columns. Structures,

Salehi, M., Sideris, P., & Liel, A. B. (2017). Numerical simulation of hybrid sliding-rocking columns subjected to earthquake excitation. *Journal of structural engineering, 143*(11), 04017149.

Salehi, M., Sideris, P., & Liel, A. B. (2021). Experimental testing of hybrid sliding ‐ rocking bridge columns under torsional and biaxial lateral loading. *Earthquake Engineering & Structural Dynamics, 50*(10), 2817-2837.

Saljoughian, A., & Mostofinejad, D. (2018). Grooving methods in square RC columns strengthened with longitudinal CFRP under cyclic axial compression. *Engineering Structures, 174*, 724-735.

Samb, N., El-Saikaly, G., & Chaallal, O. (2021). Strengthening in shear of RC T-beams with CFRP fabrics: Multilayer versus monolayer. International Conference on Fibre-Reinforced Polymer (FRP) Composites in Civil Engineering,

Santhakumar, A. R. (1974). Ductility of coupled shear walls.

Saribiyik, A., Abodan, B., & Balci, M. T. (2021). Experimental study on shear strengthening of RC beams with basalt FRP strips using different wrapping methods. *Engineering Science and Technology, an International Journal, 24*(1), 192-204.

Sarti, F., Palermo, A., & Pampanin, S. (2016). Development and testing of an alternative dissipative post-tensioned rocking timber wall with boundary columns.

Sause, R., Ricles, J., Roke, D., Chancellor, N., & Gonner, N. (2010). Seismic performance of a self-centering rocking concentrically-braced frame. Proceeding of the 9th US National and 10th Canadian conference on earthquake engineering,

Seifi, A., Hosseini, A., Marefat, M. S., & Zareian, M. S. (2017). Improving seismic performance of old-type RC frames using NSM technique and FRP jackets. *Engineering Structures, 147*, 705-723.

Sengun, K., & Arslan, G. (2022). Parameters affecting the behaviour of RC beams strengthened in shear and flexure with various FRP systems. Structures,

Shaheen, I., Cruz-Noguez, C., & Lau, D. (2013). Seismic Retrofit of RC Shear Walls with Externally Bonded FRP Tow-Sheets. 3rd Speciality Conference on Disaster Prevention and Mitigation, CSCE 2013,

Shaheen, I. K. (2014). *Seismic Retrofit and Strengthening of Deficient Reinforced Concrete Shear Walls Using Externally Bonded Fibre Reinforced Polymer Sheets* Carleton University].

Shannag, M. J., Al-Akhras, N. M., & Mahdawi, S. F. (2014). Flexure strengthening of lightweight reinforced concrete beams using carbon fibre-reinforced polymers. *Structure and Infrastructure Engineering, 10*(5), 604-613.

Shao, Y., Zhu, Z., & Mirmiran, A. (2006). Cyclic modeling of FRP-confined concrete with improved ductility. *Cement and Concrete composites, 28*(10), 959-968.

Sheikh, S. A., & Li, Y. (2007). Design of FRP confinement for square concrete columns. *Engineering Structures, 29*(6), 1074-1083.

Shen, J., Huang, Z., Song, X., & Yao, Y. (2022). Deformation performance analysis of concrete shear wall with CFRP grids based on the modified uniaxial shear-flexural model. *Journal of Building Engineering, 54*, 104621.

Sherzer, G. L., Alghalandis, Y. F., & Peterson, K. (2022). Introducing fracturing through aggregates in LDPM. *Engineering Fracture Mechanics, 261*, 108228.

Shin, J., & Jeon, J.-S. (2022). Seismic damage mitigation strategy using an FRP column jacketing system in gravity-designed reinforced concrete building frames. *Composite Structures, 279*, 114700.

Shiu, K., Barney, G., Fiorato, A., & Corley, W. (1978). Reversing load tests of reinforced concrete coupling beams. Proceedings of the Central American Conference on Earthquake Engineering,

Shook, D., Roschke, P., Lin, P.-Y., & Loh, C.-H. (2008). Experimental investigation of super-elastic semi-active damping for seismically excited structures. Structures Congress 2008: 18th Analysis and Computation Specialty Conference,

Siddika, A., Al Mamun, M. A., Alyousef, R., & Amran, Y. M. (2019). Strengthening of reinforced concrete beams by using fiber-reinforced polymer composites: A review. *Journal of Building Engineering, 25*, 100798.

Siddika, A., Al Mamun, M. A., Ferdous, W., & Alyousef, R. (2020). Performances, challenges and opportunities in strengthening reinforced concrete structures by using FRPs–A state-of-the-art review. *Engineering Failure Analysis, 111*, 104480.

Sideris, P., Aref, A. J., & Filiatrault, A. (2014). Quasi-static cyclic testing of a large-scale hybrid sliding-rocking segmental column with slip-dominant joints. *Journal of Bridge Engineering, 19*(10), 04014036.

Singh, S. B. (2013). Shear response and design of RC beams strengthened using CFRP laminates. *International Journal of Advanced Structural Engineering, 5*(1), 1-16.

Sinh, L. H., Komuro, M., Kawarai, T., & Kishi, N. (2022). Failure Modes of Reinforced Concrete Beams Strengthened in Flexure with Externally Bonded Aramid Fiber-Reinforced Polymer Sheets under Impact Loading. *Buildings, 12*(5), 584.

Smith, B., Kurama, Y., & McGinnis, M. (2011). Comparison of hybrid and emulative precast concrete shear walls for seismic regions. Structures Congress 2011,

Smith, B. S., & Coull, A. (1991). Tall building structures: analysis and design. . *United States of America*.

Soares, M. M., Palermo, D., & Cortes-Puentes, W. L. (2021). Modelling of mid-rise concrete shear walls reinforced with superelastic shape memory alloys: Nonlinear analysis. *Engineering Structures, 247*, 113049.

Song, X., Huang, Z., Shen, J., & Yao, Y. (2020). Experimental study on cyclic behavior of hybrid CFRP grids-steel shear walls. Structures,

Speicher, M., DesRoches, R., & Leon, R. T. (2008). Analytical study of SDOF systems with superelastic shape memory alloy properties. Structures Congress 2008: 18th Analysis and Computation Specialty Conference,

Sritharan, S., Aaleti, S., Henry, R. S., Liu, K. Y., & Tsai, K. C. (2015). Precast concrete wall with end columns (PreWEC) for earthquake resistant design. *Earthquake Engineering & Structural Dynamics, 44*(12), 2075-2092.

Su, X., Yan, S., Sun, X., & Wang, T. (2024). Resilient performance of self-centering hybrid rocking walls with curved interface under pseudo-static loading. *Earthquake Engineering and Engineering Vibration, 23*(1), 65-85.

Subedi, N. K. (1991). RC coupled shear wall structures. II: ultimate strength calculations. *Journal of structural engineering, 117*(3), 681-698.

Tafsirojjaman, T., Fawzia, S., Thambiratnam, D. P., & Zhao, X.-L. (2021). FRP strengthened SHS beam-column connection under monotonic and large-deformation cyclic loading. *Thin-Walled Structures, 161*, 107518.

Tang, T., & Saadatmanesh, H. (2003). Behavior of concrete beams strengthened with fiber-reinforced polymer laminates under impact loading. *Journal of Composites for Construction, 7*(3), 209-218.

Tassios, T. P., Moretti, M., & Bezas, A. (1996). On the behavior and ductility of reinforced concrete coupling beams of shear walls. *Structural Journal, 93*(6), 711-720.

Teng, J., Chen, J.-F., Smith, S. T., & Lam, L. (2002). *FRP: strengthened RC structures*. Wiley-VCH.

Thomsen, J. H., & Wallace, J. W. (1995). *Displacement-based design of RC structural walls: an experimental investigation of walls with rectangular and T-shaped cross-sections*. Clarkson University, Department of Civil Engineering.

Tolou-Kian, M. J., & Cruz-Noguez, C. (2022). Performance design of reinforced concrete shear walls detailed with self-centering reinforcement. *Engineering Structures, 252*, 113533.

Torabian, A., & Mostofinejad, D. (2017). Externally Bonded Reinforcement on Grooves Technique in Circular Reinforced Columns Strengthened with Longitudinal Carbon Fiber-Reinforced Polymer under Eccentric Loading. *ACI Structural Journal, 114*(4).

Toranzo, L., Restrepo, J., Mander, J., & Carr, A. (2009). Shake-table tests of confined-masonry rocking walls with supplementary hysteretic damping. *Journal of Earthquake Engineering, 13*(6), 882-898.

Tremblay, R., & Atkinson, G. M. (2001). Comparative study of the inelastic seismic demand of eastern and western Canadian sites. *Earthquake Spectra, 17*(2), 333-358.

Tremblay, R., Atkinson, G. M., Bouaanani, N., Daneshvar, P., Léger, P., & Koboevic, S. (2015a). Selection and scaling of ground motion time histories for seismic analysis using NBCC 2015. 11th Canadian Conference on Earthquake Engineering (11CCEE), Victoria, BC, Canada,

Tremblay, R., Atkinson, G. M., Bouaanani, N., Daneshvar, P., Léger, P., & Koboevic, S. (2015b). Selection and scaling of ground motion time histories for seismic analysis using NBCC 2015. Proceeding 11th Canadian Conference on Earthquake Engineering, Victoria, BC, Canada, 21-24 July,

Triantafillou, T., & Plevris, N. (1992). Strengthening of RC beams with epoxy-bonded fibre-composite materials. *Materials and structures, 25*(4), 201-211.

Vassiliou, M. F., & Makris, N. (2015). Dynamics of the vertically restrained rocking column. *Journal of Engineering Mechanics, 141*(12), 04015049.

Vecchio, F. J., & Collins, M. P. (1986). The modified compression-field theory for reinforced concrete elements subjected to shear. *ACI J., 83*(2), 219-231.

Wallace, J. W. (1994). New methodology for seismic design of RC shear walls. *Journal of Structural Engineering, 120*(3), 863-884.

Wallace, J. W. (2012). Behavior, design, and modeling of structural walls and coupling beams—Lessons from recent laboratory tests and earthquakes. *International Journal of Concrete Structures and Materials, 6*(1), 3-18.

Wallace, J. W., & Moehle, J. P. (1992). Ductility and detailing requirements of bearing wall buildings. *Journal of structural engineering, 118*(6), 1625-1644.

Wang, B., Zhu, S., Chen, K., & Huang, J. (2020). Development of superelastic SMA angles as seismic-resistant self-centering devices. *Engineering Structures, 218*, 110836.

Wang, D., & Filiatrault, A. (2008). Shake table testing of a self-centering post-tensioned steel frame. Proceedings of the 14th World Conference on Earthquake Engineering,

Wang, Z., Wang, D., Smith, S. T., & Lu, D. (2012). CFRP-confined square RC columns. I: Experimental investigation. *Journal of Composites for Construction, 16*(2), 150.

White, T., & Adebar, P. (2004). Estimating rotational demands in high-rise concrete wall buildings. 13th World Conference on Earthquake Engineering, Victoria, BC, Canada, 1-6 August,

Wiebe, L., Christopoulos, C., Tremblay, R., & Leclerc, M. (2013a). Mechanisms to limit higher mode effects in a controlled rocking steel frame. 1: Concept, modelling, and low‐amplitude shake table testing. *Earthquake Engineering & Structural Dynamics, 42*(7), 1053-1068.

Wiebe, L., Christopoulos, C., Tremblay, R., & Leclerc, M. (2013b). Mechanisms to limit higher mode effects in a controlled rocking steel frame. 2: large‐amplitude shake table testing. *Earthquake Engineering & Structural Dynamics, 42*(7), 1069-1086.

Wight, G. D., Ingham, J. M., & Kowalsky, M. J. (2006). Shaketable testing of rectangular post-tensioned concrete masonry walls. *ACI Structural Journal, 103*(4), 587.

Wu, H., Zhou, Y., & Liu, W. (2019). Collapse fragility analysis of self-centering precast concrete walls with different post-tensioning and energy dissipation designs. *Bulletin of Earthquake Engineering, 17*(6), 3593-3613.

Wu, X. (2014). A Study of Nonlinear Time History Analysis vs. Current Codes Analysis Procedure of Comparing Linear Dynamic Demand with Nonlinear Static Capacity for Ordinary Standard Bridge. In *Challenges and Advances in Sustainable Transportation Systems* (pp. 467-480). American Society of Civil Engineers (ASCE).

Xu, L., Lu, X., Zou, Q., Ye, L., & Di, J. (2019). Mechanical behavior of a double-column self-centering pier fused with shear links. *Applied Sciences, 9*(12), 2497.

Xu, L., Xiao, S., & Li, Z. (2018). Hysteretic behavior and parametric studies of a self-centering RC wall with disc spring devices. *Soil Dynamics and Earthquake Engineering, 115*, 476-488.

Xu, T., Liu, J., & Guo, Y. (2021). Design method of short circular FRP-steel composite tubed RC columns under eccentric compression. *Composite Structures, 262*, 113359.

Yang, C.-S. W., DesRoches, R., & Leon, R. T. (2010). Design and analysis of braced frames with shape memory alloy and energy-absorbing hybrid devices. *Engineering Structures, 32*(2), 498-507.

Yang, J., Liang, S., Zhu, X., Sun, C., & Guo, Z. (2017). Seismic behavior of precast concrete coupled shear walls with engineered cementitious composite (ECC) in the critical cast-in-place regions. *Science China Technological Sciences, 60*, 1244-1254.

Yang, K.-H., Mun, J.-H., & Oh, N.-K. (2022). Flexural Behavior of Lightweight Aggregate Concrete Shear Walls with Boundary Element. *Journal of structural engineering, 148*(1), 04021243.

Ye, L., Lu, X., & Zhao, S. (2008). Analysis on seismic damage of buildings in the Wenchuan earthquake. *J. Build. Struct, 29*, 1-9.

Yi, W.-J., Xian, Q.-l., Ding, H.-T., & Zhang, H.-y. (2006). Experimental study of RC columns strengthened with CFRP sheets under eccentric compression. *Special Publication, 238*, 395-410.

Yun, H.-D., Kim, S.-W., Jeon, E., Park, W.-S., & Lee, Y.-T. (2008). Effects of fibre-reinforced cement composites' ductility on the seismic performance of short coupling beams. *Magazine of Concrete Research, 60*(3), 223-233.

Zadeh, H. J., & Nanni, A. (2013). Design of RC columns using glass FRP reinforcement. *Journal of Composites for Construction, 17*(3), 294-304.

Zareian, M. S., Esfahani, M. R., & Hosseini, A. (2020). Experimental evaluation of self-centering hybrid coupled wall subassemblies with friction dampers. *Engineering Structures, 214*, 110644.

Zeng, J.-J., Liao, J., Liang, W.-F., Guo, Y.-C., Zhou, J.-K., Lin, J.-X., & Yan, K. (2022). Cyclic Axial Compression Behavior of FRP-Confined Seawater Sea-Sand Concrete-Filled Stainless Steel Tube Stub Columns. *Frontiers in Materials, 9*, 872055.

Zhang, S. S., Yu, T., & Chen, G. (2017). Reinforced concrete beams strengthened in flexure with near-surface mounted (NSM) CFRP strips: Current status and research needs. *Composites Part B: Engineering, 131*, 30-42.

Zhang, T. (2019). *Seismic assessment of reinforced concrete walls in pre-1970s multi-story buildings* Dept. of Civil and Environmental Engineering, Univ. of Auckland].

Zhang, T., Elwood, K., & Henry, R. (2018). Testing of singly reinforced concrete walls used in existing buildings. 2018 NZSEE Annual Conference,

Zhao, Q., Zhao, J., Dang, J.-T., Chen, J.-W., & Shen, F.-Q. (2019). Experimental investigation of shear walls using carbon fiber reinforced polymer bars under cyclic lateral loading. *Engineering Structures, 191*, 82-91.

Zhao, Z., Kwan, A., & He, X. (2004). Nonlinear finite element analysis of deep reinforced concrete coupling beams. *Engineering Structures, 26*(1), 13-25.

Zhijun, L. (2006). *Seismic vulnerability of RC frame and shear wall structures in Singapore* National university of singapore].

Zhong, C., & Christopoulos, C. (2022a). Self-centering seismic-resistant structures: Historical overview and state-of-the-art. *Earthquake spectra, 38*(2), 1321-1356.

Zhong, C., & Christopoulos, C. (2022b). Shear‐controlling rocking‐isolation podium system for enhanced resilience of high‐rise buildings. *Earthquake Engineering & Structural Dynamics, 51*(6), 1363-1382.

Zhou, K.-J., Yi, W.-J., Chen, H., Zhou, Y., & Zhang, W.-X. (2021). Shear strength and deformation modeling of conventionally reinforced short coupling beams. *Engineering Structures, 239*, 112282.

Zhou, S., Demartino, C., Xu, J., & Xiao, Y. (2021). Effectiveness of CFRP seismic-retrofit of circular RC bridge piers under vehicular lateral impact loading. *Engineering Structures, 243*, 112602.

Zhu, R., Guo, T., & Mwangilwa, F. (2020). Development and test of a self-centering fluidic viscous damper. *Advances in Structural Engineering, 23*(13), 2835-2849.

Zhu, S., & Zhang, Y. (2008). Seismic analysis of concentrically braced frame systems with self-centering friction damping braces. *Journal of structural engineering, 134*(1), 121-131.